SYNTHESIS AND BIOLOGICAL ACTIVITY OF ALOIN DERIVATIVES

ADUSHAN PILLAY

SYNTHESIS AND BIOLOGICAL ACTIVITY OF ALOIN DERIVATIVES

By

ADUSHAN PILLAY

B.Sc.Hons (University of KwaZulu-Natal)

Submitted in fulfillment of the requirements of the degree of

Master of Science

In the

School of Chemistry

University of KwaZulu-Natal

Pietermaritzburg

December 2008

Declaration

I hereby certify that this research is a result of my own investigation and has not already been accepted in substance for any degree and is not being submitted in candidature for any other degree.

Signed…….
Adushan Pillay

We, the undersigned, hereby certify that the above statement is true and correct.

Signed…….
Professor F. R. van Heerden
Supervisor

Signed…….
Doctor E. Elliott
Co-Supervisor

Signed…….
Doctor C. P. Parkinson
Co-Supervisor

School of Chemistry
University of KwaZulu-Natal
Pietermaritzburg

December 2008

ACKNOWLEDGEMENTS

I like to thank my supervisor, Professor Fanie van Heerden for her guidance, patience, support and never-ending encouragement throughout this project, and my co-supervisors, Dr Edith Elliot and Dr Christopher Parkinson, for their invaluable contributions. I would also like to express thanks to Professor Siegfried Drewes for useful discussions.

Recognition is also due to the following, without whom this work would have never been completed:

- My colleagues of both the Warren Organic Chemistry laboratory and the Biochemistry laboratory (lab 43) for the insightful discussions and for creating a pleasant ambience
- Mr C. Grimmer for running NMR spectra and for his friendship
- Doctor F. Khan for running LC-MS spectra
- Doctor C. Southway for assistance with the HPLC
- Professor O. Q. Munro for assistance with IR and for his input
- Mr R. Somaru, Mr F. Shaik, and Mr S. Ball for technical assistance
- Mr C. Mortlock and Mr P. Forder for glassblowing

I am indebted to my family for all the love and support they have offered.
I also acknowledge the financial support from the NRF and the CSIR.

TABLE OF CONTENTS

CHAPTER FOUR: ANTIPLASMODIAL ACTIVITY OF ALOIN AND DERIVATIVES

CHAPTER FIVE: CONCLUSIONS AND FUTURE WORK

ABSTRACT

This project is focused on the synthesis and biological activity of aloin and derivatives. Aloin is a *C*-glucoside anthrone that is found in *Aloe marlothii*, a common Southern African plant used in traditional medicine. Aloin was isolated from *A. marlothii*, employing a selective chelation isolation procedure. This compound is known to have numerous biologically active properties, and can be used as a laxative, an anti-bacterial agent, an anti-oxidant, and as a cytotoxic drug against breast and ovarian tumour cell lines. More relevant to this research investigation, was the reported anti-inflammatory activity of aloin. Specifically, the inhibitory activity of aloin on matrix metalloproteinases, which when excessively secreted, can lead to the development of osteoarthritis and cancer metastasis. Aloin has also been reported to have antiplasmodial activity, which was also investigated.

Aloin was synthetically transformed into several derivatives, which could be potentially useful medicinal compounds. The choice of derivatives to be made was based upon (i) known biologically active compounds (e.g. aloe-emodin) and (ii) interesting biologically active functional groups (e.g. amines). These aloin derivatives include aloe-emodin, rheinal, rhein and three amine derivatives. Homonataloin, an aloin-analogue, which was also isolated from *A. marlothii*, was synthetically transformed into nataloe-emodin. These two compounds serve as aloin structural analogues for the biological testing. Aloin and derivatives were characterised using NMR, HR-MS, UV and IR, which allowed for their unambiguous structural elucidation.

Aloin and derivatives were all tested for (i) possible inhibition towards MMP-2 and MMP-9, which are the two most common MMPs in the blood, and (ii) antiplasmodial activity against chloroquine sensitive *Plasmodium falciparum* parasites. Doxycycline, a clinical tetracycline drug, was used as a reference compound for the biological assays, since it shares many common structural features with aloin and derivatives. 11-(Piperidin-1-yl)chrysophanol and 11-(morpholin-1-yl)chrysophanol proved to be the most potent selective MMP-2 inhibitors. 11-(Piperidin-1-yl)chrysophanol was also found to be the most potent against *P. falciparum* parasite, along with 11-(pyrrolidin-1-yl)chrysophanol.

Aloin has been shown to be a cheap, easily obtainable lead compound that could facilitate the production of a range of powerful medicinal drugs.

LIST OF FIGURES

LIST OF TABLES

LIST OF ABBREVIATIONS

Ac	acetyl
A. marlothii	aloe marlothii
br s	broadened singlet
BCIP	5-bromo-4-chloro-3-indoyl phosphate
BuLi	butyllithium
ChC	*Clostridium histolyticum* collagenase
COSY	correlated spectroscopy
CMC	critical micelle concentration
DMSO	dimethyl sulfoxide
d	doublet
dd	doublet of doublets
DEPT	distortionless enhancement polarization transfer
d.H_2O	distilled water
DMF	dimethylformamide
EtOAc	ethyl acetate
ECM	extracellular matrix
EDTA	ethylenediaminetetraacetic acid
Fig	figure
h	hour
HMBC	heteronuclear multiple binuclear coherence
HSQC	heteronuclear singlet quantum coherence
HRMS	high resolution mass spectrometry
Hz	hertz
IBX	*o*-idoxybenzoic acid
IR	infrared spectroscopy
IgG	immunoglobulin G
kDa	kilodalton
LC	liquid chromatography
NBT	nitroblue tetrazolium chloride

NMR	nuclear magnetic resonance spectroscopy
MeOH	methanol
min	minute
MS	mass spectrometry
MMP	matrix metalloproteinase
MT-MMP	membrane-type matrix metalloproteinase
M_r	molecular weight
PAF	platelet activating factor
PAGE	polyacrylamide gel
%T	percentage transmittance
PI	proteinase inhibitor
PPAK-γ	peroxisome proliferators-activated receptor gamma
s	singlet
salen	2,2'-ethylenebis(nitrilomethylidene)diphenol
sp	species
RT	room temperature
t	triplet
TBS	tris buffered saline
TEMPO	2,2,6,6-tetramethylpiperidine-1-oxyl
TEMED	tetramethyethylenediamine
THF	tetrahydrofuran
TIMP	tissue-inhibitor of metalloproteinases
TLC	thin-layer chromatography
TNF-α	tumour necrosis factor alpha
UV	ultraviolet spectroscopy

CHAPTER ONE

AN INTRODUCTION TO *ALOE* CHEMISTRY

1.1 Introduction

The total synthesis of medicinally useful compounds is a highly daunting and challenging task. This requires both high skills levels and financial capital outlay. The goal of obtaining a medicinally valuable compound by partial synthesis, starting from a readily available starting material is an extremely attractive one. Such a compound may be aloin (**1.1**), which is a naturally occurring *C*-glucoside anthrone that has been reported to have many potentially useful biological properties[1]. The most interesting biological activity of aloin (**1.1**) is the reported non-competitive inhibitory action against the extracellular matrix-degrading enzyme, metalloproteinase-8[2]. Metalloproteinase-8 belongs to a family of enzymes called matrix metalloproteinases (MMPs). These enzymes are finely regulated at three stages, but sometimes, this control is altered or lost. The result is excessive tissue breakdown at an unbalanced replacement build-up rate, leading to medical conditions such as osteoarthritis, tumour growth and metastasis, and periodontal disease[3]. The *in vitro* antiplasmodial activity of aloin (**1.1**) against the chloroquine-resistant *Plasmodium falciparum* strain has also been reported, with an IC_{50} value of 107.20 ± 4.14 μg ml^{-1} [4]. Aloin (**1.1**) is found in moderate amounts in the leaf exudate of two common, robust, easily-cultivatable *Aloe* plants, *i.e*. *Aloe marlothii* A.Berger subsp. *marlothii* and *Aloe ferox* Mill. Thus, aloin (**1.1**) is a natural product with commercial potential that can be obtained from a cheap, easily obtainable, renewable resource. The investigation of the biological properties of aloin (**1.1**) and synthetic derivatives could prove to be invaluable from a medicinal perspective.

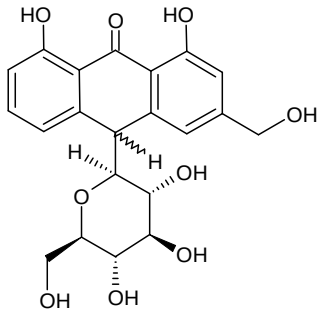

(1.1)

1.2 The genus *Aloe L.*

The genus *Aloe* comprises approximately 600 species, most of which occur naturally in Sub-Saharan Africa, except for the moist lowland forest regions and the western part of West Africa. Some species are found in the Arabian Peninsula and in Madagascar. A few *Aloe* species, formerly in the genus *Lomatophyllum*, are known from some of the smaller Indian Ocean islands[5].

Aloe plants are perennial, leaf-succulent xerophytes. Xerophytes are plants adapted to survive in areas of low or erratic precipitation, and these adaptations may include structural and physiological features. One kind of xerophytic adaptation is succulence, which is the development of water storage tissue, consisting of large thin-walled cells in which water is held in mucilage. The enlargement of leaves or stems in *Aloe* plants is a modification to accommodate the water storage tissue. The leaf cuticle is thick and is covered by a layer of wax, which has distinct patterns of ridges and/or micro papillae and sunken stomata. Many *Aloe* species have groups of cells associated with the vascular bundles, called aloin or aloitic cells that store and possibly secrete a mixture of compounds with medicinal value, with the composition varying in different species. The breakage of leaves exposes this exudate, normally yellow in colour, strong smelling and bitter in taste[1].

The bitter leaf exudates of some *Aloe* species are of commercial importance. These serve as renewable sources of the laxative aloe drug. This exudate has also been employed as a bittering agent in alcoholic beverages. *Aloe* gel is the clear jelly-like substance obtained from the leaf pulp. The mechanical extrusion of the mucilaginous gel from the fibrous fraction of the pulp gives a 70% yield with a water content of 99%. This gel is used in the cosmetic industry in shampoos, shaving and skin care creams and in the treatment of skin

disorders, especially, as topical medication for the treatment of burns. Medicinally, the gel and dried leaf exudates of *Aloe* species have been used by ancient civilizations of the Egyptians, Greeks and Mediterranean people[6].

1.2.1 *Aloe marlothii* and *Aloe ferox*

A. marlothii (Fig. 1.1) is a large single-stemmed plant occurring in South Africa, Botswana, Mozambique and Zimbabwe[7]. *A. marlothii* was previously commercially harvested for the production of the drug 'aloes' but this was ceased due to the erratic chemical variance of anthrones, i.e. aloin (**1.1**) and homonataloin (**1.2**) in the plant. This species is now only utilized in traditional medicine. This includes the treatment of round-worm infections, using the powdered dry leaves in snuff, for stomach troubles, and for weaning breastfed children by rubbing green leaf pulp over the breasts[8]. The leaves of *A. marlothii* are used by communal stock owners in the North West Province of South Africa to treat and prevent gallsickness (*Anaplasma marginale* infection in cattle), to treat parasitic helminthiasis, diarrhoea, constipation, general ailments, retained placenta, dystocia, to remove maggots from wounds and to reduce tick burdens[9].

(A) http://en.wikipedia.org/wiki/Image:Aloe_marlothii00.jpg

(B) http://commons.wikimedia.org/wiki/Image:Aloe_ferox.JPG

Figure 1.1. (**A**) *A. marlothii* and **(B**) *A. ferox* plants during flowering season.

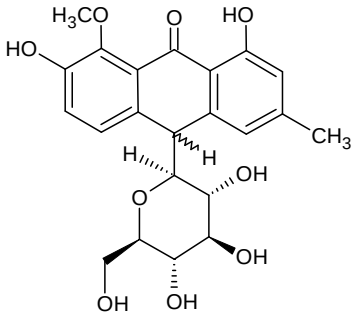

(**1.2**)

A. ferox (Figure 1.1) is the major *Aloe* species that is commercially used in South Africa. It is a plant similar to *A. marlothii*, both physiologically and in its chemistry. Commercially *A. ferox* is preferred over *A. marlothii*, due to minimal chemical variance in terms of its phenolics[1]. *A. ferox* is found predominantly in the lower western half of South Africa and is known as the 'Cape *Aloe*'. *A. marlothii* on the other hand, is found in the upper eastern half of South Africa, and prefers more mountainous terrain, and is therefore called 'mountain *Aloe*'. There are regions where these plants coexist, and hybridization between the two is a very common occurrence[10].

1.3 Chemical Constituents of *Aloe* Species

A variety of secondary metabolites are produced in the leaves and roots of *Aloe* plants. Many different classes of compounds are represented here including alkaloids, anthraquinones, anthrones, bianthraquinoids, chromones, coumarins and pyrones. The most important constituents of *Aloe* bitters are the anthrones, aloin A (**1.3**) and B (**1.4**), and the chromones aloesin (**1.5**) and aloeresin A (**1.6**)[1]. These compounds are all found in the leave exudate of both *A. marlothii* and *A. ferox*.

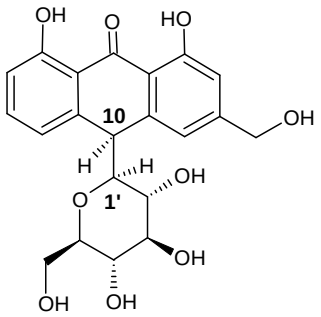

(1.3)

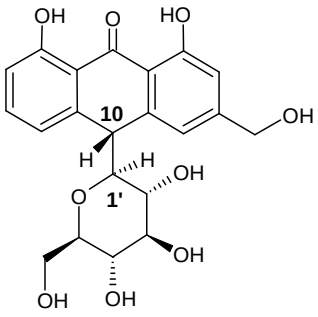

(1.4)

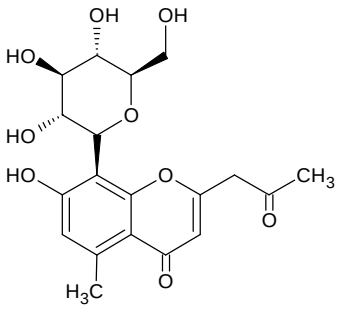

(**1.5**)

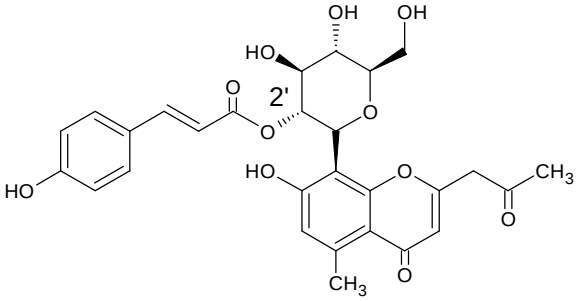

(1.6)

1.3.1 Anthrones: Aloin (1.1)

Of all the classes of compounds occurring in *Aloe* species, anthrones are considered to be the most important. Within this class itself, the most abundant is aloin (**1.1**), which was first isolated from *A. arborescens* in the 1800's[11]. Aloin consists of a mixture of aloin A (**1.3**) and aloin B (**1.4**), two diastereomeric *C*-glucosides that differ in the configuration at C-10 of the aloe-emodin anthrone moiety[6]. A biosynthetic study carried out by Grún and Franz in 1980 has shown that aloin B (**1.4**) is the true natural product, which is produced by the plant and is enzymatically converted to aloin A (**1.3**)[12]. That study also established that aloin B (**1.4**) is formed by attachment of *D*-glucose to aloe-emodin anthrone, a compound detected so far in flowers but not in the leaves of *Aloe* plants. In aloin B (**1.3**), the glucose moiety attached to C-10 has the α-orientation (i.e., 10*R*, 1'*S*) and conversely, in aloin A (**1.2**), the β-orientation (i.e., 10*S*, 1'*S*).

The carbon-carbon bond between the sugar and the anthrone (i.e. the bond from C-10 on anthrone) is quite resistant to acid and alkaline conditions. The cleavage of this bond is achieved by oxidation, rather than hydrolysis, and only under drastic conditions of acid in combination with an oxidant. This bond is also resistant to β-glycosidase of plants and most plant bacteria, however, the intestinal microflora of humans and animals have been shown to cleave this *C*-glucosyl bond, although considerable variation in response among animal species occurs[13].

The percentage of aloin (**1.1**) in the leaf exudate varies from species to species, from season to season, and depends on plant or leaf age. The aloin (**1.1**) content of leaf exudate from different *Aloe* species was analysed by numerous methods and was found to be 10-

25% on a dry weight basis of the leaf exudate[12]. A recent chemotaxonomic survey of 380 species of *Aloe* showed that aloin is found in 36 (10%) of the species[14]. The occurrence of aloin is not confined only to *Aloe* species as it has also been found in the extracts of *Rhamnus purshiana*[1].

Homonataloin (**1.2**) is another anthrone which has a similar structure to that of aloin (**1.1**). Homonataloin (**1.2**), which also occurs as diastereomers, was found to occur in 47 (12%) of 380 *Aloe* species tested, including *A. marlothii*[14]. The distribution of homonataloin (**1.2**) is more restricted compared to that of aloin (**1.1**). The chemical occurrence of aloin (**1.1**) and homonataloin (**1.2**) has been found to be mutually exclusive in *Aloe* species, with *A. mutabilis* being a notable exception[1]. Thus, within a specific *Aloe* plant, that is known to produce the anthrones, either aloin (**1.1**) or homonataloin (**1.2**) may occur, but not both simultaneously. This chemical variance between homonataloin (**1.2**) and aloin (**1.1**) in *A. marlothii* was the major factor in stopping the commercial harvesting of the plant.

1.3.2 Biological Activity of Aloin (1.1)

The most well-documented yet mechanistically unknown activity of aloin (**1.1**) is its purgative/laxative action in animals. Aloin (**1.1**) has been shown to be metabolized to the reactive aloe-emodin (**1.7**) by the colonic flora (*Eubacterium species)* in the gut. It has been demonstrated that aloe-emodin (**1.7**) exerts its action on the colonic mucosa, but its mechanism of action is still uncertain. It is postulated that aloe-emodin (**1.7**) acts by disturbing the equilibrium between the absorption of water from the intestinal lumen via an active sodium transport and the secretion of water into the lumen by a prostaglandin-dependent mechanism. Aloe-emodin (**1.7**) also stimulates the release of platelet-activating factor (PAF) in human ileal and colonic mucosa, which could also contribute to this purgative effect[15].

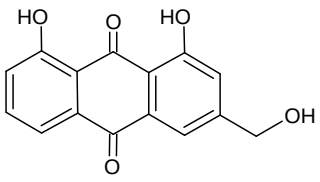

(**1.7**)

Other reported biological activities of aloin (**1.1**) include: the induction of programmed cell death (apoptosis) in Jurkat cells[16], cytotoxicity against certain breast and ovarian cancer cell lines[17], the increase in the rate of alcohol oxidation in rats[18] and the inhibition of histamine release from mast cells[19].

Aloin (**1.1**) has been reported to possess a dose-dependent inhibitory effect on MMPs. Aloin (**1.1**) has shown good inhibitory activity on both *Clostridium histolyticum* collagenase (ChC) and MMP-8 via a predominantly non-competitive inhibitory mechanism. The inhibitory activity of aloin (**1.1**) on MMP-8 was comparable to that of the modified tetracycline doxycycline (**1.8**), which is the enzyme's most powerful known inhibitor[2].

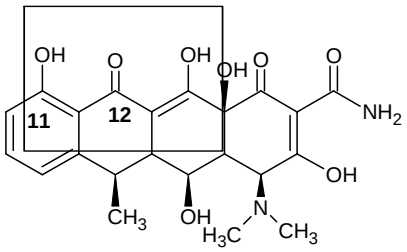

(**1.8**)

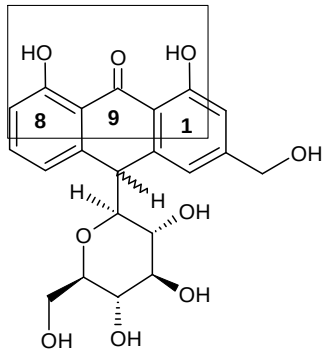

(**1.1**)

The carbonyl oxygen at C-12 and the OH group at C-11 on the doxycyline (**1.8**) structure appear essential for activity. Comparing the structures of doxycycline (**1.8**) to the structure of aloin (**1.1**), the carbonyl group at C-9, between the hydroxyls at C-8 and C-1 on the anthrone, is consistent with that pharmacophore profile and it seems reasonable to postulate that the aloin (**1.1**) inhibition of the MMPs is due to an interaction similar to that between doxycycline (**1.8**) and MMPs[2].

1.3.3 Anthraquinones: Aloe-emodin (1.7)

Aloe-emodin (**1.7**) is found in both the leaves and roots of many *Aloe* and *Senna* species. This anthraquinone usually occurs in combination with its glycosides or in a reduced (anthrone) form. The amount of aloe-emodin (**1.7**) in plants is very low, as it is thought to arise through the oxidative decomposition of its glycosides, rather than through direct

biosynthesis. Despite being such a minor constituent of the plants, many studies have proven that aloe-emodin (**1.7**) is the active metabolite of both aloin (**1.1**) and sennosides[13].

1.3.4 Biological Activity of Aloe-emodin (**1.7**)

The list of the biological properties of aloe-emodin (**1.7**) increases regularly as more studies are carried out on this highly active molecule.

The mechanism of the anti-inflammatory and immunodulatory effects of aloe-emodin (**1.7**) and other anthraquinones are proposed to involve curbing oxidation[20]. Many reactive oxygen species and free radical-mediated reactions are involved in inflammatory responses. Since anthraquinones such as aloe-emodin (**1.7**) act as both anti-oxidants and radical scavengers, they can combat many of these responses. Aloe-emodin (**1.7**) reduces the inflammation of lymphocytes and Kupfer cells in the liver. Pre-treatment of the liver with aloe-emodin (**1.7**) reduces the damage caused by toxic species such as carbon tetrachloride[20].

Aloe-emodin (**1.7**) also displays anti-bacterial activity, dose-dependently inhibiting the growth of *Helicobacter pylori*, which is a possible causative agent of gastric cancer[20]. Aloe-emodin (**1.7**) possesses contradictory activities on cell growth. It was found to stimulate the growth of primary rat hepatocytes and, conversely, was found to have apoptosis-inducing effect in human lung squamous cell carcinoma and to selectively inhibit neuroectodermal tumour growth *in vivo*[20].

Despite all of these medically-promising biological activities, anthraquinones also have harmful effects. These include genotoxic, mutagenic, and tumour-promoting effects. Thus caution should be exercised with regard to the anthraquinones, and further studies need to be carried out to more accurately define the activities of each component[20].

1.3.5 Chromones: Aloesin (1.5) and Aloeresin A (1.6)

Aloesin (**1.5**), which can be regarded as the parent compound of the aloe chromones was first described in 1970 by Haynes and coworkers[21]. Similarly to aloin (**1.1**), aloesin (**1.5**) has a *C*-glucoside sugar. It should be noted that the carbon-carbon bond connecting the

sugar to the aglycone is also difficult to break. This chromone is widespread throughout the genus, occurring in around 40% of species examined[14].

Aloeresin A (**1.6)** is another common chromone found in many *Aloe* species and differs from aloesin (**1.5**) by a *p*-coumaroyl group, which is connected to the C-2' position. This ester bond is considerably more labile than the *C*-glucoside bond, and can be hydrolysed under acidic conditions to afford aloesin (**1.5**)[22].

1.3.6 Biological Activity of Aloesin (1.5) and Aloeresin (1.6)

Both aloesin (**1.5**) and aloeresin A (**1.6**) show skin-whitening activity. These compounds display inhibitory activity against the enzyme tyrosinase. Tyrosinase is a copper-containing monooxygenase enzyme which catalyses the conversion of tyrosine to dopa, dopaquinone and subsequent autopolymerisation to melanin[23]. Pigmentation in skin results from the synthesis and distribution of melanin[22].

1.4 Project Aims

The aims of this investigation were:

1. To develop a procedure to isolate aloin from *A. marlothii* leaf exudate.

2. To synthesise several aloin derivatives, based on potentially interesting biologically active functional groups.

3. To test the potential inhibitory properties of aloin and its synthetic derivatives on MMP-2 and MMP-9.

4. To screen aloin and its synthetic derivatives for in vitro antiplasmodial activity against a chloroquine-sensitive strain of *P. falciparum*.

1.5 References

1. Reynolds, T., *Aloes: The Genus Aloe*, CRC Press LLC, New York, 2004, pp. 3-6, 39-41, 128, 336.

2. Barrantes, E., Guinea, M., *Life Sciences*, 2003, **72**, 843-850.

3. Cawston, T. E., *Pharmacology and Therapeutics*, 1996, **70**, 163-182.

4. van Zyl, R. L., Viljoen, A. M., South African Journal of Botany, 2002, **68**, 106-110.

5. Capasso, F., Borrelli, R., Capasso, R., Di Carlo, G., Izzo, A. A., Pinto, L., Mascolo, S., Castaldo, S., Longo, R., *Phytotherapy Research*, 1998, **12**, 124-127.

6. Dagne, E., *Bulletin of the Chemical Society of Ethiopia*, 1996, **10**, 89-103.

7. Biscrat, D., Dagne, E., van Wyk, B-E., Viljoen, A., *Phytochemistry*, 2000, **55**, 949-952.

8. van der Bank, H., van Wyk, B-E., van der Bank, M., *Biochemical Systematics and Ecology*, 1995, **23**, 251-256.

9. Spickett, A. M., van der Merwe, D., Matthee, O., *Experimental and Applied Acarology*, 2007, **41**, 139-146.

10. Van Wyk, B-E., Smith, G., *Guide to the Aloes of South Africa*, Briza Publications, Pretoria, South Africa, 1996, pp. 52, 58.

11. Hay, J. E., Haynes, L. J., *Journal of the American Chemical Society*, 1956, 3141-3147.

12. Grun, M., Franz, G., *Planta Medica*, 1980, **39**, 288.

13. Boudreau, M. D., Beland, F. A., *Journal of Environmental Science and Health*, 2006, **24**, 103-154.

14. Viljoen, A. M., *A Chemotaxomonic Study of Phenolic Leaf Compounds in the Genus Aloe*, 1999, PhD Thesis, Rand Afrikaans University.

15. Izzo, A. A., Sautebin, L., Borrelli, F., Longo, R., Capasso, F., *European Journal of Pharmacology*, 1999, **368**, 43-48.

16. Buenz, E. J., *Toxicology in Vitro*, 2008, **22**, 422-429.

17. Metenawy, E., Wafaa, H., Esmat, A. Y., *Cancer Molecular Biology*, 1996, **3**, 851-864.

18. Chung, J., Cheong, J., Lee, J., Roh, H., Cha, Y., *Biochemical Pharmacology*, 1996, **52**, 1461-1468.

19. Gutterman, Y., Chauser-Volfson, E., *Biochemical Systematics and Ecology*, 2000, **28**, 825-838.

20. Choi, S., Chung, M., *Seminars in Integrative Medicine*, 2003, **1**, 53-62.

21. Haynes, L. J., Holdsworth, D. K., *Journal of the Chemical Society (C)*, 1970, 2581-2586.

22. Steenkamp, L. H., Mitra, R. K., Heggie, S. J., Phehane, V. N., PCT, 2006, WO 2006/097811 A1.

23. Piao, L. Z., Park, H. R., Park, Y. K., Lee, S. K., Park, J. H., Park, M. K., *Chemical and Pharmaceutical Bulletin*, 2002, **50**, 309-311.

24. Tsuji-Naito, K., Hatani, T., Okada, T., Tehara, T., *Biorganic and Medicinal Chemistry*, 2007, **15**, 1967-1975.

CHAPTER TWO

ISOLATION OF *ALOE* COMPOUNDS AND SYNTHESIS OF ALOIN DERIVATIVES

2.1 Introduction

Aloin (**2.1**) has been shown to be a highly biologically active compound. Its numerous biological effects, as mentioned in Chapter 1, have been attributed to both its electron-rich ring system and its chelating ability. Aloin (**2.1**) has been reported to inhibit MMPs via a non-competitive chelation mechanism[1]. This property of aloin (**2.1**) was investigated in this research project. One of the aims of this project was to synthesise a variety of aloin derivatives and to test and compare their potential MMP-2 and MMP-9 inhibitory properties. By analyzing the structure of aloin (**2.1**) the benzylic hydroxy group at C-11 presents itself as a region of possible functionalisation for derivative formation. Aloin (**2.1**) will serve as a useful starting compound with many possibilities for the synthesis of derivatives. Aloin (**2.1**) occurs in many *Aloe* species[2], yet it is an expensive compound to purchase. The most effective and cost-efficient manner of obtaining aloin (**2.1**) is to isolate it from a plant that contains aloin (**2.1**) in reasonable amounts, i.e. *A. marlothii*. *A. marlothii* also contains two other major compounds in its leaf exudate; aloeresin A (**2.2**) and aloesin (**2.3**)[3]. Besides these chromones, an aloin analogue called homonataloin (**2.4**) is also known to occur[4]. The occurrence of aloin (**2.1**) and homonataloin (**2.4**) is mutually exclusive in *A. marlothii* plants. Thus an individual *A. marlothii* plant may contain either aloin (**2.1**) or homonataloin (**2.4**), but not both simultaneously. Homonataloin (**2.4**) should serve as a highly useful compound, having a methoxy group at C-8 compared to a hydroxy in aloin (**2.1**). This chemical variance could have an interesting effect on its activity.

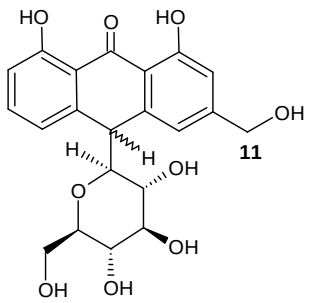

(**2.1**)

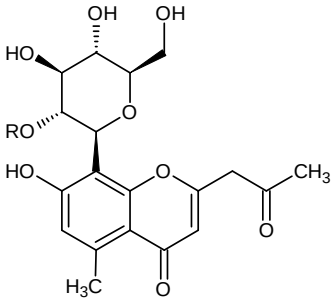

(**2.2**) R = *p*-coumaroyl
(**2.3**) R = H

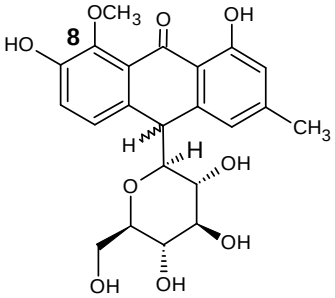

(**2.4**)

2.2 Anthraquinones

Anthraquinones are widely studied compounds having many remarkable properties and uses. Many anthraquinones occur naturally, whilst others are either synthetic or semi-synthetic. Examples of different classes of anthraquinones, along with their biological activities will be discussed briefly in this chapter to illustrate the importance and significance of these compounds.

2.2.1 Natural Anthraquinones

Dynemicin A (**2.5**) is a structurally interesting compound that has received considerable interest over the last 15 years due to its potential anticancer applications[5]. This molecule is a member of the enediyne family of antibiotics which cause cell death through irreversible oxidative strand scissions of DNA. Dynemicin A (**2.5**) has not been used as a drug due to its lack of specificity towards tumour cells, despite the high levels of cytotoxity it displays.

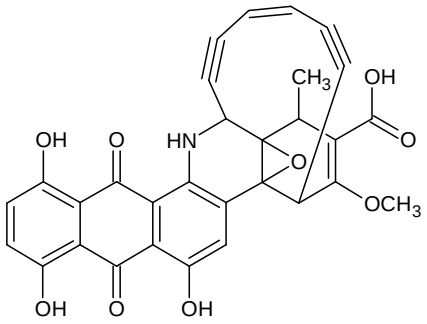

(2.5)

Chlorocyclinone C (**2.6**) is a novel anthraquinone compound which has been isolated from the mycelium of *Streptomyces sp.* strain DSM 17045[6]. This compound has been shown to antagonize rosiglitazone-induced peroxisome proliferator-activated receptor gamma (PPAR-γ) activation with $IC_{50's}$ < 0.4 μM *in vitro*. PPAR-γ antagonists provide a therapeutic option to patients in need of effective antidiabetic therapies.

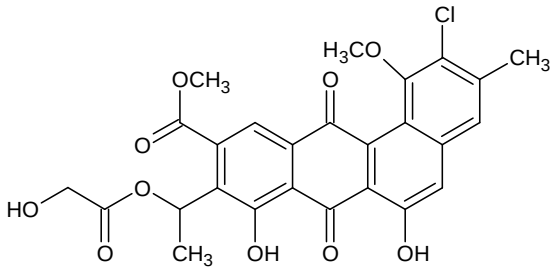

(2.6)

A pentacyclic anthraquinone compound (**2.7**) has been isolated from *Juglans mandshurica*[7]. This compound efficiently induced apoptosis in HeLa cells (a cancer cell line) through a mitochondria dependent pathway and activation of the caspase cascade. This may prove to be a potential chemotherapeutic candidate for the treatment of cancer.

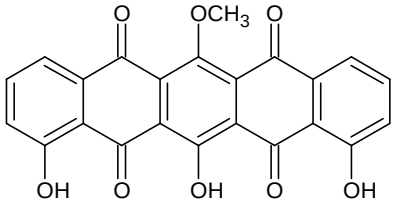

(2.7)

A recent phytochemical study of the fruits of *Vismia laurentii* resulted in the isolation of three structurally related anthraquinones; laurentiquonones A (**2.8**), B (**2.9**) and C (**2.10**)[8]. The combined extracts of these compounds displayed anti-plasmodial activity against the W2 strain of *P. falciparum*.

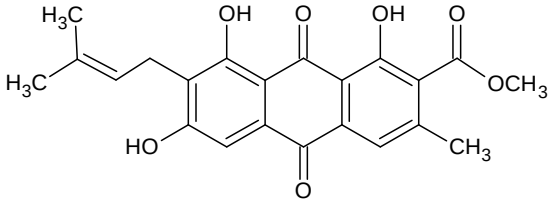

(2.8)

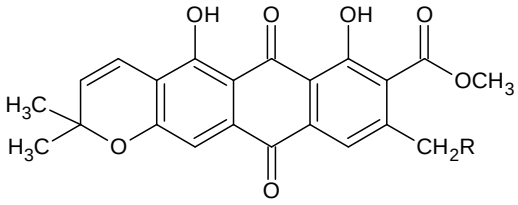

(**2.9**) R = H

(**2.10**) R = OAc

Altersolanol A (**2.11**), a tetrahydroanthraquinone, showed good cytotoxic activity *in vitro* towards L5178Y mouse lymphoma lines[9]. This compound also exhibited antimicrobial activity against gram-positive pathogens, i.e. *Staphylococcus epidermidis*, *Staphylococcus aureus* and *Enterococcus faecalis*. It has been discovered that altersolanol A (**2.11**) acts as an electron acceptor in the bacterial membrane and thus inhibits bacterial growth. This bioactive metabolite was isolated from the endophytic fungus *Ampelomyces sp*. which was isolated from the Egyptian plant *Urospermum picroides*.

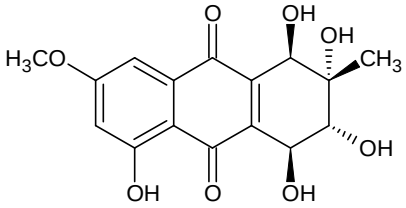

(2.11)

Brasilquinolone C (**2.12**), a benz[a]anthraquinone antibiotic, was isolated from fermentations of *Nocardia brasiliensis*[10]. This compound exhibited antimycobacterial activity towards *Mycobacterium smegmatis* with an MIC value of 12.5 μg ml^{-1}. Mild cytotoxicity towards murine leukaemia cell line L1210 and P388 was also observed.

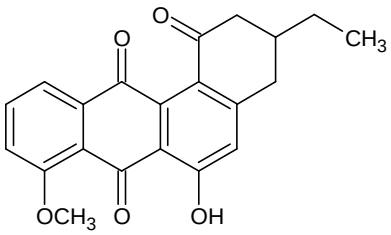

(2.12)

The anthracyclinone celasramycin B (**2.13**) was isolated from an unidentified species of *Streptomyces*[10]. Celasramycin B (**2.13**) displayed an MIC of 3.1 μg ml^{-1} towards *Mycobacterium vaccae*.

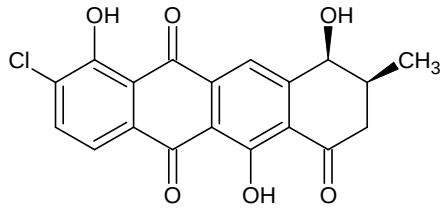

(2.13)

Mumbaistatin (**2.14**) has been found to be the most potent natural inhibitor of glucose 6-phosphate transporter 1 (G6PT1), a key enzyme in the regulation of glucose homeostasis, making it an important therapeutic target in type II diabetes[11]. Mumbaistatin was isolated from cultures of *Streptomyces sp*. DSM 11641.

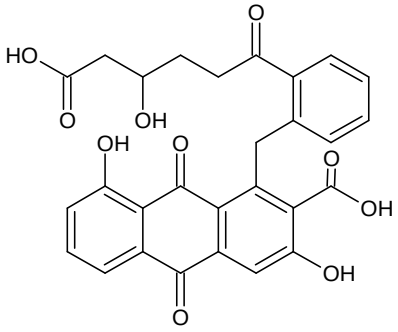

(2.14)

Natural anthraquinones are valuable medicinal compounds. These are biosynthesized via the polyketide synthase pathway. Many of these compounds play a crucial role in the fight against infectious diseases.

2.2.2 Synthetic Anthraquinones

The anthraquinone (**2.15**) has exhibited *in vitro* cytotoxicity against several different cancer lines through apoptosis. Apoptosis has become a focus of interest in oncology because a disregulation of the apoptosis process can prompt malignancy of tumours[12].

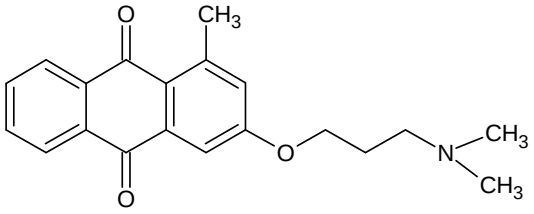

(2.15)

Mitoxanthrone dihydrochloride **(2.16**) is an important compound used clinically as an anticancer agent. It is used for treating leukemia, lyphomas, and advanced breast and ovarian cancer in combination with other treatment[13]. The reaction mechanism of the anti-tumour activity of anthraquinones is probably multimodal in nature, and studies have suggested that its intercalative interaction with DNA may play a role.

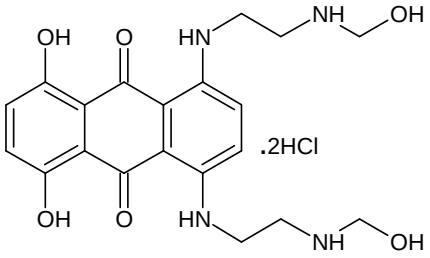

(2.16)

The anthracycline antibiotics daunomycin (**2.17**) and doxorubicin (**2.18**) are clinically effective anti-tumour agents[14]. They display good potency and are used commonly in the treatment of a wide range of cancers. However, they are expensive and quite toxic.

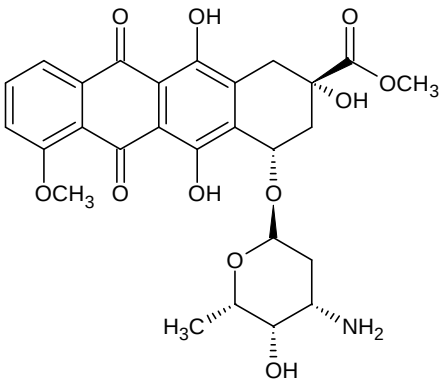

(2.17)

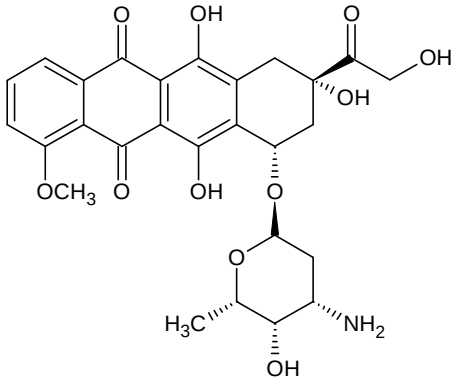

(2.18)

Synthetic anthraquinones, that are used medicinally, are usually less structurally complex than the naturally occurring ones. Many synthetic anthraquinones are created from a lead compound, which is commonly a natural product.

2.2.3 Semi-Synthetic Anthraquinones

Emodin (**2.19**) and chrysophanol (**2.20**) are naturally occurring anthraquinones that have been used as starting materials for synthesis. These compounds were isolated from crude rhubarb extract. Their structural aromatic features indicate that these compounds and their derivatives (especially positively charged ones) may intercalate into the double helix of DNA[15]. Libraries of their derivatives were prepared for structure-activity relationship studies of anticancer activity against mouse leukemia L1210 and human leukemia HL-60 cells. In general, it was also reported that anthraquinones bearing an amino function interact with DNA. There was no straightforward correlation apparent between the derivative affinity for DNA and their cytotoxic effects. This study concluded that the cytotoxicity produced by these derivatives is time dependent and is not a direct result of initial inhibition of DNA replication.

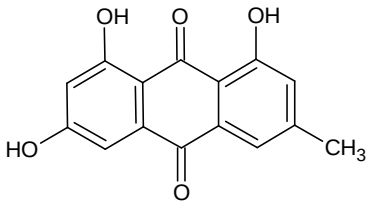

(2.19)

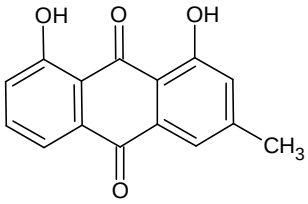

(2.20)

The use of semi-synthetic anthraquinones as potential medicinal drugs is becoming more common. It is often quicker and cheaper to synthetically modify an existing anthraquinone framework than the *de novo* synthesis of the product.

2.3 Isolation of *A. marlothii* Leaf Exudate Compounds

2.3.1 Isolation of Aloin (2.1) and Homonataloin (2.4)

It is well documented that the levels of aloin (**2.1**) within *Aloe* species varies from species to species, seasonally, and relative to the environmental conditions of the specific *Aloe* plant[3]. Thus it is rather difficult to obtain a source of *A. marlothii* leaf exudate that has consistently high aloin (**2.1**) content. Furthermore, without TLC pre-analysis of the *A. marlothii* plants' chemical constituents, it is impossible to determine whether the plant contains either aloin (**2.1**) or homonataloin (**2.4**). The *A. marlothii* sample which was obtained in Ladysmith, was a collection of different plants and as expected contained both aloin (**2.1**) and homonataloin (**2.4**). This was a beneficial complication as it provided us with a source of both aloin (**2.1**) and homonataloin (**2.4**), which have sufficiently different R_f values on TLC to allow for separation by column chromatography.

2.3.2 Column Chromatography of *A. marlothii* Leaf Exudate

The *Aloe* leaf exudate was freeze-dried and then fractionated by column chromatography employing a solvent system containing ethyl acetate, methanol and water in a 77:13:10 ratio[16]. This tried and tested eluent system gives optimal separation of leaf components. Thus, this chromatography technique was utilized on the acquired *A. marlothii* leaf exudate sample, resulting in good separation of the sample components. The order of elution of the compounds was: homonataloin (**2.4**) (R_f = 0.75), aloeresin A (**2.2**) (R_f = 0.65), aloin (**2.1**) (R_f = 0.58) and then aloesin (**2.3**) (R_f = 0.38). However, one major problem with this system was that water was present in each fraction. The only procedure to remove water other than freeze-drying is by the addition of toluene. Toluene forms a stable azeotrope with water, thus allowing for easier removal. High temperatures (boiling point of toluene is 110 ^{o}C) are required for the solvent removal, which risks the degradation of the isolated products. Thus it was necessary that a more volatile solvent system be developed. This was achieved by replacement of the water with another polar solvent, acetonitrile, which has a boiling point of 81 ^{o}C. It was discovered that a 75:10:2 ratio of ethyl acetate (EtOAc), methanol (MeOH) and acetonitrile (CH_3CN) afforded a degree of separation highly comparable to that of the mixture containing water.

2.3.3 Structural Confirmation of Aloin A (2.21)

The ^{1}H NMR spectrum (Plate 1a) had peaks characteristic of an aromatic compound with an attached sugar. The aromatic region has five protons, i.e., H-7 (δ_H 6.68, *d*, *J* = 8.6 Hz), H-2 (δ_H 6.78, *d*, *J* = 1.5 Hz), H-5 (δ_H 6.94, *d*, *J* = 1.5 Hz), H-4 (δ_H 7.04, *d*, *J* = 8.6 Hz), H-6(δ_H 7.47 (1H, *t*, *J* = 7.9), which are expected for aloin (**2.1**). The splitting pattern of the proton attached to C-10 (δ_H 4.69, *d*, *J* = 2.4 Hz) confirmed a *C*-glucosidic linkage. The signals for the sugar protons H-5' (δ_H 2.84, *m*), H-4' (δ_H 2.85, *t*, *J* = 9.2 Hz), H-2' (δ_H 2.96, *t*, *J* = 9.2 Hz), H-3' (δ_H 3.28, *t*, *J* = 9.2 Hz), H-6'b (δ_H 3.33, *m*), H-1' (δ_H 3.33, *t*, *J* = 9.2 Hz) and H-6'a (δ_H 3.44, *m*) are well resolved and allow for unambiguous assignment. The methylene proton H-11 (δ_H 4.56, *d*) shift corresponds to that of a benzylic primary alcohol. The phenolic hydroxy protons 8-OH (δ_H 11.35, br *s*, D_2O exchangeable) and 1-OH (δ_H 11.68, br *s*, D_2O exchangeable) of aloin (**2.1**) can also be clearly seen.

The ^{13}C NMR spectrum (Plate 1b) displayed a total of 21 carbon atoms. Two CH_2 carbons, eleven CH carbons and nine non-protonated carbons were identified. In the ^{13}C NMR spectrum, six signals (δ_C 63.3, 71.8, 72.0, 80.0, 81.6, 86.6) were characteristic of a *C*-glucose moiety, five aromatic signals (δ_C 114.4, 116.8, 119.1, 120.0, 137.0,), four signals (δ_C 117.7, 118.7, 143.2, 146.6) and a signal depicting a benzylic methylene group (δ_C 64.5). Two signals characteristic of phenolic carbons (δ_C 162.9, 163.4) and one of a ketone (δ_C 195.5) are also observed.

The DEPT 135 spectrum (Plate 1c) corresponded to the ^{13}C spectrum, confirming the identity of the two CH_2 groups as well as that of the nine CH carbons. The HSQC experiment (Plate 1e) allowed for the correlation of all protonated carbon atoms with well-resolved protons. An HMBC experiment (Plate 1f) showed connections of C-8a with H-7 and H-5, of C-1a with 2-H and 4-H, and of C-3 with 11-H_2.

It was interesting to note that only aloin A (**2.21**) was isolated from the leaf exudate, and not a mixture of both the aloin A (**2.21**) and aloin B (**2.22**) diastereomers as expected. The acquired NMR data corresponds with the ^{1}H and ^{13}C NMR assignments of aloin A (**2.21**) found in the literature[17].

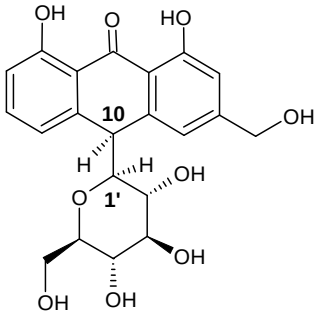

(2.21)

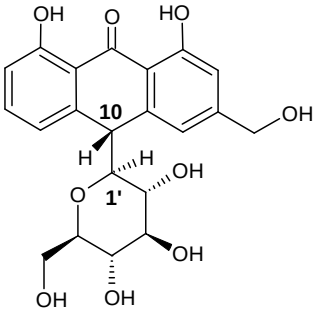

(2.22)

2.3.4 Structural Elucidation of Homonataloin (2.4)

The ^{1}H NMR spectrum (Plate 4a) of homonataloin (**2.4**) displays a mixture of two compounds, i.e. homonataloin A (**2.23**) and homonataloin B (**2.24**) in a 4:1 ratio. The aromatic region depicts four protons for each diastereomer. For homonataloin A (**2.23**) these are singlets for protons H-2, H-4 (δ_H 6.62 and 6.76) and doublets for protons H-5 and H-6 (δ_H 7.08 and 7.13). Similarly for homonataloin B (**2.24**) H-2 and H-4 (δ_H 6.65 and 6.84) are singlets and H-5 and H-6 (δ_H 7.12 and 7.09) are doublets. The sugar protons resonate in a region (δ_H 2.6-4.5) similar to those of the sugar in the ^{1}H NMR spectrum aloin A (Plate 1a), both being *C*-glucosides. The 11-methyl group (δ_H 2.29) and methoxy group (δ_H 3.74) clearly differentiate the ^{1}H NMR spectrum of homonataloin (**2.23**) from that of aloin A (**2.21**) (Plate 1a). The shift of the 1-hydroxy proton (δ_H 12.1) is similar to that of aloin A (**2.21**) (Plate 1a), whilst the hydroxy at H-7 (δ_H 9.55) is not observed in the spectrum.

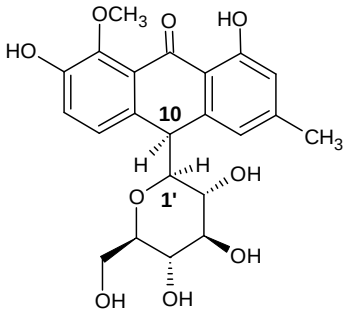

(2.23)

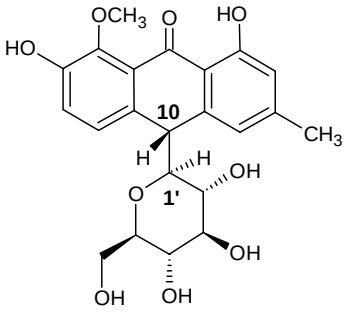

(2.24)

The ^{13}C NMR spectrum (Plate 4b) displayed a total of 16 carbons for each homonataloin diastereomer, one more than that of aloin A (Plate 1a). One CH_2 carbon, one CH_3 carbon,

ten CH carbons and nine non-protonated carbons were identified. In the ^{13}C NMR spectrum, six signals (δ_C 60.0-85.0) were characteristic of a *C*-glucose moiety, four aromatic signals (δ_C 115.6, 119.2, 121.9, 123.8) four quaternary signals (δ_C 118.0, 127.4, 136.2, 140.8) and a signal depicting a benzylic methyl group (δ_C 21.9). Three signals characteristic of phenolic carbons (δ_C 145.2, 147.5, 160.4) and one of a ketone (δ_C 190.1) were also observed.

The DEPT 135 spectrum (Plate 1c) corresponded to the ^{13}C NMR spectrum, confirming the identity of the single CH_2 and CH_3 groups as well as that of the ten CH carbons. The methoxy group is also observed. A HSQC experiment (Plate 4e) allowed for the correlation of all protonated carbon atoms with well-resolved protons.

The ^{13}C NMR shifts of the sugar carbon atoms C-3', C-5' and C-1' were observed at δ_C 78.4, 80.4 and δ_C 84.2 respectively. The assignments of these ^{13}C NMR signals were not in accordance with the assignments reported J. M. Conner *et al*[18], which were deemed incorrect.

2.3.5 Selective Calcium Precipitation of Aloin (2.1)

Column chromatography is an effective yet a long and tedious technique for the isolation of aloin (**2.1**). It was mentioned in an article by Hay and Haynes[19] that aloin (**2.1**) could be precipitated from the leaf exudate by the addition of excess calcium salt and ammonium hydroxide. It was proposed that aloin (**2.1**) formed a calcium salt which precipitated out of solution. This aloin-calcium salt could then be filtered and re-protonated in acid. This method of aloin (**2.1**) precipitation seemed interesting and was thus investigated. The *A. marlothii* leaf exudate was dissolved in hot water, followed by the addition of excess calcium chloride and ammonia. Ammonia is a weak base (pK_b = 4.7) and thus deprotonates the aloin phenolic groups (pK_a = 10.0) in a reversible manner. However, the reverse reaction is slightly more favourable with ammonium (pK_a = 9.4) donating a proton to the deprotonated phenol (s) (pK_b = 4.0). The deprotonated phenol at either C-1/C-8 combined with the neighbouring ketone functionality at position C-9, provide an ideal ligand for metal chelation (Scheme 2.1). Thus, even though the equilibrium between the ammonia and aloin phenols favours the formation of ammonia (and not the ammonium salt), the small percentage of the phenols which are deprotonated react with the free Ca^{2+} in

solution and form the aloin calcium salt. This insoluble aloin calcium salt precipitates out of solution, thus shifting the reaction equilibrium towards the formation of the salt.

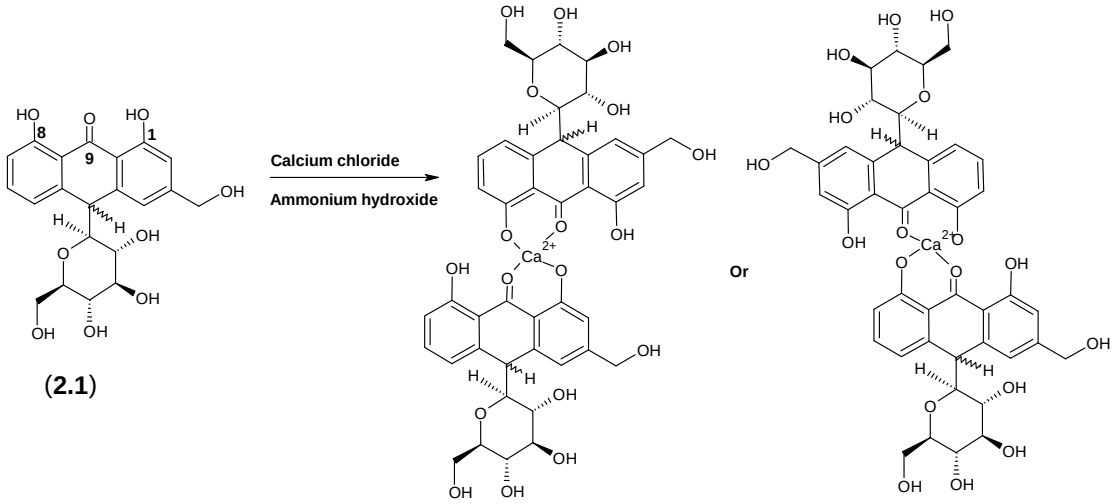

(**2.1**)

Scheme 2.1[19]

Aloin (**2.1**) can be regenerated by the addition of strong acid to this salt, which displaces the chelated calcium ion and re-protonates the phenolic hydroxy. This aqueous solution can then be washed with ethyl acetate, which should extract the aloin (**2.1**) which can be isolated upon removal of the solvent. It should also be noted that aloin (**2.1**) is roughly 2.3 times more soluble in water than in ethyl acetate (due to the polar sugar moiety), thus multiple extractions are required for removal of the aloin (**2.1**). The aloin (**2.1**) obtained from this procedure is of relatively high purity (~ 90%).

2.4 Synthesis of Aloin Derivatives

The first aim of this project was to develop an effective procedure for the isolation of aloin (**2.1**) from the *A. marlothii* leaf exudate. Since a method yielding large amounts of aloin (**2.1**) was found, the next step was to transform the anthrone into the desired synthetic anthraquinone derivatives. The choice of derivatives to be made was based upon (i) known biologically active compounds (e.g. aloe-emodin) and (ii) interesting biologically active functional groups (e.g. amines). The planned synthetic pathway is shown below (Scheme 2.2).

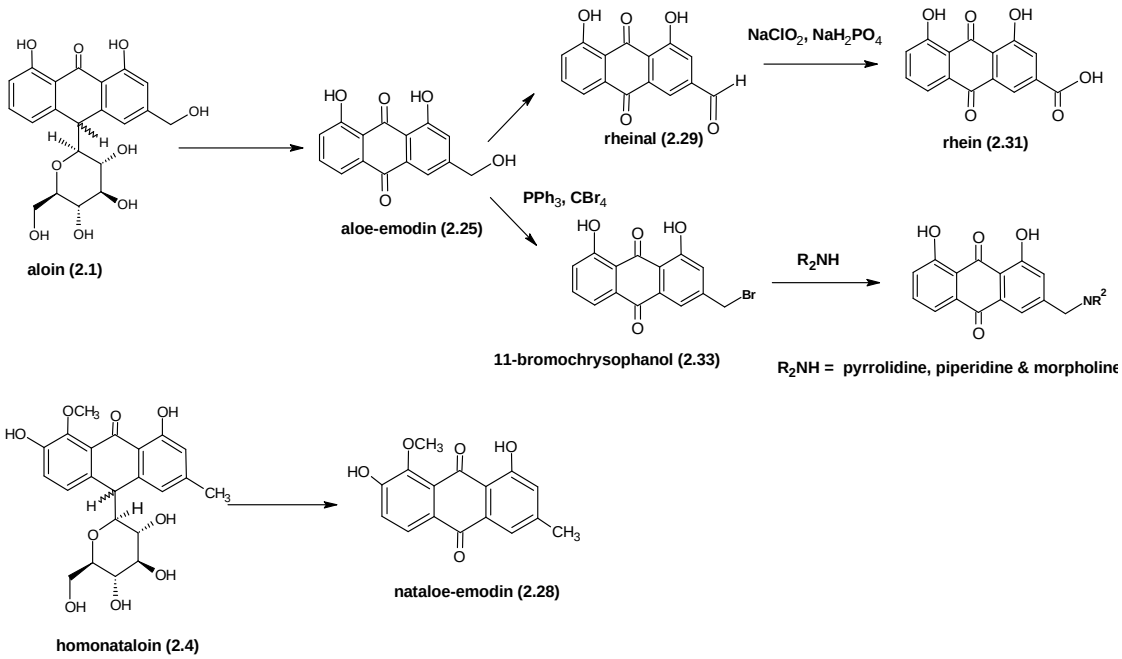

Scheme 2.2

2.4.1 Oxidation of Aloin (2.1) to Aloe-emodin (2.25)

The oxidation of aloin (**2.1**) to aloe-emodin (**2.25**) is a naturally occurring event. If aloin (**2.1**) is present in an oxidative medium, it is possible that the *C*-glucoside sugar is cleaved and the C-10 position to which it was attached is oxidized to a ketone. This is the postulated origin of aloe-emodin (**2.25**) in *Aloe* plants, as an aloin (**2.1**) breakdown product[20]. Thus it should be possible to obtain aloe-emodin (**2.25**) by simply leaving aloin (**2.1**) in an oxidative medium. This is however an unreliable, time-consuming and inefficient method to obtain aloe-emodin (**2.25**) (Scheme 2.3).

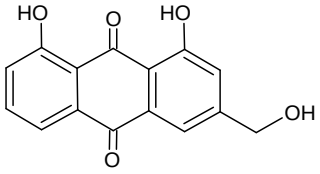

(**2.25**)

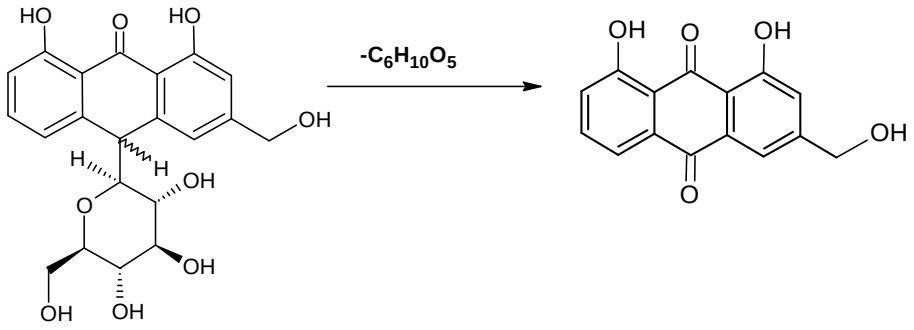

(2.1) **(2.25)**

Scheme 2.3

There are a number of published methods to oxidize aloin (**2.1**) to aloe-emodin (**2.25**), the most prominent being the $FeCl_3$-mediated process (Scheme 2.4). This reaction is low yielding (yields < 60% reported) and very inefficient as it requires a 5:1 ratio of $FeCl_3$ to aloin (**2.1**)[19]. In our hands, this reaction afforded yields of 50% and was found to be extremely messy; thus other oxidation methods for the oxidation of aloin (**2.1**) to aloe-emodin (**2.25**) were to be tested.

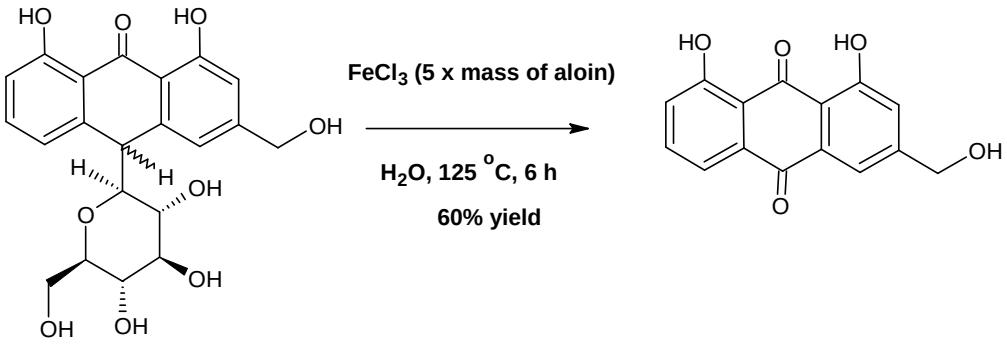

(2.1) **(2.25)**

Scheme 2.4

In this investigation, a novel procedure to efficiently oxidize aloin (**2.1**) to aloe-emodin (**2.25**) was found. A Co(II) catalyst (**2.26**) was found to do the necessary conversion in good yields, higher than those obtained in the $FeCl_3$ process (Scheme 2.5).

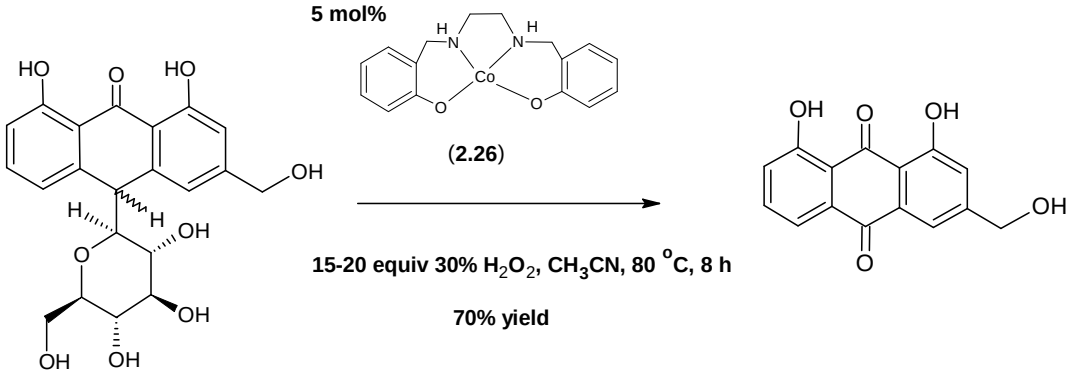

(2.1) **(2.25)**

Scheme 2.5

The Co(II) catalyst (**2.26**) was synthesized according to the published procedure[21]. The catalyst requires a source of oxygen (H_2O_2 in this case). A proposed mechanism of this oxidation is shown in Scheme 2.6. The Co(II) catalyst (**2.26**), in aqueous solution, forms a mononuclear superoxo species (**A**). Dioxygen then binds to the cobalt atom, and the Co(II) atom is oxidized to Co(III) (**B**)[22]. The substrate, aloin (**2.1**), loses hydrogen at H-10 resulting in the formation of an aloin radical (**C**). The cobalt-bound dioxygen radical and aloin radical (**C**) then each donate an electron to form a bond between them. Homolysis of the oxygen-oxygen bond and the *C*-glucosidic linkage generates aloe-emodin (**2.25**) and a glucose radical (**D**) that can be quenched by the cobalt species. The formation of a ketone at C-10 of the anthraquinone is the driving force in this last step. The extended conjugation allows for increased electron delocalization, thus promoting the stability of the anthraquinone (**2.25**).

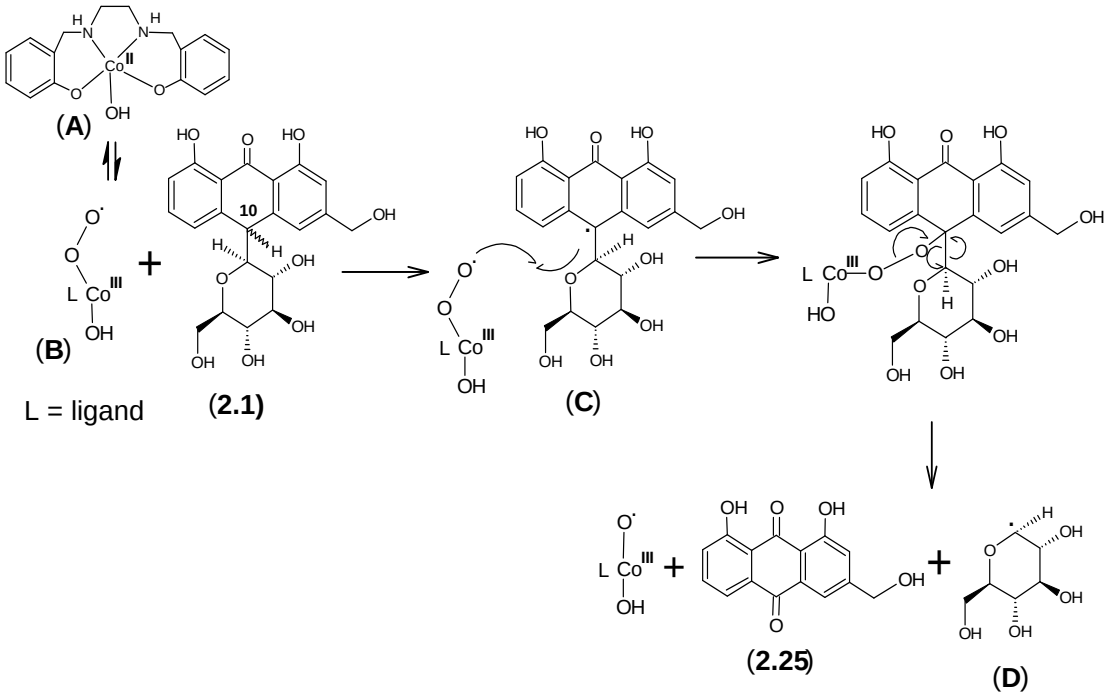

Scheme 2.6

The Cu(II) derivative (**2.27**)[23], which was reported to have the same oxidizing ability as the Co(II) complex (**2.26**), was also synthesized and tested on aloin (**2.1**) (Scheme 2.7).

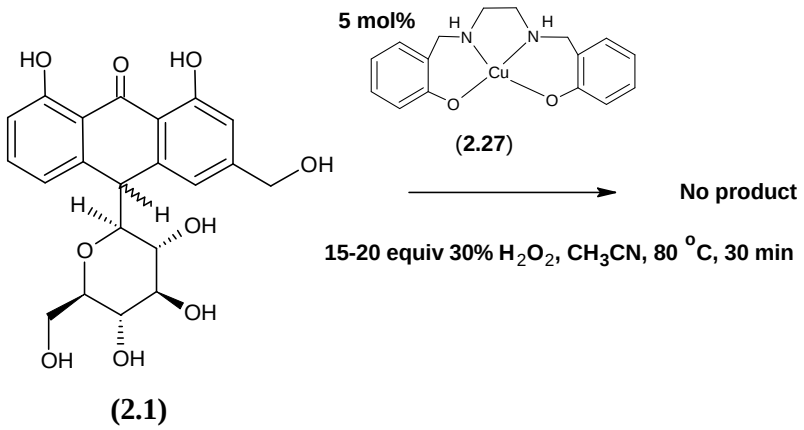

Scheme 2.7

After 30 min, no aloin (**2.1**) or aloe-emodin (**2.25**) could be detected in the reaction mixture by TLC.

2.4.2 Structural Elucidation of Aloe-emodin (2.25)

The ^{1}H NMR spectrum (Plate 5a) of aloe-emodin (**2.25**) had peaks characteristic of an aromatic compound with 10 protons. Similarly to the parent compound aloin (Plate 1a), five proton signals were observed in the aromatic region of the ^{1}H NMR spectrum, i.e., H-2 (δ_H 7.29, *s*), H-7 (δ_H 7.37, *d*, *J* = 8.2 Hz), H-4 (δ_H 7.69, *s*), H-5 (δ_H 7.70, *d*, *J* = 7.4 Hz), H-6 (δ_H 7.78, *t*, *J* = 7.9). The chemical shift of the methylene protons (δ_H 4.64, *s*) corresponds to that of a benzylic primary alcohol. The phenolic hydroxy groups OH-8/ OH-1 (δ_H 11.80, br *s*, D_2O exchangeable) can also be clearly observed downfield.

The ^{13}C NMR spectrum (Plate 5b) displayed a total of 15 carbons. One CH_2 carbon, five CH carbons and nine non-protonated carbons were identified. In the ^{13}C NMR spectrum, five aromatic signals (δ_C 117.1, 119.3, 120.7, 124.4, 137.2), four quaternary carbon peaks (δ_C 114.4, 115.8, 133.1, 133.3) and a signal depicting a benzylic methylene group (δ_C 62.1). Two signals characteristic of phenolic carbons (δ_C 161.3, 161.6) and two of ketones (δ_C 190.9, 191.6) were also observed. All these carbon NMR shifts, besides the new carbonyl carbon signal (δ_C 190.9), correlate with those of aloin (Plate 1b). The difference between the NMR spectra of the two compounds is the absence of the sugar moiety in aloe-emodin (**2.25**).

The DEPT 135 spectrum (Plate 5c) confirmed the presence of a single CH_2 group as well as that of the five aromatic CH carbons. An HSQC experiment (Plate 5e) showed correlations for all the carbon atoms with attached protons. The HMBC experiment (Plate 5f) showed correlations of C-8a with H-7 and H-5, of C-1a with 2-H and 4-H, and of C-3 with 11-H_2.

2.4.3 Oxidation of Homonataloin (2.4) to Nataloe-emodin (2.28)

Homonataloin (**2.4**) was oxidized to nataloe-emodin (**2.28**) (Scheme 2.8) using the same process used for the oxidation of aloin (**2.1**) to aloe-emodin (**2.25**) (Scheme 2.5). Nataloe-emodin (**2.28**) would provide a useful aloe-emodin (**2.25**) structural analogue for testing of biological activity.

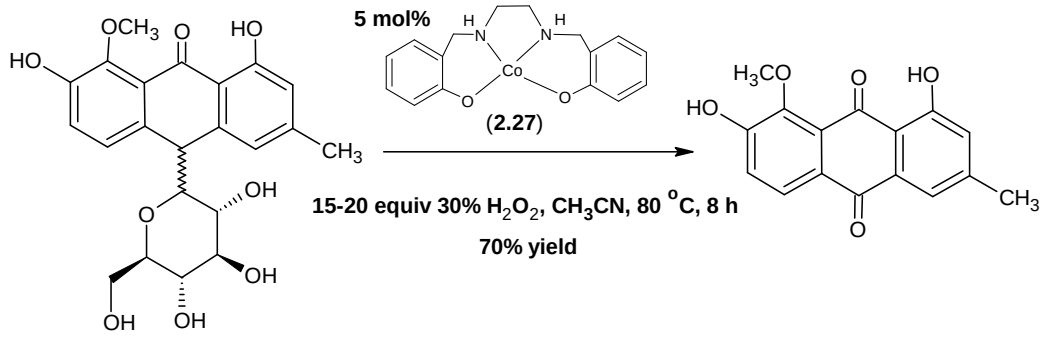

(2.4) **(2.28)**

Scheme 2.8

2.4.4 Structural Elucidation of Nataloe-emodin (2.28)

The ^{1}H NMR spectrum (Plate 6a) of nataloe-emodin (**2.28**) had peaks characteristic of an aromatic compound with 12 protons. Similarly to the parent compound homonataloin (Plate 4a), four proton signals were observed in the aromatic region of the ^{1}H NMR spectrum, i.e., H-2 (δ_H 7.15, *s*, *J* = 1.3 Hz), H-6 (δ_H 7.32, *d*, *J* = 8.2 Hz), H-4 (δ_H 7.47, *d*, *J* = 1.3 Hz), H-5 (δ_H 7.90, *d*, *J* = 8.3 Hz). Signals for the 11-methyl group (δ_H 2.42) and the methoxy group (δ_H 3.84) are also observed. The hydroxy groups 1-OH (δ_H 12.71) and 7-OH (δ_H 10.84) correlate with those of the shifts of homonataloin.

The ^{13}C NMR spectrum (Plate 6b) displayed a total of 16 carbon signals. One CH_3 carbon, one OCH_3 carbon, four CH carbons and ten non-protonated carbons were identified. In the ^{13}C NMR spectrum, there were four aromatic signals (δ_C 119.8, 122.3, 123.9, 125.6) four signals corresponding to quaternary carbon atoms (δ_C 122.4, 126.2, 126.5, 132.9) and a signal indicating a benzylic methyl group (δ_C 21.9). Three signals characteristic of phenolic carbons (δ_C 148.4, 148.6, 163.8) and two of carbonyl carbons (δ_C 188.6, 191.4) are also observed. An HSQC experiment (Plate 6e) allowed for the correlation of all protonated carbon atoms with their attached protons.

2.4.5 Oxidation of Aloe-emodin (2.25) to Rheinal (2.29)

Aloe-emodin (**2.25**) was oxidized to rheinal (**2.29**) using the highly efficient oxidizing agent *o*-idoxybenzoic acid (IBX) (**2.30**) (Scheme 2.9), which was synthesised based on the procedure provided in the literature[24]. This safe, easily accessible reagent is highly

selective in the oxidation of alcohols to their corresponding aldehydes and ketones. This is virtually a quantitative reaction which is achieved at room temperature in THF. IBX (**2.30**) is insoluble in most solvents, with THF being an exception. DMSO is often added to the reaction mixture in tiny amounts to improve the solubility of the IBX (**2.30**) and hence improve the rate and yield of the reaction[25].

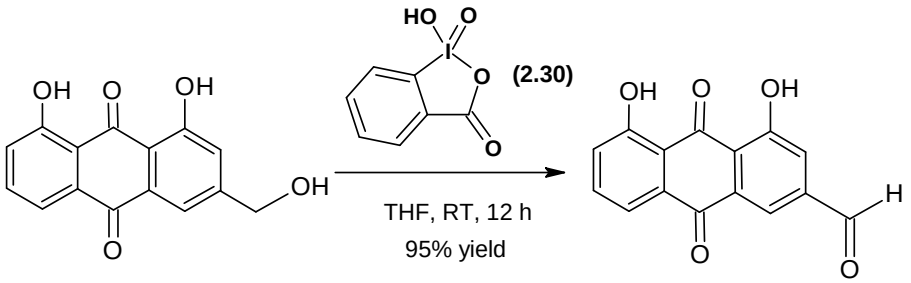

(**2.25**) (**2.29**)

Scheme 2.9

The oxidation of aloe-emodin (**2.25**) to rheinal (**2.29**) is proposed to occur by the mechanism shown in scheme 2.10[**26**].

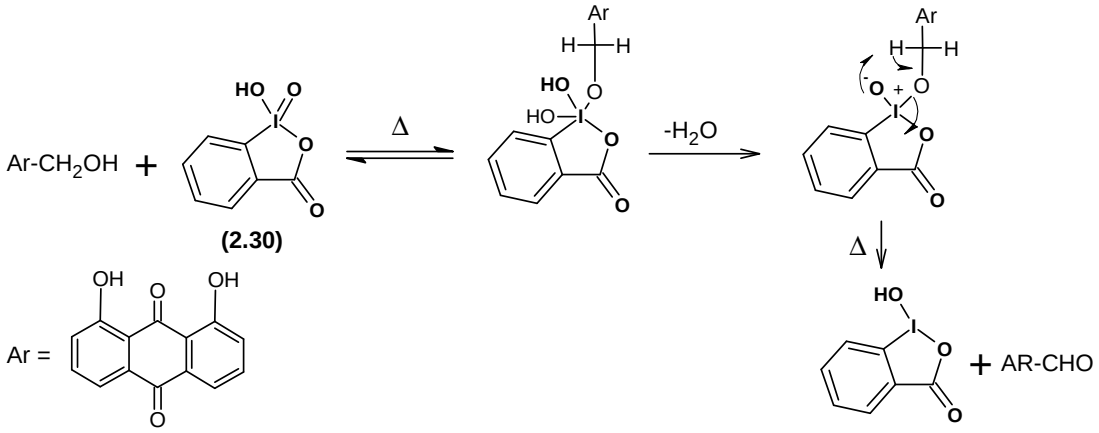

Scheme 2.10

2.4.6 Structural Elucidation of Rheinal (2.29)

The ^{1}H NMR spectrum (Plate 8a) of rheinal (**2.29**) correlates with that of the parent molecule aloe-emodin (Plate 5a). The proton spectrum of rheinal (**2.29**) differs from that

of aloe-emodin (**2.25**) by the absence of the H-11 methylene protons and the appearance of a strong aldehyde peak of H-11 (δ_H 10.12, *s*) downfield.

Similarly to the ^{1}H NMR spectrum, the ^{13}C NMR spectrum (Plate 8b) of rheinal (**2.29**) also correlates with the ^{13}C NMR spectrum of aloe-emodin (Plate 5b), except for a few differences. The C-11 CH_2 peak of aloe-emodin (**2.25**) is absent, and the aldehyde peak of rheinal (**2.29**) C-11 (δ_C 192.8) is observed. The HSQC spectrum (Plate 8d) of rheinal clearly depicts the correlation of the aldehyde proton and the carbon to which it is attached.

2.4.7 Oxidation of Rheinal (2.29) to Rhein (2.31)

Rheinal (**2.29**) was converted to rhein (**2.31**) in a high yield by using sodium chlorite in a hydrogen phosphate buffer as the oxidation reagent. (Scheme 2.11). Similarly to the IBX oxidation, this was done at room temperature. Sodium chlorite is a selective reagent for the oxidation of aldehydes to carboxylic acids, and has been utilized extensively in the carbohydrate field. However, there is a limitation in this reaction, i.e. the formation of the toxic chlorine dioxide gas. This noxious gas may cause unwanted side reactions to occur. This problem can be alleviated by the addition of a chlorine scavenger such as resorcinol[27].

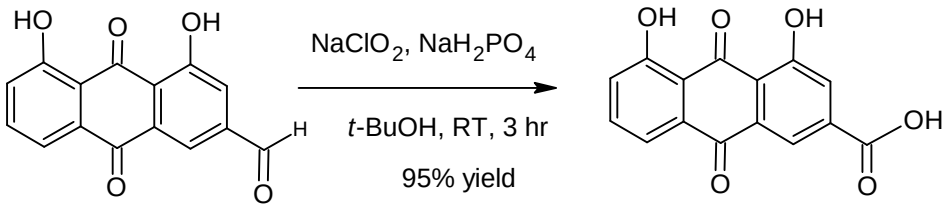

(**2.29**) (**2.31**)

Scheme 2.11

It was initially planned to obtain rhein (**2.31**) directly from aloe-emodin (**2.25**). This transformation would mean that rhein (**2.31**) could be produced by a single step as opposed to two steps. Heavy metal species such as chromic acid and potassium permanganate would very readily perform the necessary oxidations. However, it is extremely difficult to remove all traces of these metals completely, which would be unacceptable for the biological testing of the synthesized products. Several other benzylic oxidations were

tried, all of which proved either ineffective or resulted in a low yield, as described in Sections 2.4.9 to 2.4.11.

2.4.8 Structural Elucidation of Rhein (2.31)

The ^{1}H NMR spectrum (Plate 9a) of rhein (**2.31**) differs from that of rheinal (**2.29**), by the absence of the aldehyde peak of H-11. The ^{13}C NMR spectrum (Plate 9b) of rhein (**2.31**) closely resembles that of rheinal (**2.29**), except for the upfield shift of C-11 (δ_C 181.4).

2.4.9 Nickel Oxide Hydroxide Oxidation of Aloe-emodin (2.25)

When nickel(II) chloride/nickel(II) acetate is exposed to commercial bleach (~5% aqueous NaOCl), an insoluble nickel species is formed, named nickel oxide hydroxide. This compound is a heterogeneous catalyst, used at a 2.5 mol % that is particularly useful in the oxidation of organic compounds. Many different oxidations are possible: the oxidation of primary alcohols to carboxylic acids; secondary alcohols to ketones and aldehydes to carboxylic acids[28]. This promising, cost-efficient catalyst was to be tested on the oxidation of aloe-emodin (**2.25**) to rhein (**2.31**) (Scheme 2.12).

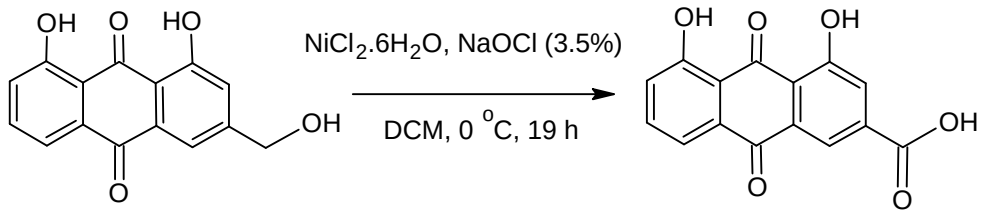

(2.25) **(2.31)**

Scheme 2.12

Analysis of the reaction mixture showed no trace of either starting material or the desired product. The fate of this reaction was most probably the decomposition of the anthraquinone molecule. The identical reaction was successfully tested on a model system, i.e., the oxidation of benzyl alcohol to benzoic acid which resulted in excellent yields (>95%). This oxidation method was repeated several times on aloe-emodin (**2.25**), varying the experimental conditions. This method was unsuccessful and thus was abandoned.

2.4.10 Oxidation of Aloe-emodin (2.25) with TEMPO (2.32)/NaOCl/$NaClO_2$

An interesting procedure to oxidize alcohols to their corresponding carboxylic acids is utilizing the combination of NaOCl, $NaClO_2$ and TEMPO (2,2,6,6-tetramethylpiperidine-1-oxyl) (**2.32**). TEMPO (**2.32**) is a radical at room temperature. The proposed mechanism for this oxidation is shown in Scheme 2.13.

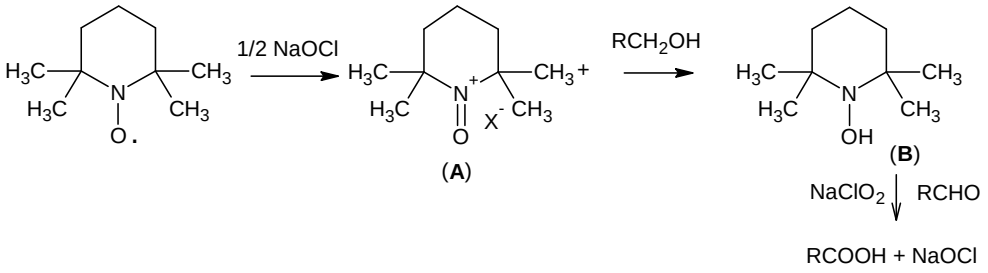

(2.32)

Scheme 2.13

TEMPO (**2.32**) is catalytically converted to the *N*-oxoammonium cation (**A**) by NaOCl. This *N*-oxoammonium cation (**A**), being the active form of TEMPO (**2.32**), rapidly oxidizes the primary alcohol to its corresponding aldehyde, itself being converted to the hydroxylamine (**B**). The aldehyde is then oxidized to its carboxylic acid derivative, generating a NaOCl molecule in the process which facilitates the initial oxidation[29]. All three of these reagents are readily available at low cost, which is an added benefit.

This oxidation method was tried on aloe-emodin (**2.25**) (Scheme 2.14), which proved unsuccessful. Even after sufficiently increased reaction times and ratios of reagents, all that was present was the starting material. It was postulated the TEMPO (**2.32**)/NaOCl/$NaClO_2$ combination was too mild to oxidize the benzylic alcohol next to an electron-rich anthraquinone system.

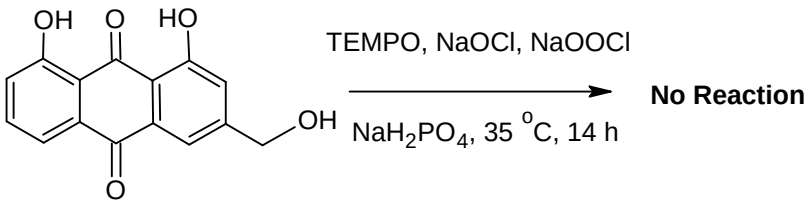

(**2.25**)

Scheme 2.14

2.4.11 Ruthenium Tetroxide Oxidation of Aloe-emodin (2.25)

Ruthenium tetroxide (RuO_4) is a powerful oxidation reagent used in organic synthesis. It is a strong oxidant for many functional groups and is capable of cleaving double bonds. RuO_4 is prepared by oxidation of either ruthenium(III) chloride or ruthenium dioxide with aqueous periodate or hypochlorite and then extracted into carbon tetrachloride. Despite being an excellent oxidizing agent, there are many drawbacks to this reagent: It is expensive, corrosive, requires CCl_4 as a co-solvent and is difficult to separate from the reaction products[30]. The oxidation of RuO_4 on aloe-emodin (**2.25**) was carried out according to the standard published protocol[31] (Scheme 2.15).

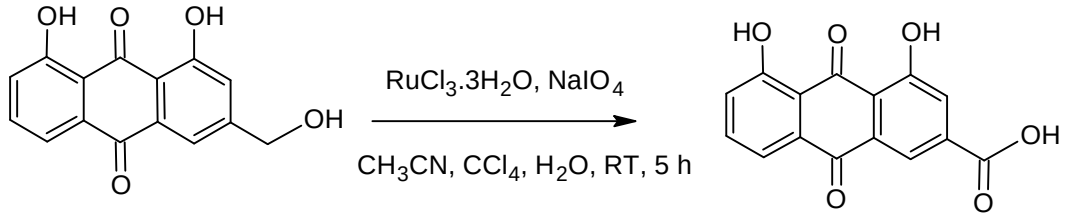

(**2.25**) (**2.31**)

Scheme 2.15

After 5 h of reaction time, the reaction was worked up and the products were isolated by chromatography. The compounds isolated were rheinal (**2.29**) (10%), aloe-emodin (**2.25**) (80%) and rhein (**2.31**) (5%). It was concluded that this reagent was not efficient enough for the oxidation of aloe-emodin (**2.25**) to rhein (**2.31**).

2.4.12 Bromination of Aloe-emodin (2.25) to 11-Bromochrysophanol (2.33)

The conversion of aloe-emodin (**2.25**) to 11-bromochrysophanol (**2.33**) was a necessary transformation to allow for a subsequent amination reaction, as bromine is a far better leaving group than oxygen. This reaction has been published using HBr as the brominating medium[32]. This is a high yielding process (89%) but milder methods were tested in order to eliminate the use of the strong acid HBr.

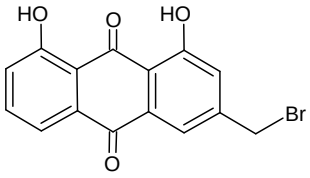

(**2.33**)

2.4.13 Bromination of Aloe-emodin (2.25) Using CuBr/CBr_4/Cu/Fe

This interesting brominating technique centres around a Cu/Fe redox system. Copper is the sacrificial anode, and iron is the cathode. This reaction does not require the supply of electricity and occurs in a purely chemical mode. The addition of 1,10-phenanthroline was reported to increase the efficiency of the reaction[33]. The bromination of aloe-emodin (**2.25**) was tested using this system (Scheme 2.16), but all that was found was starting material. It was unclear why this reaction failed.

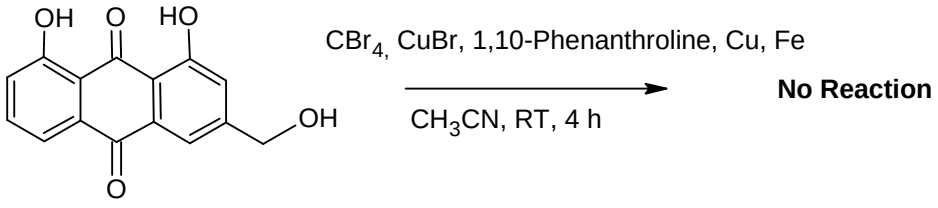

(2.25)

Scheme 2.16

2.4.14 Bromination of Aloe-emodin (2.25) to 11-Bromochrysophanol (2.33) Using CBr_4/PPh_3

The second brominating system that was tested on aloe-emodin (**2.25**) was a combination of CBr_4 and PPh_3 in THF (Scheme 2.17).

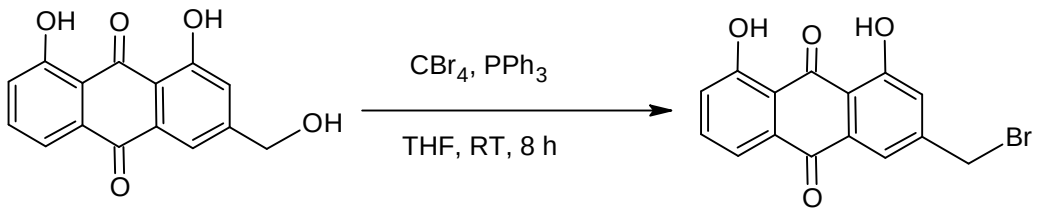

(2.25) **(2.33)**

Scheme 2.17

Initially a ratio of CBr_4/PPh_3 (1:1) to aloe-emodin (**2.25**) in toluene was tested and resulted in low yields (<50%). Thereafter an increased ratio of CBr_4/PPh_3 (4:4) to aloe-emodin (**2.25**) in THF was tested and resulted in greatly improved yields (>90%). This method was based on a benzylic bromination reported in the literature[34].

2.4.15 Structural Elucidation of 11-Bromochrysophanol (2.33)

The ^1H NMR spectrum (Plate 10a) of 11-bromochrysophanol (**2.33**) correlates closely with that of the parent molecule aloe-emodin (**2.25**). The proton spectrum of 11-bromochrysophanol (**2.33**) differs from that of aloe-emodin (**2.25**) in the downfield shift of the benzylic proton signal from δ_H 4.64, in aloe-emodin (**2.25**), to δ_H 4.81, in 11-bromochrysophanol (**2.33**). This shift of the methylene proton signal reflects the chemical transformation of the hydroxy group to a bromide.

The ^{13}C NMR spectrum (Plate 10b) of 11-bromochrysophanol (**2.33**) is similar to that of aloe-emodin (**2.25**). The carbon signal at δ_C 25.1 is due to C-11 attached to a bromine atom. The signal at δ_C 62.0 corresponds to that of a benzylic CH_2 attached to a hydroxy group (C-11), exactly like that of aloe-emodin (**2.25**). The solvent that was used for the NMR spectroscopy was deuterated DMSO, which has trace amounts of water. DMSO, being an extremely hygroscopic compound, absorbs water from the atmosphere once it is

exposed to it. It was postulated that the 11-bromochrysophanol (**2.33**) was transformed back to aloe-emodin (**2.25**) whilst undergoing the ^{13}C NMR experiment by reacting with the water present in the deuterated DMSO. The absence of signals for aloe-emodin (**2.25**) in the proton spectrum confirmed this.

2.4.16 Substitution Reaction of 11-Bromochrysophanol (2.33)

The conversion of 11-bromochrysophanol (**2.33**) to amine derivatives has been reported in the literature. Fifteen aloe-emodin amine derivatives have been synthesized by Koyama *et al*. in an attempt to produce novel potential anticancer agents[15]. More recently, Cui *et al*. completed a similar study on these aloe emodin amine derivatives[35]. The published protocol for producing these amines involves stirring 11-bromochrysophanol (**2.33**) in dry DMF in the presence of an excess of the desired amine in excess for three days. Low yields (<60%) were reported for this slow reaction. Three amine derivatives of aloe-emodin (**2.25**), i.e. 11-(pyrrolidin-1-yl)chrysophanol (**2.34**), 11-(piperidin-1-yl)chrysophanol (**2.35**) and 11-(morpholin-1-yl)chrysophanol (**2.36**) were required for this research project. Of these three aloe-emodin (**2.25**) derivatives, only the 11-(morpholin-1-yl)chrysophanol (**2.36**) is novel. It was postulated that the amination reaction would occur at a much faster rate if the amine was deprotonated. A strong base such as BuLi was required to facilitate this process.

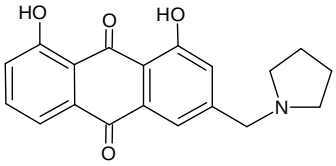

(2.34)

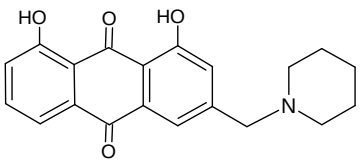

(2.35)

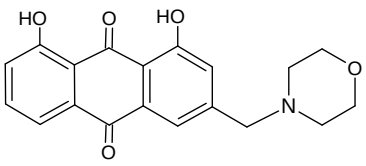

(2.36)

2.4.17 Amination Reaction of 11-Bromochrysophanol (2.33)

BuLi (**2.37**) was carefully added to freshly distilled morpholine (**2.38**) in dry THF. The deprotonated morpholine (**2.39**) was added to 11-bromochrysophanol (**2.33**) and stirred for 12 h at RT. 11-(Morpholin-1-yl)chrysophanol (**2.36**) was formed (Scheme 2.18).

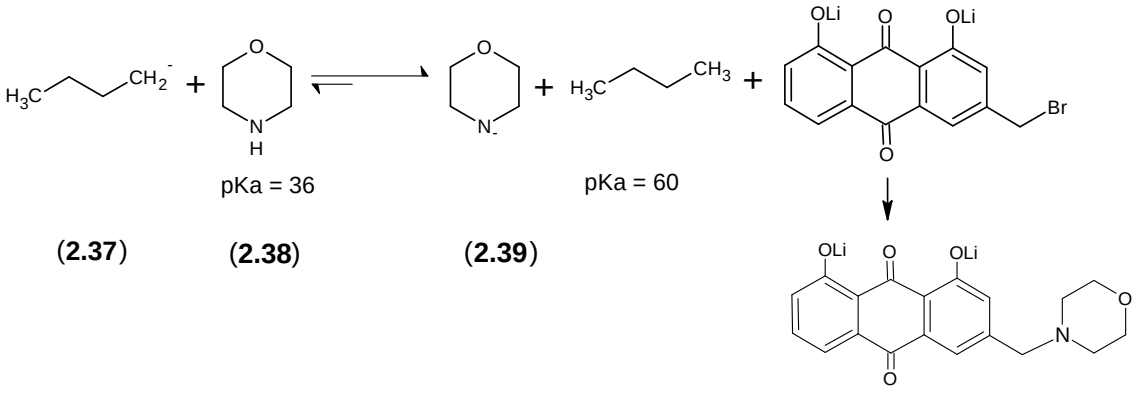

(**2.37**) (**2.38**) (**2.39**) (**2.36**)

Scheme 2.18

The work up of the reaction (Scheme 2.19) starts off with the addition of hydrochloric acid to reprotonate the two phenolic groups at positions C-1 and C-8. These phenolic protons (pK_a = 10.0) were removed by the excess deprotonated amine anions. The reaction mixture was then neutralised with $NaHCO_3$. This was done to neutralise the ammonium cation formed. The reaction mixture was chromatographed to afford the 11-(morpholin-1-yl)chrysophanol (**2.36**) product in high yields (>90%).

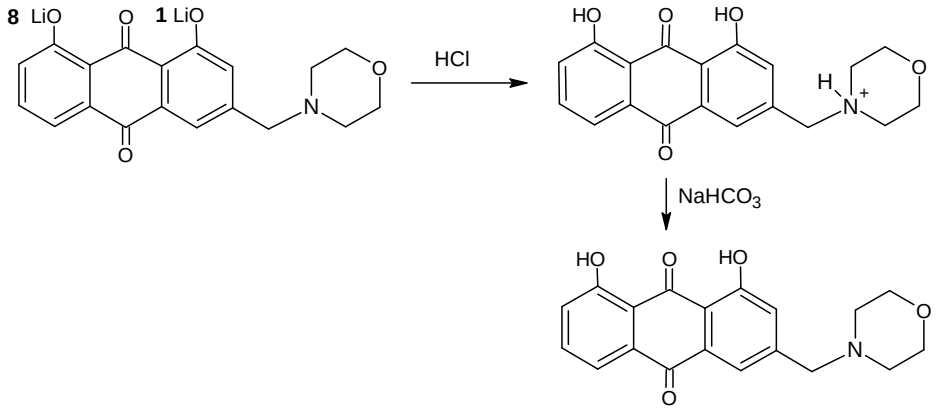

(**2.36**)

Scheme 2.19

The synthesis of 11-(morpholin-1-yl)chrysophanol (**2.36**), the 11-(piperidin-1-yl)chrysophanol (**2.35**) and 11-(pyrrolidin-1-yl)chrysophanol (**2.34**) derivatives was effected similarily.

2.4.18 Structural Elucidation of 11-(Pyrrolidin-1-yl)chrysophanol (2.34)

The proton spectrum of 11-(pyrrolidin-1-yl)chrysophanol (**2.34**) differs from that of aloe-emodin (**2.25**). Firstly, there is a considerable upfield shift of the signal for the 11-methylene protons from δ_H 4.64, in aloe-emodin (**2.25**), to δ_H 3.75, in 11-(pyrrolidin-1-yl)chrysophanol (**2.34**). This change in chemical shift reflects the substitution of the bromine atom by a nitrogen atom, *i.e.* the pyrrolidine group. The pyrrolidine-nitrogen atom, which has three covalent bonds, is less electronegative then the bromine atom and thus the methylene protons experience an upfield shift. The pyrrolidine CH_2 atoms H-2' (δ_H 1.74, *m*) and H-1' (δ_H 2.42, *m*) are also present in the spectrum, integrating to eight protons in total.

The ^{13}C NMR (Plate 11b) of 11-(pyrrolidin-1-yl)chrysophanol (**2.34**) is similar to that of aloe-emodin (**2.25**). The carbon signal at δ_C 59.1 is that of C-11 attached to the nitrogen-atom of the pyrrolidine. The shifts of the pyrrolidine carbon atoms are also observed, C-2' (δ_C 25.7) and C-1' (δ_C 54.0). The HMBC spectrum (Plate 11f) shows connections of C-11 with H-1'and *vice versa*.

2.4.19 Structural Elucidation of 1-(Piperidin-1-yl)chrysophanol (2.35)

The ^1H NMR spectrum (Plate 12a) of 1-(piperidin-1-yl)chrysophanol (**2.35**) resembles that of 11-(pyrrolidin-1-yl)chrysophanol (**2.35**), being a structurally similar compound. There are the amine, *i.e.* piperidine in this case, protons H-3' (δ_H 1.43, *m*), H-2' (δ_H 1.58, *m*) and H-1' (δ_H 2.41, *m*) present. There is also an upfield shift of the H-11 methylene protons to δ_H 3.55.

The ^{13}C NMR spectrum (Plate 12b) of 11-(piperidin-1-yl)chrysophanol (**2.35**) is similar to that of aloe-emodin (**2.25**). The carbon shift at 63.1 is that of C-11 attached to the nitrogen-atom of the piperidine. The signals for the piperidine carbon atoms are also observed, C-3' (δ_C 25.9), C-2' (δ_H 25.9) and C-1' (δ_H 54.7). The HMBC spectrum (Plate 12f) shows connections of C-11 with H-1'and *vice versa*.

2.4.20 Structural Elucidation of 11-(Morpholin-1-yl)chrysophanol (2.36)

The ^{1}H NMR spectrum (Plate 13a) of 11-(morpholin-1-yl)chrysophanol (**2.36**) correlates with that of aloe-emodin (**2.25**). There is an upfield shift of the H-11 methylene protons from δ_H 4.64, in aloe-emodin (**2.35**), to δ_H 3.60, in 11-(morpholin-1-yl)chrysophanol (**2.36**). The morpholine proton atoms H-1' (δ_H 2.40, *m*) and H-2' (δ_H 3.61, *m*), are also observed.

The ^{13}C NMR spectrum (Plate 13b) of 11-(morpholin-1-yl)chrysophanol (**2.36**) is highly similar to that of aloe-emodin (**2.25**). The carbon shift at δ_C 62.0 is that of C-11 attached to the nitrogen-atom of the morpholine. The shifts of the morpholine carbon atoms are also observed, C-1' (δ_C 53.6) and C-2' (δ_H 66.7). The HMBC spectrum (Plate 13f) shows connections of C-11 with H-1'and *vice versa*.

2.5 Conclusion

A method to isolate aloin (**2.1**) from the *A. marlothii* leaf exudate was developed using a selective calcium precipitation. Aloin (**2.1**) was successfully transformed into several derivatives, which were all purified using column chromatography. The structures of these derivatives were verified using NMR spectroscopy.

2.6 Experimental

All the required chemicals or reagents were obtained from FLUKA, SIGMA-ALDRICH or MERCK and were used without further purification. All reactions requiring anhydrous solvents were performed under a nitrogen atmosphere.

Nuclear magnetic resonance spectroscopy (NMR) of the isolated compounds was performed on either a Bruker 400 MHz or 500 MHz spectrophotometer. All NMR spectra were recorded at 25 ^{o}C and the chemical shifts were recorded in ppm referenced to the tetramethylsilane as zero. Coupling constants are calculated as observed in the ^{1}H NMR spectra. Deuterated methanol (MeOH-d_4) or DMSO-d_6 were used as solvents for polar compounds and deuterated chloroform ($CDCl_3$) was used for non-polar compounds. Mass spectra were obtained with a Waters-LCT-Premier mass-spectrometer.

Thin-layer chromatography (TLC) of the compounds was performed with glass backed silica plates (Merck 0.20 mm). The TLC-plates were viewed under UV light (λ 254 and 366 nm) and subjected to iodine or anisaldehyde spray reagent (6 g anisaldehyde in 250 ml ethanol containing 2.5 ml concentrated sulfuric acid). Once the plates were sprayed they were heated in an oven to allow for the colour development.

Normal and flash chromatography were performed with silica gel 60 (Merck 0.040-0.063 m) and on columns with diameters of 2 cm, 4 cm or 6 cm. The extracts or mixed fractions were absorbed onto silica and were then packed onto columns. Both isocratic and gradient eluent systems were employed.

2.6.1 Column Chromatography of *A. marlothii* Leaf Exudate

Homonataloin (2.4)

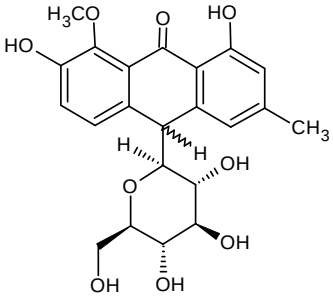

$C_{22}H_{24}O_9$

FW 432.4 g/mol

Aloin (2.1)

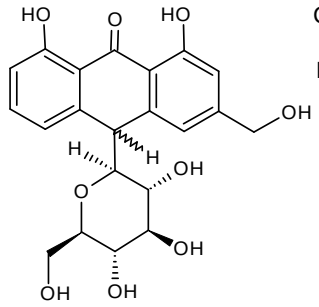

$C_{21}H_{22}O_9$

FW 418.4 g/mol

Aloesin (2.3)

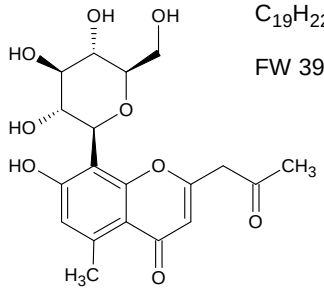

$C_{19}H_{22}O_9$

FW 394.4 g/mol

Aloeresin A (2.2)

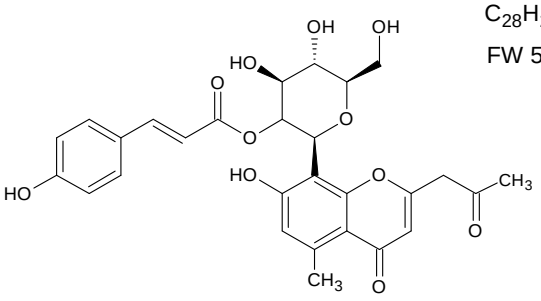

$C_{28}H_{28}011$

FW 540.5 g/mol

A. marlothii leaf exudate was sourced from Ladysmith and was obtained as follows: Leaves were harvested with sickles and carefully stacked in a circle with the cut surfaces facing inwards. A plastic sheet was placed in the middle to collect the leaf exudates. Freeze-dried *A. marlothii* leaf exudate (5.0 g) was chromatographed on silica gel, eluting

with an EtOAc-MeOH-CH_3CN [75:10:2 (v/v)] running phase. Column fractions were monitored by silica gel TLC (solvent, EtOAc-MeOH-CH_3CN, 75:10:2 v/v), and four major compounds were observed. The fractions containing each compound were collected, combined and the solvent was removed using a rotary evaporator followed by high vacuum. The four compounds were then subjected to NMR analysis. The structure of the compounds (based on the column elution order) were elucidated to be homonataloin (**2.4**) (400 mg, R_f = 0.75, 8%), aloeresin A (**2.2**) (1600 mg, R_f = 0.65, 32%), aloin (**2.1**) (1100 mg, R_f = 0.58, 22%) and aloesin (**2.3**) (1800 mg, R_f = 0.38, 36%) respectively.

Homonataloin (2.4): Yellow amorphous solid comprising an unresolved mixture of homonataloin A and homonataloin B; UV (MeOH) λ_{Max} (log ε): 213 (8.62), 295 (4.79), 352 (1.51) nm; IR (KBr) ν_{max}:. 3385, 2923, 1702, 1633, 1607, 1483, 1433, 1359, 1270, 1216, 1169 cm^{-1}.

NMR analysis revealed signals for both isomers.

Homonataloin A. ^{1}H NMR (DMSO-d_6, 400 MHz): δ_H 2.29 (3H, *s*, H-11), 2.75-2.81 (2H, *m*, H-2', H-4'), 3.11-3.16 (3H, *m*, H-1', H-6'b, H-5'), 3.31 (1H, *d*, H-6'a), 3.74 (3H, *s*, H-12), 4.38 (2H, *s*, H-10), 6.62 (1H, *s*, H-2), 6.76 (1H, *s*, H-4), 7.08 (1H, *s*, H-5), 7.13 (1H, *s*, H-6), 9.55 (1H, br *s*, D_2O exchangeable, OH-7), 12.10 (1H, br *s*, D_2O exchangeable, OH-1)(A)^{13}C NMR (DMSO-d_6, 400 MHz): δ_C 21.9 (C-11), 49.1 (C-10), 61.4 (C-12), 62.1 (C-6'), 70.8 (C-2'), 70.9 (C-4'), 78.4 (C-3'), 80.4 (C-5'), 84.2 (C-1'), 115.6 (C-2), 118.0 (C-8a), 119.2 (C-4), 121.9 (C-5), 123.8 (C-6), 127.4 (C-9a), 136.2 (C-4a), 140.8 (C-5a), 145.2 (C-7), 147.5 (C-8), 150.1 (C-3), 160.4 (C-1), 190.1 (C-9).

Homonataloin B. ^{1}H NMR (DMSO-d_6, 400 MHz): δ_H 2.29 (3H, *s*, H-11), 2.75-2.81 (2H, *m*, H-2', H-4'), 3.11-3.16 (3H, *m*, H-1', H-6'b, H-5'), 3.31 (1H, *d*, H-6'a), 3.74 (3H, *s*, H-12), 4.38 (2H, *s*, H-10), 6.64 (1H, *s*, H-2), 6.82 (1H, *s*, H-4), 7.06 (1H, *s*, H-5), 7.13 (1H, *s*, H-6), 9.51 (1H, br *s*, D_2O exchangeable, OH-7), 12.10 (1H, br *s*, D_2O exchangeable, OH-1)(B)^{13}C NMR (DMSO-d_6, 400 MHz): δ_C 21.9 (C-11), 49.1 (C-10), 61.4 (C-12), 62.1 (C-6'), 70.8 (C-2'), 70.4 (C-4'), 78.1 (C-3'), 80.1 (C-5'), 84.2 (C-1'), 115.9 (C-2), 117.7 (C-8a), 120.7 (C-5), 120.9 (C-4), 123.8 (C-6), 127.7 (C-9a), 132.0 (C-4a),140.8 (C-5a), 145.22 (C-7), 147.8 (C-8), 150.1 (C-3), 160.4 (C-1), 190.1 (C-9). HR-TOF-MS: *m/z* 431.1333 $[M-H]^-$ (calculated for $C_{22}H_{23}O_9$, 431.1342).

Aloeresin A (2.2): Yellow amorphous solid; ^{1}H NMR (400 MHz, MeOH-d_4): δ_H 2.34 (3H, *s*, H-11), 2.63 (3H, *s*, H-12), 3.44-3.57 (2H, *m*, H-4',H-5'), 3.65-3.75 (3H, *m*, H-3', H-2', H-6'b), 3.80-3.95 (3H, *m*, H-6'a, H-9), 4.53 (1H, *d*, H-1'), 5.14 (1H, *d*, H-2'), 6.06 (1H, *d*, *J* = 16.0 Hz, H-2''), 6.20 (1H, *s*, H-3), 6.58 (2H, *t*, *J* = 8.5 Hz, H-6'', H-8''), 7.32 (2H, *d*, *J* = 8.0 Hz, H-5'', H-9''), 7.40 (1H, *d*, *J* = 16.0 Hz, H-3''); ^{13}C NMR (MeOH-d_4, 400 MHz): δ_C 23.2 (C-12), 26.4 (C-11), 48.0 (C-9), 61.9 (C-6'), 72.1 (C-4'), 72.2 (C-1'), 73.8 (C-2'), 77.8 (C-3'), 82.7 (C-5'), 108.7 (C-8), 112.1 (C-3), 113.4 (C-2''), 114.9 (4a), 115.4 (C-6'', C-8''), 115.8 (C-6), 127.1 (C-4''), 131.1 (C-5'', C-9''), 159.8 (C-8a), 161.1 (C-2, C-7), 168.1 (C-1''), 182.0 (C-4), 204.7 (C-10). HR-TOF-MS: *m/z* 539.1551 $[M-H]^-$ (calculated for $C_{28}H_{27}O_{11}$, 539.1553).

Aloin (2.1): Yellow amorphous solid; UV (MeOH) λ_{Max} (log ε): 261 (5.79), 269 (5.86), 297 (5.93), 359 (6.02) nm; IR (KBr) ν_{max}: 3328, 1634, 1601, 1490, 1428, 1335, 1287, 1164 cm^{-1}; ^{1}H NMR (MeOH-d_4, 400 MHz): δ_H 2.84 (1H, *m*, H-5'), 2.85 (1H, *t*, *J* = 9.2 Hz, H-4'), 2.96 (1H, *t*, *J* = 9.2 Hz, H-2'), 3.28 (1H, *t*, *J* = 9.2 Hz, H-3'), 3.33 (1H, *m*, H-6'b), 3.35 (1H, *t*, *J* = 9.2 Hz, H-1'), 3.44 (1H, *m*, H-6'a), 4.56 (1H, *d*, $J_{a,b}$ = 14.6 Hz, H-11), 4.69 (2H, *d*, *J* = 2.4 Hz, H-10), 6.68 (1H, *d*, *J* = 8.6 Hz, H-7), 6.78 (1H, *d*, J = 1.5 Hz, H-2), 6.94 (1H, *d*, *J* = 1.5 Hz, H-5), 7.04 (1H, *d*, *J* = 8.6 Hz, H-4), 7.47 (1H, *t*, *J* = 7.9, H-6), 11.35 (1H, br *s*, D_2O exchangeable, OH-8), 11.68 (1H, br *s*, D_2O exchangeable, OH-1); ^{13}C NMR (MeOH-d_4, 400 MHz): δ_C 45.9 (C-10), 63.3 (C-6'), 64.5 (C-11), 71.8 (C-2'), 72.0 (C-4'), 80.0 (C-3'), 81.6 (C-5'), 86.6 (C-1'), 114.4 (C-2), 116.8 (C-7), 117.7 (C-9a), 118.7 (C-8a), 119.1 (C-4), 120.0 (C-5), 137.0 (C-6), 143.2 (C-4a), 146.6 (C-5a), 151.5 (C-3), 162.9 (C-1), 163.4 (C-8), 195.5 (C-9); HR-TOF-MS: *m/z* 417.1185 $[M-H]^-$ (calculated for $C_{21}H_{21}O_9$, 417.1186)

Aloesin (2.3): White powder; ^{1}H NMR (MeOH-d_4, 400 MHz): δ_H 2.29 (3H, *s*, H-11), 2.70 (3H, *s*, H-12), 3.45-3.56 (3H, *m*, H-3', H-4', H-5'), 3.75 (1H, *m*, H-6'b), 3.83-3.90 (2H, *m*, H-6'a, H-9), 4.02 (1H, *m*, H-2'), 4.98 (1H, *d*, H-1') 6.14 (1H, *s*, H-3), 6.70 (1H, *s*, H-6); ^{13}C NMR (MeOH-d_4, 400 MHz): δ_C 23.2 (C-12), 29.9 (C-11), 49.0 (C-9), 62.9 (C-6'), 70.4 (C-4'), 71.6 (C-2'), 74.2 (C-1'), 79.9 (C-3'), 82.5 (C-5'), 111.3 (C-4a), 113.4 (C-6, C-3), 116.2 (C-8), 116.8 (C-6), 143.3 (C-5), 158.4 (C-8a), 161.7 (C-7), 162.6 (C-2), 182.0 (C-1), 204.6 (C-10). HR-TOF-MS: *m/z* 395.1328 $[M-H]^-$ (calculated for $C_{19}H_{23}O_9$, 395.1342).

2.62 Isolation of Aloin (2.1) via formation of Calcium salt

A. marlothii leaf exudate (50.0 g) was dissolved in hot water (300 ml), in a large beaker, and stirred thoroughly to form a dark yellow syrupy mixture. Anhydrous $CaCl_2$ (50.0 g, 0.450 mmol) and NH_3 (25%) (~15 ml) were then added to the solution. The mixture was stirred vigorously for 10 min and allowed to settle. Within a few minutes the mixture thickened and an orange-yellow precipitate formed. The precipitate was vacuum filtered using a large Büchner funnel and flask, and the orange cake that remained was washed with water until it became a bright yellow colour. The supernatant was discarded and the yellow precipitate was transferred into a large beaker. The precipitate was slowly treated with HCl (5 M, 100 ml). The mixture was stirred slowly and water (200 ml) was added. The orange-red solution was transferred into a large separatory funnel and this aqueous layer was washed several times with ethyl acetate (10 x 300 ml). The organic layers were combined, dried over anhydrous $MgSO_4$ and filtered with a Büchner funnel and flask. The solvent was then removed using a rotary evaporator to yield a lemon-yellow powder (10.0 g). A portion of this product (0.2 g) was subjected to a silica chromatography column using an EtOAc-MeOH-CH_3CN [75:10:2 (v/v)] solvent system to afford clean aloin (**2.1**) (0.188 g, 0.45 mmol, 94%).

2.6.3 $FeCl_3$ Oxidation of Aloin (2.1)

Aloe-emodin (2.25)

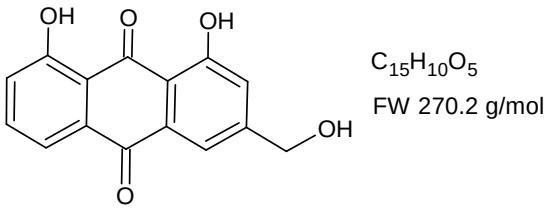

$C_{15}H_{10}O_5$
FW 270.2 g/mol

Aloin (**2.1**) (100 mg, 0.24 mmol) and anhydrous $FeCl_3$ (500 mg, 3.1 mmol) were dissolved in hot water (10 ml) in a round bottom flask equipped with a magnetic stirrer bar and reflux condenser. The dark solution was then refluxed for 6 h at 120 ^oC. The mixture was cooled to RT and cold water (10 ml) was added. The dark orange mixture was then washed with dichloromethane (3 x 20 ml). The organic layers were combined, dried over anhydrous $MgSO_4$, filtered with a Büchner funnel and flask and the solvent was then

removed using a rotary evaporator to afford aloe-emodin (**2.25**) as an orange-brown sweet smelling solid (32.4 mg, 0.12 mmol, 50%).

Aloe-emodin (2.25): Orange solid; UV (MeOH) λ_{Max} (log ε) : 255 (2.74), 276 (2.55), 286 (2.55), 429 (2.45) nm; IR (KBr) ν_{max}: 2924, 1674, 1627, 1454, 1388, 1284, 1213, 1170 cm^{-1}; ^{1}H NMR (400 MHz, DMSO-d_6): δ_H 4.64 (2H, *s*, H-11), 5.59 (1H, br *s*, D_2O exchangeable, OH-11), 7.29 (1H, *s*, H-2), 7.37 (1H, *d*, J = 8.2 Hz, H-7), 7.69 (1H, *s*, H-4), 7.70 (1H, *d*, J = 7.4 Hz, H-5), 7.78 (1H, *t*, J = 7.9 Hz, H-6), 11.80 (2H, br *s*, D_2O exchangeable, OH-1, OH-8). ^{13}C NMR (400 MHz, DMSO-d_6): δ_C 62.1 (C-11), 114.4 (C-9a), 115.8 (C-8a), 117.1 (C-4), 119.3 (C-5), 120.7 (C-2), 124.4 (C-7), 133.1 (C-4a), 133.3 (C-5a), 137.2 (C-6), 153.7 (C-3), 161.3 (C-1), 161.6 (C-8), 190.9 (C-10), 191.6 (C-9). HR-TOF-MS: *m/z* 269.0437 $[M-H]^-$ (calculated for $C_{15}H_9O_5$, 269.0450).

2.6.4 Synthesis of Co(II) Oxidation Catalyst (2.26)

Co(II) Catalyst (2.26)

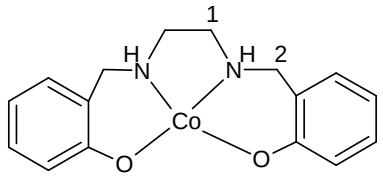

$C_{16}H_{18}N_2O_2Co$
FW 329.3 g/mol

Salicylaldehyde (1.22 g, 10 mmol) and ethylene diamine (300 mg, 5 mmol) were reacted together in MeOH (50 ml) and stirred rapidly in a round bottom flask, which resulted in the rapid formation of a lemon yellow precipitate (salen[2,2'-ethylenebis(nitrilomethylidene)diphenol]-H2, 1.80 g, 67%) $NaBH_4$ (400 mg, 10 mmol) was slowly added to the mixture, and stirred for 2 h at RT. The solvent was then removed using a rotary evaporator to yield a colourless powder (salen-H_4, 1.40 g, 62%), which was washed with distilled water (20 ml) and air dried. IR (KBr) ν_{max}: 3288, 2909, 2868, 2827, 1608, 1565, 1398, 1260, 999 cm^{-1}; ^{1}H NMR (400 MHz, $CDCl_3$): δ_H 2.85 (4H, *s*, H-2), 3.9 (4H, *dd*, H-1), 6.7-7.2 (8H, *m*, benzene). Salen-H_4 (150 mg, 0.55 mmol) and Co(II) acetate (200 mg, 1.10 mmol) were dissolved in MeOH (10 ml) and stirred for 2.5 h under N_2 at 50 ^{o}C. The removal of the solvent on a rotary evaporator afforded a powder which chromatographed on a silica chromatography column using a mixture of EtOAc-MeOH (15:5) to afford the Co(II) catalyst (**2.26**) as a green powder (110 mg, 0.33 mmol, 61%):

UV (CH_3CN): λ_{max} 262 (2.86), 384 (2.08) nm. HR-TOF-MS: *m/z* 330.0700 $[M+H]^+$ (calculated for $C_{16}H_{18}O_2N_2Co$, 329.0700).

2.6.5 Co(II) Catalysed (2.26) Oxidation of Aloin (2.1) to Aloe-emodin (2.25)

Aloin (**2.1**) (200 mg, 0.487 mmol), Co(II) catalyst (**2.26**) (25 mg, 0.076 mmol) and 30% H_2O_2 (3 ml, 26 mmol) were dissolved in CH_3CN (5 ml) in a round bottom flask equipped with magnetic stirrer and reflux condenser. The mixture was refluxed for 8 h at 80 ^oC and then allowed to cool to RT. The solution was then extracted with diethyl ether (3 x 80 ml), dried over anhydrous $MgSO_4$, filtered and the solvent was removed via a rotary evaporator. The orange material was then subjected to column chromatography, using diethyl ether as the eluent. The first fast running orange band was collected, and the solvent was removed to afford aloe-emodin (**2.25**) as a dull orange solid (92 mg, 0.34 mmol, 70%).

2.6.6 Synthesis of Cu(II) Oxidation Catalyst (2.27)

Cu(II) Catalyst (2.27)

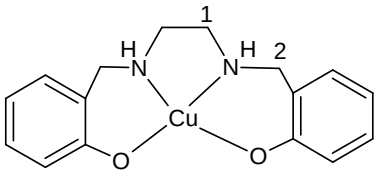

$C_{16}H_{18}N_2O_2Cu$
FW 333.9 g/mol

Salicylaldehyde (1.22 g, 10 mmol) and ethylene diamine (300 mg, 5 mmol) were stirred together in MeOH (50 ml), which resulted in the rapid formation of a lemon yellow precipitate (salen-H2, 1.80 g, 67%). $NaBH_4$ (400 mg, 10 mmol) was slowly added to the mixture, and stirred for 2 h at RT. The solvent was then removed using a rotary evaporator to yield a colourless powder (salen-H_4, 1.40 g, 62%), which was washed with distilled water (20 ml) and air dried. IR (KBr) ν_{max}: 3288, 2909, 2868, 2827, 1608, 1565, 1398, 1260 cm^{-1}; ^1H NMR (400 MHz, $CDCl_3$): δ_H 2.85 (4H, *s*, H-2), 3.9 (4H, *dd*, H-1), 6.7-7.2 (8H, *m*, benzene). Salen-H_4 (150 mg, 0.55 mmol) and Cu(II) acetate (200 mg, 1 mmol) were dissolved in MeOH (10 ml) and stirred for 2.5 h under N_2 at 50 ^oC. The removal of the solvent on a rotary evaporator afforded a powder which was chromatographed on a silica chromatography column using a EtOAc-MeOH (15:5) eluent to afford the Cu(II) catalyst (**2.27**) as a green powder (160 mg, 0.48 mmol, 87%): UV (CH_3CN) λ_{max} (log ε) :

385 (2.39), 585 (1.88) nm. HR-TOF-MS: *m/z* 334.0757 $[M+H]^+$ (calculated for $C_{16}H_{18}O_2N_2Cu$, 334.0743).

2.6.7 Cu(II) Catalysed (2.27) Oxidation of Aloin (2.1)

Aloin (**2.1**) (200 mg, 0.487 mmol), Cu(II) catalyst (**2.27**) (25 mg, 0.075 mmol) and 30% H_2O_2 (3 ml, 26 mmol) were dissolved in CH_3CN (5 ml) in a round bottom flask equipped with magnetic stirrer and reflux condenser. The mixture was refluxed for 8 h at 80 ^oC and then allowed to cool to RT. TLC analysis of the reaction showed no trace of starting material [aloin (**2.1**)] or of the expected product [aloe-emodin(**2.25**)], only the presence of the Cu(II) catalyst and its breakdown products.

2.6.8 Co (II) Catalysed (2.26) Oxidation of Homonataloin (2.4) to Nataloe-emodin (2.28)

Nataloe-emodin (2.28)

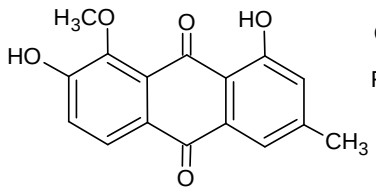

$C_{16}H_{12}O_5$

FW 284.26 g/mol

Homonataloin (**2.4**) (1000 mg, 2.31 mmol), Co(II) catalyst (**2.27**) (100 mg, 0.30 mmol) and 30% H_2O_2 (15 ml, 130 mmol) were dissolved in CH_3CN (50 ml) in a round bottom flask equipped with magnetic stirrer and reflux condenser. The mixture was refluxed for 8 h at 80 ^oC and then allowed to cool to RT. The solution was then extracted with diethyl ether (3 x 80 ml), dried over anhydrous $MgSO_4$, filtered and the solvent was removed via a rotary evaporator. The orange material was then chromatographed on a silica column, using diethyl ether as the eluent. The first fast running orange band was collected, and the solvent was removed to afford nataloe-emodin (**2.28**) as a dull orange solid (460 mg, 1.06 mmol, 70%).

Nataloe-emodin (2.28): Orange solid; UV (MeOH) λ_{Max} (log ε): 274 (3.68), 295 (2.32), 329 (5.67), 401 (1.22) nm; IR (KBr) ν_{max}: 2924, 2854, 1637, 1606, 1566, 1481, 1427, 1362, 1295, 1205, 1157 cm^{-1}; ^1H NMR (DMSO-d_6, 400 MHz): δ_H 2.42 (3H, *s*, H-11), 3.84

(3H, *s*, H-12), 7.15 (1H, *d*, *J* = 1.3 Hz, H-2), 7.32 (1H, *d*, *J* = 8.2 Hz, H-6), 7.47 (1H, *d*, *J* = 1.3 Hz, H-4), 7.90 (1H, *d*, *J* = 8.3 Hz, H-5), 10.84 (1H, br *s*, D_2O exchangeable, OH-7) 12.71 (1H, br *s*, D_2O exchangeable, OH-1).[13]C NMR (DMSO-d_6, 400 MHz): δ_C 21.9 (C-11), 60.9 (C-12), 115.3 (C-3), 119.8 (C-4), 122.3 (C-6), 122.4 (C-4a), 123.9 (C-2), 125.6 (C-5), 126.2 (C-8a), 126.5 (C-9a), 132.9 (C-4a), 148.4 (C-8), 148.6 (C-7), 158.4 (C-5a), 163.8 (C-1), 188.6 (C-10), 191.4 (C-9). HR-TOF-MS: *m/z* 283.0602 $[M-H]^-$ (calculated for $C_{16}H_{11}O_5$, 283.0606).

2.6.9 Synthesis of IBX (2.30)

***o*-Iodoxybenzoic acid (2.31)**

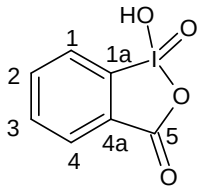

$C_7H_5O_4I$
FW 280.0 g/mol

$KBrO_3$ (4.00 g, 24 mmol) was dissolved in H_2SO_4 (2 M, 38 ml) in a two-necked round bottom flask equipped with a magnetic stirrer bar, reflux condenser and thermometer. The clear solution was heated to 60 ^oC and *o*-iodobenzoic acid (4.00 g, 16 mmol) was added over 40 min in small (0.5 g) portions. The mixture became a bright orange colour as Br_2 gas was evolved and a white precipitate emerged. After the addition was complete, the temperature was maintained at 65 ^oC for 3 h. The solution was then cooled in an ice bath and the solid material was collected by vacuum filtration with a Büchner funnel and flask. The white precipitate was washed with cold H_2O (500 ml), cold EtOH (500 ml) followed by cold water (500 ml). The IBX (**2.30**) was air dried and weighed (2.00 g, 7.14 mmol, 44%).

IBX (2.30): White powder; [1]H NMR (400 MHz, DMSO-d_6): δ_H 7.83 (1H, *t*, *J* = 8.3 Hz, H-3), 7.98 (1H, *t*, *J* = 8.3 Hz, H-2), 8.02 (1H, *d*, *J* = 12.8 Hz, H-4), 8.14 (1H, *d*, *J* = 12.8 Hz, H-1); [13]C NMR (400 MHz, DMSO-d_6): δ_C 125.5 (C-1), 130.6 (C-4), 131.6 (C-4a), 133.5 (C-3), 134.9 (C-2), 147.0 (C-1a), 168.0 (C-5); HR-TOF-MS: *m/z* 278.9154 $[M-H]^-$ (calculated for $C_7H_4O_6I$, 278.9154).

2.6.10 IBX (2.30) Oxidation of Aloe-emodin (2.31) to Rheinal (2.29)

Rheinal (2.29)

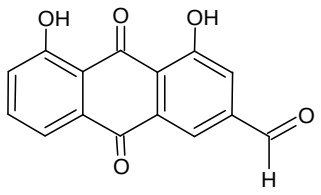

$C_{15}H_8O_5$
FW 268.2 g/mol

Aloe-emodin (**2.25**) (100 mg, 0.37 mmol) was dissolved in dry THF (8 ml). IBX (**2.30**) (155 mg, 0.55 mmol) and DMSO (2 ml) were added to the mixture which was stirred for 8 h at RT. The solution was transferred to a separatory funnel, where H_2O (20 ml) was added and the resulting orange mixture was washed with diethyl ether (4 x 50 ml). The organic layers were combined, dried over anhydrous $MgSO_4$ and filtered with a Buchner funnel and flask. The solvent was then removed using a rotary evaporator to yield an orange-yellow solid which was purified by silica column chromatography using diethyl ether as the eluent. Rheinal (**2.29**) was obtained in excellent yields (94.2 mg, 0.35 mmol, 95%)

Rheinal (2.29): Orange amorphous solid; UV (MeOH) λ_{Max} (log ε) : 253 (2.69), 274 (2.37), 285 (2.36), 429 (2.43) nm; IR ν_{max} (neat) :. 2922, 2640, 1670, 1622, 1602, 1427, 1400, 1287, 1264, 1157, 1108 cm^{-1}; ^1H NMR (500 MHz, DMSO-d_6): δ_H 7.42 (1H, *d*, *J* = 8.3 Hz, H-7), 7.76 (1H, *d*, *J* = 7.5 Hz, H-5), 7.82 (1H, *s*, H-2), 7.84 (1H, *t*, *J* = 8.1 Hz, H-6), 8.13 (1H, *d*, *J* = 1.2 Hz, H-4), 10.12 (1H, s, H-11) 11.83 (2H, br *s*, D_2O exchangeable, OH-1, OH-8); ^{13}C NMR (500 MHz, DMSO-d_6): δ_C 116.8 (C-8a), 118.5 (C-4), 119.9 (C-5), 120.1 (C-9a), 124.8 (C-2), 125.2 (C-7), 133.8 (C-4a), 134.8 (C-5a), 138.1 (C-6), 141.9 (C-3), 161.4 (C-1), 162.0 (C-8), 191.9 (C-10), 192.8 (C-9), 192.8 (C-11); HR-TOF-MS: *m/z* 267.0289 $[M-H]^-$ (calculated for $C_{15}H_7O_5$, 267.0293).

2.6.11 Oxidation of Aloe-emodin (2.25) with Nickel Oxide Hydroxide

Aloe-emodin (**2.25**) (150 mg, 0.56 mmol), $NiCl_2.6H_2O$ (12.5 mg, 0.053 mmol), H_2O (0.1 ml) and DCM (0.2 ml) were added together and cooled in an ice bath. Cold NaOCl (3.5%, 10 ml) was added and, instantaneously, a black slurry formed. The mixture was stirred for

8 h (5 ml NaOCl was added after 3 h) at 0 ^{o}C and for 11 h at RT. The reaction mixture was acidified using HCl (5 M) and extracted with EtOAc (3 x 20 ml). The organic layers were combined, dried over anhydrous $MgSO_4$ and filtered with a Buchner funnel and flask. The solvent was then removed using a rotary evaporator. No trace of starting material [aloe-emodin (**2.25**)] or of desired product [rhein (**2.31**)] were found.

2.6.12 Oxidation of Aloe-emodin (2.25) with TEMPO (2.32)/NaOCl/$NaClO_2$

Aloe-emodin (**2.25**) (50 mg, 0.185 mmol), TEMPO (**2.32**) (2.2 mg, 0.011 mmol) and NaH_2PO_4 buffer (0.75 ml, pH = 6.7) were added together in a round bottom flask and the solution was heated to 35 ^{o}C. Next, NaOCl (46 mg, 0.4 mmol in 0.2 ml H_2O) and NaOCl (3.5%, 1 ml) were added to the stirred reaction over 2 h. The deep-purple reaction mixture was then stirred for 12 h at 35 ^{o}C. The solution was then acidified with HCl (3 M). TLC analysis showed only starting material.

2.6.13 RuO_4 Oxidation of Aloe-emodin (2.25)

Aloe-emodin (**2.25**) (50 mg, 0.19 mmol), $NaIO_4$ (214 mg, 1 mmol, 5 mol%), CH_3CN (0.8 ml), CCl_4 (0.8 ml) and H_2O (1.2 ml) were added together in a round bottom flask equipped with magnetic stirrer. The mixture was stirred for 5 min at RT and $RuCl_3.3H_2O$ (13.1 mg, 0.050 mmol, 0.25 mol%) was added. The reaction was stirred vigorously for 5 h at RT. The reaction material was chromatographed on silica gel, eluting with a diethyl ether/petroleum ether (15:10 v/v) running phase. Thee compounds were isolated, aloe-emodin (**2.25**) (43 mg, 0.16 mmol, 84%), rheinal (**2.29**) (5 mg, 0.019 mmol, 10%) and rhein (**2.31**) (3 mg, 0.0095 mmol, 5%).

2.6.14 Oxidation of Rheinal (2.29) to Rhein (2.31) with Sodium Chlorite

Rhein (2.31)

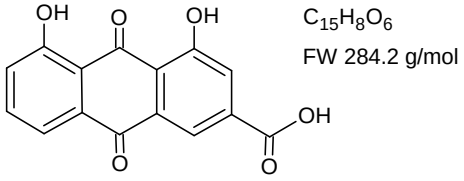

$C_{15}H_8O_6$

FW 284.2 g/mol

Rheinal (**2.29**) (150 mg, 0.56 mmol) was dissolved in ^{t}BuOH (10 ml) in a round bottom flask equipped with a magnetic stirrer bar. A solution of $NaClO_2$ (640 mg, 12.28 mmol) and $NaH_2PO_4.H_2O$ (640 mg, 16.32 mmol) in distilled H_2O (6 ml) was added over 5 min. The reaction mixture was stirred vigorously for 3 h at RT. The solution was dried over anhydrous $MgSO_4$, filtered and the mixture was absorbed on dry silica via a rotary evaporator. The silica-adsorbed material was chromatographed on silica gel, initially eluting with several bed volumes of diethyl ether, followed by MeOH to elute a bright yellow band. The solvent was removed using a rotary evaporator and rhein (**2.31**) was obtained as a bright yellow solid (151 mg, 0.53 mmol, 95%).

Rhein (2.31): Pale yellow powder; UV (MeOH) λ_{Max} (log ε) : 257 (2.56), 285 (2.17), 432 (2.32) nm; IR ν_{max} (KBr) :. 3435, 2892, 1699, 1675, 1630, 1470, 1398, 1269, 1217, 1167 cm^{-1}; ^{1}H NMR (500 MHz, DMSO-d_6): δ_H 7.41 (1H, *dd*, J = 8.4, *J* = 1.1 Hz, H-7), 7.75 (1H, *dd*, *J* = 7.5, J = 1.1 Hz, H-5), 7.78 (1H, *d*, *J* = 1.7 Hz, H-2), 7.84 (1H, *t*, *J* = 8.3 Hz, H-6), 8.15 (1H, *d*, *J* = 1.6 Hz, H-4), 11.90 (2H, br *s*, D_2O exchangeable, OH-1, OH-8); ^{13}C NMR (500 MHz, DMSO-d_6): δ_C 116.81 (C-8a), 118.80 (C-4), 119.50 (C-1a), 119.46 (C-5), 120.02 (C-9a), 124.14 (C-2), 124.62 (C-7), 137.62 (C-6), 161.11 (C-1), 161.44 (C-8), 165.46 (C-11), 161.43 (C-1), 191.87 (C-10), 192.75 (C-9); HR-TOF-MS: *m/z* 283.0249 $[M-H]^-$ (calculated for $C_{15}H_7O_6$, 283.0243).

2.6.15 Attempted Bromination of Aloe-emodin (2.25)

A round bottom flask, equipped with magnetic stirrer, was charged with CuBr (1.3 mg, 0.009 mmol), 1,10-phenantholine monohydrate (3.6 mg, 0.018 mmol), Cu powder (35 mg, 0.55 mmol), Fe powder (51 mg, 0.91 mmol) and CBr_4[36] (242 mg, 0.73 mmol). Aloe-emodin (**3.23**) (50 mg, 0.185 mmol) in dry CH_3CN (5 ml) was added to the reaction flask and the resulting solution was stirred vigorously for 4 h under an atmosphere of N_2. TLC analysis of the reaction showed only starting material.

2.6.16 Bromination of Aloe-emodin (2.25) to 11-Bromochrysophanol (2.33)

11-Bromochrysophanol (2.33)

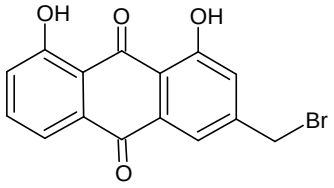

$C_{15}H_9O_4Br$
FW 333.1 g/mol

Aloe-emodin (**2.25**) (200 mg, 0.7 mmol) and PPh_3 (1.00 g, 3.8 mmol) were dissolved in dry THF (10 ml) in a round bottom flask equipped with a magnetic stirrer bar. CBr_4 (1.4 g, 4.2 mmol) was added and the mixture was stirred for 12 h under an atmosphere of N_2 at RT. The bright orange solution was dried on anhydrous $MgSO_4$, filtered and absorbed to dry silica via a rotary evaporator. The silica-absorbed material was chromatographed on silica gel, eluting with a diethyl ether-petroleum ether [15:10 (v/v)] running phase. The solvent was removed using a rotary evaporator and the desired product was obtained as a bright yellow solid (210 mg, 0.63 mmol, 90%)

11-Bromochrysophanol (2.33): Bright orange crystals; UV (MeOH) λ_{Max} (log ε) : 257 (2.27), 287 (1.99), 312 (1.73) nm; IR ν_{max} (neat) :. 2921, 1983, 1728, 1669, 1623, 1603, 1567, 1476, 1377, 1202, 1125 cm^{-1}; ^1H NMR (500 MHz, DMSO-d_6): δ_H 4.81 (2H, *s*, H-11) 7.40 (1H, *dd*, *J* = 8.32, *J* = 1.2 Hz, H-7), 7.47 (1H, *d*, *J* = 1.6 Hz, H-2), 7.73 (1H, *dd*, *J* = 7.5, 1.1 Hz, H-5), 7.79 (1H, *d*, *J* = 1.7 Hz, H-6), 7.81 (1H, *t*, *J* = 8.3 Hz, H-6), 11.91 (2H, br *s*, D_2O exchangeable, OH-1, OH-8).^{13}C NMR (500 MHz, DMSO-d_6): δ_C 25.1 (C-11), 114.5 (C-9a), 115.9 (C-8a), 117.1 (C-5), 119.4 (C-4), 120.7 (C-7), 124.4 (C-2), 133.2 (C-4a), 133.4 (C-5a), 137.4 (C-6), 153.7 (C-3), 161.4 (C-8), 161.6 (C-1) 181.6 (C-10), 191.7 (C-9). HR-TOF-MS: *m/z* 330.9613 $[M-H]^-$ (calculated for $C_{15}H_8O_4Br^{79}$, 330.9606).

2.6.17 Substitution Reaction of 11-Bromochrysophanol (2.33) to 11-(Pyrrolidin-1-yl)chrysophanol (2.34)

11-(Pyrrolidin-1-yl)chrysophanol (2.34)

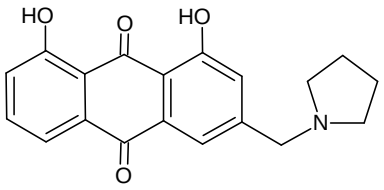

$C_{19}H_{17}O_4N$
FW 323.34 g/mol

BuLi (**2.37)** (1.2 ml, 12.0 mmol) was added to freshly distilled pyrrolidine (1.0 ml, 12.0 mmol) in dry THF (5 ml) under N_2 at 0 ^oC. After being stirred vigorously for 30 min at RT, 11-bromochrysophanol (**2.33**) (140 mg, 0.42 mmol) in dry THF (15 ml) was added. The deep purple mixture was stirred for 12 h at RT before being acidified with conc. HCl. This was followed by the addition of $NaHCO_3$ until the solution was neutralized. The solvent was removed via a rotary evaporator and the resulting solid material was chromatographed on a silica column eluting with ethyl acetate. 11-(Pyrrolidin-1-yl)chrysophanol (**2.34**) was collected as a brown residue (110 mg, 0.34 mmol, 80%).

11-(Pyrrolidin-1-yl)chrysophanol (2.34): Orange solid; UV (MeOH) λ_{Max} (log ε) : 269 (3.10), 272 (2.74), 322 (4.20), 429 (2.68) nm; IR (KBr) ν_{max}:. 3417, 2936, 2924, 1672, 1628, 1570, 1353, 1352, 1215, 1159 cm^{-1}; ^1H NMR (DMSO-d_6, 400 MHz): δ_H 1.74 (4H, *m*, H-2'), 2.54 (4H, *m*, H-1'), 3.75 (2H, *d*, H-11), 7.31 (1H, *d*, *J* = 1.1 Hz, H-2), 7.36 (1H, *dd*, *J* = 8.2 Hz, *J* = 1.1 Hz, H-7), 7.69 (1H, *d*, *J* = 1.1 Hz, H-4), 7.72 (1H, *dd*, *J* = 7.9 Hz, *J* = 1.2 Hz, H-5), 7.78 (1H, *t*, *J* = 8.3 Hz, H-6) 11.80 (2H, br *s*, D_2O exchangeable, OH-1, OH-8).^{13}C NMR (DMSO-d_6, 400 MHz): δ 25.66 (C-2'), 54.01 (C-1'), 59.21 (C-11), 115.23 (C-9a), 116.38 (C-8a), 119.80 (C-4), 119.88 (C-5), 123.77 (C-2), 124.88 (C-7), 133.68 (C-4a), 133.80 (C-5a), 137.82 (C-6), 150.09 (C-3), 161.82 (C-1), 162.04 (C-8), 181.93 (C-10), 194.04 (C-9). HR-TOF-MS: *m/z* 322.1089 $[M-H]^-$ (calculated for $C_{19}H_{16}O_4N$, 322.1079).

2.6.18 Substitution Reaction of 11-Bromochrysophanol (2.33) to 11-(Piperidin-1-yl)chrysophanol (2.35)

11-(Piperidin-1-yl)chrysophanol (2.35) $C_{20}H_{19}O_4N$

FW 337.37 g/mol

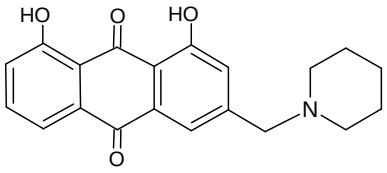

BuLi (**2.37**) (1.15 ml, 11.6 mmol) was added to freshly distilled piperidine (1.0 ml, 11.6 mmol) in dry THF (5 ml) under N_2 at 0 ^oC. After being stirred vigorously for 30 min at RT, 11-bromochrysophanol (**2.33**) (140 mg, 0.42 mmol) in dry THF (15 ml) was added. The deep purple mixture was stirred for 12 h at RT before being acidified with conc. HCl. This was followed by the addition of $NaHCO_3$ until the solution was neutralized. The solvent was removed via a rotary evaporator and the resulting solid material was chromatographed on a silica column eluting with an ethyl acetate mobile phase. 11-(piperidin-1-yl)chrysophanol (**2.35**) was collected as a brown precipitate (108 mg, 0.32 mmol, 75%).

11-(Piperidin-1-yl)chrysophanol (2.35): brown solid; UV (MeOH) λ_{Max} (log ε) : 268 (1.38), 285 (0.97), 346 (0.16), 429 (0.74) nm; IR (KBr) ν_{max}:.2929, 1672, 1632, 1570, 1469, 1452, 1425, 1370, 1279, 1162 cm^{-1}; ^1H NMR ($CDCl_3$, 400 MHz): δ_H 1.43 (2H, *m*, H-3'), 1.58 (4H, *m*, H-2'), 2.41 (4H, *m*, H-1'), 3.55 (2H, *s*, H-11), 7.28 (1H, *dd*, *J* = 8.0 Hz, *J* = 1.1 Hz, H-7), 7.34 (1H, *d*, *J* = 1.1 Hz, H-2), 7.63 (1H, *t*, *J* = 8.3 Hz, H-6), 7.80 (1H, *d*, *J* = 1.1 Hz, H-4), 7.82 (1H, *dd*, *J* = 8.1 Hz, *J* = 1.1 Hz, H-5) 12.05 (2H, br *s*, D_2O exchangeable, OH-1, OH-8).^{13}C NMR ($CDCl_3$, 400 MHz): δ_C 24.2 (C-3') 25.9 (C-2'), 54.7 (C-1'), 63.1 (C-11), 100.1 (C-7), 114.9 (C-9a), 115.9 (C-8a), 119.5 (C-5), 120.7 (C-4), 124.1 (C-2), 133.4 (C-4a), 133.8 (C-5a), 137.0 (C-6), 149.6 (C-3), 162.5 (C-1), 162.8 (C-8), 181.9 (C-10), 192.6 (C-9). HR-TOF-MS: *m/z* 336.1223 $[M-H]^-$ (calculated for $C_{20}H_{18}O_4N$, 336.1238).

2.6.19 Substitution Reaction of 11-Bromochrysophanol (2.33) to 11-(Morpholin-1-yl)chrysophanol (2.36)

11-(Morpholin-1-yl)chrysophanol (2.36)

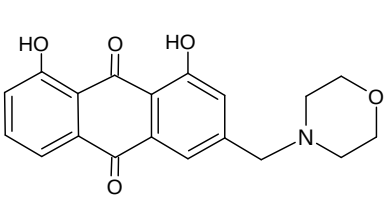

$C_{19}H_{17}O_5N$
FW 339.34 g/mol

BuLi (**2.37**) (1.1 ml, 11.5 mmol) was added to freshly distilled morpholine (**2.38**) (1.0 ml, 11.5 mmol) in dry THF (5 ml) under N_2 at 0 ^oC. After being stirred vigorously for 30 min at RT, 11-bromochrysophanol (**2.33**) (140 mg, 0.42 mmol) in dry THF (15 ml) was added. The deep purple mixture was stirred for 12 h at RT before being acidified with conc. HCl. This was followed by the addition of $NaHCO_3$ until the solution was neutralized. The solvent was removed via a rotary evaporator and the resulting solid material was chromatographed on a silica column eluting with diethyl ether. 11-(Morpholin-1-yl)chrysophanol (**2.36**) was collected as a dull orange solid (128 mg, 0.38 mmol, 90%).

11-(Morpholin-1-yl)chrysophanol (2.36): Orange solid; UV (MeOH) λ_{Max} (log ε) : 270 (2.23), 272 (1.96), 338 (0.24), 429 (1.52) nm; IR (KBr) ν_{max}:. 2844, 2855, 1672, 1619, 1576, 1467, 1347, 1291, 1206, 1111 cm^{-1}; ^1H NMR (DMSO-d_6, 400 MHz): δ_H 2.40 (4H, *m*, H-1'), 3.60 (2H, *d*, H-11), 3.61 (4H, *m*, H-2'), 7.32 (1H, *d*, *J* = 1.1 Hz, H-2), 7.37 (1H, *d*, *J* = 8.2 Hz, H-7), 7.69 (1H, *d*, *J* = 1.1 Hz, H-4), 7.70 (1H, *d*, *J* = 7.9 Hz, H-5), 7.78 (1H, *t*, *J* = 8.3 Hz, H-6) 11.80 (2H, br *s*, D_2O exchangeable, OH-1, OH-8).^{13}C NMR (DMSO-d_6, 400 MHz): δ_C 53.6 (C-1'), 62.0 (C-11), 66.7 (C-2'), 115.3 (C-9a), 116.4 (C-8a), 119.8 (C-4), 120.1 (C-5), 124.1 (C-2), 124.9 (C-7), 133.7 (C-4a), 133.8 (C-5a), 137.8 (C-6), 149.6 (C-3), 161.8 (C-1), 161.9 (C-8), 181.9 (C-10), 194.3 (C-9). HR-TOF-MS: *m/z* 338.1033 $[M-H]^-$ (calculated for $C_{19}H_{16}O_5N$, 338.1028).

2.7 References

1. Barrantes, E., Guinea, M., *Life Sciences*, 2003, **72**, 843-850.

2. Reynolds, T., *Aloes: The Genus Aloe*, CRC Press LLC, New York, 2004, pp. 39-41.

3. Viljoen, A. M, *A Chemotaxomonic Study of Phenolic Leaf Compounds in the Genus Aloe*, 1999, PhD Thesis, Rand Afrikaans University.

4. Beaumont, J., Reynolds, T., Vaughn, J. G., *Planta Medica*, 1984, **50**, 505-508.

5. Tuttle, T., Kraka, E., Thiel, W., Cremer, D., *Journal of Physical Chemistry B*, 2007, **111**, 8321-8328.

6. Potterat, O., Puder, C., Wagner, K., Bolek, W., Vetterman, R., Kauschke, S. G., *Journal of Natural Products*, 2007**, 70**, 1934-1938.

7. Li, Z., Wang, J., Jiang, B., Zhang, X., An, L., Bao, Y., *Phytomedicine*, 2007, **14**, 846-852.

8. Noungoue, D. T., Antheaume, C., Chaabi, M., Ndjakou, B. L., Ngouela, S., Lobstein, A., Tsamo, E., *Phytochemistry*, 2008, **69**, 1024-1028.

9. Aly, A. H., Edrada-Ebel, R., Wray, V., Muller, W. E. G., Koszytska, S., Hentschel, U., Proksch, P., Ebel, R., *Phytochemistry*, 2008, **69**, 1716-1725.

10. Copp, B., *Natural Product Reports*, 2003, **20**, 535-557.

11. Lee, T. S., Das, A., Khosala, C., *Bioorganic and Medicinal Chemistry*, 2007, **15**, 5207-5218.

12. Wei, B., Wu, S., Chung, M., Won, S., Lin, C., *European Journal of Medical Chemistry*, 2000, **35**, 1089-1098.

13. Huang, H., Chioy, J., Fong, Y., Hou, C., Lu, V., Wang, J., Shih, J., Pan, Y., Lin, J., *Journal of Medicinal Chemistry*, 2003, **46**, 3300-3307.

14. Alexander, J., Bhatia, A. V., Mitscher, L. A., Omoto, S., Suzuki, T., *Journal of Organic Chemistry*, 1980, **45**, 20-24.

15. Koyama, M., Takahashi, K., Chou, T., Darzynkiewicz, Z., Kapuscinski, J., Kelly, T. R., Wantabe, K. A., *Journal of Medicinal Chemistry*, 1989, **32**, 1594-1599.

16. Dagne, E., *Bulletin of the Chemical Society of Ethiopia*, 1996, **10**, 89-103.

17. Manitto, P., Monti, D., Speranza, G., *Journal of the Chemical Society, Perkin Transations 1*, 1990, 1297-1300

18. Conner, J. M., Gray, A. I., Reynolds, T., Water, P. G., *Phytochemistry*, 1990, **29**, 941-944.

19. Hay, J. E., Haynes, L. J., *Journal of American Chemical Society*, 1956, 3141-3147.

20. Wamer, W. G., Vath, P., Falvey, D. E., *Free Radical Biology and Medicine*, 2003, **34**, 233-242.

21. Das, S., Punniyamourthy, T., *Tetrahedron Letters*, 2003, **44**, 6033-6035.

22. Kervinen, K., Allmendinger, M., Leskela, M., Repo, T., Rieger, B., *Physical Chemistry*, 2003, **5**, 4450-4454.

23. Velusamy, S., Punniyamurhty, T., *European Journal of Organic Chemistry*, 2003, 3913-3915.

24. Ireland, R. E., Liu, L., *Journal of Organic Chemistry*, 1993, **58**, 2899.

25. Moore, J. D., Finney, N. S., *Organic Letters*, 2002, **4**, 3001-3003.

26. Moorthy, J. M., Singhal, N., Venkatakrishnan, *Tetrahedron Letters*, 2004, **45**, 5419-5424.

27. Lindgren, B. O., Nilson, T., *Acta Chemica Scandinavica*, 1973, **27**, 888-890.

28. Grill, J. M., Ogle, J. W., Miller, S. A., *Journal of Organic Chemistry*, 2006, **71**, 9291-9296.

29. Zhao, M. Li, J., Mano, E., Song, Z., Tschaen, D. M., Grabowski, J. J., Reider, P. J., *Journal of Organic Chemistry*, 1999, **64**, 2564-2566.

30. Burke, S. D., Danheiser, R. L., *Handbook of Reagents for Organic Synthesis : Oxidising and Reducing Agents*, Copyright © John Wiley & Sons Ltd, Chichester, United Kingdom, 1999, 346.

31. Singh, A. K., Varma, R. S., *Tetrahedron Letters*, 1992, **33**, 2307-2310.

32. Alexander, J. Bhatia, A. V., Clark, G. W., Leutzow, A., Mitscher, L. A., Omoto, S., Suzuki, T., *Journal of Organic Chemistry*, 1980, **45**, 24-28.

33. Leonel, E., Paugam, J. P., Nedelec, J. Y., *Journal of Organic Chemistry*, 1997, **62**, 7061-7064.

34. Seo, J., Kim, H., Yoon, C. M., Ha, D. C., Gong, Y. D., *Tetrahedron*, 2005, **61**, 9305, 9311.

35. Cui, X., Takahashi, K., Shimamura, T., Koyanagi, J., Komada, F., Saito, S., *Chemical Pharmacology Bulletin*, 2008, **56**, 497-503.

CHAPTER THREE

ALOIN AND DERIVATIVES AS POTENTIAL MMP INHIBITORS

3.1 Introduction

Connective tissues, such as cartilage, are crucial to maintain the healthy structure and efficient functioning of the body. Matrix metalloproteinases (MMPs) are calcium-dependent zinc-containing endopeptidases that are responsible for the controlled degradation of many components of the extracellular matrix (ECM), including cartilage tissue[1]. Release of these enzymes is usually finely regulated. However, sometimes, this control is altered or lost, resulting in excessive tissue breakdown at an unbalanced replacement build-up rate, leading to medical conditions such as osteoarthritis, tumour growth and metastasis, and periodontal disease. Developing proteinase inhibitors that are therapeutically active is a challenging problem. Tetracylines, such as doxycycline (**3.1**) and minocycline (**3.2**), are examples of a class of MMP inhibitors that are used clinically to treat some of these diseases[1].

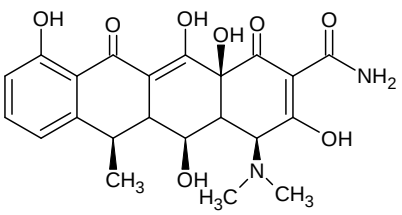

(**3.1**)

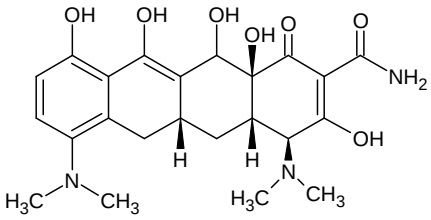

(**3.2**)

The most interesting biological property of aloin (**3.3**), as far as this investigation is concerned, is its reported ability to inhibit granulocyte MMP-8. Aloin (**3.3**), which is a naturally occurring *C*-glucoside anthrone, also has many structural features similar to that of doxycycline (**3.1**), suggesting similar activity with regard to MMP inhibition[2]. Thus, aloin (**3.3**), and its synthetic derivatives (see Chapter 2) were screened for their ability to inhibit MMP-2 and MMP-9, the two most prominent MMPs in mammalian blood. Their

inhibitory activity, if any at all, will be compared to that of known MMP inhibitors such as doxycycline (**3.1**) and ethylenediamine tetraacetic acid (EDTA).

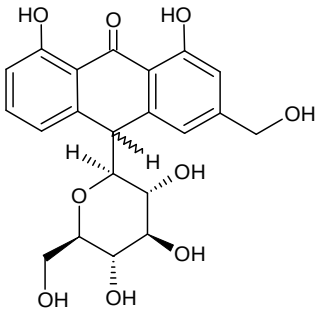

(3.3)

3.2 Matrix Metalloproteinases

3.2.1 Introduction

Matrix metalloproteinases are a family of potent enzymes that can degrade different components of the ECM. Thus, they are involved in numerous biological processes. These include: embryonic development, blastocyst implantation, organ morphogenesis, nerve growth, ovulation, cervical dilatation, postpartum uterine involution, endometrial cycling, hair follicle cycling, bone remodelling, wound healing, angiogenesis and apoptosis[3]. The pathological roles include roles in arthritis, cancer, cardiovascular disease, nephritis, neurological disease, breakdown of brain blood barrier, periodontal disease, skin ulceration, gastric ulcer, corneal ulceration, liver fibrosis, emphysema and fibrotic lung disease[3].

3.2.2 Structural Diversity of MMPs

The complete set of MMPs produced by human cells has been defined due to the sequencing of the complete human genome[4]. Twenty-four distinct genes have been found to encode members of the MMP family. These enzymes are classified based on their structural design, rather than their substrate specificities (Fig. 3.1). Structurally, MMPs are organized around a conserved catalytic domain, which contains a propeptide that is necessary to maintain enzyme latency. There is also a signal peptide which directs their

secretion from the cell, and in most MMPs, a C-terminal hemopexin domain which contributes to substrate specificity and to interactions with endogenous inhibitors.

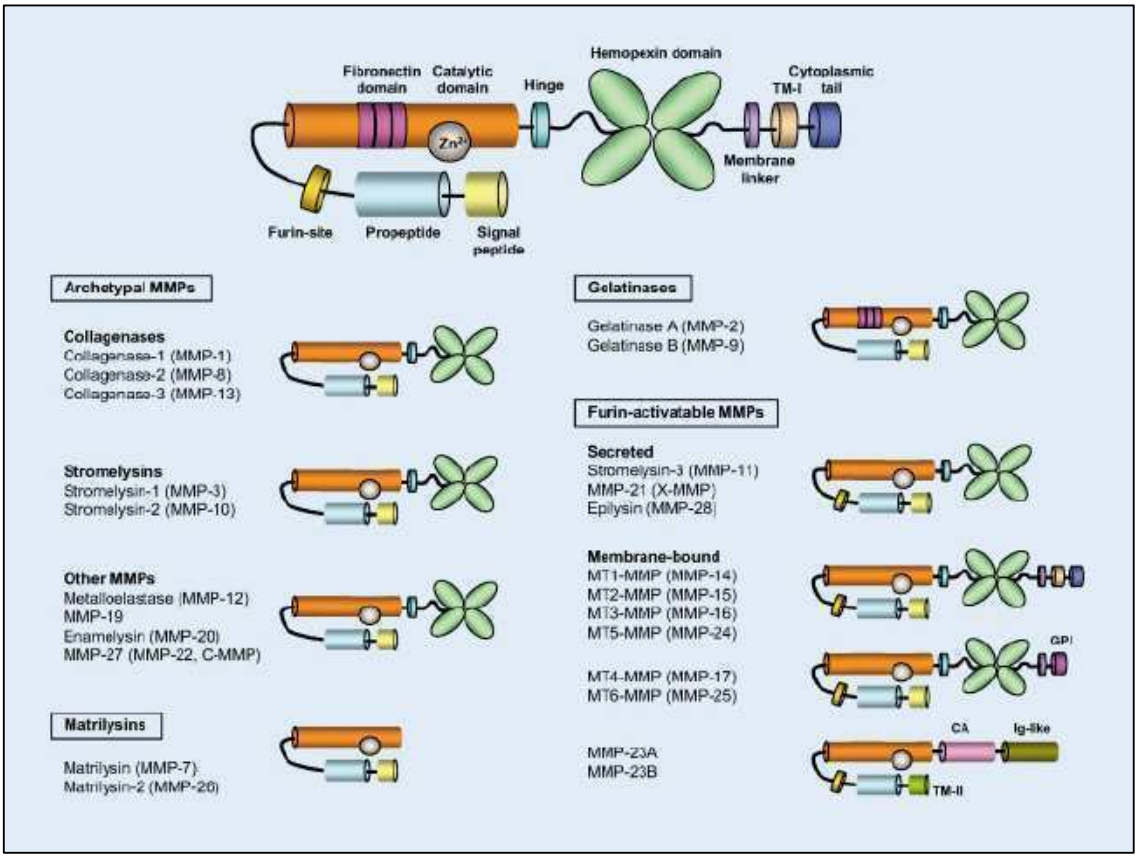

Figure 3.1. Structural classification of human MMPs based on their domain organization[4].

Since these enzymes consist of similar domains (Fig. 3.1), they contain many common properties: (i) they are secreted as inactive zymogens; (ii) their activation can be achieved proteolytically or by treatment with mercurial compounds; (iii) they contain a zinc catalytic centre; (iv) the active enzymes function at neutral pH and require calcium for activity; and (v) the active enzymes are inhibited by tissue-inhibitors of metalloproteinases (TIMPs)[1].

There are four main groups of the MMP family; (i) the stromelysins; (ii) the collagenases; (iii) the gelatinases and (iv) the membrane type-MMPs (MT-MMPs). Each member of the MMP family has been allocated a MMP number and the different numbers, molecular weights (M_r), substrate specificities and common names are listed in Table 3.1.

TABLE 3.1 The MMP Family-Names, Numbers, Molecular Weights (kDa)* and Known Matrix Substrates[5]

The Collagenases	Known As	M_r	Substrates
Interstitial Collagenases	MMP-1	**55**/45	Collagen type I, II, III, VI, X, gelatin, aggrecan, proteoglycan link protein, tenascin, entactin, α_1-proteinase inhibitor (PI) and $\alpha_2$macroglobulin
Neutrophil Collagenase	MMP-8	**75**/58	Collagen type I, II, III, V, VII, VIII, X, gelatin, aggrecan, α_1-PI, α_2-antiplasmin and fibronectin
Collagenase-3	MMP-13	**60**/48	Collagen type I, II, III, IV, VII, X, gelatin, plasminogen activator inhibitor 2, aggrecan and tenascin
Collagenase-4	MMP-18	**55**/42	Collagen type I and gelatin
The Gelatinases			
Gelatinase-A	MMP-2	**72**/66	Collagens type I, IV, V, VII, X, XI, XIV, gelatin type I, II, III, fibronectin, elastin, vitronectin, aggrecan, link protein, α_1-PI and activates MMP-9 and MMP-13[a]
Gelatinase-B	MMP-9	**92**/86	Collagens type III, IV, V, gelatin type I, V, aggrecan, elastin, fibronectin, link protein and α_1-PI.
The Stromelysins			
Stromelysin-1	MMP-3	**57**/45	Proteoglycan, link protein, fibronectin, laminin, elastin, gelatins type I, III, IV, V, collagens III, IV, V, IX, α_1-PI, α2-M and activates MMP-1, -7, -8, -9, and -13
Stromelysin-2	MMP-10	**57**/54	Gelatins type I, III, IV, V, collagens types III, IV, V, fibronectin, aggrecan, elastin, fibronectin and activates MMP-1 and MMP-8

Stromelysin-3	MMP-11	**51**/44	α_1-PI and N-terminal domain cleaves casein
The Membrane-Bound MMPs			
MT MMP-1	MMP-14	**66**/56	Collagens type I, II, III, IV, gelatin, elastin, aggrecan, proteoglycan, fibronectin, vitronectin and activates MMP-2 and MMP-13
MT MMP-2	MMP-15	**72**/60	Collagens type I, II, gelatin, fibronectin, tenascin, laminin, proteoglycan, and activates MMP-2
MT MMP-3	MMP-16	**64**/52	Activates MMP-2 and possibly other MMPs
MT MMP-4	MMP-17	**57**/63	Gelatin
MT MMP-5	MMP-24	**63**/45	Gelatin, fibronectin, proteoglycan and activates MMP-2
MT MMP-6	MMP-25	**63**/?	Activates MMP-2, MMP-9 and α_1-PI
Other Enzymes			
Matrilysin	MMP-7	**28**/19	Collagens type IV, X, gelatins type I, III, IV, V, proteoglycan, fibronectin, aggrecan, link protein, tenascin, laminin, elastin, entactin, α_1-PI and activates MMP-1, -2 and -9.
Metalloelastase	MMP-12	**54**/45,22	Collagen type IV, elastin, gelatin, α 1-PI, fibronectin, vitronectin and laminin
-	MMP-19	**54**/45	Aggrecan
Enamelysin	MMP-20	**54**/22	Not known
XMMP	MMP-21	**70**/53	Gelatin
CMMP	MMP-22	**52**/43	Gelatin
-	MMP-23	?/?	Not known
Endometase	MMP-26	**28**/?	Gelatin and α_1-PI

*Molecular weight (M_r) of the latent (in bold) and active forms.

3.2.3 Control of the Matrix MMPs

Due to the potent proteolytic nature of MMPs, they are carefully controlled. Control of activity is regulated at a number of points: (i) at the synthetic level of cytokines and growth factors; (ii) at the secretion level by secretion of pro-MMPs; (iii) via regulation of activation by proenzymes and (iv) the inhibition of the active enzymes via inhibitors (Fig. 3.2).

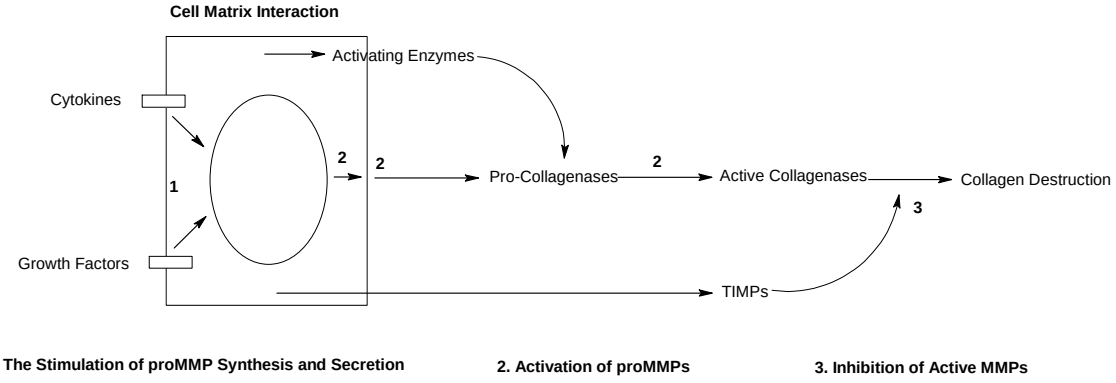

Figure 3.2. Levels of MMP control using collagenase as an example[1].

3.2.3.1 Synthesis and Secretion of MMPs

MMPs are secreted by a variety of connective tissue and pro-inflammatory cells including fibroblasts, osteoblasts, endothelial cells, macrophages, neutrophils and lyphocytes[6]. The pro-inflammatory cytokines interleukin-1 (IL-1) and tumour necrosis factor-α (TNF-α) stimulate numerous cell types, including chondrocytes, to secrete both collagenase and stromelysin[7]. Recent studies have shown that direct contact between T-lymphocytes and monocytes is a major pathway to up-regulate MMP biosynthesis and factors produced by T-cells can also increase collagenase synthesis by dermal fibroblasts[8].

3.2.3.2 Activation of the Proenzymes

All MMPs are secreted in a proenzyme (zymogen) form. A propeptide, containing a conserved sequence PRCGVPD, is lost during activation. A cysteine residue is attached to the catalytic zinc ion, and disruption of this interaction initiates activation[9]. Complete *in*

vivo activation is achieved by removal of the propeptide proteolytically, either autocatalytically or by other proteinases. The active enzyme can now bind to its substrate, and the zinc ion at the active site can hydrolyse susceptible bonds in the protein substrates[10].

3.2.3.3 Inhibition of Active Enzymes

Active MMPs are inhibited by TIMPs, which are found connective tissue[11]. TIMP-1 is a 28-kDa glycoprotein held by 6 disulfide bonds to form two main domains. The protein is highly stable to both low pH and temperature. The mechanism of inhibition by TIMP-1 is unknown. The inhibitor binds tightly to the active forms of MMPs in a 1:1 ratio[12]. TIMPs play an important role in controlling connective tissue breakdown by blocking the action of the activated MMPs and also preventing activation of the proenzymes[13].

3.2.4 The Gelatinases: MMP-2 and MMP-9

These two MMPs are the most abundant enzymes of the family, occurring prominently in mammalian blood. MMP-2 (Fig. 3.3) and MMP-9 (Fig. 3.4) play a crucial role in the breakdown of the extracellular matrix during cell migration and tissue remodelling[14]. The gelatinases are also indicated in a growing number of chronic chromic cardiovascular pathologies including heart failure, atherosclerosis and abdominal aneurysms. MMP-2 has also recently been implicated in many acute cardiovascular processes such as: platelet aggregation, regulation of vascular tone and modulation of the inflammatory response[15]. MMP-9 is most closely involved with metastasis of cancer cells[16].

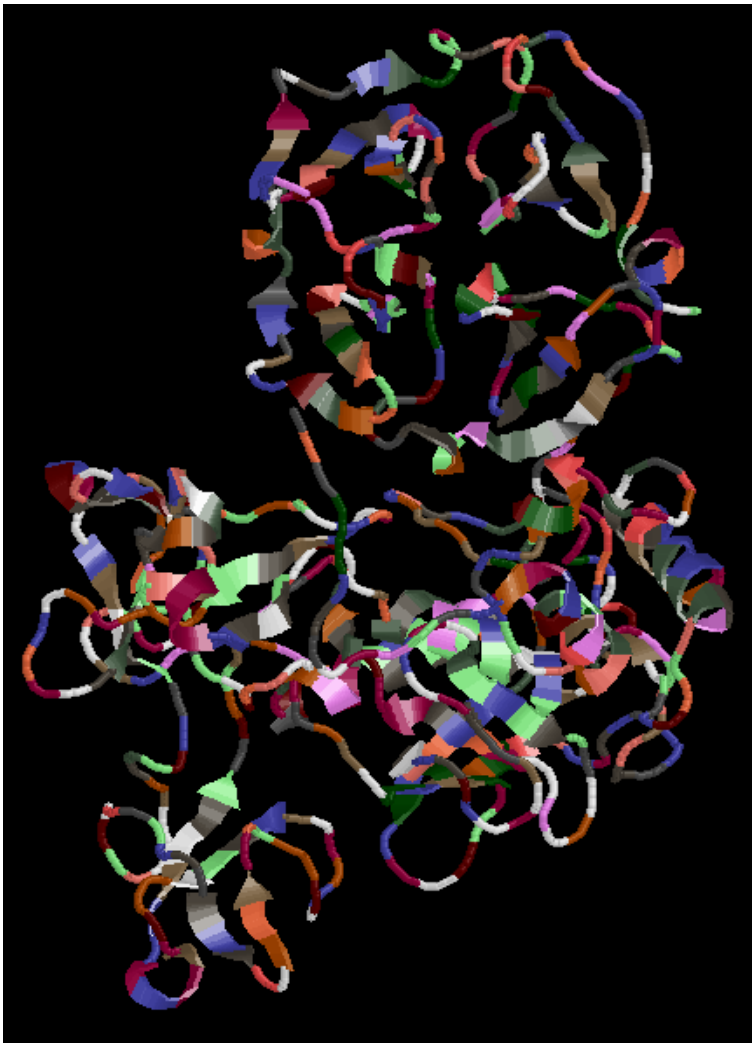

Figure 3.3. Structure of MMP-2[17].

Figure 3.4. Structure of MMP-9[18].

3.2.5 Prospects for the Therapeutic Inhibition of MMPs

MMPs have been heralded as promising targets for cancer therapy, and consequently a large number of natural and synthetic MMP inhibitors have been identified as cytostatic and anti-angiogenic agents. Many of these compounds have begun to undergo clinical trials[6]. Creating proteinase inhibitors that are therapeutically active is a daunting task. Besides having the required potency, the compound needs to be bioavailable, preferably after oral dosing. After administration, the drug must enter the circulation and reach the

desired concentration in the tissues. The compound must be specific for the target enzyme family and must not be antigenic. Any toxic side effects should also be eliminated[19].

3.2.6 Design of MMP Inhibitors

The direction that has been employed in the design of inhibitors is to select a zinc chelating ligand and attach it to a peptide that mimics the cleavage site in the MMPs target substrates[1]. Therefore, metalloproteinase inhibitors can be based on: (i) substrate cleavage sites[20]; (ii) sites cleaved in proteinase inhibitors[21]; (iii) inhibitory sequences such as the propeptide zinc-binding region[22] and (iv) sequences cleaved during activation of one MMP by another[21]. It has been suggested that the principle of MMP inhibition should initially be tested with broad-spectrum inhibitors to determine the potential of these compounds.

3.2.6.1 Tetracyclines as Inhibitors of MMP

The antibiotic tetracycline (**3.4**) and related compounds, such as doxycycline (**3.1**) and minocycline (**3.2**), exhibit inhibitory activity against collagenase, although the mechanism of inhibition is unknown. These tetracyclines have MMP inhibitory activity that is distinct from their antimicrobial property. These compounds are already in clinical use, and may give valuable information on MMP inhibition[1]. Doxycycline (**3.1**) is the most potent inhibitor of MMPs in this class of compounds, and has been shown to interact with Ca^{2+} and Zn^{2+} structural ions[15].

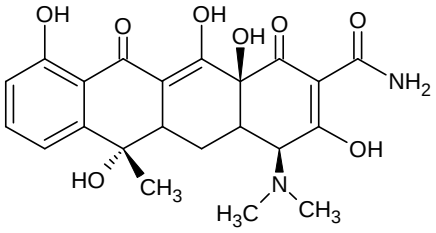

(**3.4**)

3.3 Results and Discussion

3.3.1 Western Blot of MMP-2 and MMP-9

A western blot was used to confirm the identity of MMP-2 and MMP-9 in the horse serum, using primary antibodies (rabbit anti-MMP-2 and chicken anti-MMP-9) that bind specifically to MMP-2 and MMP-9. Specific enzyme-linked secondary antibodies (anti-rabbit IgG alkaline phosphatase conjugate for MMP-2 and anti-chicken IgG alkaline phosphatase conjugate for MMP-9) and an appropriate substrate (BCIP and NBT) were used.

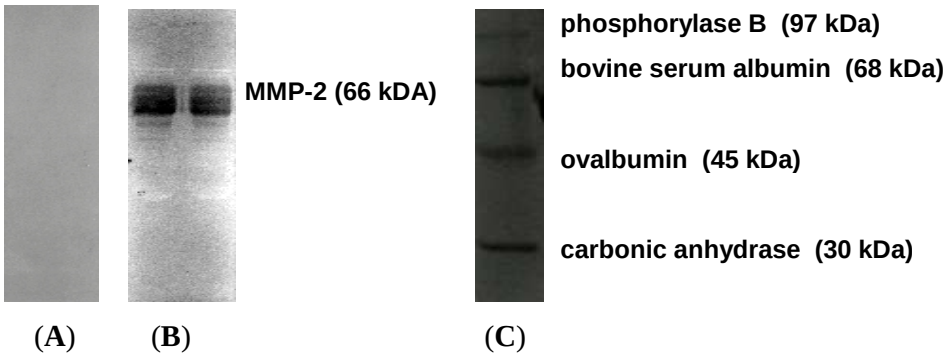

Figure 3.5. Western blots of control (**A**) of MMP-2 in horse serum, showing a negative result for MMP-2 in the absence of a MMP-2 pre-immune antibody, horse serum sample (**B**) displaying a positive result for the presence of MMP-2 in the presence of an MMP-2 pre-immune antibody and blot (**C**) is a lane containing M_r markers.

The Western blot for MMP-2 (**B**) which was treated with MMP-2 pre-immune shows specificity of the primary antibody for MMP-2, at 66 kDa [determined by a M_r marker (**C**)], confirming the presence of MMP-2 in horse serum (Fig. 3.5). Omission of the MMP-2 pre-immune antibody during preparation showed no bands (**A**).

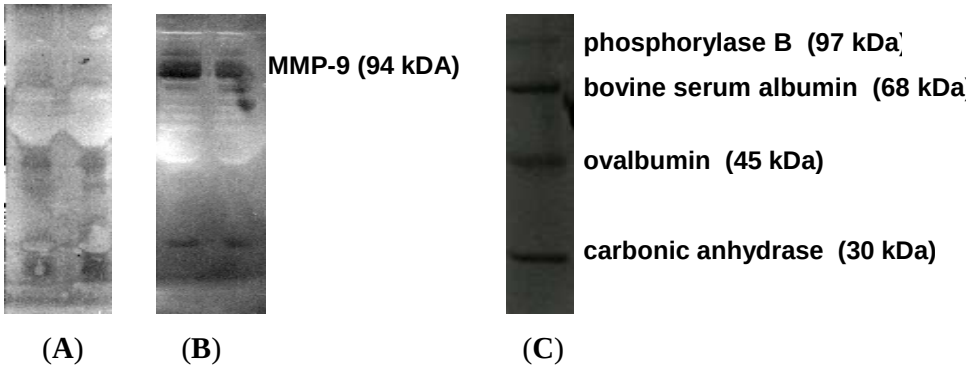

Figure 3.6. Western blots of control (**A**) of MMP-9 in horse serum, showing a negative result for MMP-9 in the absence of a MMP-9 pre-immune antibody, horse serum sample (**B**) displaying a positive result for the presence of MMP-9 in the presence of an MMP-9 pre-immune antibody and blot (**C**) is a lane containing M_r markers.

The Western blot for MMP-9 (**B**) which was treated with MMP-2 pre-immune shows specificity of the primary antibody for MMP-9, at 94 kDa [determined by a M_r marker (**C**)], confirming the presence of MMP-9 in horse serum (Fig. 3.6). Omission of the MMP-2 pre-immune antibody during preparation showed no bands (**A**).

3.3.2 Zymography

Aloin (**3.3**) and synthetic derivatives were screened for their possible gelatinolytic inhibitory characteristics, using zymography (see Section 3.5.1.2), against horse serum MMP-2 and MMP-9. The compounds were applied at concentrations ranging from 10 mM to 0.05 mM. EDTA, a strong zinc chelator, was used as an indication of complete enzyme inhibition. The inhibitory activity of aloin (**3.3**) and derivatives was compared to that of doxycycline (**3.1**), used clinically as a MMP inhibitor. Proteolytic activity was indicated by the presence of clear bands on a dark background and the intensity of the band being proportional to the MMP-2 and MMP-9 activity.

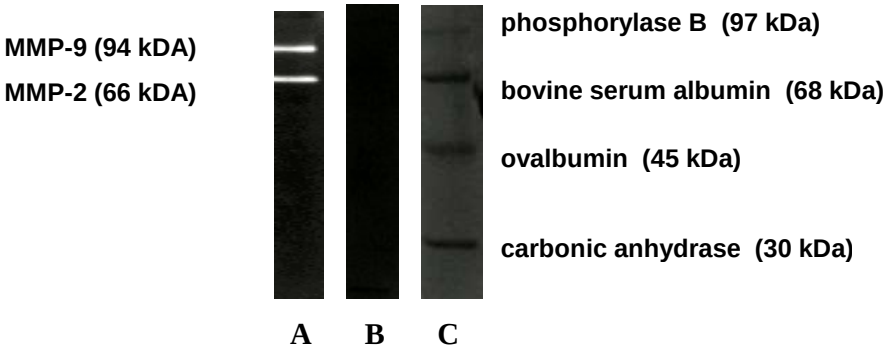

Figure 3.7. Positive control (**A**) zymogram in gelatinase buffer showing native activity of MMP-9 and MMP-2 in horse blood, negative control (**B**) zymogram in gelatinase buffer containing EDTA, displaying complete inhibition of MMP-9 and MMP-2 and gel (**C**) is a lane containing M_r markers.

The identity of both MMP-9 and MMP-2 were confirmed by their M_r, judged using M_r markers (Fig. 3.7) and a western blot (see Section 3.3.1**)**. The positive control (**A**) served as a reference for the subsequent zymograms containing potential MMP-2 and MMP-9 inhibitors derived from aloin. The negative control (**B**) contains EDTA, which binds strongly to the catalytic zinc ion and other ions in the MMPs structure. This results in the inhibition of MMP activity, indicating what would be observed in the absence of MMP activity and confirms the identity of the enzymes being metalloproteinases. Cathepsins, enzymes also capable of gelatinase activity, are also occasionally found in mammalian serum[23]. Since no activity was observed in the presence of EDTA, it can be concluded that the gelatinase activity was due to metallo-proteinases, and not cathepsins.

3.3.2.1 Doxycycline (3.1) Zymograms

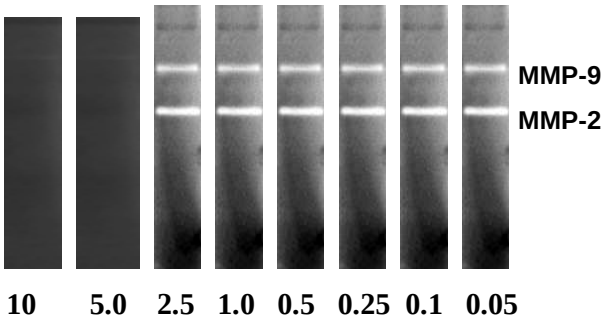

Figure 3.8. Zymograms displaying the effect of various doxycyline (**3.1**) concentrations, i.e. from 10 mM to 0.05 mM incorporated into the gelatinase buffer.

Doxycycline (**3.1**) inhibits both MMP-2 and MMP-9 at concentrations of 10 mM and 5 mM. Activity is restored when concentrations are dropped to 2.5 mM to 0.05 mM (Fig. 3.8).

3.3.2.2 Aloin (3.3) Zymograms

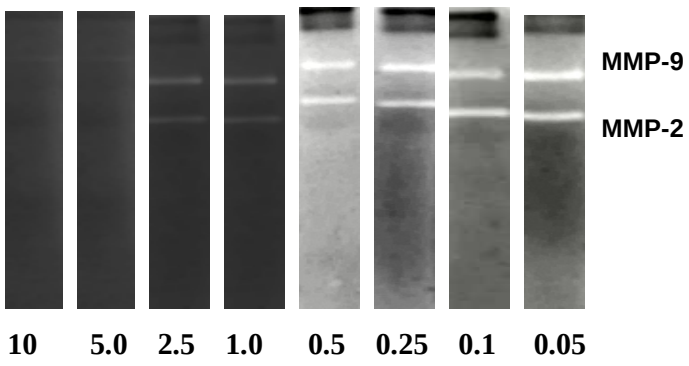

Figure 3.9. Zymograms displaying the effect of various aloin (**3.3**) concentrations, i.e. from 10 mM to 0.05 mM incorporated into the gelatinase buffer.

Aloin (**3.3**) inhibits both MMP-2 and MMP-9 at a concentration of 10 mM. MMP-2 and MMP-9 activity is partially restored at aloin (**3.3**) concentrations of 5.0 mM to 1.0 mM (Fig. 3.9). Complete MMP-2 and MMP-9 activity is restored at aloin (**3.3**) concentrations of 0.5 mM to 0.05 mM.

3.3.2.3 Homonataloin (3.5) Zymograms

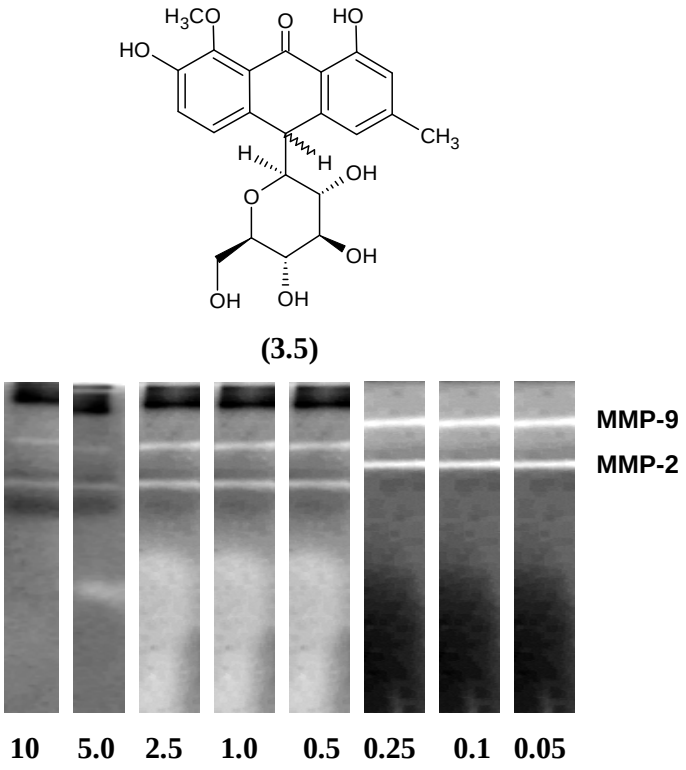

(3.5)

Figure 3.10. Zymograms displaying the effect of various homonataloin (**3.5**) concentrations, i.e. from 10 mM to 0.05 mM incorporated into the gelatinase buffer.

Homonataloin (**3.5**) displays slight inhibitory activity of both MMP-2 and MMP-9 at concentrations of 10 mM to 5.0 mM (Fig. 3.10). Complete MMP-2 and MMP-9 activity was restored from homonataloin (**3.5**) concentrations of 2.5 mM to 0.05 mM.

3.3.2.4 Aloe-emodin (3.6) Zymograms

(3.6)

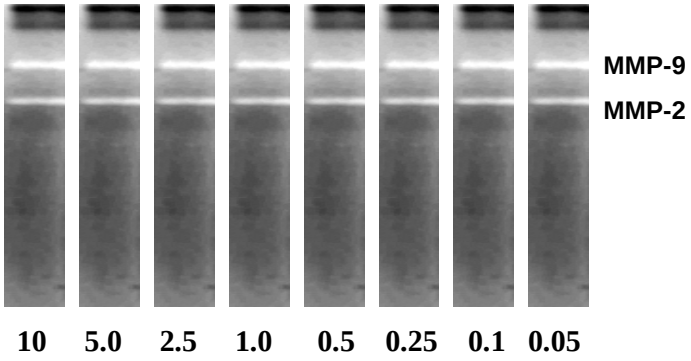

Figure 3.11. Zymograms displaying the effect of various aloe-emodin (**3.6**) concentrations, i.e.,from 10 mM to 0.05 mM incorporated into the gelatinase buffer. Aloe-emodin (**3.6**), which was virtually insoluble in the gelatinase buffer, displayed no inhibitory effects on neither MMP-2 nor MMP-9 at aloe-emodin (**3.6**) concentrations at10 mM to 0.05 mM (Fig. 3.11).

3.3.2.5 Nataloe-emodin (3.7) Zymograms

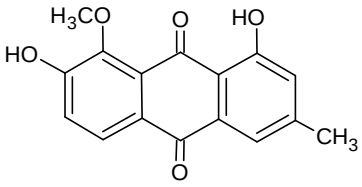

(3.7)

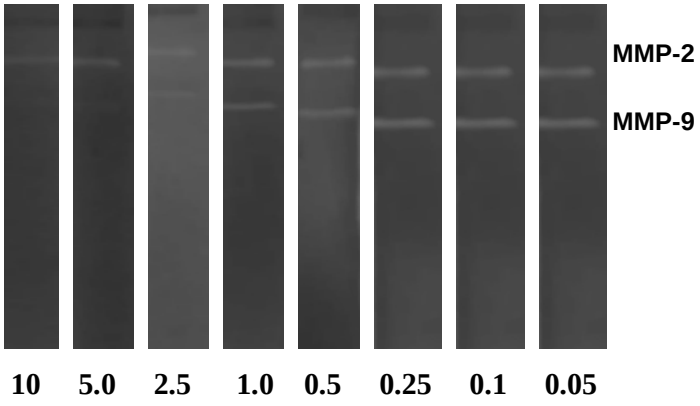

Figure 3.12. Zymograms displaying the effect of various nataloe-emodin (**3.7**) concentrations, i.e. from 10 mM to 0.05 mM incorporated into the gelatinase buffer.

Nataloe-emodin (**3.7**) shows high inhibition of MMP-2 and moderate inhibition of MMP-9 at 10 MM and 5.0 mM inhibitor concentrations (Fig. 3.12). The activity of both MMP-2 and MMP-9 is slightly reduced at a nataloe-emodin concentration of 2.5 mM. Complete MMP-2 and MMP-9 activity is restored from nataloe-emodin (**3.7**) concentrations of 1.0 mM to 0.05 mM.

3.3.2.6 Rheinal (3.8) Zymograms

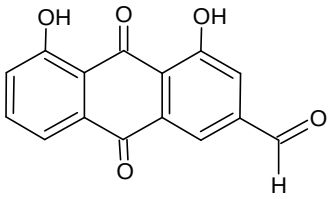

(3.8)

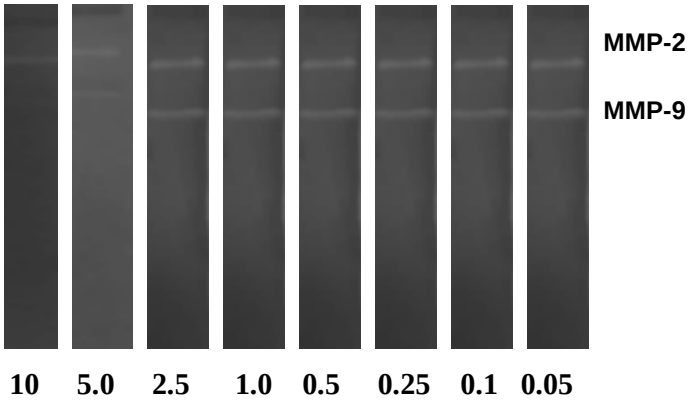

Figure 3.13. Zymograms displaying the effect of various rheinal (**3.8**) concentrations, i.e. from 10 mM to 0.05 mM incorporated into the gelatinase buffer.

Rheinal (**3.8**) shows high inhibition of MMP-2 and moderate inhibition of MMP-9 at 10 MM and 5.0 mM inhibitor concentrations (Fig. 3.13). The activity of both MMP-2 and MMP-9 is restored at rheinal (**3.8**) concentrations of 2.5 mM to 0.05 mM.

3.3.2.7 Rhein (3.9) Zymograms

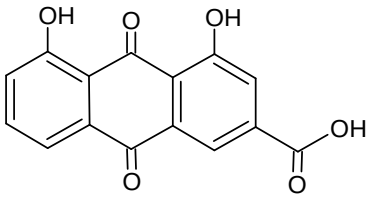

(3.9)

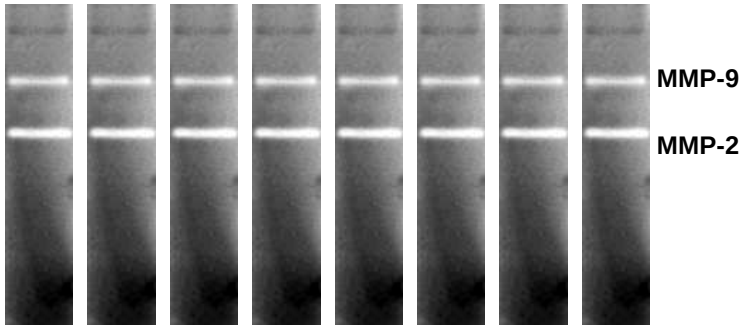

10 5.0 2.5 1.0 0.5 0.25 0.1 0.05

Figure 3.14. Zymograms displaying the effect of various rhein (**3.9**) concentrations, i.e. from 10 mM to 0.05 mM incorporated into the gelatinase buffer.

Rhein (**3.9)** displayed no inhibitory effects on neither MMP-2 nor MMP-9 at rhein (**3.9**) concentrations at 10 mM to 0.05 mM (Fig. 3.14).

3.3.2.8 11-(Pyrrolidin-1-yl)chrysophanol (3.10) Zymograms

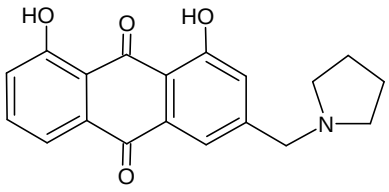

(3.10)

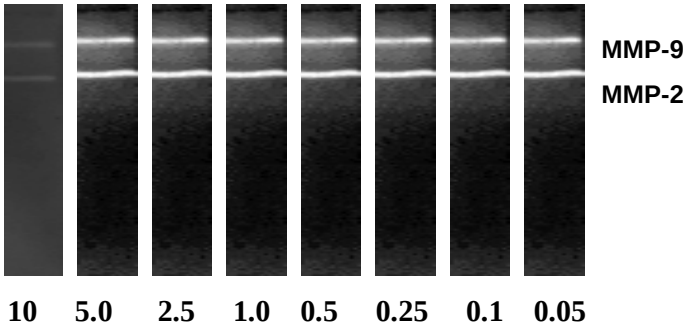

Figure 3.15. Zymograms displaying the effect of various 11-(pyrrolidin-1-yl)chrysophanol (**3.10**) concentrations, i.e. from 10 mM to 0.05 mM incorporated into the gelatinase buffer.

11-(Pyrrolidin-1-yl)chrysophanol (**3.10)** displayed no inhibitory effects on neither MMP-2 nor MMP-9 at 11-(pyrrolidin-1-yl)chrysophanol (**3.10)** concentrations from 10 mM to 0.05 mM (Fig. 3.15).

3.3.2.9 11-(Piperidin-1-yl)chrysophanol (3.11) Zymograms

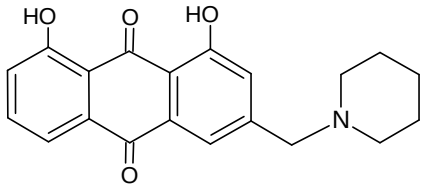

(**3.11**)

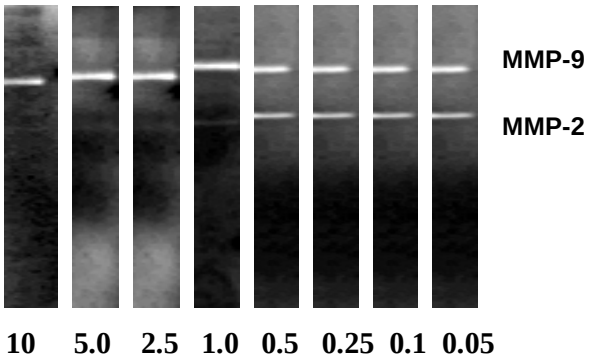

Figure 3.16. Zymograms displaying the effect of various 11-(piperidin-1-yl)chrysophanol (**3.11**) concentrations, i.e. from 10 mM to 0.05 mM incorporated into the gelatinase buffer.

11-(Piperidin-1-yl)chrysophanol (**3.11**) at concentrations of 10 mM to 1.0 mM showed remarkably high selective inhibition of MMP-2. The activity of MMP-2 was restored from 11-(piperidin-1-yl)chrysophanol (**3.11**) concentrations of 0.5 mM to 0.05 mM (Fig. 3.16). MMP-9 activity was unaffected at all concentrations of 11-(piperidin-1-yl)chrysophanol (**3.11**).

3.3.2.10 11-(Morpholin-1-yl)chrysophanol (3.12) Zymograms

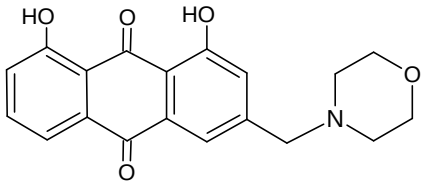

(3.12)

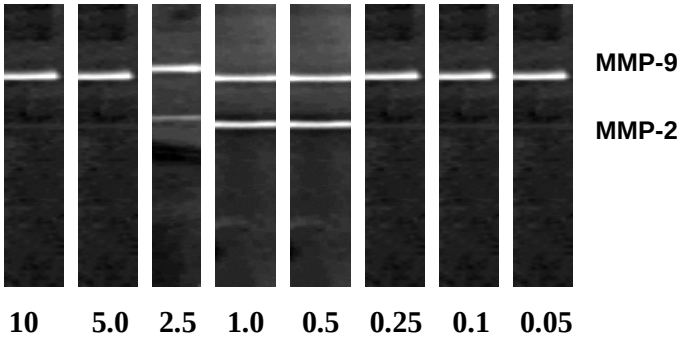

Figure 3.17. Zymograms displaying the effect of various 11-(morpholin-1-yl)chrysophanol (**3.12**) concentrations, i.e. from 10 mM to 0.05 mM incorporated into the gelatinase buffer.

11-(Morpholin-1-yl)chrysophanol (**3.11**), at concentrations of 10 mM to 5.0 mM displayed high inhibition of MMP-2. Strangely, at 11-(morpholin-1-yl)chrysophanol (**3.11**) concentrations of 2.5 mM to 0.5 mM, MMP-2 activity was fully restored, only to diminish again at 11-(morpholin-1-yl)chrysophanol (**3.11**) concentrations of 0.25 mM to 0.05 mM. This effect is possibly attributed to experimental error. MMP-9 activity was unaffected at all concentrations of 11-(morpholin-1-yl)chrysophanol (**3.11**).

3.3.2 Inferences and Discussion of Zymograms

A study by Barrentes and Guinea[2] reported that aloin (**3.3**) displayed good inhibitory properties against *Clostridium histolyticum* collagenase (ChC) and granulocyte MMP-8. The inhibitory action of aloin was compared to that of doxycycline (**3.1**), a structurally similar anthraquinone that is a well known broad range MMP-inhibitor. The anthrones aloin (**3.3**) and homonataloin (**3.5**) and their synthetic derivatives, which were either isolated or synthesized, have never been tested for their possible inhibitory activity against MMP-2 and MMP-9. These two enzymes play essential regulatory roles in the body, but are also involved in a growing number of pathological conditions[15,16]. Most MMP-2 and MMP-9 inhibitors target the zinc ion in the enzymes catalytic site[5]. The action of doxycycline (**3.1**) and aloin (**3.3**) has been reported to proceed via a non-competitive mechanism[2], implying that these compounds indirectly affect the zinc catalytic site. Thus, studying the mode of action of this class of compounds could be very useful in designing new MMP-inhibitors.

Aloin (**3.3**) and doxycycline inhibited both MMP-2 and MMP-9 at concentrations of 5 mM and 10 mM. Aloin (**3.3**) continued to moderately inhibit these enzymes at concentrations of 2.5 mM and 1.0 mM. At these concentrations for doxycycline (**3.1**) enzyme activity was completely returned, implying that aloin (**3.3**) displays higher MMP-2 and MMP-9 inhibitory properties than doxycycline (**3.1**). A similar result has been reported for MMP-8[2], which further reinforces the inhibitory activities found in this investigation.

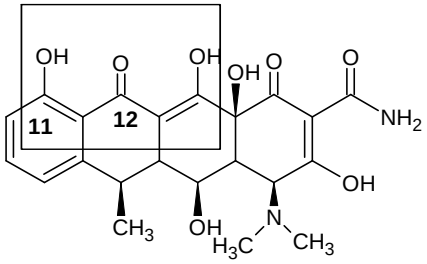

(**3.1**)

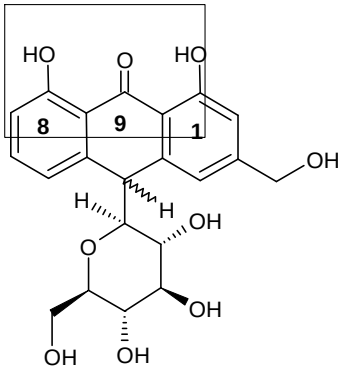

(**3.3**)

The ketone at C-12 and the OH group at C-11 on the doxycyline (**3.1**) structure have been reported to be essential for activity[2]. Comparing the structures of doxycycline (**3.1**) to the structure of aloin (**3.3**), the carbonyl group at C-9, between the hydroxyls at C-8 and C-1 on the anthrone, is consistent with that pharmacophore profile and it seems reasonable to postulate that the aloin (**3.3**) inhibition of the MMPs is due to an interaction similar to that between doxycycline (**3.1**) and MMPs.

Aloin (**3.3**) has a moderately high affinity for binding to calcium ions, as this is experimentally shown in the aloin-calcium salt formation (see Chapter 2, Section 2.3.5). This was used as a method of selectively precipitating an aloin-calcium salt from the *A. marlothii* leaf exudate that contains many other chemical constituents[24]. MMPs require Ca^{2+} as enzymatic cofactors that are necessary for their activity[2]. MMPs also contain calcium ions within their quaternary protein structure which are vital for maintaining the structural integrity of these enzymes[1]. Thus based on the affinity aloin (**3.3**) has for calcium ions, it can be proposed that aloin (**3.3**) interacts/chelates with either (i) the Ca^{2+} cofactors in solution or (ii) the calcium ions incorporated into the MMP-structure. These aloin-calcium interactions could lead to either diminished MMP activity, due to lack of Ca^{2+} cofactors, or result in a change in the structural conformation of the enzyme, rendering the catalytic zinc site inactive.

Homonataloin (**3.5**) displays slight inhibition against MMP-2 and MMP-9 at high concentrations, i.e. at 10 mM and 5 mM. Comparing the structures of homonataloin (**3.5**) to aloin (**3.3**), it can be seen that homonataloin (**3.5**) has a methoxy-group at C-8 compared to the hydroxyl-group in aloin (**3.3**). This methyl-group attached to the oxygen atom at C-8 sterically restricts interactions of the C-8 oxygen with other groups. Since it has been proposed that the interaction of this C-8 oxygen atom plays a role in MMP-inhibition, it seems logical to assume that this methoxy-group lowers the MMP-inhibitory properties of homonataloin (**3.5**) compared to that of aloin (**3.3**).

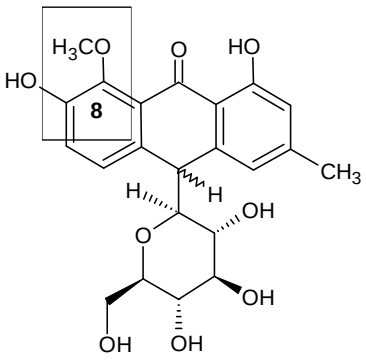

(**3.5**)

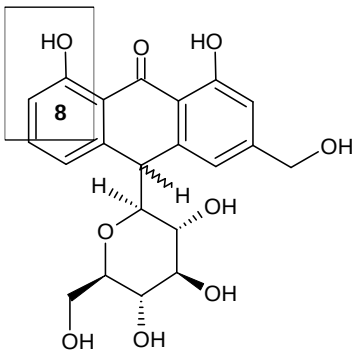

(**3.3**)

The biggest problem with using aloin (**3.3**) or homonataloin (**3.5**) as MMP-inhibitors is that they are unstable in solution since they are susceptible to oxidation of their sugar moieties[25]. Thus creating aloin/homonataloin derivatives without the sugar moieties should greatly increase their stability in solution.

Aloe-emodin (**3.6**) was poorly soluble in the gelatinase buffer solution and consequently showed no inhibition of MMP-2 or MMP-9 at any concentration. Nataloe-emodin (**3.7**), which has better solubility in the gelatinase buffer than aloe-emodin (**3.6**), showed complete inhibition of MMP-2 and MMP-9 at concentrations of 10 mM, and moderate inhibition of these enzymes at concentrations of 5 mM and 2.5 mM. Similarly to aloe-emodin (**3.6**), rheinal (**3.8**), was poorly soluble in the gelatinase buffer solution but displayed good inhibition of both MMP-2 and MMP-9 at concentrations of 10 mM and 5 mM. In contrast, rhein (**3.9**) had excellent solubility in the gelatinase buffer solution yet failed to inhibit the MMPs at any concentration.

Rhein (**3.9**) is the active metabolite of diacerein (**3.13**), which is a drug that has been used in clinical studies to treat to the symptoms of osteoarthritis. Rhein (**3.9**) has been reported by Tamura *et al*. to down-regulate the production of pro-MMPs -1, -3, -9 and -13 and up-regulate the production of TIMPs in cultured rabbit articular chondrocytes[26]. The exact mechanism of the therapeutic action of rhein on osteoarthritis is unknown, but it has not been reported to be an MMP-inhibitor, specifically of MMP-2 or MMP-9, which was also established in this study.

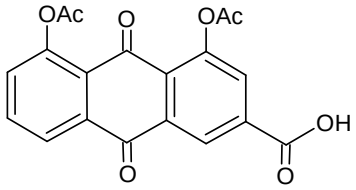

(**3.9**)

11-(Pyrrolidin-1-yl)chrysophanol (**3.10**) did not show any MMP-2 or MMP-9 inhibition, whilst 11-(piperidin-1-yl)chrysophanol (**3.11**) and 11-(morpholin-1-yl)chrysophanol (**3.12**) did. 11-(Piperidin-1-yl)chrysophanol (**3.11**) and 11-(morpholin-1-yl)chrysophanol (**3.12**) have 6-membered nitrogen-containing rings and 11-(pyrrolidin-1-yl)chrysophanol (**3.10**) has a 5-membered nitrogen-containing ring. Thus it can be assumed that this difference in ring size plays a role in the inhibition of MMP-2 and MMP-9. This difference in ring size is most probably influential in a peripheral ligand interaction of the nitrogen-atom in the 6-membered ring and a region in the protein structure.

11-(Piperidin-1-yl)chrysophanol (**3.11**) showed selective inhibition of MMP-2 at concentrations of 10 mM to 1.0 mM. Similarly, 11-(morpholin-1-yl)chrysophanol (**3.12**) selectively inhibited MMP-2 at concentrations of 10 mM and 5 mM. These results are highly promising as selective MMP-2 inhibition is an attractive proposition, since MMP-2 is one of the major enzymes involved in cancer metastasis[16].

3.4 Conclusion

The inhibitory activity of aloin (**3.3**) and derivatives were successfully tested against MMP-2 and MMP-9 using zymography. Aloin (**3.3**), nataloe-emodin (**3.7**) and rheinal (**3.8**) displayed mild inhibition against MMP-2 and MMP-9. Homonataloin (**3.5**), aloe-emodin (**3.6**), rhein (**3.9**) and 11-(pyrrodin-1-yl)chrysophanol (**3.10**) also showed either poor or no inhibition against MMP-2 and MMP-9. 11-Piperidin-1-yl)chrysophanol (**3.11**) and 11-(morpholin-1-yl)chrysophanol (**3.12**) displayed selective inhibition against MMP-2. Zymography is a qualitative biochemical technique, thus a quantitative study is also necessary to determine the stoichiometric efficacy of the inhibitors.

3.5 Experimental

All the chemicals used in this biochemical component of this research project were purchased from Sigma Aldrich.

3.5.1 General

3.5.1.1 Sodium Dodecyl Sulfate (SDS) Polyacrylamide Gel Electrophoresis (PAGE)

Polyacrylamide gel electrophoresis enables protein separation by differential migration to either the cathode or anode through a chemically inert matrix. This matrix is comprised of acrylamide and *N*,*N*′-methylene bisacrylamide co-monomers that undergo a free radical mediated polymerization to create a meshwork of pores that sterically constrict protein movement. Ammonium persulfate is the polymerization radical-initiator, and tetramethyethylenediamine (TEMED) (a donor and acceptor of free radicals) is the catalyst facilitating the process. The molecular weight (M_r) range of protein separation is determined by the total acrylamide concentration (acrylamide and bisacrylamide) and the acrylamide : bisacrylamide ratio[27].

When SDS is absent, the direction and extent of protein migration depends mainly on the individual mass-to-charge ratios and complicates M_r determinations. SDS partially denatures non-sulfide-linked oligomeric structures and the secondary structure of proteins, adding a nett-negative charge on the proteins due to the strongly anionic group on the detergent. The micelle formed by the SDS may otherwise be unilamellar (due to hydrophobic interactions) or bilamellar (due to electrostatic interactions). The addition of a reducing agent (e.g. β-mercaptoethanol), combined with heating, allows the intra- and inter-disulfide bridges to be broken, and the polypeptide chains to be linearised by thermally overcoming folding kinetics. The resulting peptide chain can bind to SDS, allowing protein migration in an electric field to solely rely on the basis of M_r (assuming a constant SDS binding ratio). This occurs as all the proteins now carry a nett negative charge and, therefore, migrate to the anode[27].

3.5.1.2 Zymography

Zymography is a SDS-PAGE gel that enables the detection of enzyme activity, after the proteins have been electrophoresed[28]. In zymography, the resolving gel contains incorporated proteinase substrate (e.g. gelatin, collagen, fibrin, casein). Substrate concentration is crucial for optimal band formation, resolution and detection. Non-reducing and non-heating conditions are used to retain enzyme activity. The gel was washed with Triton X-100, after electrophoresis, to removes SDS bound to the protein and renature the enzyme. The SDS become easily detached at this dilution, having a significantly higher critical micelle concentration (CMC) than Triton X-100 (CMC_{SDS} = 8.27 mM; $CMC_{TX\text{-}100}$ = 0.24 mM[27]). The gel was subsequently incubated at optimal temperature in the appropriate buffer, which contains the necessary enzyme cofactors and at the optimum enzyme pH. Enzyme activity was detected by staining the gels with either a Coomassie Blue or Amido black solution. Activity appears as clear, translucent bands against a stained undigested background.

Zymography, using fresh horse blood, was utilized in this study for the detection of MMP-2 and MMP-9. Whole blood was allowed to clot before it was centrifuged, and the serum was separated from the lower red blood cell layer. The MMP substrate chosen was gelatin, a substrate cleaved by a broad range of proteinases from other classes (e.g. cathepsins) in addition to MMP-2 and MMP-9. MMP specificity was ensured by the use of additional gelatinase buffer containing EDTA

Activity of these gelatinases, and not the cathepsins (if present) will be inhibited by the EDTA, owing to the chelation of the metal in the catalytic active site.

3.5.1.3 Western Blotting

Western blotting is a biochemical technique that provides information about antibody specificities, the target antigen, M_r, activation status (i.e. enzyme pro-form vs. active species), oligomeric arrangement or post-translational modifications.

The thickness of the SDS-PAGE gel and % transmittance (%T) affects the protein transfer time, as well the efficiency of the transfer onto the nitrocellulose membrane. Generally a

thinner gel (0.1-0.5 mm) promotes better protein transfer, but may limit the amount of protein that can be loaded. When a SDS-PAGE gel has a high %T, protein transfer is greatly hindered. Also, if the %T of the SDS-PAGE gel is too low, band resolution and separation is reduced.

Blocking steps prevent non-specific protein association with the nitrocellulose membrane.

3.5.2 Materials and Methods

3.5.2.1 SDS-PAGE Gel Reagents

Acrylamide/bisacrylamide monomer stock solution (30% T, 2.67 C). Acrylamide monomer (58.4 g) and *N,N'*-methylene bisacrylamide (1.60 g) were dissolved in d.H_2O (200 ml). The solution was then filtered through Whatman No. 1 filter paper and stored at RT in an amber bottle.

Running gel buffer (1.5 M Tris-HCl, pH 8.8). Tris (36.3 g) was dissolved in d.H_2O (180 ml), titrated to pH 8.8 with HCl [30% (v/v)], and made up to 200 ml. The solution was stored in a plastic bottle at 4 ^{o}C.

Stacking gel buffer (500 mM Tris-HCl, pH 6.8). Tris (12.0 g) was dissolved in d.H_2O (180 ml), titrated to pH 6.8 with HCl (30% v/v), and made up to 200 ml. The solution was stored in a plastic bottle at 4 ^{o}C.

SDS stock solution [10% (w/v)]. SDS (10 g) was dissolved in d.H_2O (100 ml) and stored at RT.

Electrode buffer [25 mM Tris-HCl, 192 mM glycine, 0.1% (m/v) SDS, pH 8.3]. Tris (0.75 g), glycine (3.6 g), and SDS stock (2.5 ml) were dissolved in d.H_2O (247.5 ml).

Ammonium persulfate initiator solution [10 % (w/v)]. Ammonium persulate (0.05 g) were dissolved in d.H_2O (0.5 ml) and stored at 4 ^{o}C for up to a week.

Non-reducing sample loading buffer [62.5 mM Tris, 10% (v/v) glycerol, 2% (w/v) SDS, 0.025% (w/v) bromophenol blue, pH 6.6]. Stacking gel buffer (1 ml), d.H_2O (3.4 ml), glycerol (1.6 ml), SDS [1.6 ml of a 10% (w/v) solution] and bromophenol, blue [0.4 ml of a 0.5% (w/v) solution in d.H_2O] were stirred together.

Renaturation solution [2.5 % (v/v) Triton X-100]. Triton X-100 (6.25 ml) was dissolved in d.H_2O (250 ml) and stored at 4 ^oC.

Stock gelatin solution [1% (w/v)]. Porcine skin gelatin (300 bloom) (0.1 g) was added to d.H_2O (10 ml). The solution was heated whilst stirring vigorously to dissolve the gelatin.

Gelatinase Zymography buffer [50 mM Tris-HCl, 200 mM NaCl, 5 mM $CaCl_2$, 0.02% (v/v) Brij 35, pH 7.5 at 37^{o}C]. Tris (0.1 g), NaCl (1.17 g), $CaCl_2.2H_2O$ (0.109 g) and Brij 35 [67 µl of a 30% (v/v)] solution were dissolved in d.H_2O (90 ml) and heated to 37 ^oC. The pH was titrated to 7.5 with HCl [30% (v/v)] and the volume was made up to 100 ml.

Amido Stain Stock Solution [1% (w/v)]. Amido black (1.0 g) was dissolved in d.H_2O (100 ml) by stirring for 1 h at RT. The solution was then filtered through Whatman no. 1 filter paper and stored at RT.

Staining Solution [0.1% (w/v) amido black, 30% (v/v) methanol, 10% (v/v) acetic acid]. Stain stock solution (50 ml), methanol (150 ml), acetic acid (50 ml) and d.H_2O (300 ml) were mixed together at RT.

Destaining Solution [30% (v/v) methanol, 10% (v/v) acetic acid]. Methanol (150 ml), acetic acid (50 ml) and d.H_2O (300 ml) were mixed together at RT.

M_r markers. Standards for M_r determination were: phosporylase b (94 kDa), bovine serum albumin (68 kDa), ovalbumin (45 kDa), carbonic anhydrase (30 kDa), soybean trypsin inhibitor (20.1 kDa) and lysozyme (14 kDa). The lysophilised markers were reconstituted in non-reducing treatment buffer (100 ml), and aliquots were stored at 4 ^oC.

3.5.2.2 SDS-PAGE gel/Zymogram Procedure

The SDS-PAGE electrophoresis unit (Hoefer® Mighty Small) was assembled according to the manufacturers' instructions. The glass plates, plastic combs, plastic spacers and glass backings were cleaned with detergent and then with acetone. These components were then assembled in a gel caster.

Acrylamide monomer, gel buffer, d.H_2O, stock gelatin solution, SDS, ammonium persulfate and TEMED as indicated for the running gel (Table 3.2), were mixed together thoroughly. This running gel mixture was then carefully loaded onto the gel caster apparatus (overlaid with d.H_2O to exclude oxygen), to a depth of 2.5 cm from the top of the glass plate, and allowed to polymerise. After the running gel had set (~45 min), the d.H_2O was poured out and the desired stacking gel solution was made up as described in Table 3.2. The stacking gel mixture was then layered on top of the polymerised running gel. Plastic 10 well combs were placed into the stacking gel and polymerisation was allowed to occur (~20 min). The combs were removed and the gels were assembled into the electrophoresis apparatus. The serum is mixed with sample loading buffer (1:6 dilution ratio of serum : loading buffer) and the mixture is then agitated for 10 min at RT. Electrode buffer was made up, added, and the samples (10 µl) were carefully loaded onto the gels. During electrophoresis, the gels were cooled using a circulatory water bath (4 ^{o}C) and protein samples were separated at 36 mA (unlimited voltage).

Table 3.2. Reagent composition and proportions for two Tris-glycine gels containing 0.1% (w/v) gelatin

	Running gel (%)			**Stacking gel (%)**	
Reagent	12.5%	7.5%	5%	4%	3%
Monomer (ml)	6.25	3.75	2.5	0.94	0.71
Running gel buffer (ml)	3.75	3.75	3.75	-	-

Stacking gel buffer (ml)	-	-	-	1.75	1.75
10% SDS (µl)	150	150	150	70	70
d.H_2O (ml)	3.275	5.775	7.025	4.3	4.53
Ammonium Persulfate (µl)	75	75	75	50	50
TEMED (µl)	7.5	7.5	7.5	15	15
1% (w/v) Gelatin/Collagen (ml)	1.475	1.475	1.475	-	-

Once electrophoresis was complete, the gels were carefully removed and were soaked in renaturation solution (2 x 30 min, RT) and shaken on an orbital shaker. The gels were then rinsed in d.H_2O (30 min).

For gelatinase assays, the controls: (+) no inhibitor (d.H_2O); (-) known inhibitors (doxycyline, EDTA); and potential inhibitors (aloin and derivatives) were freshly solubilised in the gelatinase Tris-HCl incubation buffer used for developing the zymogram. The gel was cut into slices corresponding to the lanes which were put in different tanks and incubated at 37 ^{o}C for 36 h in the incubation buffer

The slabs were then stained (15-30 min) in amido black staining solution, and destained in the same solution without the amido black dye. After destaining, a light translucent band over a blue background was detected for gelatinase activity. The gels were then photographed and analysed.

3.5.2.3 Western Blot Reagents

Gershoni blotting buffer [25 mM Tris-HCl, 192 mM glycine, 20% (v/v) methanol, 0.01% (w/v) SDS, pH 8.3]. Tris (6.05 g), glycine (28.8 g) and SDS [2 ml of a 10% (w/v) solution] were dissolved in d.H_2O (1.6 l). Methanol (400 ml) was added to the solution, which was stored at -20 ^oC.

Ponceau S protein stain solution [0.1% (w/v) in 1% (v/v) acetic acid]. Ponceau S (0.1 g) and acetic acid (1 ml) were added to a 100 ml volumetric flask and made up to volume with d.H_2O.

Tris-buffered saline (TBS: 20 mM Tris-HCl, 200 mM NaCl, pH 7.4). Tris (2.42 g) and NaCl (11.69 g) were dissolved in d.H_2O (950 ml). The pH was adjusted to 7.4 with HCl and the volume was made up to 1 l with d.H_2O.

Blocking solution [5% (w/v) non-fat milk powder in TBS]. Non-fat milk powder (5 g) was dissolved in TBS (100 ml).

Alkaline phosphatase detection buffer (50 mM Tris-HCl, 5 mM $MgCl_2$, pH 9.5). Tris (0.61 g) and $MgCl_2.2H_2O$ (0.10 g) were dissolved in d.H_2O (90 ml). The pH was adjusted to 9.5 with HCl and the volume was made up with d.H_2O.

Alkaline phosphatase substrate solution [0.015% (w/v) BCIP, 0.03% (w/v) NBT in detection buffer]. BCIP (1.5 mg in 1 ml DMF) and NBT (3 mg) were dissolved in detection buffer (10 ml) just before use.

MMP-2 primary (pre-immune) antibody [L43 Cat P1 (20 µg/ml)]. L43 Cat P1 [14 µl of a 17.32 mg/ml stock solution] was dissolved in TBS (12 ml) just before use.

MMP-2 primary (immune) antibody (20 µg/ml). Rabbit anti-MMP-2 primary antibody [12 µl of a 19.76 mg/ml stock solution] was dissolved in TBS (12 ml) just before use.

MMP-9 primary (pre-immune) antibody [L43 Cat P1 (20 µg/ml)]. L43 Cat P1 [34 µl of a 7.00 mg/ml stock solution] was dissolved in TBS (12 ml) just before use.

MMP-9 primary (immune) antibody (20 µg/ml). Chicken anti-MMP-9 primary antibody [16 µl of a 15.04 mg/ml stock solution] was dissolved in TBS (12 ml) just before use.

MMP-2 secondary antibody [anti-rabbit IgG alkaline phosphatase conjugate]. MMP-2 secondary antibody [1 µl of a mg/ml stock solution] was dissolved in TBS (150 ml) just before use.

MMP-9 secondary antibody [anti-chicken IgG alkaline phosphatase conjugate]. MMP-9 secondary antibody [1 µl of a mg/ml stock solution] was dissolved in TBS (30 ml) just before use.

3.5.2.4 Western Blot Procedure

Following SDS-PAGE (Section 3.4.2.2), the gel was removed from the electrophoresis unit, and submerged (30 min) in ice-cold transfer buffer together with Hybond^{TM-C} nitrocellulose hybridization transfer membrane (0.45 µm) and Whatman filter paper. The transfer cassette (Hoefer® TE Series Transphor Electrophoresis Unit) was assembled and orientated in the electrophoresis chamber to ensure that the membrane was closest to the anode. The chamber was filled with ice-cold transfer buffer and stirred with a magnetic stirrer continuously. Protein transfer was performed at a constant current of 90 mA for 18 h. The gel and transfer membrane were then carefully removed from the cassette, and the outline of the gel was marked onto the membrane. The nitrocellulose membrane was rinsed with d.H_2O and then stained with Ponceau S to visualize the M_r markers, the sample protein profiles and to assess the efficiency of the transfer. The positions of the lanes and the markers were marked by pricking the membrane gently with a needle point. The Ponceau S was decolourised with TBS and the membrane was air-dried before probing.

The membrane was incubated (1 h, 10 ml/lane) with blocking solution to prevent non-specific adsorption of antibodies. The membrane was then washed in TBS (3 x 5 min, 10 ml/wash) and incubated with the appropriate primary antibody (2 h, 10 ml/lane). Following washing in TBS (3 x 5 min, 10 ml/wash), the membrane was incubated with the appropriate enzyme conjugated secondary antibody (1 h, 10 ml/lane). The membrane was washed as previously, immersed in the appropriate substrate solution (10 ml/lane) and

developed (5-10 min) until distinct bands were observed against a lightly coloured background. The membrane was rinsed with d.H_2O, dried and stored in the dark until photographed.

3.6 References

1. Cawston, T. E., *Pharmacology and Therapeutics*, 1996, **70**, 163-182.

2. Barrantes, E., Guinea, M., *Life Sciences*, 2003, **72**, 843-850.

3. Nagase, H., Woessner, J. F., *The Journal of Biological Chemistry*, 1999, **274**, 21491-21494.

4. Folgueras, A. R., Pendas, A. M., Sanchez, L. M., Lopez-otin, C., *International Journal of Developmental Biology*., 2004, 48, 411-424.

5. Bigg, H. F., Rowan, A. D., *Current Opinion in Pharmacology*, 2001, **1**, 314-320.

6. Verma, R. P., Hansch, C., *Bioorganic and Medicinal Chemistry*, 2007, **15**, 2223-2268.

7. Saklatvala, J., Pilsworth, L. M. C., Sarsfield, S. J., Gavinlovic, J., Heath, J., *Journal of Biochemistry*, 1984, **224**, 461-466.

8. Miltenburg, A. M. M., Lacraz, S., Welgus, H. G., Dayer, J. M., *Journal of Immunology*, 1995, **154**, 2655-2667.

9. Van Wart, H. E., Birkedal-Hansen, H., *Proceedings of the National Academy of Sciences*, 1990, **87**, 5578-5582.

10. Kleiner, D. E., Jr., Stetler-Stevenson, G., *Current Biology*, 1993, **5**, 891-897.

11. Cawston, T. E., Galloway, W. A., Mercer, E., Murphy, G., Reynolds, J. J., *Journal of Biochemistry*, 1981, **195**, 159-165.

12. Cawston, T. E., Murphy, G. M., Mercer, E., Galloway, W. A., Hazleman, B. L., Reynolds, J. J., *Journal of Biochemistry*, 1983, **211**, 313-318.

13. Denhardt, D. T., Feng, B., Edwards, D. R., Cocuzzi, E. T., Malyankar, U. M., *International Journal of Clinical Pharmacology Therapy and Toxicology*, 1993, **59**, 329-341.

14. Briknarova, K., Grishaev, A., Banyai, L., Tordai, H., Patthy, L., Llinas, M., *Col-2 Structure, Function and Dynamics*, 1999, **7**, 1235-1245.

15. Lalu, M. M., Cena, J., Chowdhury, R., Lam, A., Schulz, R., *British Journal of Pharmacology*, 2006, **149**, 31-42.

16. Seo, U. K., Lee, Y. J., Kim, J. K., Cha, B. Y., Kim, D. W., Nam, K. S., Kim, C. H., *Journal of Ethnopharmacology*, 2005, **97**, 101-106.

17. Morgunova, E., Tuuttila, A., Bergmann, U., Isupov, M., Lindqvist, Y., Schneider, G., Tryggvason, K., *Science*, 1999, **284,** 1667-1670.
18. Rowsell, S., Hawtin, P., Minshull, C.A., Jepson, H., Brockbank, S.M., Barratt, D.G., Slater, A.M., McPheat, W.L., Waterson, D., Henney, A.M., Pauptit, R.A., *Journal of Molecular Biology*, 2002, **319,** 173-181.
19. Docherty, A. J. P., O'Conell, J., Crabbe, T., Angal, S., Murphy, G., *Trends in Biotechnology*, 1992, **10**, 200-207.
20. Gray, S. D., Saneii, H. H., Spatola, A. F., *Biochemical and Biophysical Research Communications*, 1981, **101**, 1251-1258.
21. Sottrup-Jensen, L., Birkedal-Hansen, H., *Journal of Biological Chemistry*, 1989, **264**, 15781-15789.
22. Hanglow, A. C., Lugo, A., Walsky, R., Finch-Arieta, Lusch, M., Visnick, L., Fotouchi, N.,*Agents Actions 39 (Special Conference Issue)*, 1993, C148-C150.
23. Ishido, K., Kominami, E., *Biological Chemsitry*, 1998, 379, 131-135.
24. Reynolds, T., *Aloes: The Genus Aloe*, CRC Press LLC, New York, 2004, pp. 39-41.
25. Wamer, W. G., Vath, P., Falvey, D. E., *Free Radical Biology and Medicine*, 2003, **34**, 233-242.
26. Tamura, T., Kosaka, N., Ishiwat, J., Sato, S., Nagase, H., Ito, A., *Journal of the Osteoarthritis Research Society International*, 2001, 9, 257-263.
24. Price, B., *Neutrophil Tissue Inhibitor of Matrix Metalloproteinas-1: Novel Localisation, Mobilisation and Possible Role*, 2001, PhD thesis, University of KwaZulu-Natal.
25. Gabriel, O., Gersten, D. M., *Analytical Biochemistry*, 1992, **203**, 1-21

CHAPTER FOUR

ANTIPLASMODIAL ACTIVITY OF ALOIN AND DERIVATIVES

4.1 Introduction

Malaria affects 300-500 million people annually and 0.5-2.5 million people die from the disease[1]. The rapid spread of malaria together with the emergence of resistance against conventional anti-malarial drugs has put enormous pressure on public health systems to introduce new treatments. Chloroquine (**4.1**) and artemisinin derivatives are currently the two most widely used classes of antimalarials. Artemisinin (**4.2**), a natural product, has proven to be an invaluable lead compound in the production of potent antimalarials[2].

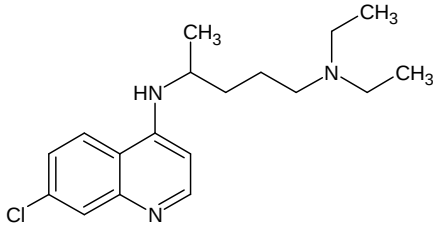

(**4.1**)

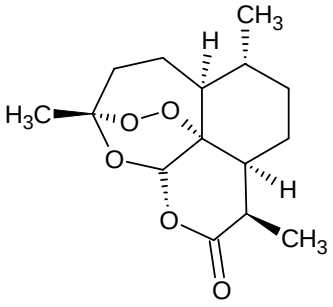

(**4.2**)

The *in vitro* antiplasmodial activity of aloin (**4.3**) against the chloroquine-resistant *Plasmodium falciparum* strain has been reported, with an IC_{50} value of 107.20 ± 4.14 μg ml^{-1} [3]. Homonataloin (**4.4**), an aloin analogue, displays more potent antiplasmodial activity then aloin (**4.3**), with an IC_{50} value of 13.46 ± 1.36 μg ml^{-1} [3]. Similarly to artemisinin (**4.2**), aloin (**4.3**) and homonataloin (**4.4**) are naturally occurring compounds which display considerable antiplasmodial activity. Thus the investigation of the antiplasmodial activity of derivatives of aloin (**4.3**) and homonataloin (**4.4**) could prove to be extremely valuable and useful from a medicinal perspective.

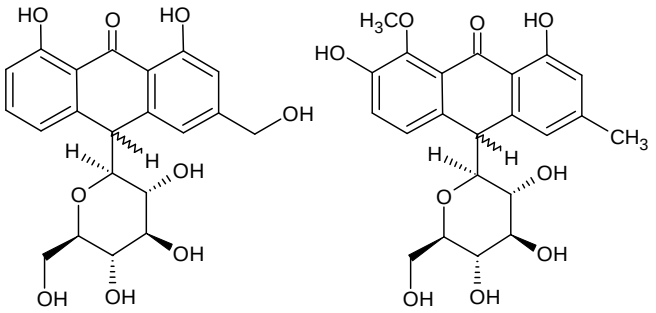

(4.3) **(4.4)**

4.2 Malaria and Antimalarials

4.2.1 Introduction

Malaria is a parasitic disease that is caused by the *Plasmodium* protozoa (single-celled parasites), which is mainly transmitted by the female *Anopheles* mosquito[4]. Malaria is prevalent throughout Africa, Asia and Latin America[5]. There are four species of the human malarial parasite: *P. falciparum* (most deadly), *P. vivax, P. malariae* and *P. ovale*[6]. When a victim is bitten by an infected mosquito, the parasites cause an initial asymptomatic infection of the liver cells. After an incubation period of approximately one week, the parasites enter the blood stream. The parasites infect, develop and multiply within host erythrocytes. A small proportion of these parasites develop into the so-called gametocytes (sexual stages), which are able to infect a new mosquito host when they are taken up with a meal of blood. The clinical symptoms of malaria are caused exclusively by the parasite erythrocytic stages.

Considering this complex life-cycle of the plasmodial parasite, there are many stages that need to be considered as targets for therapy. Thus, it is now common to take a combination of anti-malarial drugs for treatment to combat the different blood stages of the parasite life-cycle. The efficacy of commercial antimalarial drugs such as chloroquine (**4.1**), when used as monotherapies, are quickly decreasing. There is a growing demand for active compounds with a novel mode of action to replace the current ineffective drugs. For thousands of years, plants have been the basis of sophisticated traditional medicine systems and more recently, natural products have provided an excellent source of medicinal lead compounds. Quinine (**4.5**), which is an alkaloid isolated from *Cinchona* bark, is the most

important lead compound against malaria. Quinine (**4.5**) was used as a template in the creation of chloroquine (**4.1**) and mefloquine (**4.6**). Artemisinin (**4.2**), which is isolated from the Chinese plant *Artemisia annua* L., has been successfully used against chloroquine-resistant malarial parasites[6].

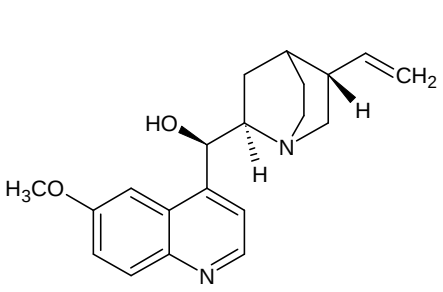

(**4.5**)

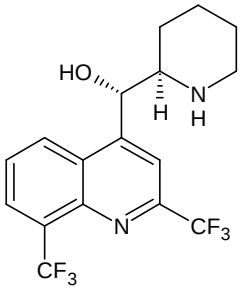

(**4.6**)

4.2.2 Established Anti-malarial Drugs

4.2.2.1 Chloroquine (4.1) and Mefloquine (4.6)

Chloroquine (**4.1**), a 4-aminoquinonline, was first synthesized in 1934, but was only used in 1946 because it was initially considered to be too toxic[1]. Since then, it has turned out to be the most important and effective antimalarial compound and consequently become the drug of choice in many programmes aimed at the global eradication of malaria. A major factor promoting the use of chloroquine (**4.1**) was the low cost required to produce the drug. Today, chloroquine-resistant strains of *P. falciparum* are common in all endemic areas worldwide[1].

Mefloquine (**4.6**) is considered the standard therapeutic alternative for chloroquine-resistant malaria. The use of this drug is limited due to the high costs and appearance of neuropsychiatric side effects[1].

The mode of action of these 4-aminoquinolines is generally accepted to involve the interference with the detoxification of free heme, which is generated during the degradation of haemoglobin. Haemoglobin is ingested by the parasite and transported into a central food vauole (Fig. 4.1), where it is digested into small peptides. These peptides are required for the parasite for growth and multiplication. The resulting heme moiety that

is released during haemoglobin degradation is potentially toxic to the parasite through an oxidative mechanism, and is therefore converted to insoluble crystals called hemozoin[1].

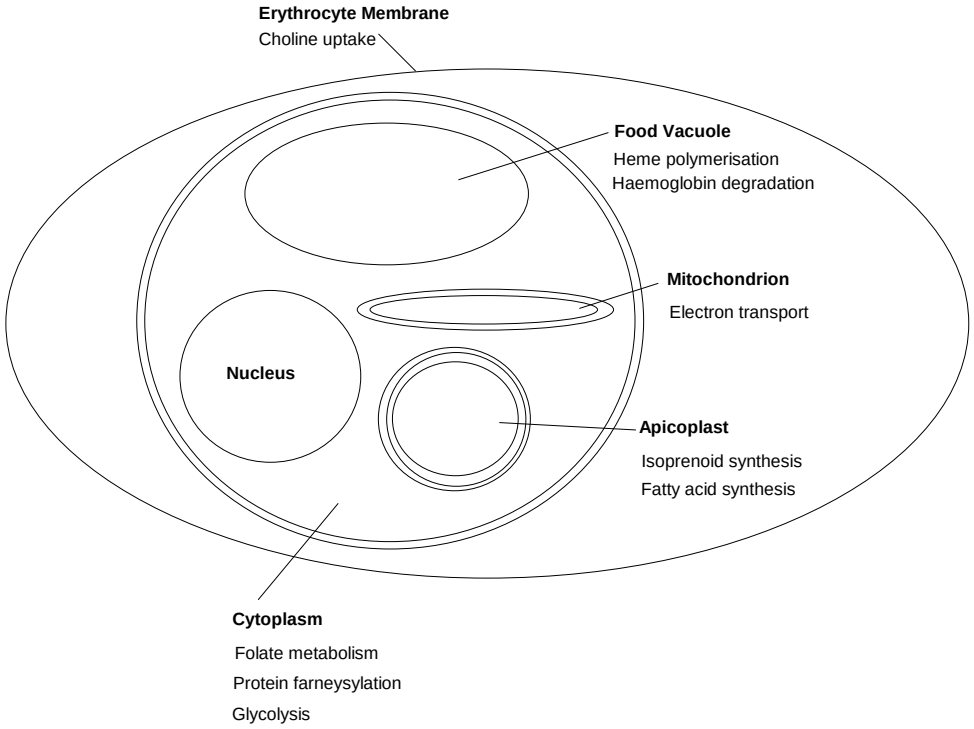

Figure 4.1. Schematic representation of an erythrocyte infected with *P. falciparum*, indicating the subcellular localization of different drug targets[1].

4.2.2.2 Artemisinin (4.2)

Artemisinin (**4.2**) is a sequiterpene trioxane lactone that was first isolated in 1971. Artemisinin (**4.2**) and its derivatives, dihydroartemisinin (**4.7**), artemether (**4.8**), arteether (**4.9**) and artesunate (**4.10**), represent a new class of antimalarial drugs that contain an endoperoxide group. Artemisinin (**4.2**) on its own has limited therapeutic value, due to its low solubility, low bioavailability, short life and neurotoxicity[7]. Thus semi-synthetic derivatives with better pharmacokinetic properties have been prepared. These drugs are all metabolized to dihydroartemisinin (**4.7**), which is the main bioactive compound[1].

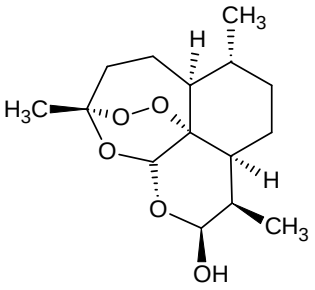

(**4.7**)

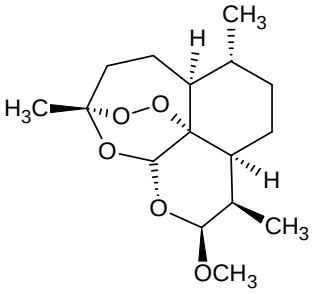

(**4.8**)

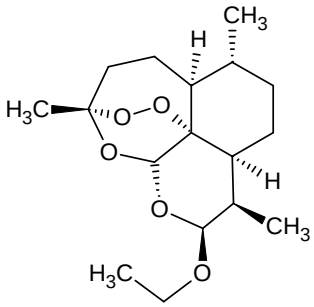

(**4.9**)

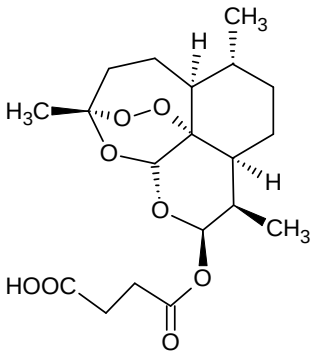

(**4.10**)

The artemisinins act faster than any other malarial drugs, with an approximate parasite and fever clearance time of 32 h. This is substantially quicker than the 2-3 days required for the conventional antimalarial drugs to alleviate the symptoms. Moreover, the artemisinins act against the sexual parasitic stages, which are responsible for the infection of the female *Anopheles* mosquito and consequently for the transmission of the disease. These drugs have a short plasma half-life and treatment is necessary for 5-7 days to fully eliminate the parasites[1].

The mechanism of action of the artemisinins evidently depends on the peroxide bond cleavage after contact with Fe(II) heme inside the food vacuole (Fig. 4.2). This results in the generation of free radicals that can alkylate the heme molecule. By this action, the detoxification of free heme may be inhibited[1].

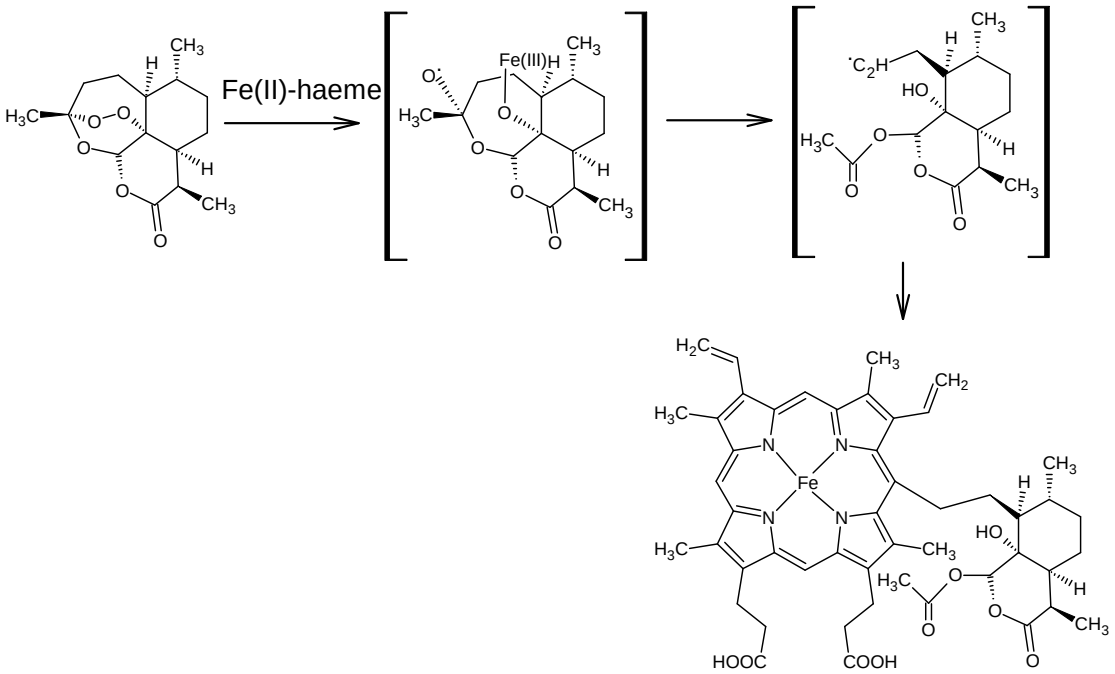

Figure 4.2. Hypothetical mechanism for the radical alkylation of heme by artemisinin (**4.2**)[1].

4.2.3 Antibiotics

Many antibiotics that are known to be antibacterial agents also display antimalarial activity. Their mode of action depends on the fact that the malarial parasites contain an unusual plastid-like organelle called an apicoplast[1] (see Figure 4.1). The apicoplast fulfils different metabolic processes, such as the synthesis of fatty acids, isoprenoids and potentially heme. Enzymes involved in metabolic functions within the apicoplast are encoded by the nuclear genome and are transported to the apicoplast by a specific terminal-amino sequence. Doxycycline (**4.11**) is the most commonly used antibiotic in anti-malarial therapy. It is used either on its own as a prophylactic, or in combination with quinine (**4.5**)/artensuate (**4.10**) for treatment in cases of chloroquine-resistant parasites. Tetracyclines such as doxycycline (**4.11**) inhibit protein synthesis inside the apicoplast and possibly in the mitochondria.

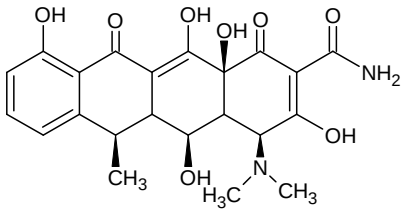

(**4.11**)

Due to the structural similarities between doxycyline and aloin (**4.3**) (and derivatives), it is possible that they have comparable biological activities (see Chapter 3). Thus the potential antiplasmodial activity of aloin (**4.3**) and derivatives was tested.

4.3 Results and Discussion

Aloin (**4.3**) and derivatives were screened for their possible antiplasmodial activities, using chloroquine (**4.1**) as a reference. The methodology used for this testing is in section 4.4. The IC_{50} values of aloin (**4.3**) and derivatives are displayed in table 4.1 below.

Table 4.1. *In vitro* antiplasmodial activity against *P. falciparum* (chloroquine-sensitive) D10 strain of aloin (4.3) and derivatives, along with 'drug-likeness' data.*

Compound	IC_{50} (μg/ml)	IC_{50} (μM)	LogP	H-bond Donors	H-bond Acceptors	Lipinski Rules Obeyed
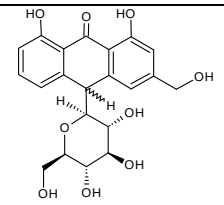 (**4.3**)	66.22	158	1.86 ± 0.71	7	9	No
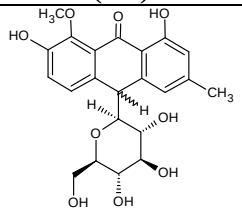 (**4.4**)	13.18	30	2.25 ± 0.85	6	9	No
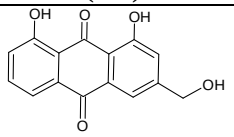 (**4.12**)	80.35	297	3.38 ± 0.77	3	5	Yes
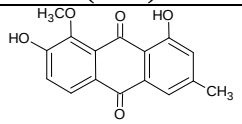 (**4.13**)	insoluble	-	4.18 ± 1.12	2	5	Yes
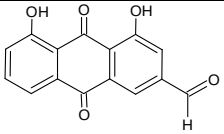 (**4.14**)	insoluble	-	4.33 ± 1.34	2	5	Yes

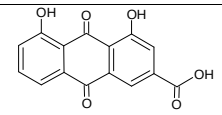 (**4.15**)	42.86	155	4.58 ± 1.35	3	6	Yes
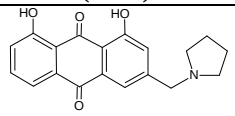 (**4.16**)	3.72	11	4.54 ± 0.78	2	5	Yes
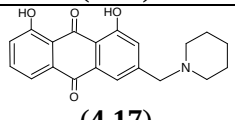 (**4.17**)	2.65	7	5.10 ± 0.78	2	5	Yes
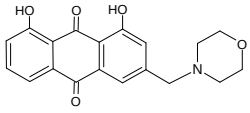 (**4.18**)	46.67	30	3.52 ± 0.88	2	6	Yes
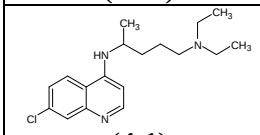 (**4.1**)	0.01782	0.56	4.69 ± 0.32	1	3	Yes

* Definitions of 'drug-likeness' descriptors are given in Section 4.3.1.

Homonataloin (**4.4**) is approximately 5 times more active than aloin (**4.3**). There are 3 structural differences (Table 4.2) between the two *C*-glucosides which possibly contribute to this difference in antiplasmodial activity.

Table 4.2 Structural differences between aloin (**4.3**) and homonataloin (**4.4**).

Carbon	Aloin (4.3)	Homonataloin (4.4)
11	CH_2OH	CH_3
8	OH	OCH_3
7	H	OH

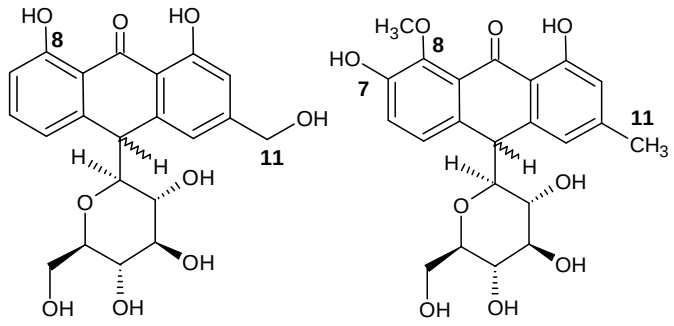

(4.3) **(4.4)**

A study carried out by Winter *et al*. on hydroxy-anthraquinones established the effect that the position of the hydroxyl group has on antiplasmodial activity[8]. A series of hydroxy and polyhydroxy-anthraquinones based on the potent antiplasmodial compound rufigallol (**4.19**) ($IC_{50} \approx 10.5$ ng/ml) were assayed. The results of this structure-activity study were used as a guideline to help explain the differences in antiplasmodial activity between aloin (**4.3**) and homonataloin (**4.4**).

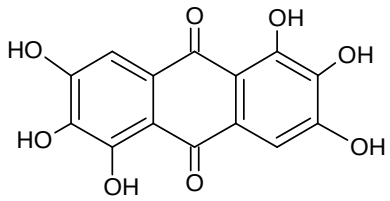

(**4.19**)

Octahydroxy-9,10-anthraquinone (**4.20**) (IC_{50} = 800 ng/ml) has hydroxyl groups at C-8/4 and C-1/8, along with 9- and 10-carbonyl groups which form a chelating moiety, similar to that found in aloin (**4.3**). Rufigallol (**4.19**) lacks the hydroxyl groups at C-8/4, but maintains the C-2,3,6,7 hydroxyl groups. These hydroxyl groups, along with the C-1/5-hydroxy and C-9/10-ketone moieties resemble the structural make-up of the anthrone part of homonataloin (**4.4**). Rufigallol (**4.19**) is 22 times more active against plasmodial parasites then octahydroxy-9,10-anthraquinone (**4.20**). The only difference between the two is that rufigallol (**4.19**) lacks the hydroxyl groups at C-8/4. Homonataloin (**4.4**) has a methoxy-group at C-8, which 'blocks' the activity of the hydroxyl-group, which is found in aloin (**4.3**). Rufigallol (**4.19**), octahydroxy-9,10-anthraquinone (**4.20**) and homonataloin (**4.4**) contain hydroxyl groups at C-7/3 which possibly plays a role in antiplasmodial activity. The absence of this C-7 hydroxyl group along with the C-8 hydroxyl group in aloin (**4.3**) compared to homonataloin (**4.4**), have thus been proposed to be the constituents that are responsible for the differences in their antiplasmodial activity.

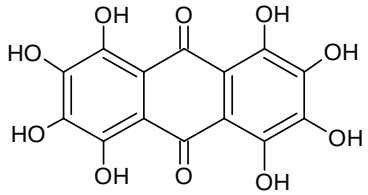

(**4.20**)

Aloe-emodin (**4.12**) displayed low antiplasmodial activity compared to aloin (**4.3**). This was probably influenced by the poor solubility displayed by aloe-emodin (**4.12**) in aqueous media. Rheinal (**4.13**) and nataloe-emodin (**4.14**) were insoluble in the plasmodial buffer medium and therefore could not be tested. Rhein (**4.15**) also showed poor antiplasmodial activity, despite having high solubility.

The antiplasmodial activity of the amine derivatives of aloe-emodin proved to be among the highest of the derivatives. The order of antiplasmodial activity was: 11-(piperidin-1-yl)chrysophanol (**4.17**) > 11-(pyrrolidin-1-yl)chrysophanol (**4.16**) > 11-(morpholin-1-yl)chrysophanol (**4.18**). This trend was also observed by Stocks *et al.*[9] who synthesized a series of short chain chloroquine derivatives, such as (**4.21**), (**4.22**) and (**4.23**), in which the diethylamino side chains were replaced by functional groups that were more resistant to dealkylation. This investigation was carried out to increase the half-life of chloroquine (**4.1**), which is extensively metabolized by dealkylation of the side chains[7]. It was found that the addition of piperidyl (**4.21**) and pyrrolidyl (**4.22**) rings to the 4-amino side chain resulted in enhanced activity against chloroquine-resistant *P. falciparum*. Interestingly, the addition of a morphinyl (**4.23**) ring resulted in a a considerably lower antiplasmodial activity than the piperidyl and pyrrolidyl derivatives, suggesting that the lipophilicity of the cyclic amine influences the activity of the drug.

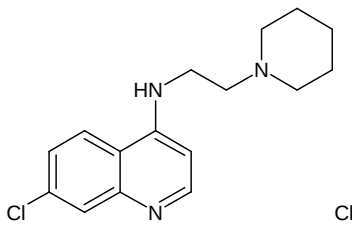

(**4.21**)

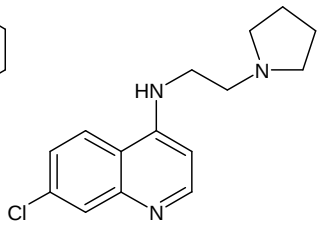

(**4.22**)

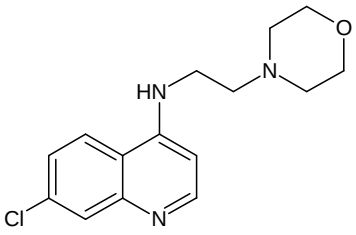

(**4.23**)

4.3.1 'Drug-Likeness' of Aloin (4.3) and Derivatives

As part of this investigation, aloin (**4.3**) and derivatives were investigated, based on their structural features, to determine if they could serve as potential medicinal drugs. The parameters of Lipinski's 'rule of 5' were used as a reference for this study. C. A. Lipinski and co-workers at Pfizer studied the data of drug candidates and discovered that there were

some reasonably clear cut-offs for oral absorption and general cell permeability[10]. They consequently constructed the ‘rule of five’ which serves as a tool to define the ‘drug-likeness’ of a potential drug candidate based on four parameters. The "rule-of-5" states that poor absorption or permeation is more likely when:

1. The LogP is larger than 5.
2. There are more then 5 hydrogen-bond donors (expressed as the sum of the OH’s and NH’s).
3. There are more than 10 hydrogen-bond acceptors (expressed as the sum of nitrogen and oxygen atoms).
4. The molecular weight is over 500.

Most of the aloin derivatives satisfy all these criteria, increasing the possibility of their use as medicinal drug targets.

The logP value of a compound is the logarithm of its partition coefficient between n-octanol and water [$\log(c_{octanol}/c_{water})$]. This is a well-established measure of the compound's hydrophilicity. Low hydrophilicities and therefore high logP values (> 5.0) cause poor absorption or permeation. The distribution of calculated logP values of more than 3000 drugs on the market underlines this fact.

Optimizing compounds for high activity on a biological target is generally accompanied by increased molecular weights. However, compounds with higher molecular weights are less likely to be absorbed and therefore to ever reach the site of action. Thus, trying to keep molecular weights as low as possible is crucial.

4.3.2 Mechanism of Action of Aloin (4.3) and Derivatives

The antiplasmodial action of aloin (**4.3**) and derivatives were compared to those of doxycycline (**4.11**) and rufigallol (**4.19**), which have many structural features in common with aloin (**4.3**) and its derivatives.

In Chapter 3, aloin (**4.3**) and its derivatives were tested for their MMP-2 and MMP-9 inhibitory properties, using doxycycline (**4.11**) as a reference. Besides being a MMP-

inhibitor, doxycycline (**4.11**) is a powerful antimalarial drug. Doxycycline (**4.11**) has been reported to have an IC_{50} value of 4800 nM (W2 Strain), in comparison to chloroquine (**4.1**) which has an IC_{50} value of 100 nM. A mechanism of action of doxycycline was recently proposed by Dahl *et al*[11]. Doxycycline (**4.11**) causes the apicoplast to become dysfunctional in progeny parasites. Late-stage parasites were those most susceptible to doxycycline (**4.11**). This effect of doxycycline (**4.11**) is evident in mature parasites from the second generation, which did not rupture to release viable merozoites.

The amine derivatives of aloe-emodin, i.e. 11-(piperidin-1-yl)chrysophanol (**4.17**), 11-(pyrrolidin-1-yl)chrysophanol (**4.16**) and 11-(morpholin-1-yl)chrysophanol (**4.18**) resemble the pharmacophore profile of doxycycline (**4.11**) very closely, and thus could share its mechanism of action. Comparing the structures of doxycycline (**4.11**) and 11-(piperidin-1-yl)chrysophanol (**4.17**), it can be seen that they both share many common structural features. Firstly, they both contain the same chelating moiety **A**, i.e. the C-11/13 hydroxy-C-12 ketone combination in doxycycline (**4.11**) and C-1/8 hydroxyl-C-9 ketone combination in 11-(piperidin-1-yl)chrysophanol (**4.17**). This chelating feature is common to all the aloin derivatives. Secondly, doxycycline has a tertiary amine nitrogen atom 3-carbon atoms away from the C-13 hydroxyl group (**B**). This structural feature is also found in 11-(piperidin-1-yl)chrysophanol (**4.17**).

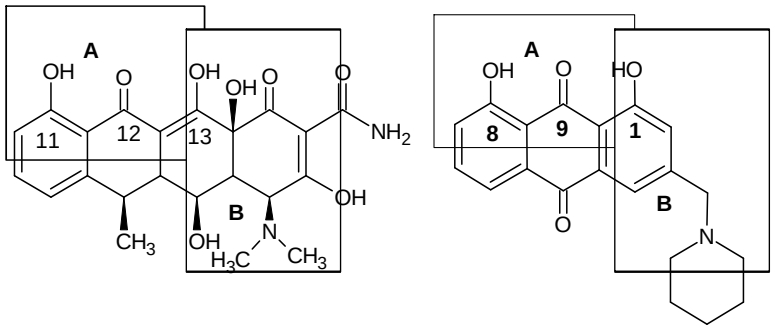

(**4.11**) (**4.17**)

The antimalarial action of rufigallol (**4.19**) is postulated to involve an iron chelation mechanism, similar to that of desferroxamine (desferal) (**4.24**)[8]. The antimalarial effect of desferroxamine (**4.24**) has been shown to involve chelation of iron, which required for cellular metabolism and DNA synthesis of the parasite. Desferroxamine has also been shown to extract ferric iron from the hemozoin (see section 4.2.2.1).

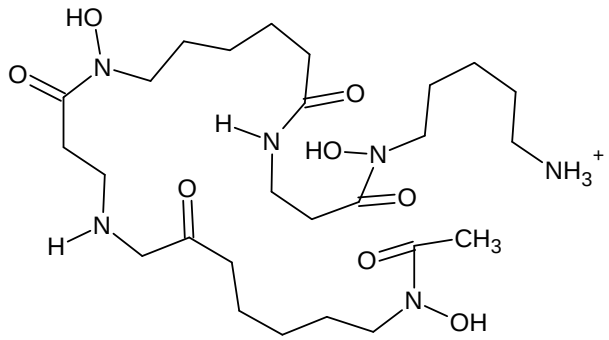

(**4.24**)

4.4 Conclusion

Aloin (**4.3**) and its derivatives displayed fairly good activity against the chloroquine-sensitive strain of *P. falciparum*. The two amine derivatives, i.e. 11-(pyrrodin-1-yl)chrysophanol (**4.16**) and 11-piperidin-1-yl)chrysophanol (**4.17**) showed the best antiplasmodial activities. It was noteworthy to discover that homonataloin (**4.4**) was fives times more active against the Plasmodium parasites than aloin (**4.3**). Thus it can be concluded that aloin (**4.3**) and possibly homonataloin (**4.4**) can serve as lead compounds in the designing of novel antiplasmodial drugs.

4.5 Experimental

Aloin (**4.3**) and its derivatives were sent to the Division of Pharmacology at the University of Cape Town for the screening of *in vitro* plasmodial activity. The methodology that was used at this institute was as follows:

The test compounds were tested in duplicate on one occasion against chloroquine-sensitive (CQS) strain of *P. falciparum* (D10). Continuous *in vitro* cultures of asexual erythrocyte stages of *P. falciparum* were maintained using a modified method of Trager and Jensen[12]. Quantitative assessment of antiplasmodial activity *in vitro* was determined via the parasite lactate dehydrogenase assay using a modified method described by Makler[13].

The samples were prepared as 2 mg/ml stock solutions in 10% DMSO or 10% methanol and were sonicated to enhance solubility. Samples were tested as a suspension if not completely dissolved. Stock solutions were stored at -20 ºC. Further dilutions were prepared on the day of the experiment. Chloroquine (**4.1**) was used as the reference drug

in all experiments. A full dose-response was performed for all compounds to determine the concentration inhibiting 50% of parasite growth (IC_{50} value). Test samples were tested at a starting concentration of 100 μg/ml, which was then serially diluted 2-fold in complete medium to give 10 concentrations; with the lowest concentration being 0.2 μg/ml. The same dilution technique was used for all samples. Chloroquine (**4.1**) was tested at a starting concentration of 100 ng/ml. The highest concentration of solvent to which the parasites were exposed had no measurable effect on the parasite viability (data not shown). The IC_{50}-values were obtained using a non-linear dose-response curve fitting analysis via Graph Pad Prism v.4.0 software.

4.6 References

1. Wiesner, J., Ortmann, R., Jomaa, H., Schlitzer, M., *Angewandte Chemie International* Edition, 2003, **42**, 5274-5293.

2. De Ridder, S., van der Kooy, F., Verpoorte, R., Journal of Ethnopharmacology, 2008, article in press.

3. van Zyl, R. L., Viljoen, A. M., *South African Journal of Botany*, 2002, **68**, 106-110.

4. Caniato, R., Puricelli, L., *Critical Reviews in Plant Sciences*, 2003, **22**, 79-105.

5. Stratton, L., O'Neill, M. S., Kruk, M. E., Bell, M. L., *Social Science and Medicine*, 2008, **67**, 854-862.

6. Schwikkard, S., van Heerden, F. R., *Natural Product Reports*, 2002, **19**, 675-692.

7. Mital, A., *Current Medicinal Chemistry*, 2007, **14**, 759-773.

8. Winter, R. W., Cornell, K. A., Johnson, L. L., Isabelle, L. M., Hinrich, Riscoe, M. K., *Bioinorganic and Medicinal Chemistry Letters*, 1995, **5**, 1927-1932.

9. Stocks, P. A., Raynes, K. J., Bray, P. G., Park, B. K., O'Neill, P. M., Ward, S. A., *Journal of Medicinal Chemistry*, 2002, **45**, 4975-4983.

10. Lipinski, C. A., Lombardo, F., Dominy, B. W., Feeney, P. J., *Advanced Drug Delivery Reviews*, 1997, **23**, 3-25.

11. Dahl, E. L., Shock, J. L., Shenai, B. R., Gut, J., DeRisi, J. L., Rosenthal, P. J., *Antimicrobial Agents and Chemotherapy*, 2006, **50**, 3124-3131.

12. Trager, W., Jensen, J. B., *Science*, 1976, **193**, 673-675.

13. Makler, M. T., Ries, J. M., Williams, J. A., Bancroft, J. E., Piper, R. C., Gibbins, B. L., Hinrichs, D. J., *The American Society of Tropical Medicine and Hygiene*, 1993, **48**, 739-741.

CHAPTER FIVE

CONCLUSIONS AND FUTURE WORK

5.1 Conclusion

Aloe marlothii is known to be a rich source of phenolic compounds, especially aloin (**5.1**). Aloin (**5.1**) was isolated from the *A. marlothii* leaf exudate by both conventional (column chromatography) and novel (calcium-salt precipitation) methods. Aloin (**5.1**), being unstable in solution, was chemically transformed into a more stable derivative, i.e. aloe-emodin (**5.2**) which lacks the sugar moiety. Aloe-emodin (**5.2**) was then transformed into several derivatives with potentially useful biological activities. Aloin (**5.1**) and derivatives were tested for (i) their potential as MMP-2 and MMP-9 inhibitors and for (ii) their potential antiplasmodial activity against a strain of chloroquine-sensitive *Plasmodium falciparum* parasites. Doxycyline (**5.3**), a clinical drug that is structurally similar to aloin and derivatives, was used as a reference compound in both of the biological assays. 11-(Piperidin-1-yl)chrysophanol (**5.4**) and 11-(morpholin-1-yl)chrysophanol (**5.5**) proved to be the most potent selective MMP-2 inhibitors. 11-(Piperidin-1-yl)chrysophanol (**5.4**) was also found to be the most potent against *P. falciparum* parasite, along with 11-(pyrrolidin-1-yl)chrysophanol (**5.6**). Aloin (**5.1**) has been thus shown to be a cheap, easily obtainable starting material that can be transformed chemically into biologically active derivatives.

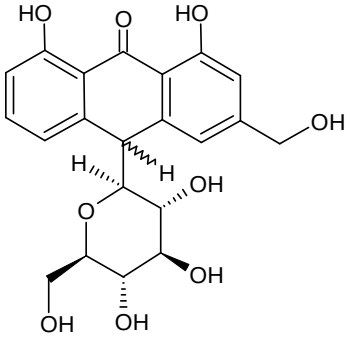

(**5.1**)

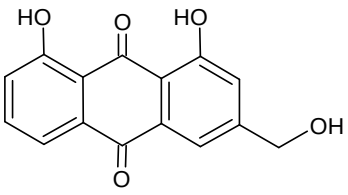

(**5.2**)

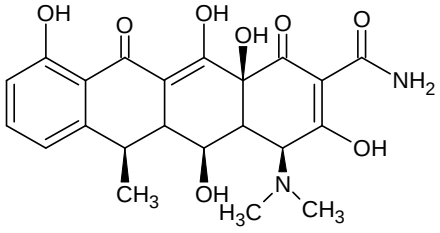

(**5.3**)

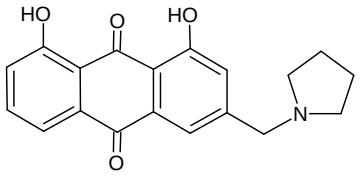

(**5.4**)

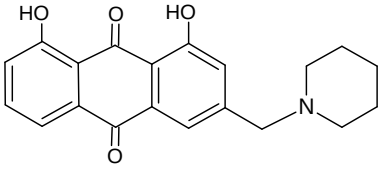

(**5.5**)

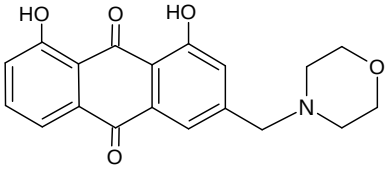

(**5.6**)

5.2 Future Work

The results obtained from both of the biochemical assays provide useful information for the development of more potent drugs. With regard to the MMP-inhibitory studies, 6-membered rings, with varied substituents (**5.7**), may prove to be highly active against MMP-2. The incorporation of even larger rings or more highly substituted rings should also be examined. Molecular modelling would also be a powerful tool in understanding the mechanism of the compounds' inhibitory action, thus aiding the process of designing new inhibitors once sufficient species with activity has been prepared.

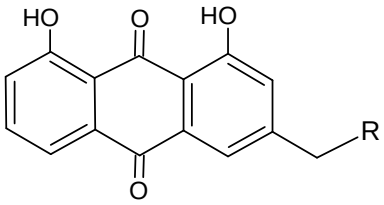

R = substituted 6-membered nitrogen-containing ring

(**5.7**)

Based on the results obtained from the antiplasmodial studies, it was established that the aloin (**5.1**) analogue, homonataloin (**5.8**), contained a structural motif that was more potent towards the *P. falciparum* parasites then aloin (**5.1**). Thus, homonataloin (**5.8**), which can be isolated from specific *A. marlothii* plants, would serve as a far more useful starting compound in the preparation of antiplasmodial drugs. The synthesis of compounds shown in Fig. 5.1 may result in considerably higher antiplasmodial activities.

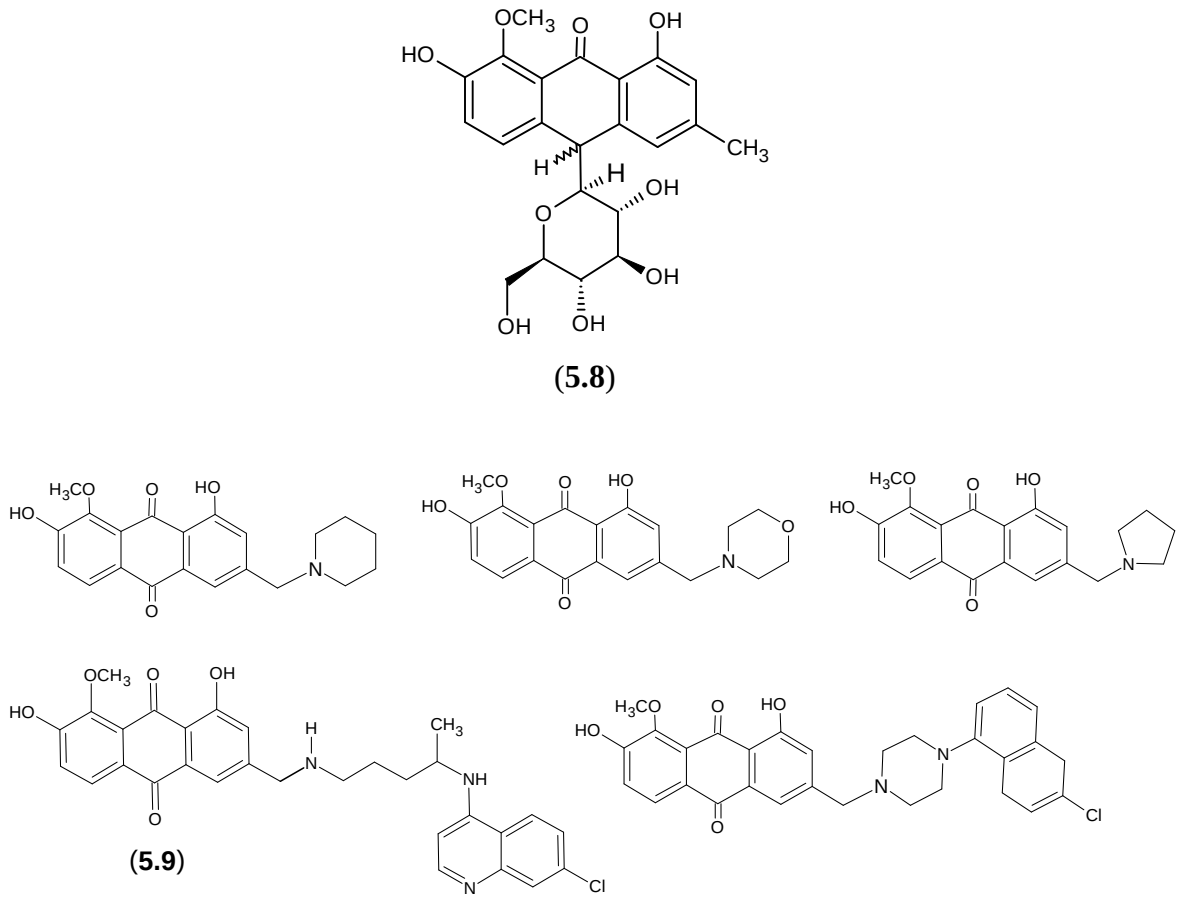

(**5.8**)

(**5.9**)

Figure 5.1. Potential antiplasmodial compounds derived from homonataloin (**5.8**).

Compound (**5.9**) contains a quinoline moeity, based on chloroquine, which is known to have antiplasmodial activity.

The toxicity of aloin and derivatives would also need to be investigated, to clearly distinguish between the toxicity of the drugs and their biological properties.

APPENDIX

Plate 6b: ^{13}C NMR Spectrum of nataloe-emodin (**2.28**) in DMSO-d_6

Plate 6C: DEPT 135 (i) and DEPT 90 (ii) NMR Spectra of nataloe-emodin (**2.28**) in DMSO-d_6

Plate 6d: COSY NMR Spectrum of nataloe-emodin (**2.28**) in DMSO-d_6

Plate 6e: HSQC NMR Spectrum of nataloe-emodin (**2.28**) in DMSO-d_6

Plate 6f: HMBC NMR Spectrum of nataloe-emodin (**2.28**) in DMSO-d_6

Plate 7a: ^{1}H NMR Spectrum of rheinal (**2.29**) in DMSO-d_6

Plate 7b: ^{13}C NMR Spectrum of rheinal (**2.29**) in DMSO-d_6

Plate 7c: COSY NMR Spectrum of rheinal (**2.29**) in DMSO-d_6

Plate 7d: HSQC NMR Spectrum of rheinal (**2.29**) in DMSO-d_6

Plate 7e: HMBC NMR Spectrum of rheinal (**2.29**) in DMSO-d_6

Plate 8a: ^{1}H NMR Spectrum of IBX (**2.30**) in DMSO-d_6

Plate 8b: ^{13}C NMR Spectrum of IBX (**2.30**) in DMSO-d_6

Plate 8c: COSY Spectrum of IBX (**2.30**) in DMSO-d_6

Plate 8d: HSQC Spectrum of IBX (**2.30**) in DMSO-d_6

Plate 8e: HMBC Spectrum of IBX (**2.30**) in DMSO-d_6

Plate 9a: ^{1}H NMR Spectrum of rhein (**2.31**) in DMSO-d_6

Plate 9b: ^{13}C NMR Spectrum of rhein (**2.31**) in DMSO-d_6

Plate 9c: COSY NMR Spectrum of rhein (**2.31**) in DMSO-d_6

Plate 9d: HSQC NMR Spectrum of rhein (**2.31**) in DMSO-d_6

Plate 9e: HMBC NMR Spectrum of rhein (**2.31**) in DMSO-d_6

Plate 10a: ^{1}H NMR Spectrum of 11-bromo-chrysophanol (**2.33**) in DMSO-d_6

Plate 10b: ^{13}C NMR Spectrum of 11-bromo-chrysophanol (**2.33**) in DMSO-d_6

Plate 10c: COSY NMR Spectrum of 11-bromo-chrysophanol (**2.33**) in DMSO-d_6

Plate 10d: HSQC NMR Spectrum of 11-bromo-chrysophanol (**2.33**) in DMSO-d_6

Plate 11a: ^{1}H NMR Spectrum of 11-(pyrrolidin-1-yl)chrysophanol (**2.34**) in DMSO-d_6

Plate 11b: ^{13}C NMR Spectrum of 11-(pyrrolidin-1-yl)chrysophanol (**2.34**) in DMSO-d_6

Plate 11c: DEPT 90 (i) and Dept 135 (ii) NMR Spectrum of 11-

Plate 1a: ^{1}H NMR Spectrum of aloin A (2.1) in MeOH-d_4

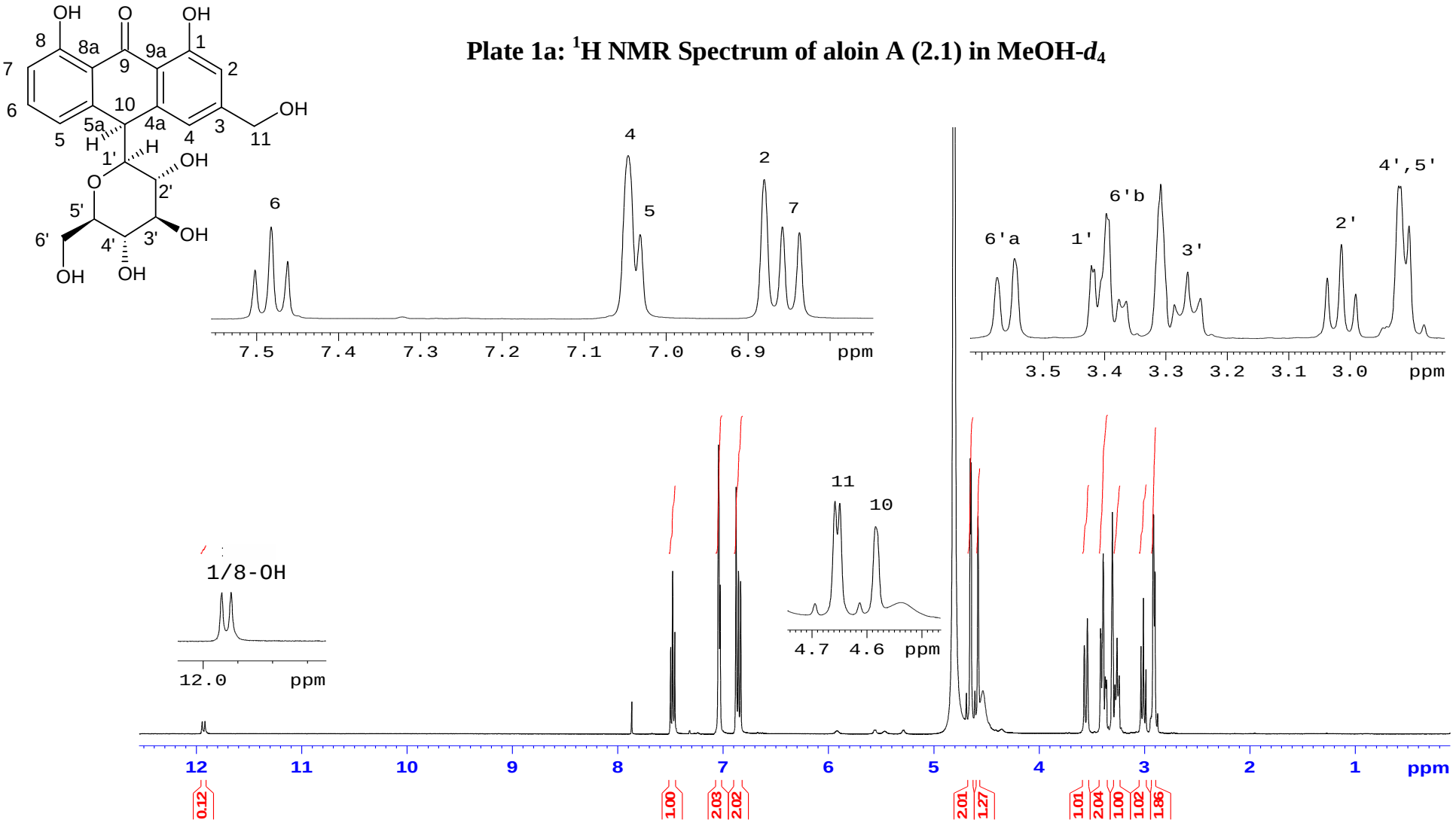

Plate 1b: ^{13}C NMR Spectrum of aloin A (2.1) in MeOH-d_4

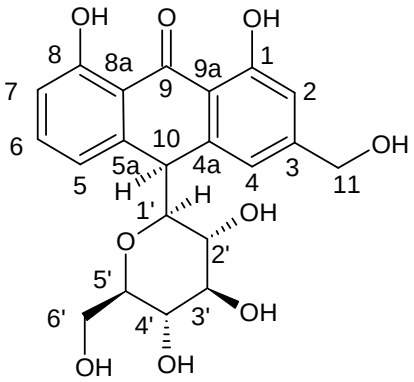

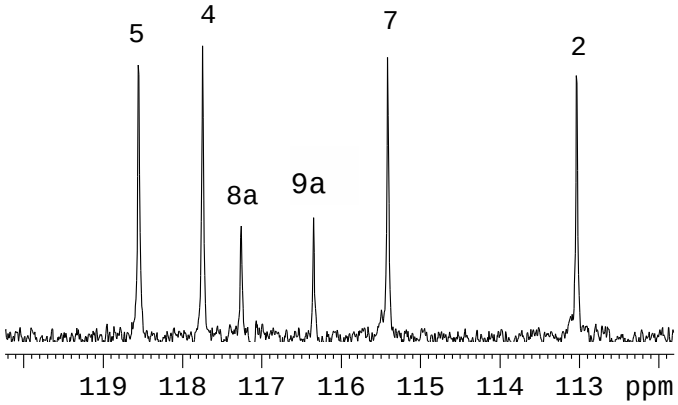

Plate 1c: DEPT 135 NMR Spectrum of aloin A (2.1) in MeOH-d_4

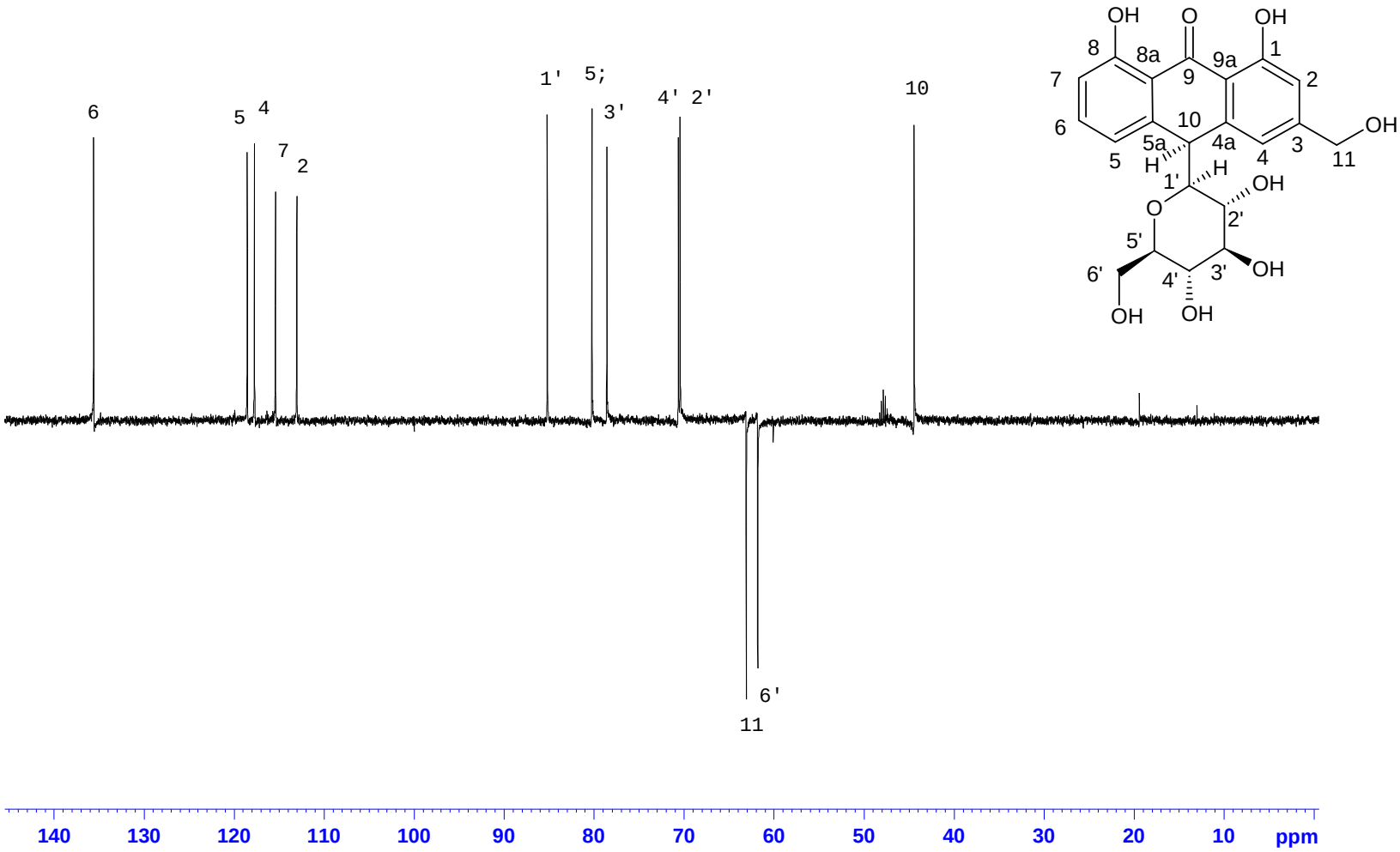

Plate 1d: COSY NMR Spectrum of aloin (2.1) in MeOH-d_4

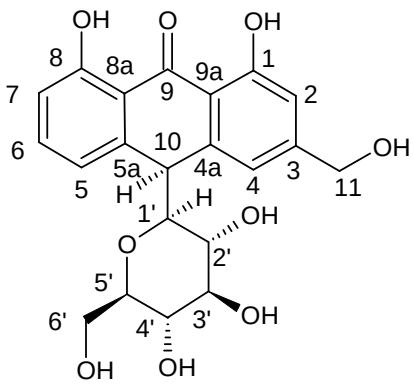

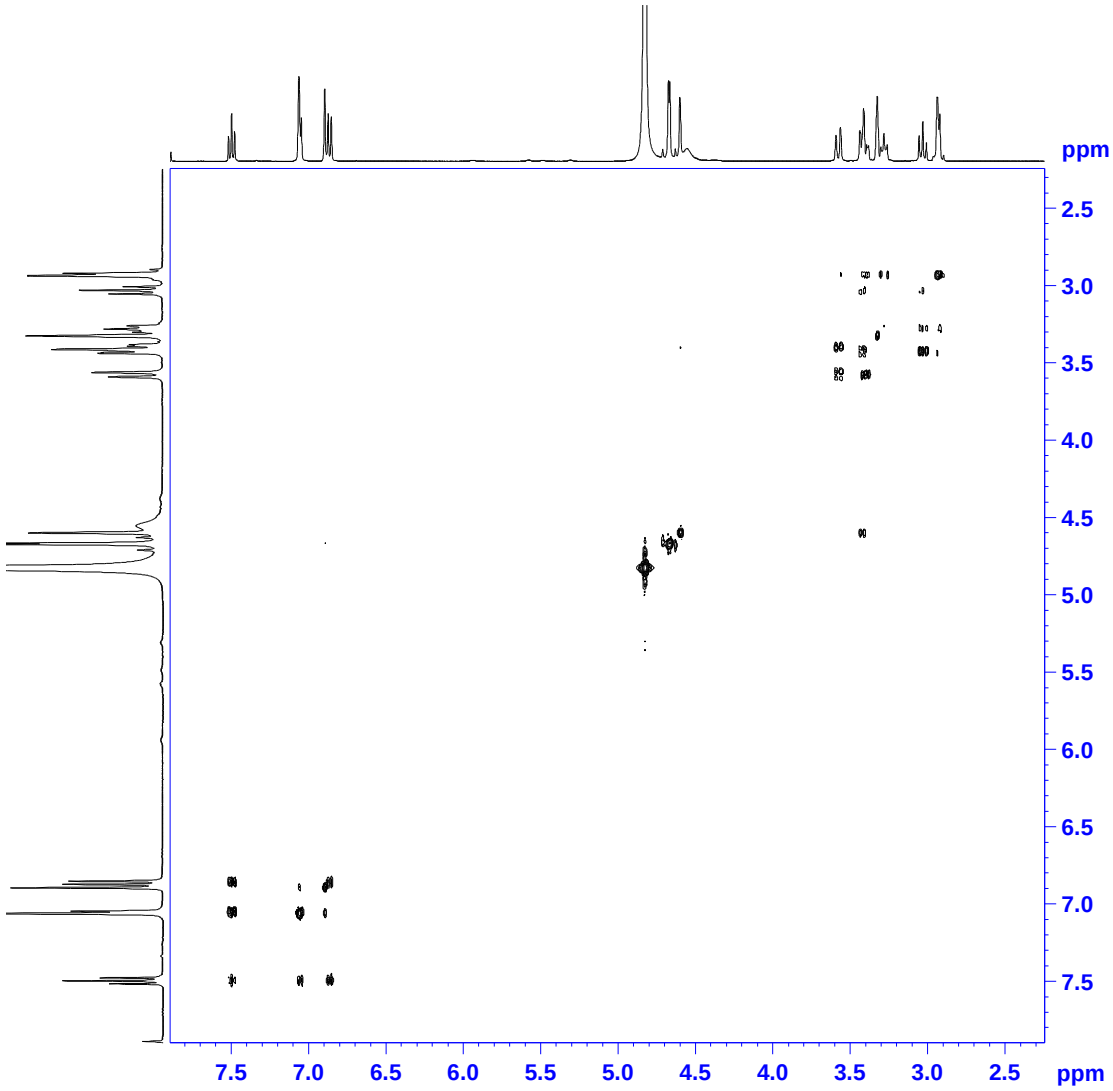

Plate 1e: HSQC NMR Spectrum of aloin (2.1) in MeOH-d_4

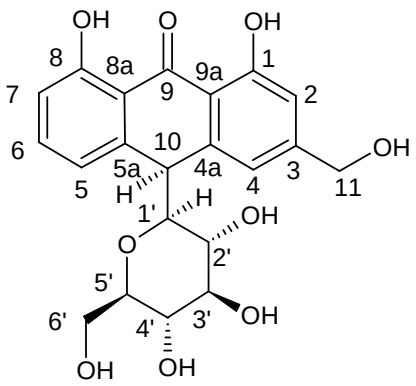

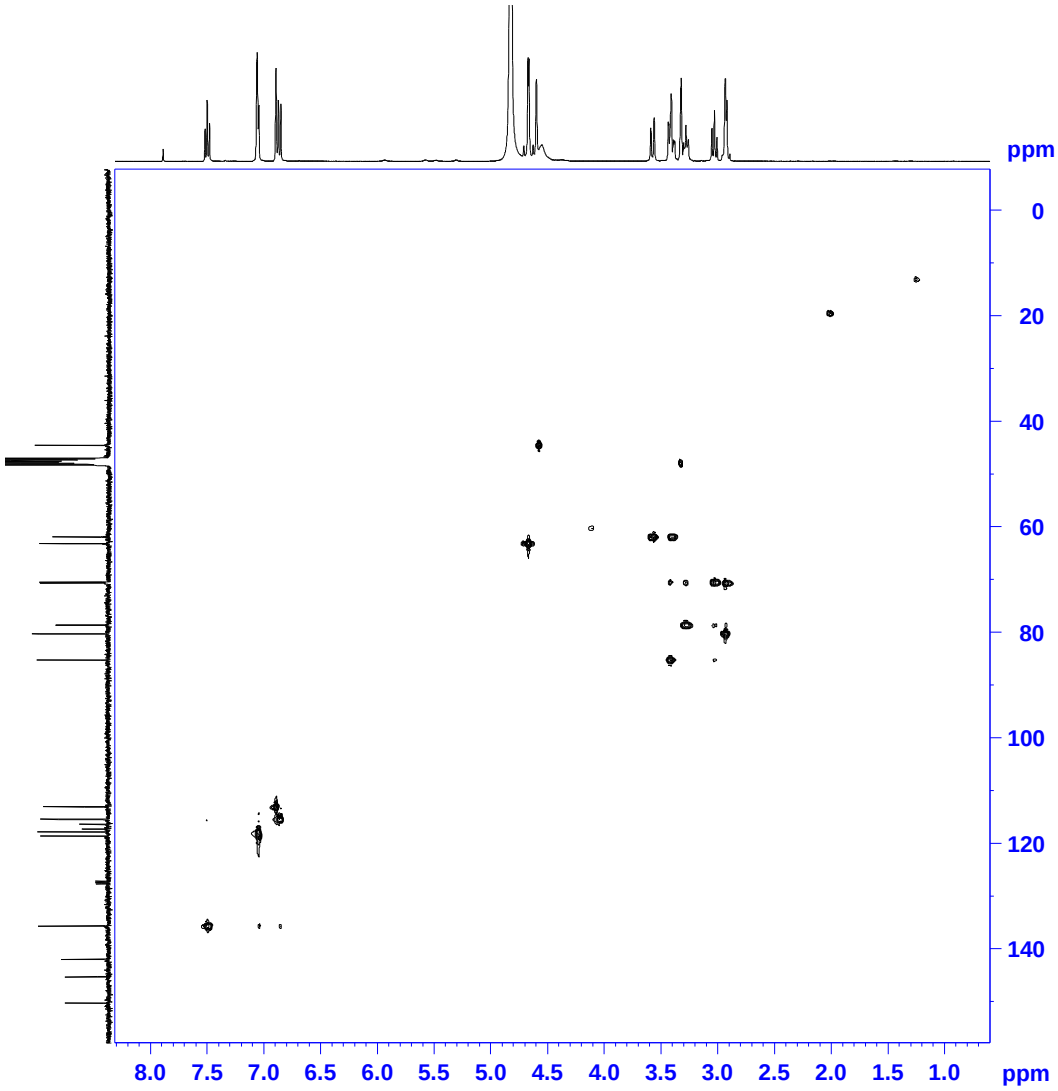

Plate 1f: HMBC NMR Spectrum of aloin (2.1) in MeOH-d_4

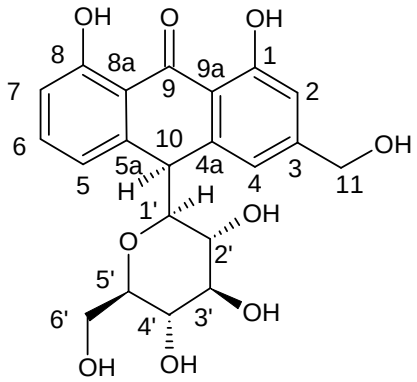

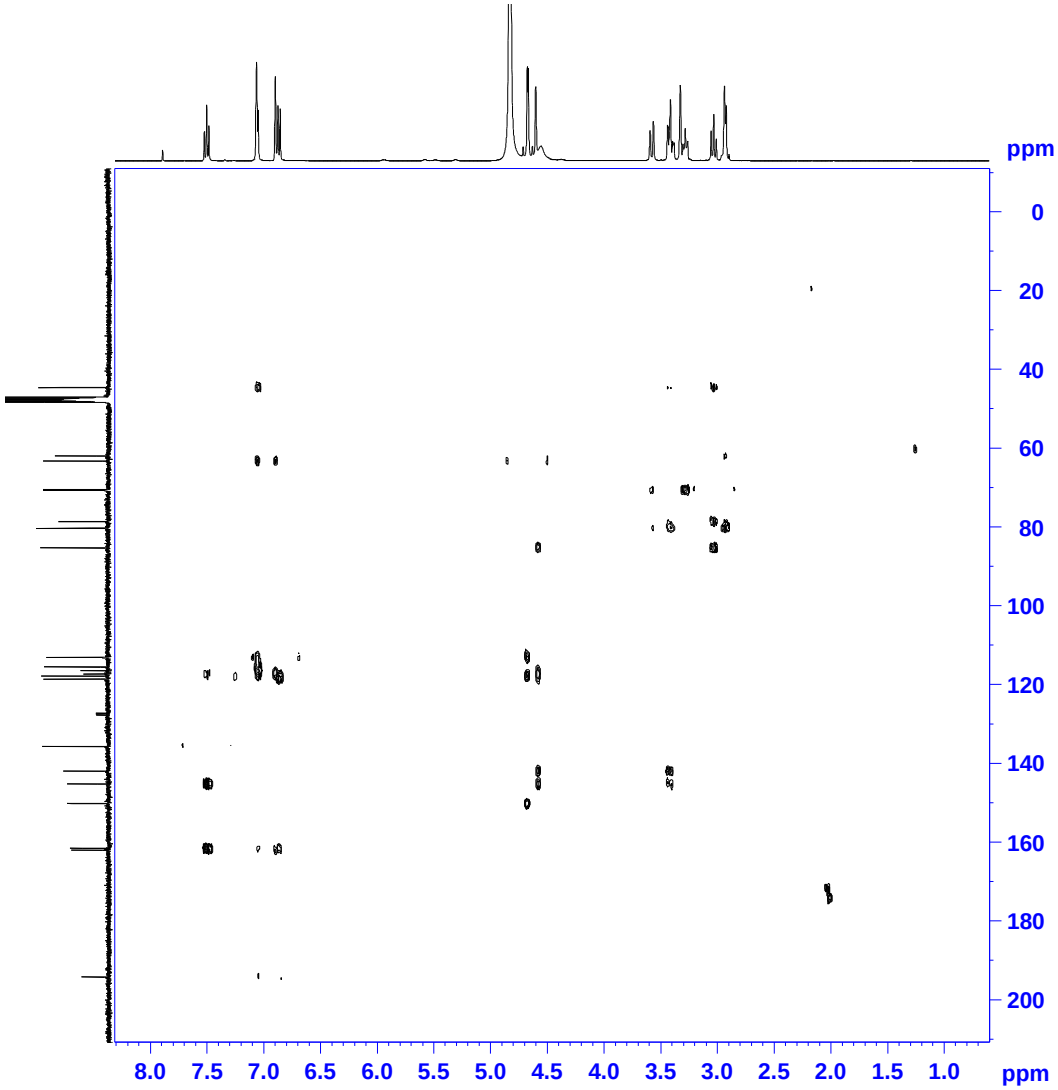

Plate 2a: ^{1}H NMR Spectrum of aloeresin A (2.2) in MeOH-d_4

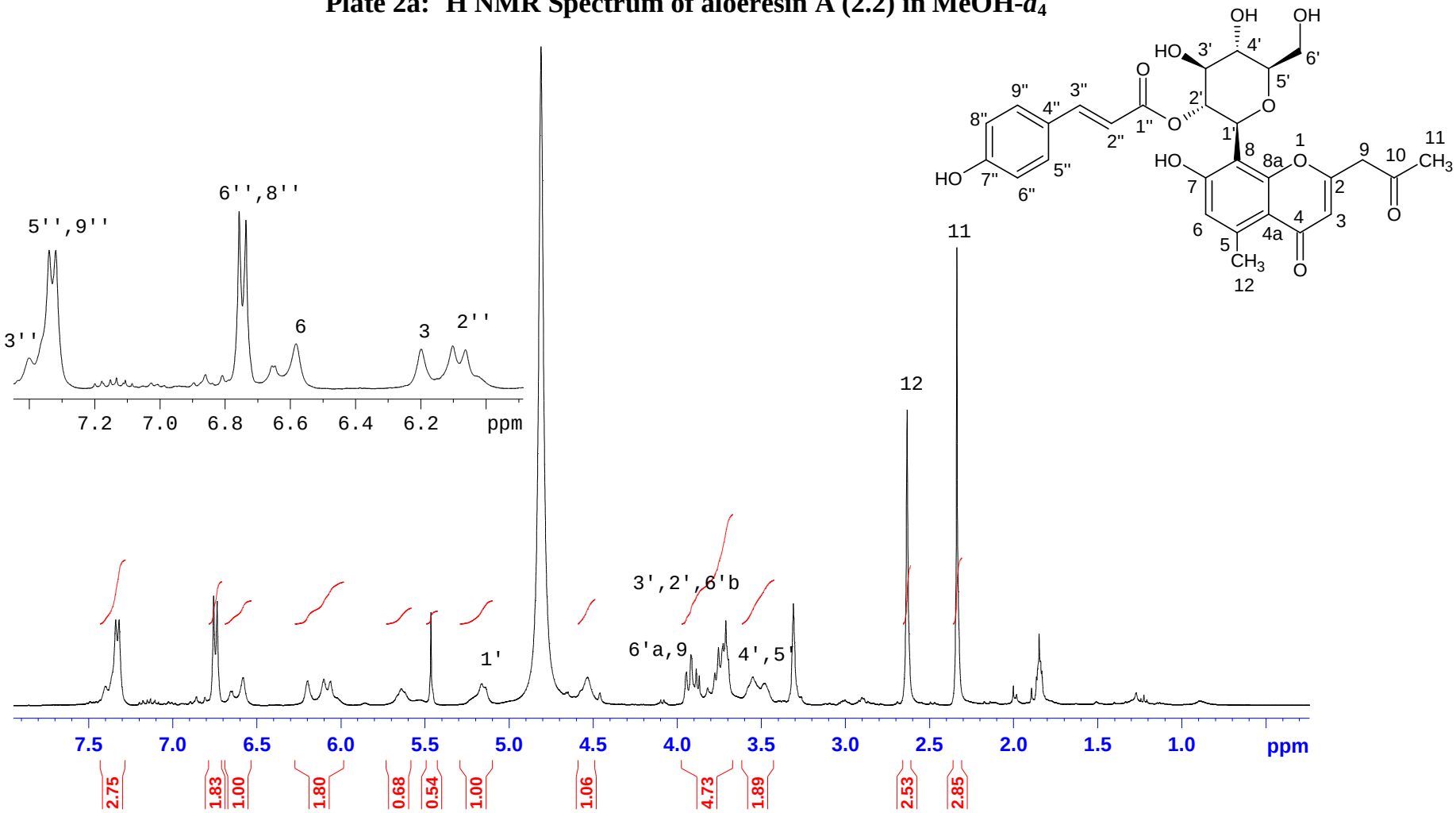

Plate 2b: ^{13}C NMR Spectrum of aloeresin A (2.2) in MeOH-d_4

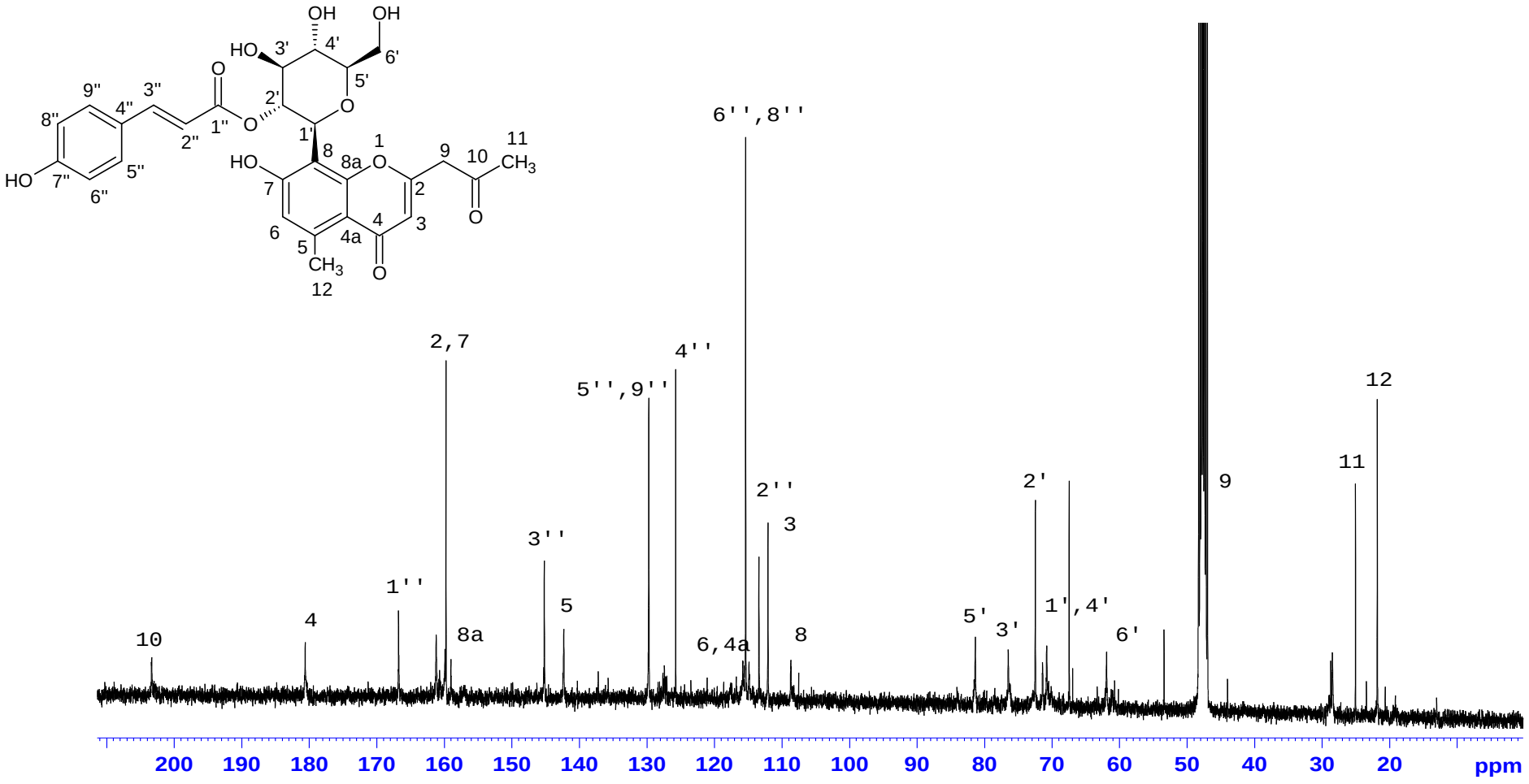

Plate 2c: DEPT 135 NMR Spectrum of aloeresin A (2.2) in MeOH-d_4

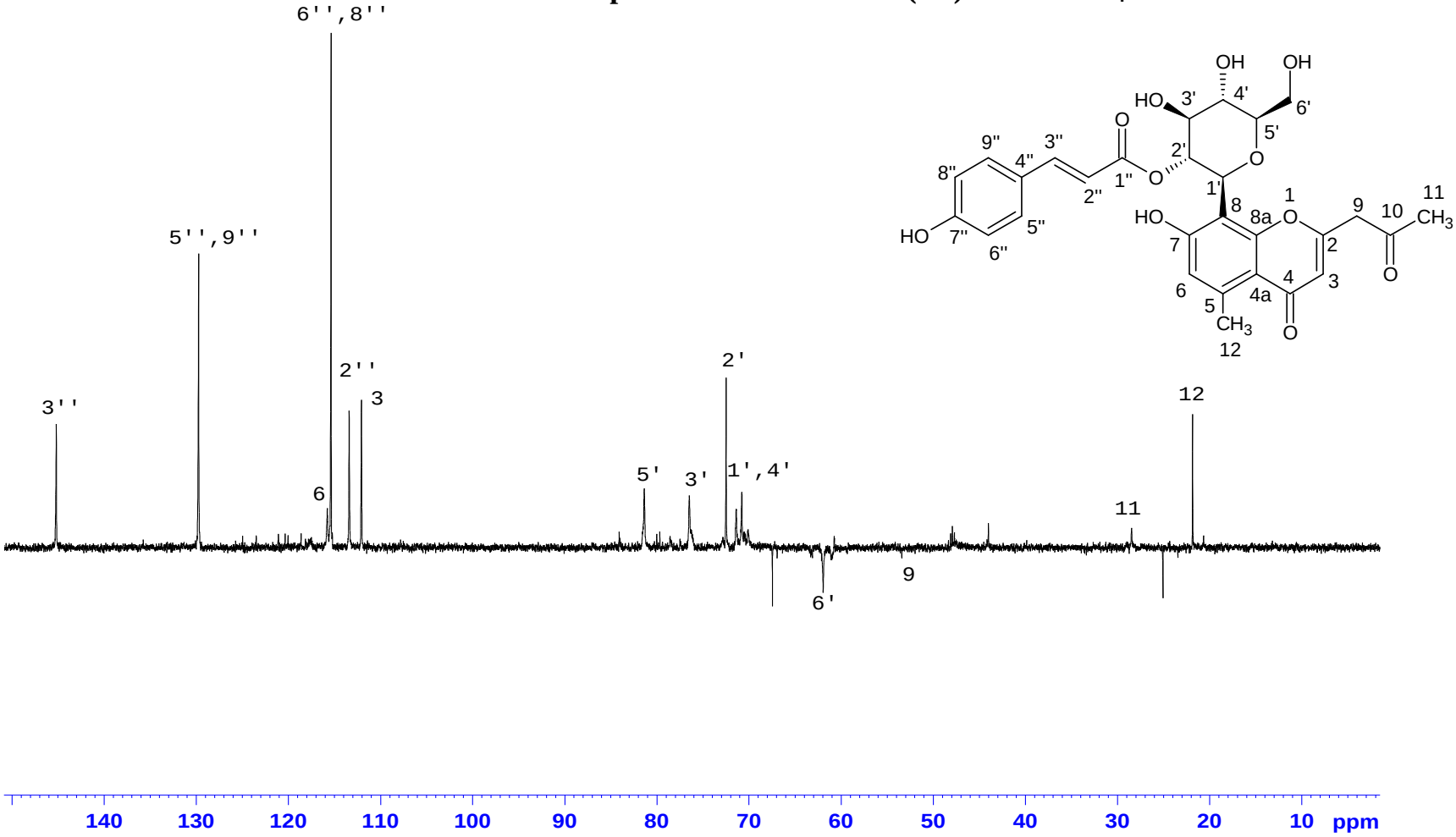

Plate 2d: COSY NMR Spectrum of aloeresin A (2.2) in MeOH-d_4

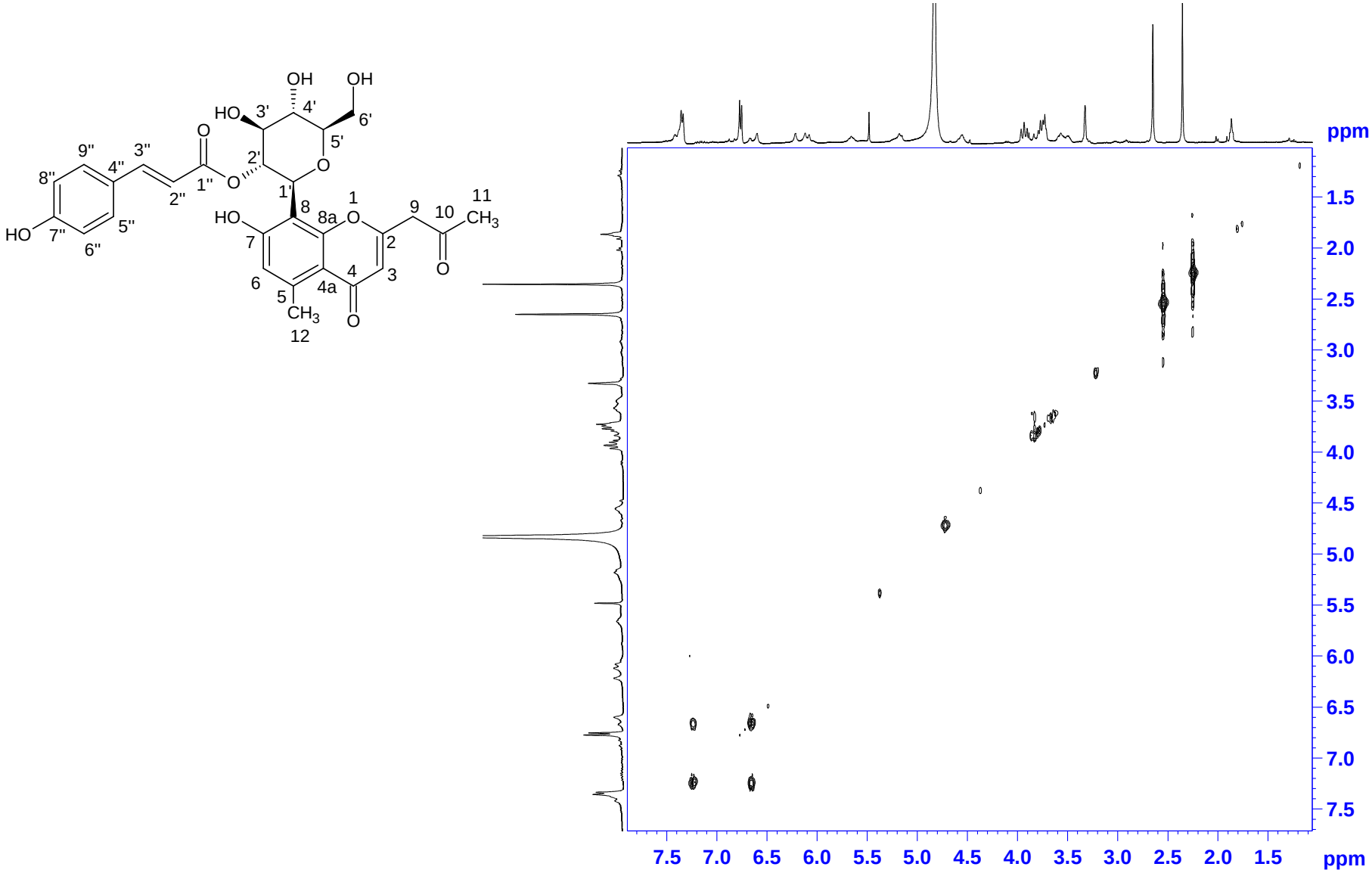

Plate 2e: HSQC NMR Spectrum of aloeresin A (2.2) in MeOH-d_4

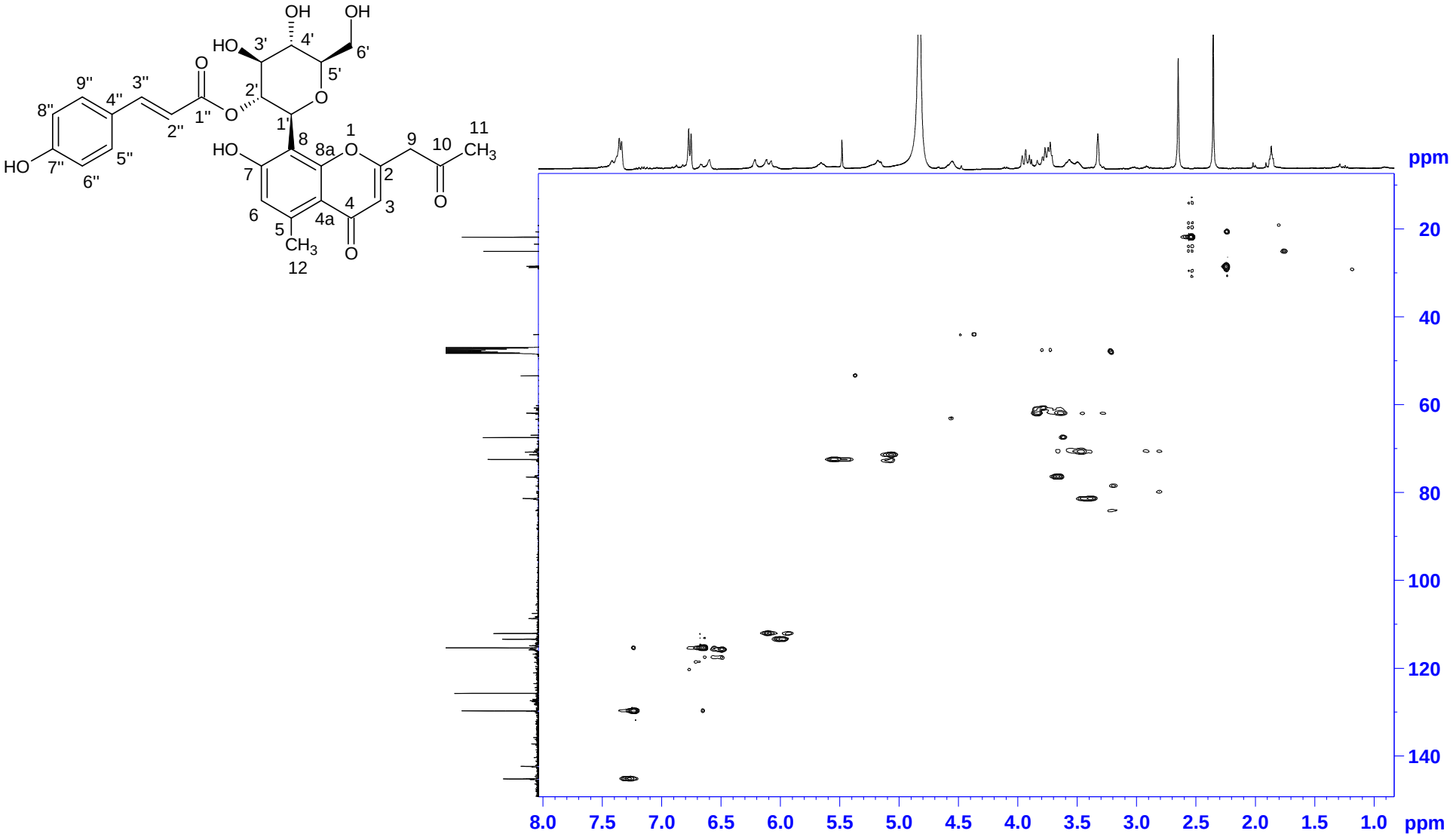

Plate 2f: HMBC NMR Spectrum of aloeresin A (2.2) in MeOH-d_4

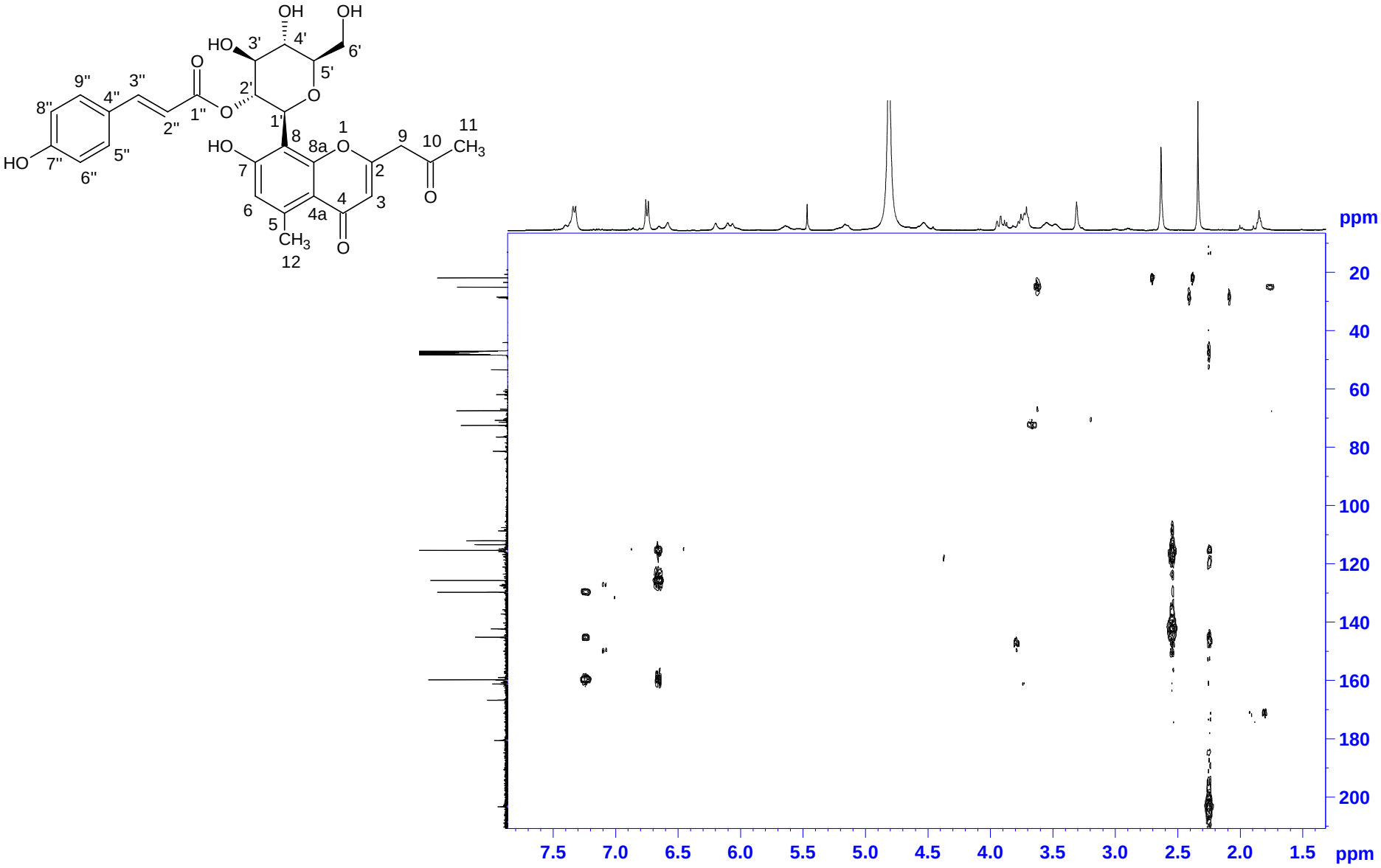

Plate 3a: ^{1}H NMR Spectrum of aloesin (2.3) in MeOH-d_4

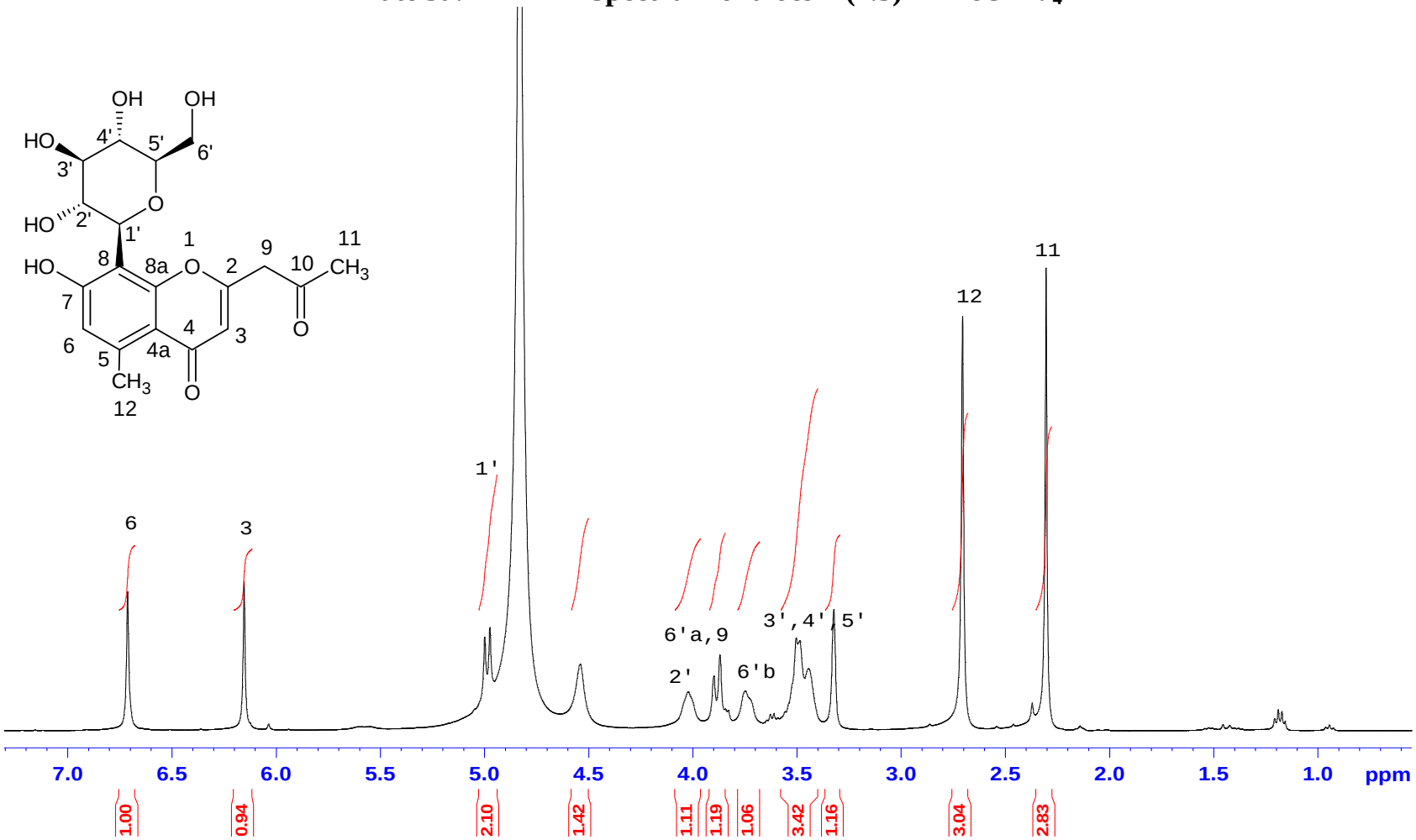

Plate 3b: ^{13}C NMR Spectrum of aloesin (2.3) in MeOH-d_4

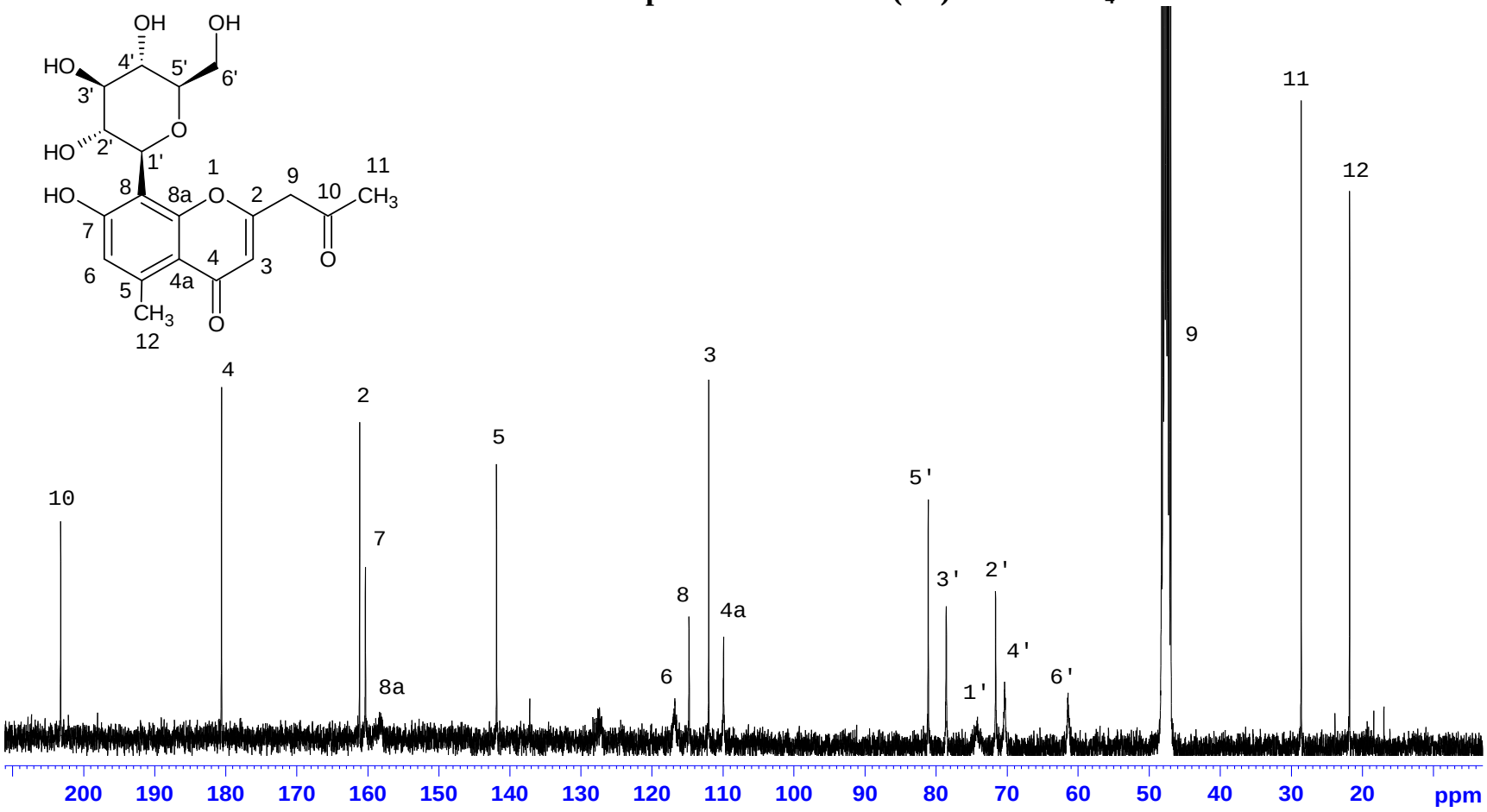

Plate 3c: DEPT NMR Spectrum of aloesin (2.3) in MeOH-d_4

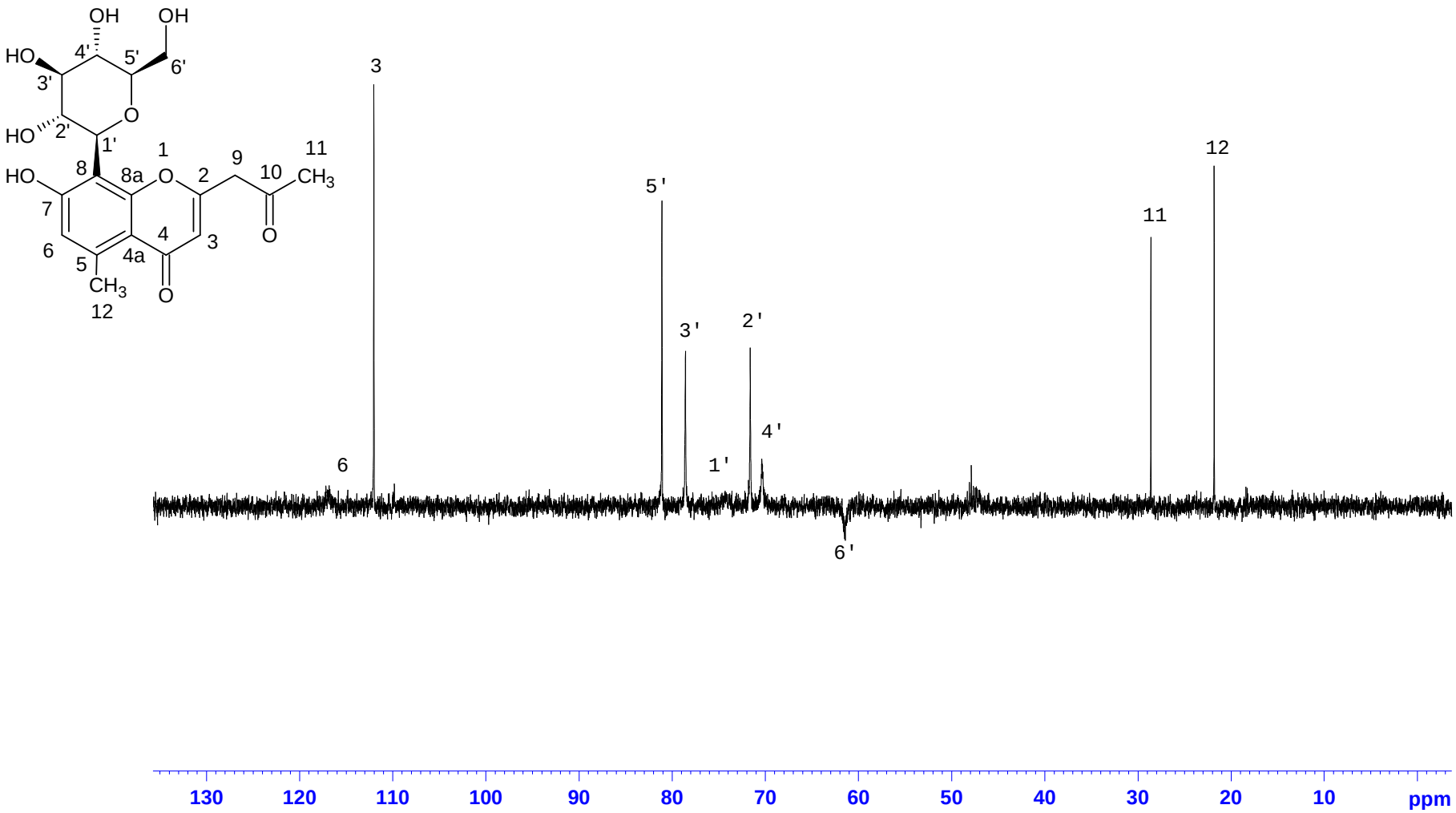

Plate 3d: COSY Spectrum of aloesin (2.3) in MeOH-d_4

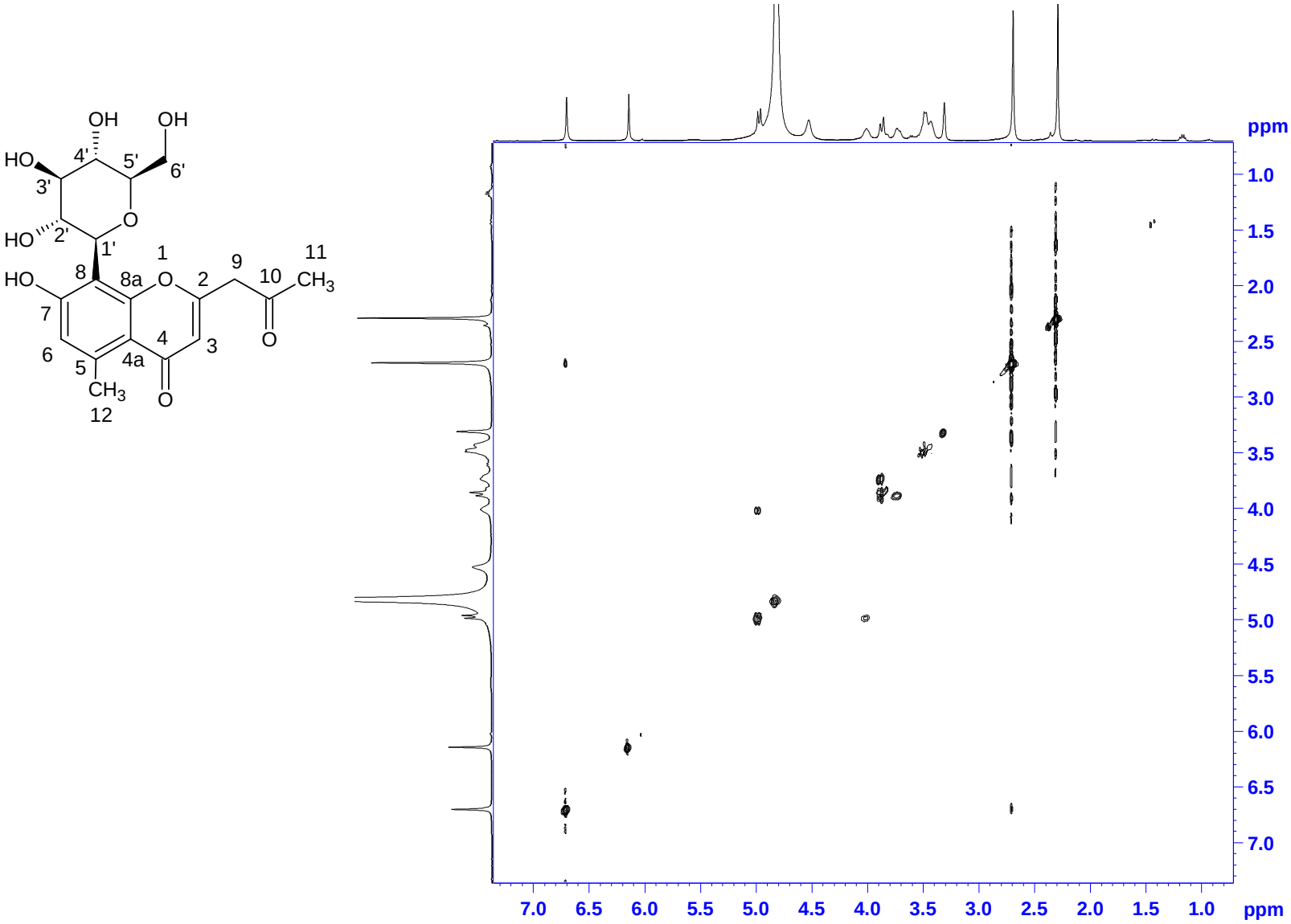

Plate 3e: HSQC NMR Spectrum of aloesin (2.3) in MeOH-d_4

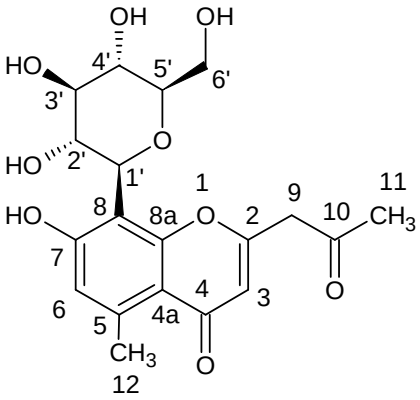

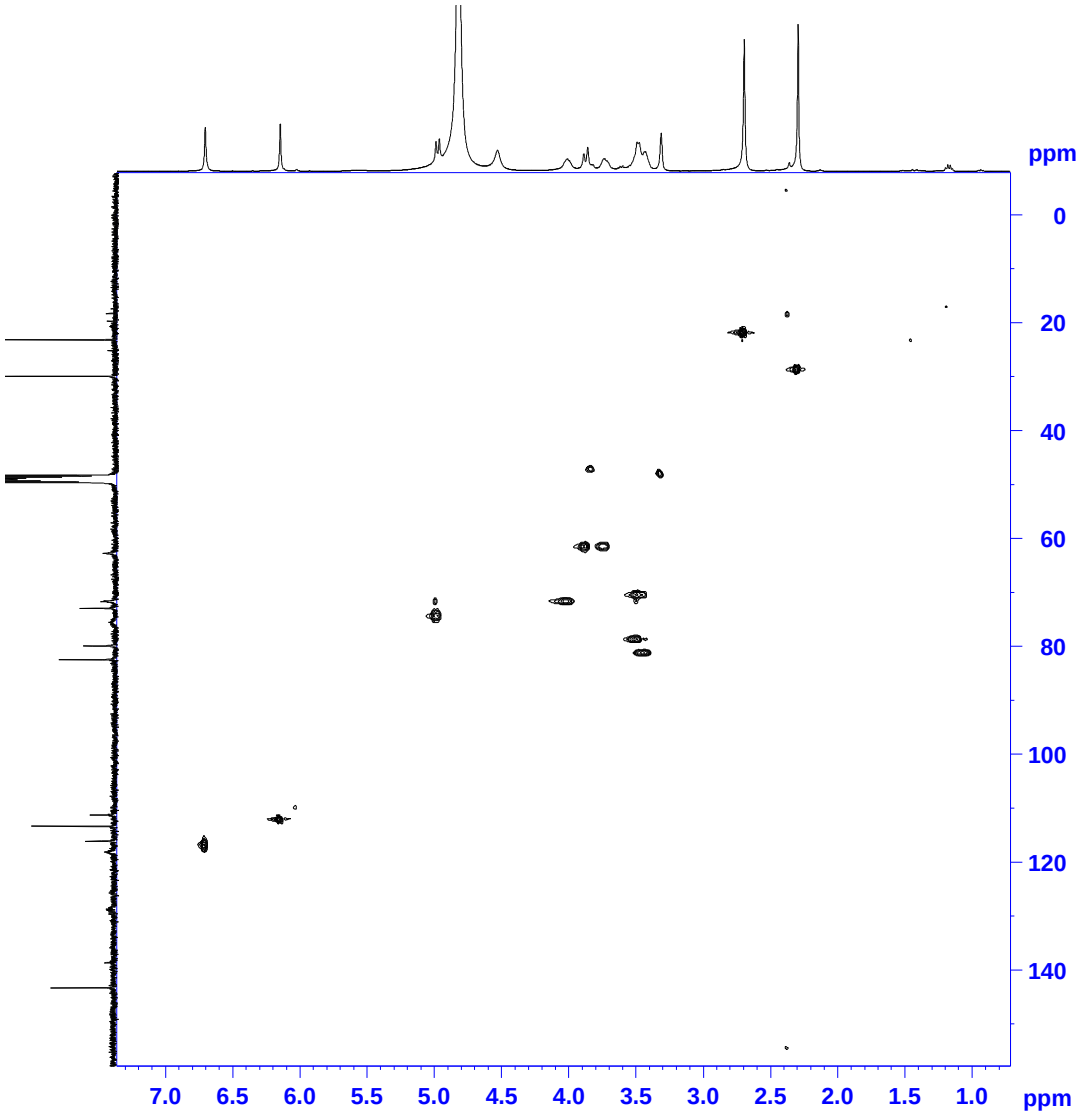

Plate 3f: HMBC Spectrum of aloesin (2.3) in MeOH-d_4

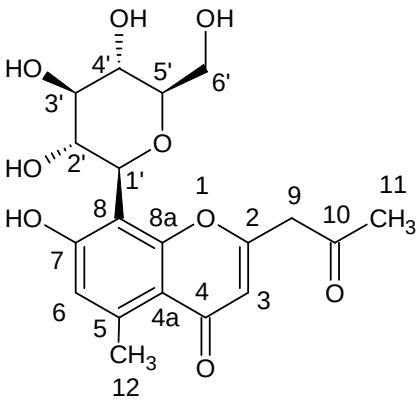

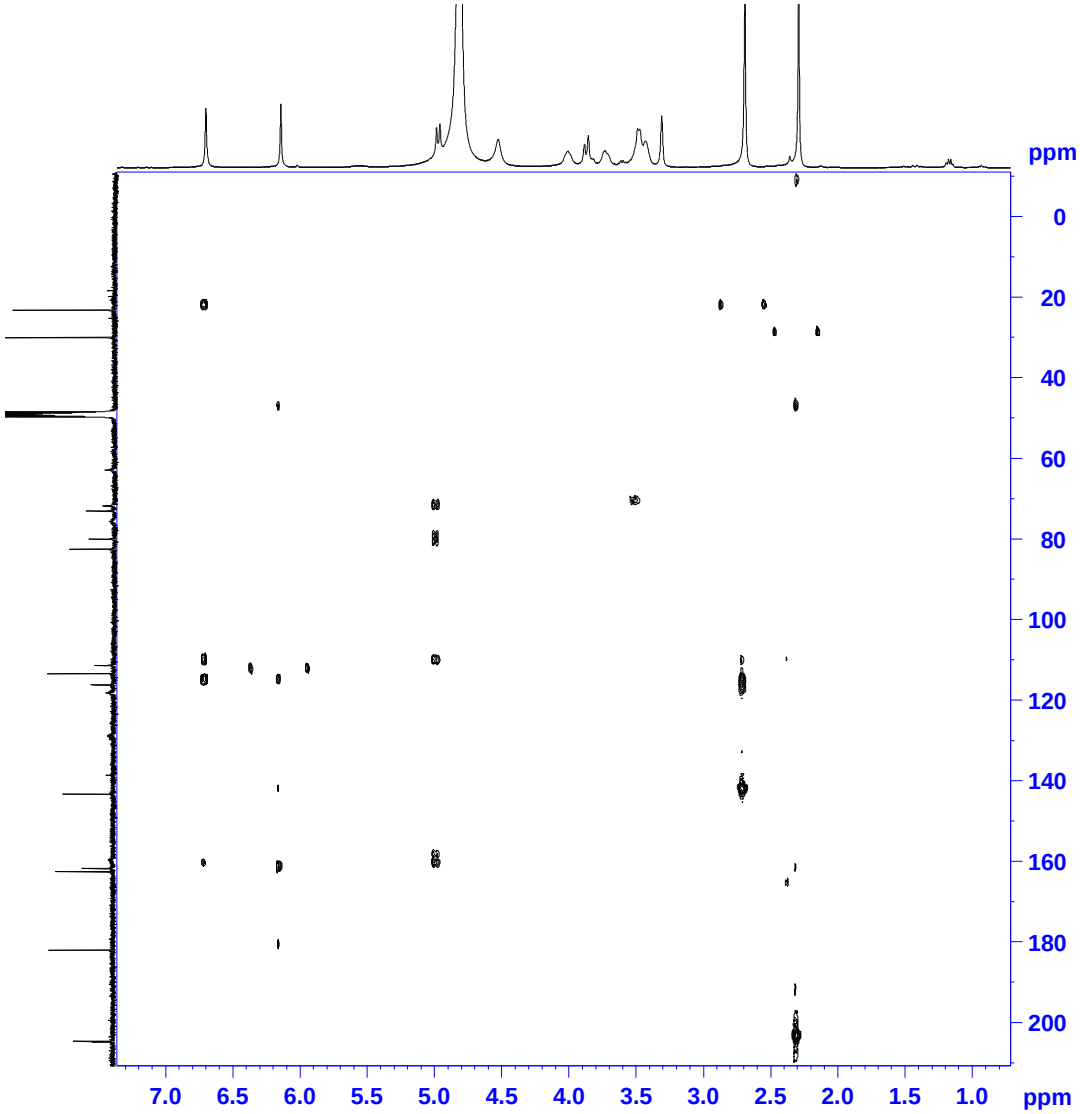

Plate 4a: ^{1}H NMR Spectrum of homonataloin (2.4) in DMSO-d_6

A: - isomer
B: + isomer

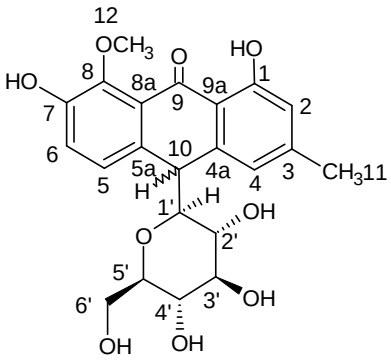

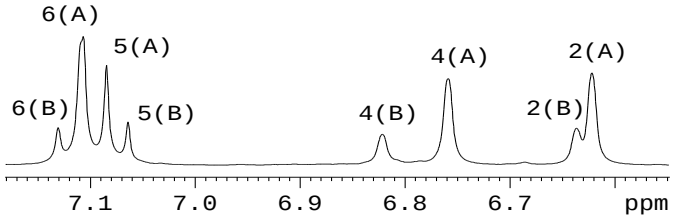

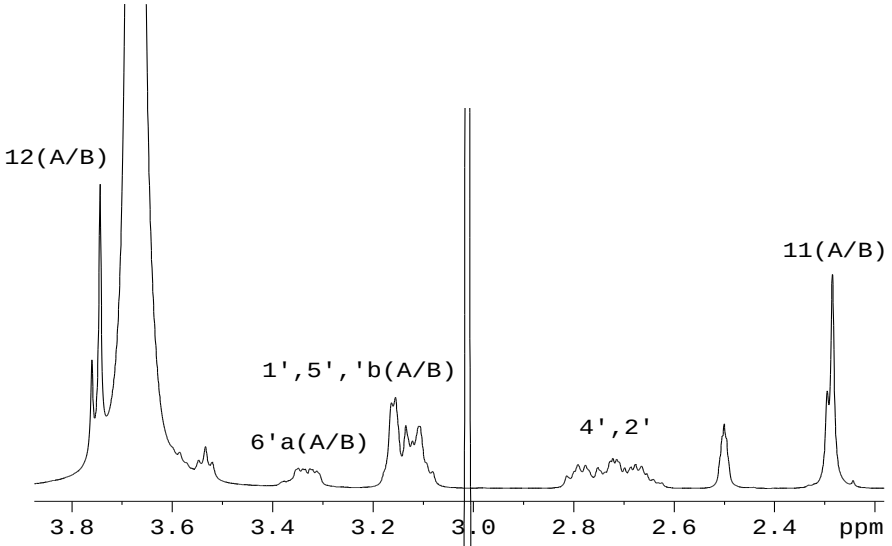

Plate 4b: ^{13}C NMR Spectrum of homonataloin (2.4) in DMSO-d_6

A: -isomer
B: + isomer

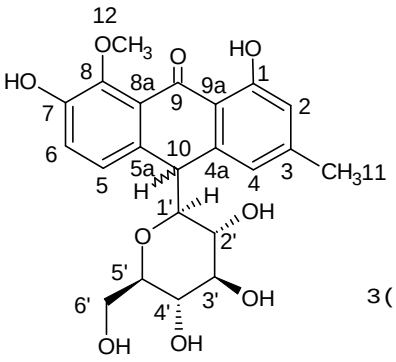

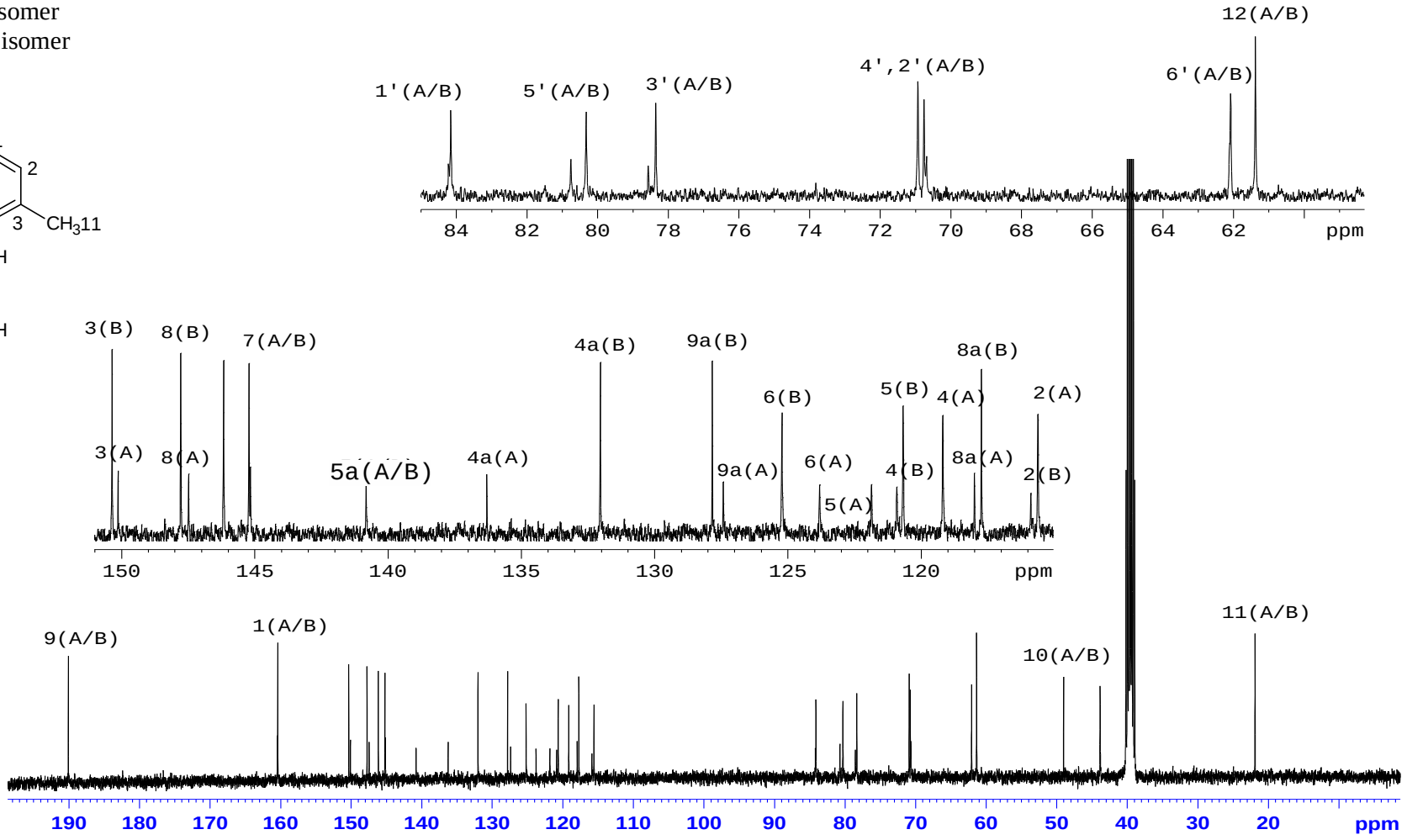

Plate 4c: DEPT 135 NMR Spectrum of homonataloin (2.4) in DMSO-d_6

A: -isomer
B: + isomer

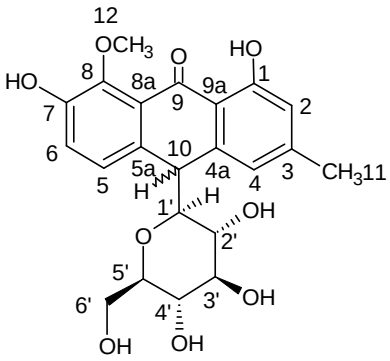

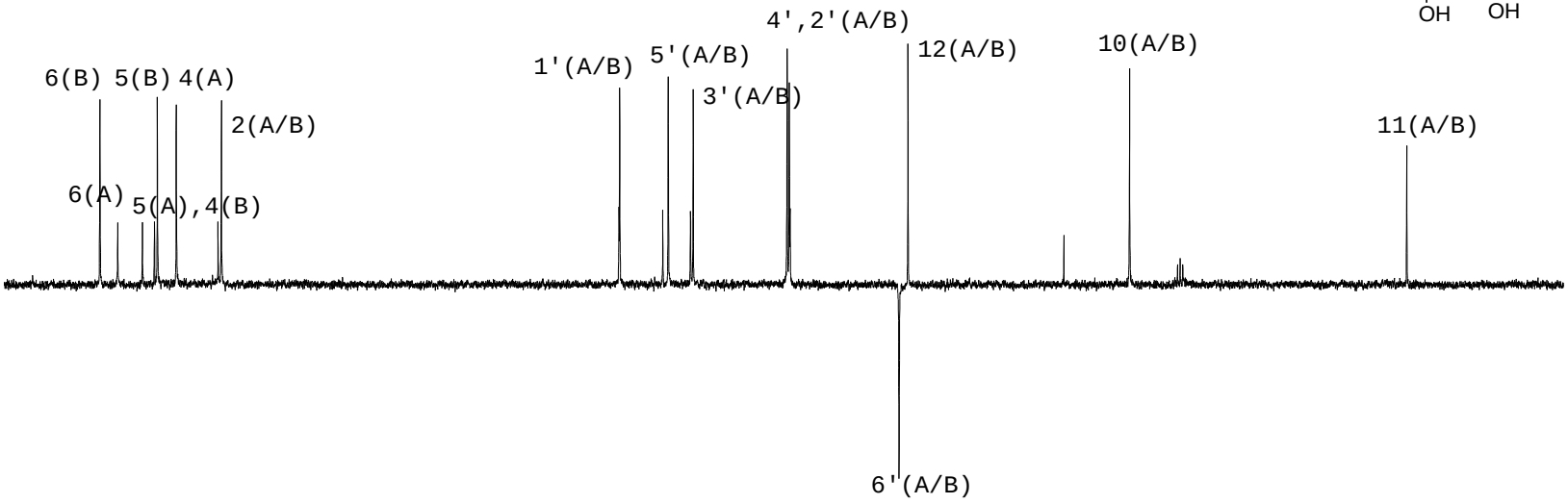

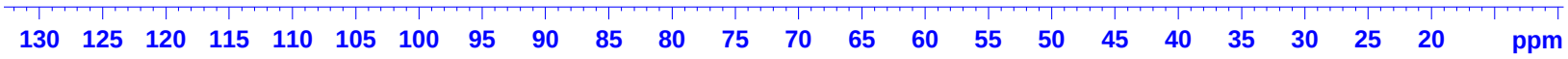

Plate 4d: COSY NMR Spectrum of homonataloin (2.4) in DMSO-d_6

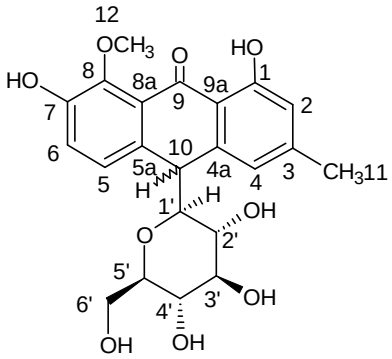

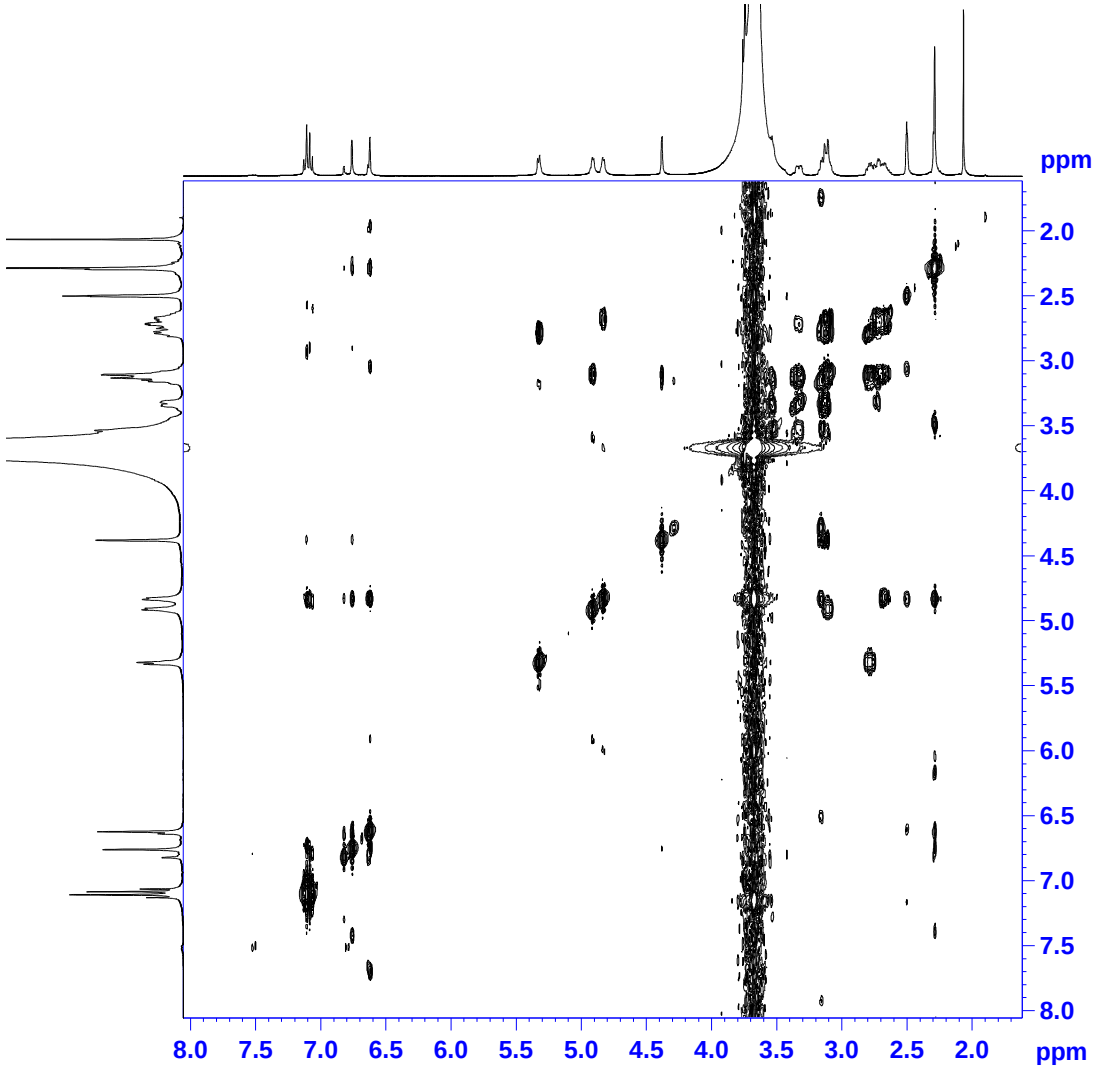

Plate 4e: HSQC NMR Spectrum of homonataloin (2.4) in DMSO-d_6

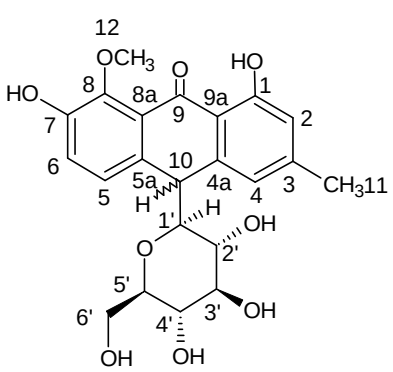

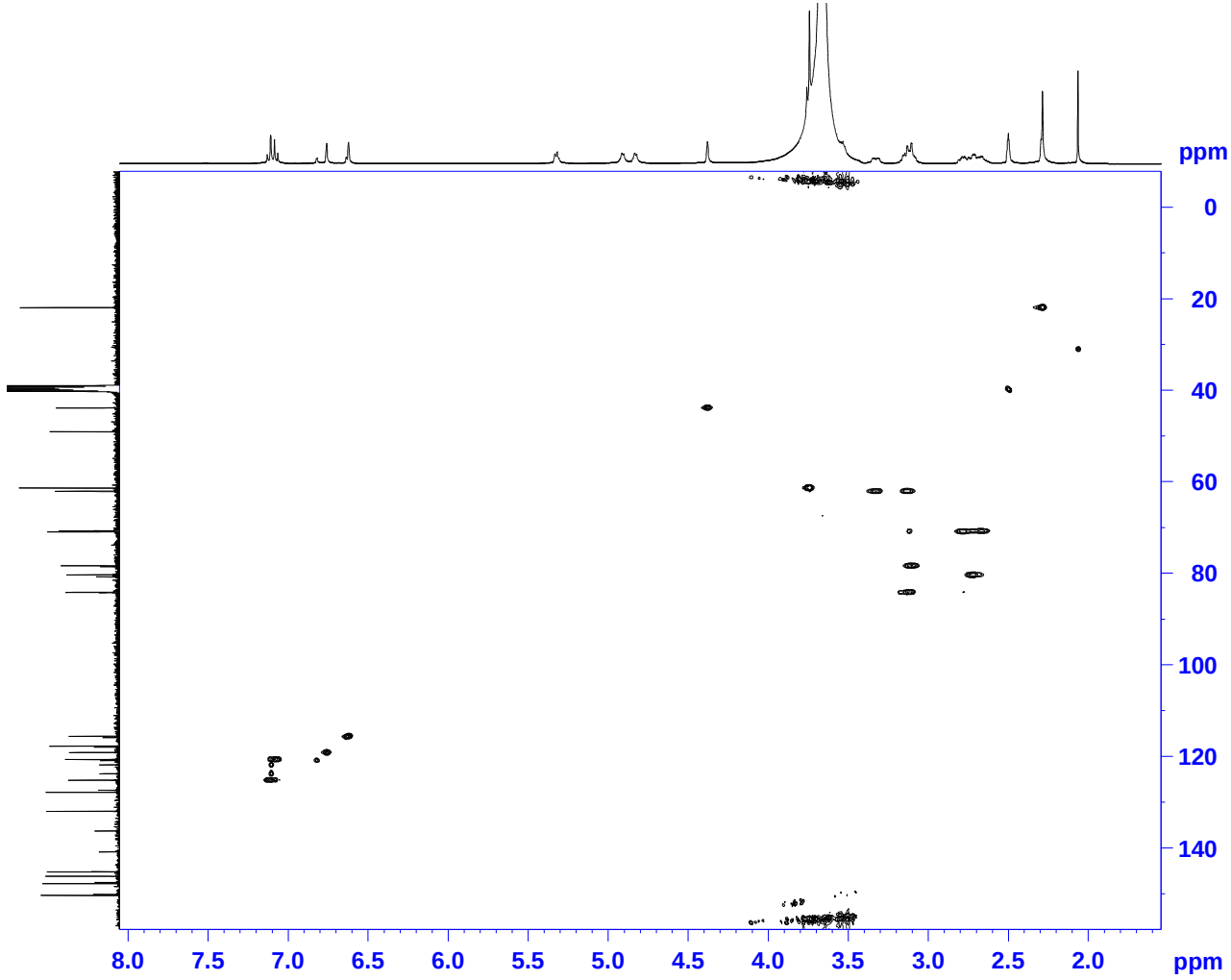

Plate 4f: HMBC NMR Spectrum of homonataloin (2.4) in DMSO-d_6

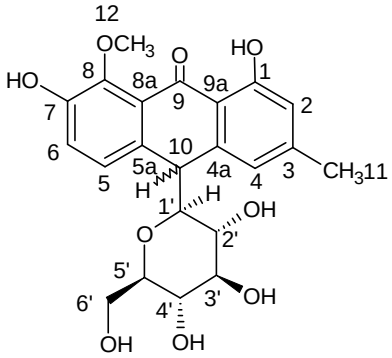

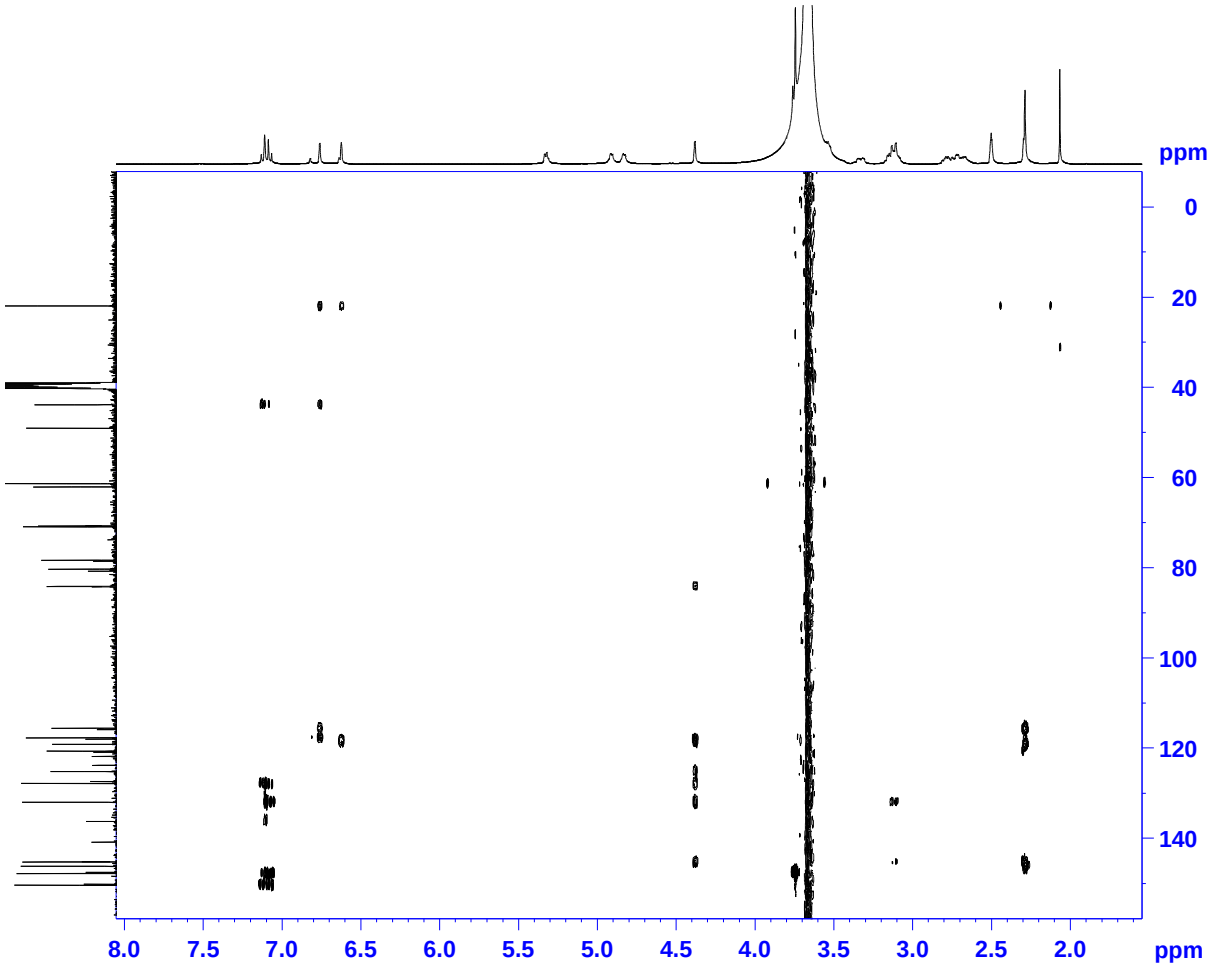

Plate 5a: ^{1}H NMR Spectrum of aloe-emodin (2.25) in DMSO-d_6

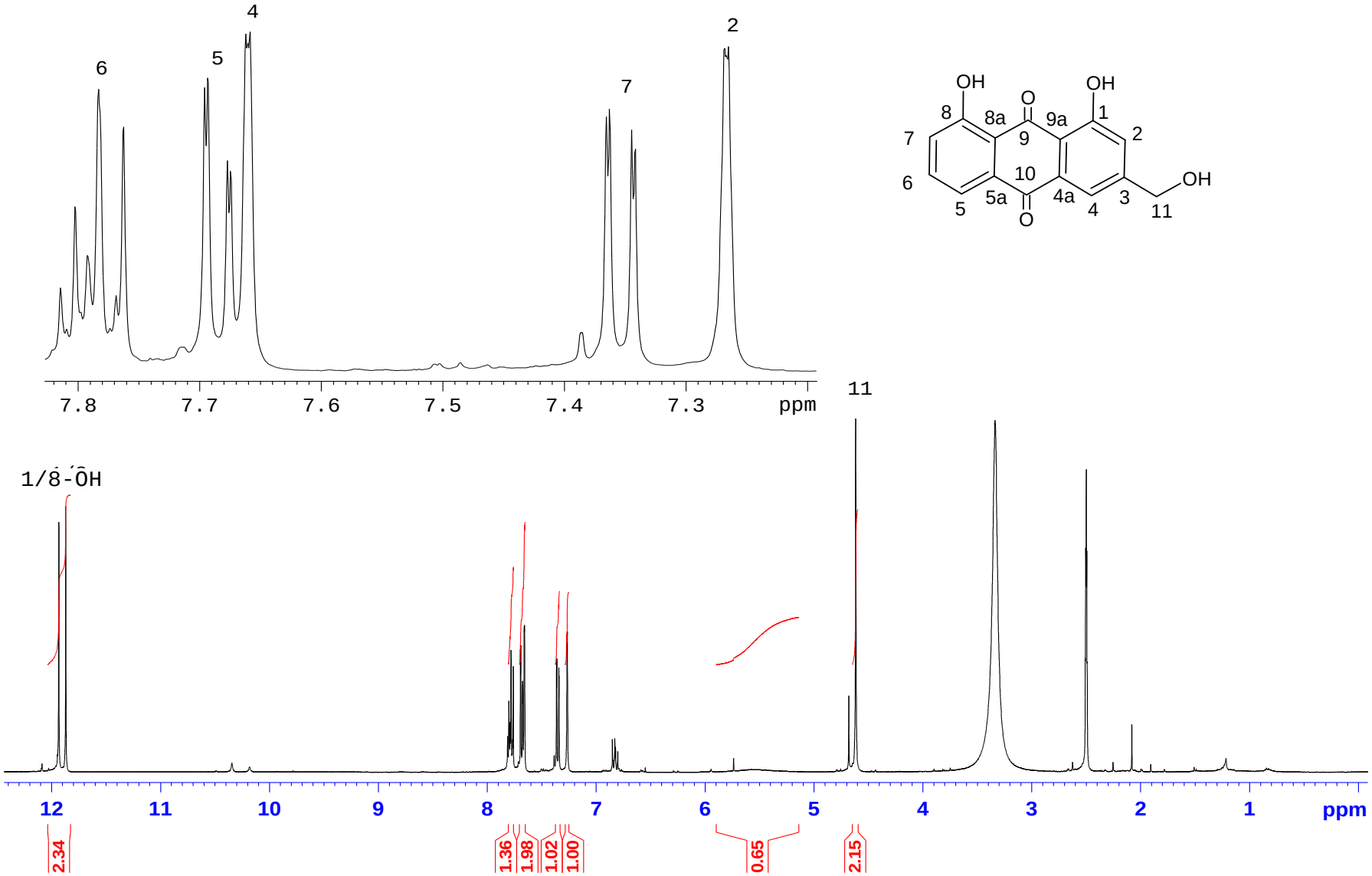

Plate 5b: ^{13}C NMR Spectrum of aloe-emodin (2.25) in DMSO-d_6

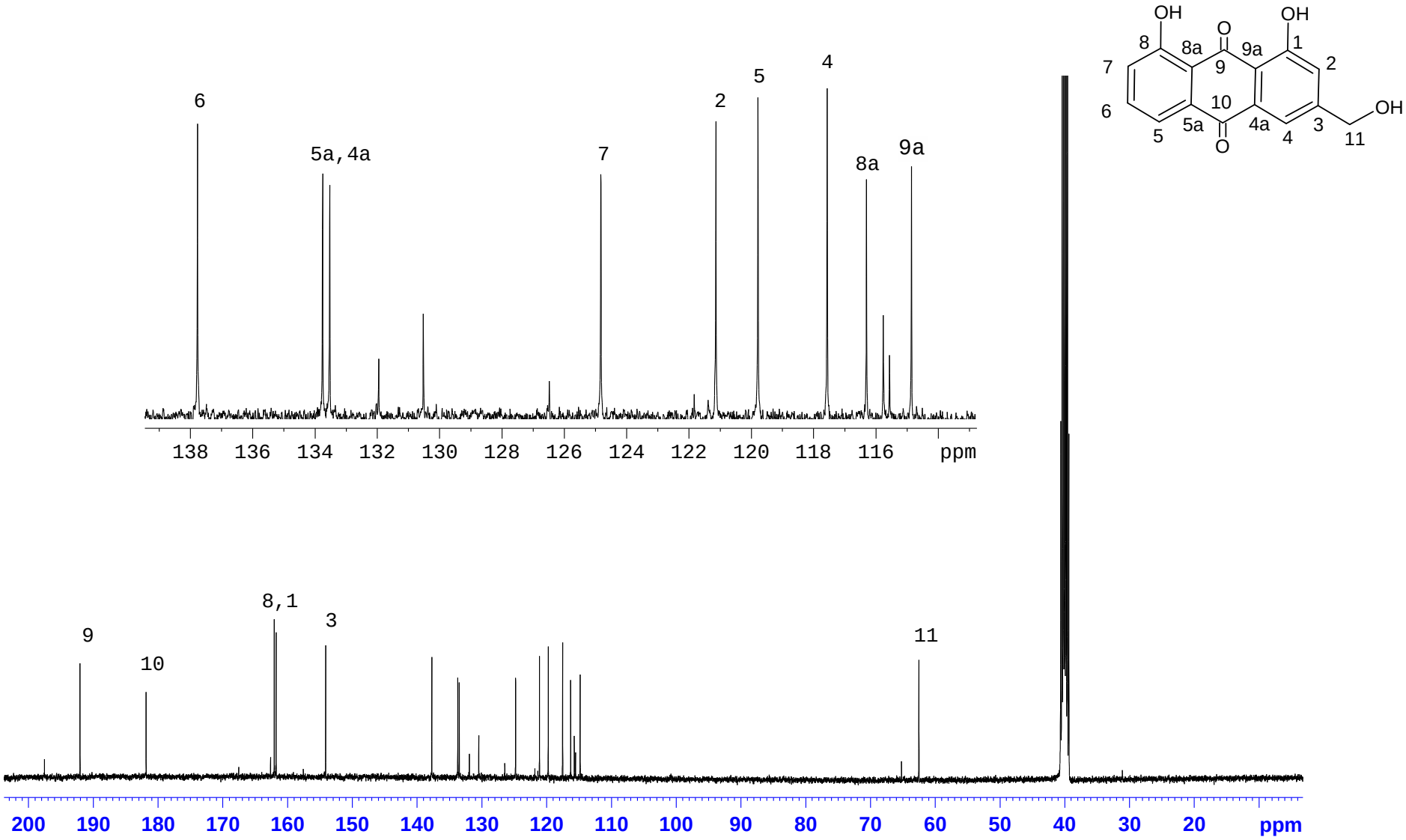

Plate 5c: DEPT 90 NMR Spectrum of aloe-emodin (2.25) in DMSO-d_6

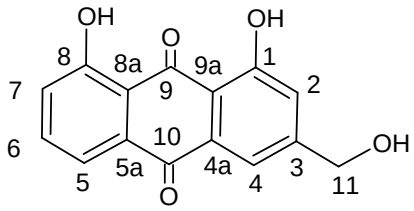

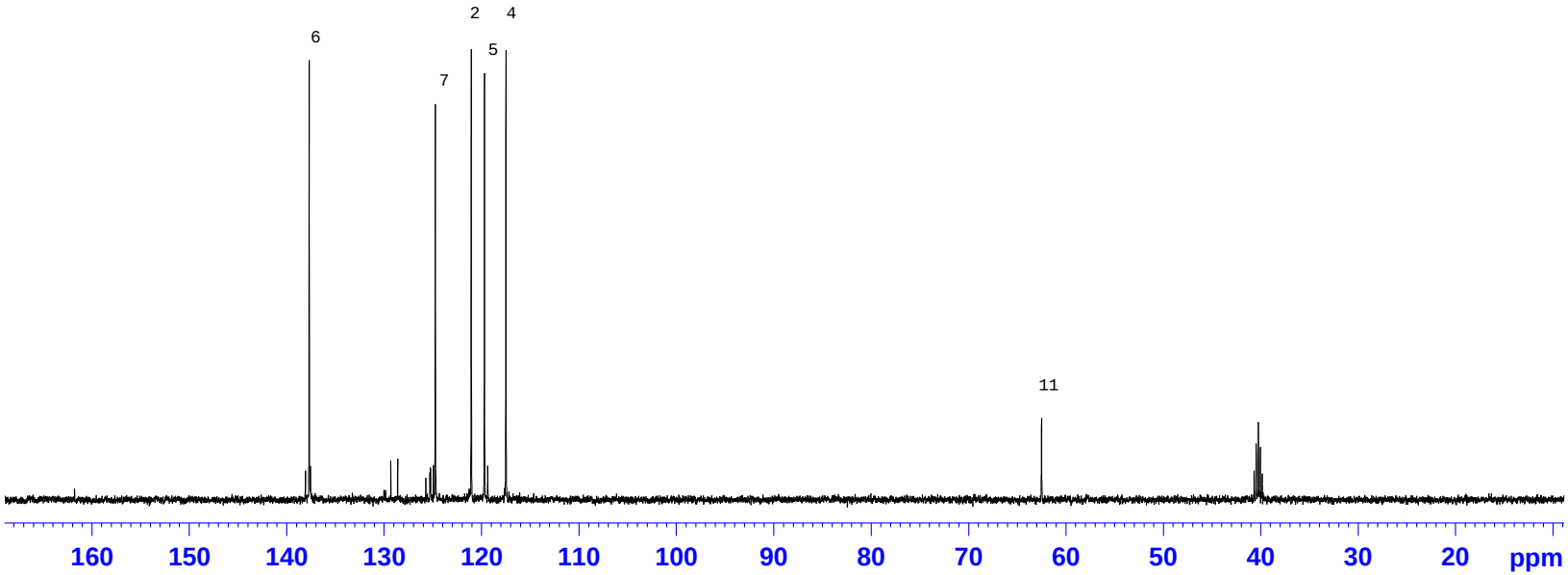

Plate 5d: COSY NMR Spectrum of aloe-emodin (2.25) in DMSO-d_6

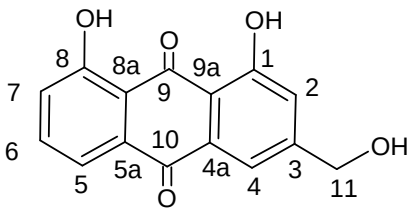

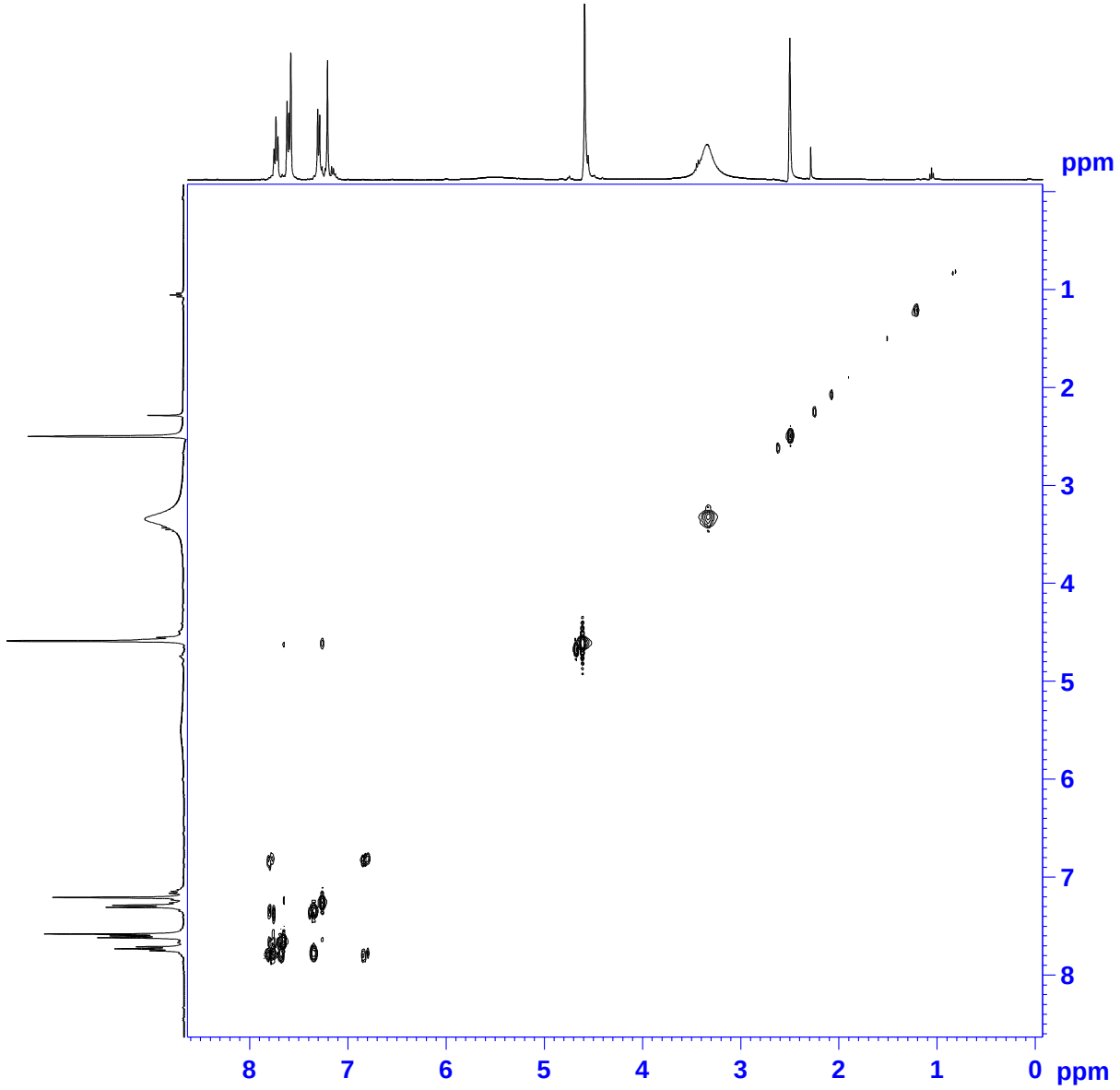

Plate 5e: HSQC NMR Spectrum of aloe-emodin (2.25) in DMSO-d_6

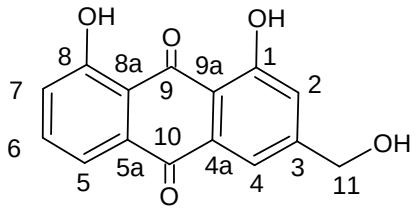

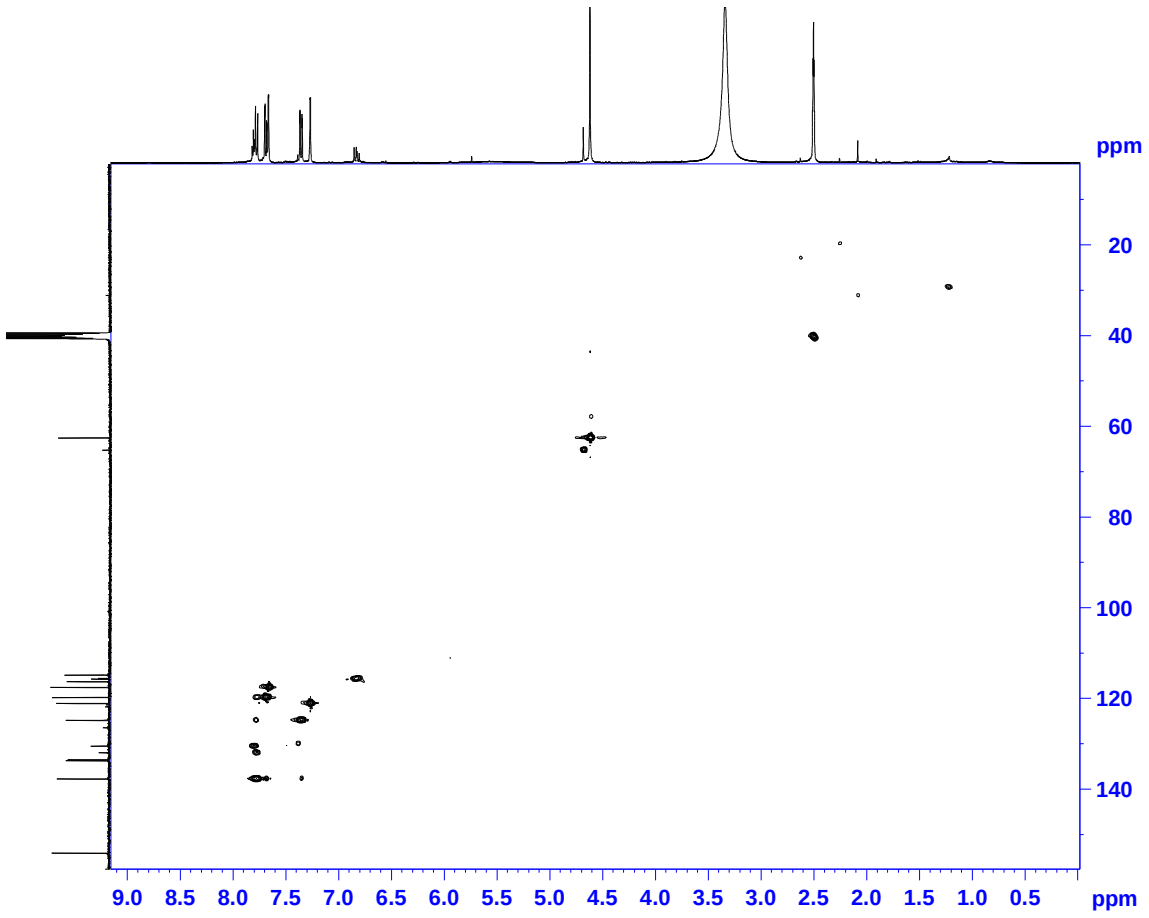

Plate 5f: HMBC NMR Spectrum of aloe-emodin (2.25) in DMSO-d_6

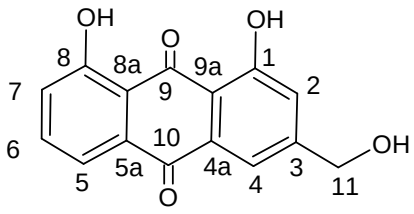

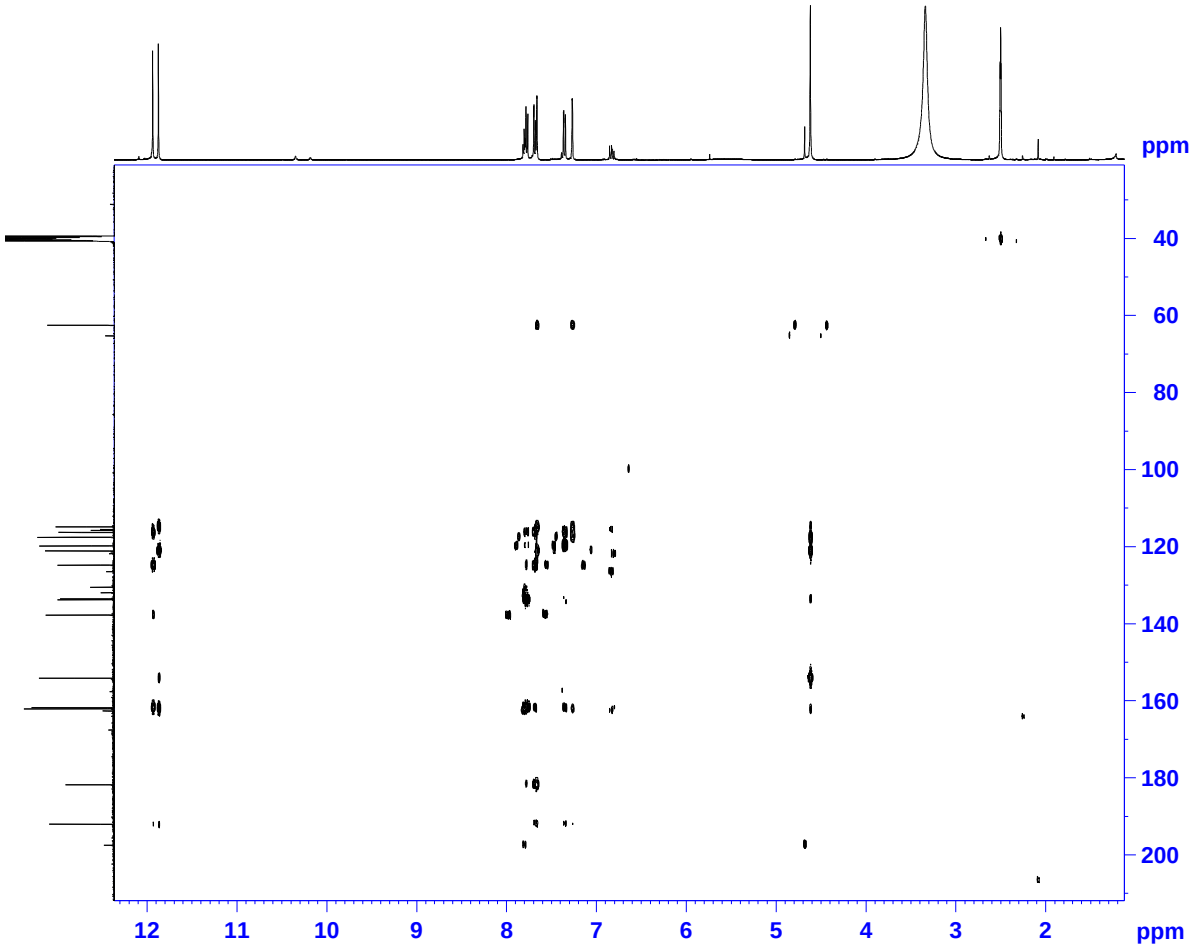

Plate 6a: ^{1}H NMR Spectrum of nataloe-emodin (2.28) in DMSO-d_6

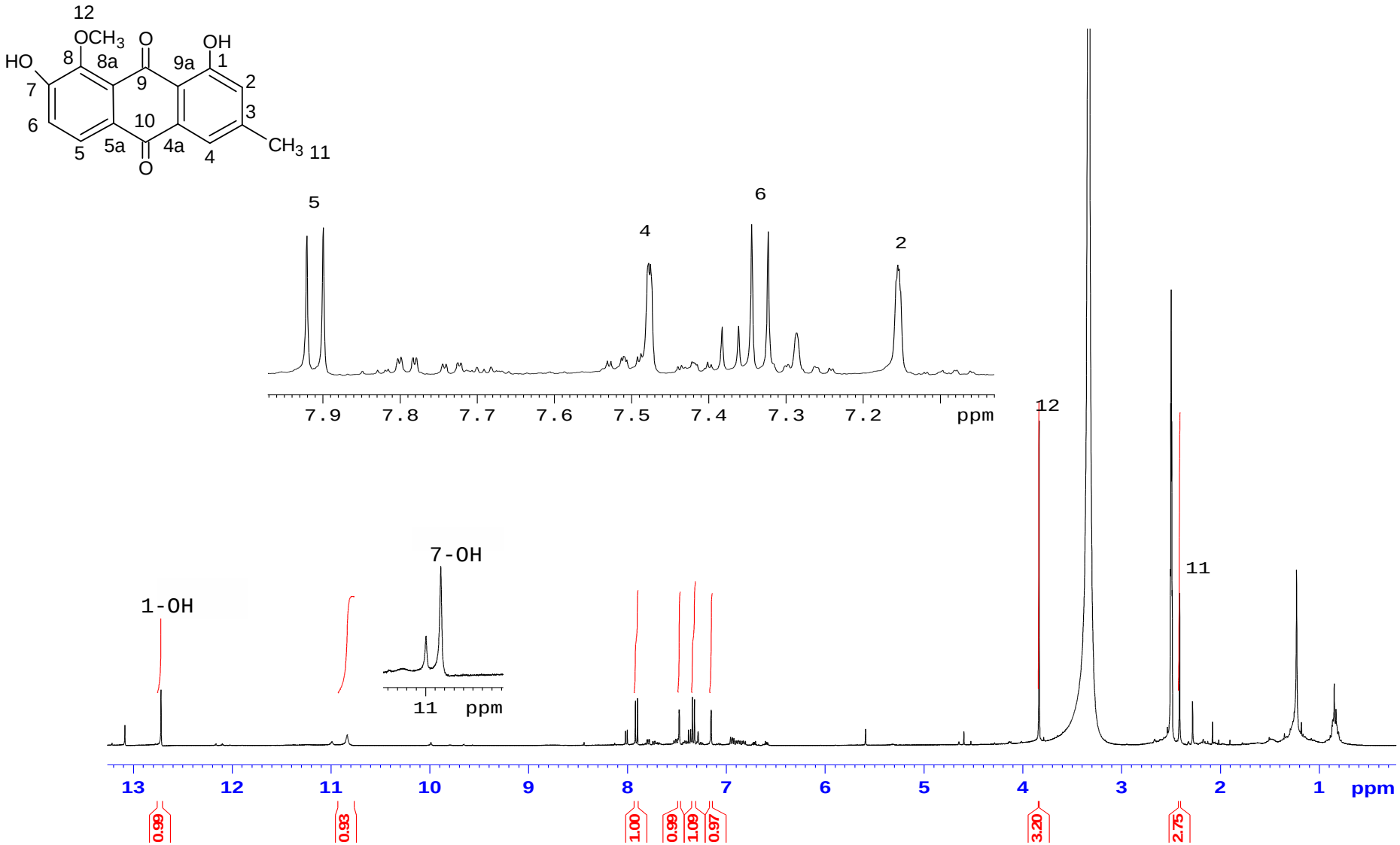

Plate 6b: ^{13}C NMR Spectrum of nataloe-emodin (2.28) in DMSO-d_6

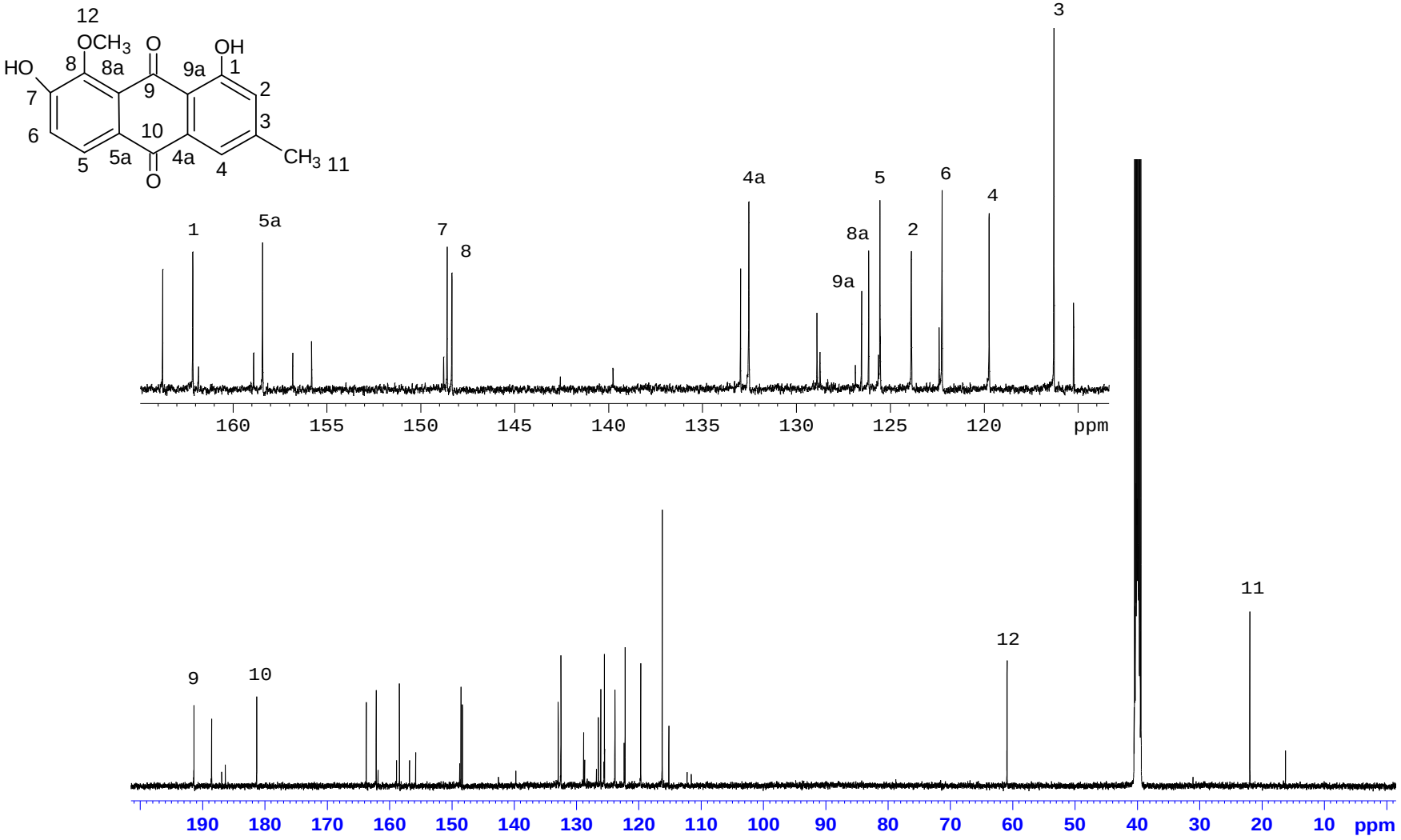

Plate 6C: DEPT 135 (i) and DEPT 90 (ii) NMR Spectra of nataloe-emodin (2.28) in DMSO-d_6

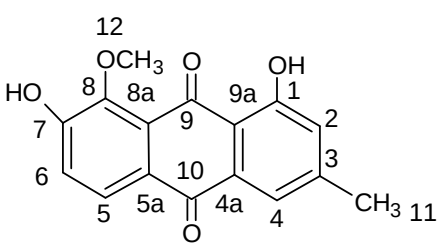

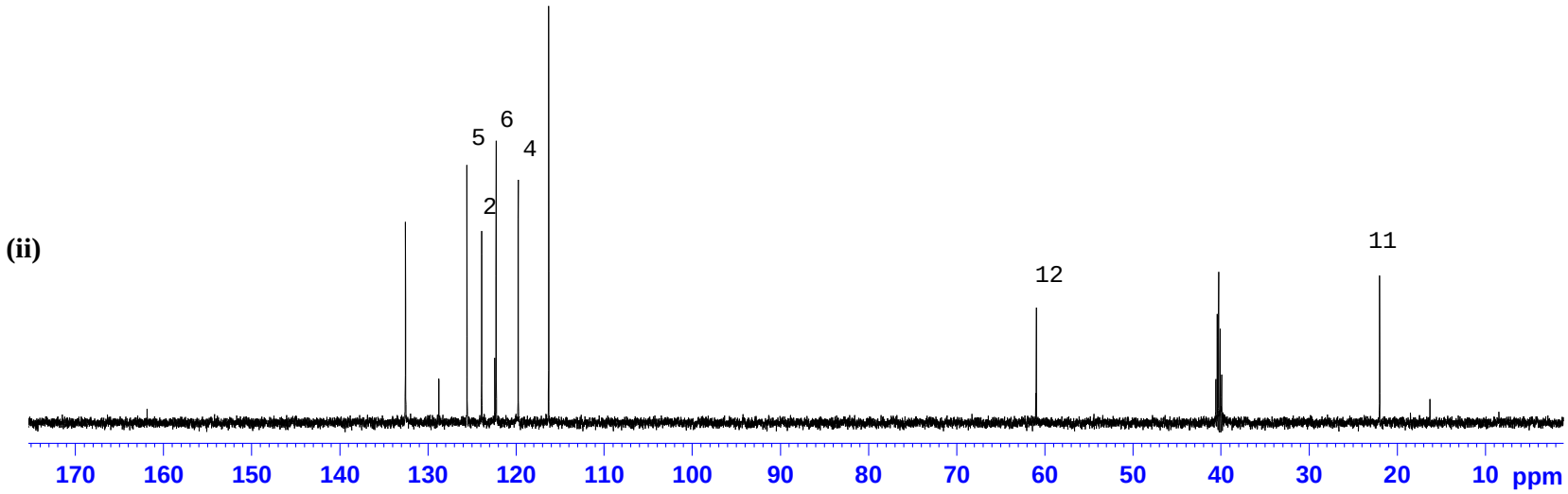

Plate 6d: COSY NMR Spectrum of nataloe-emodin (2.28) in DMSO-d_6

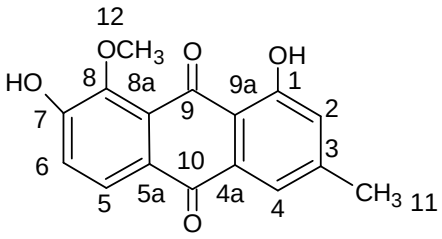

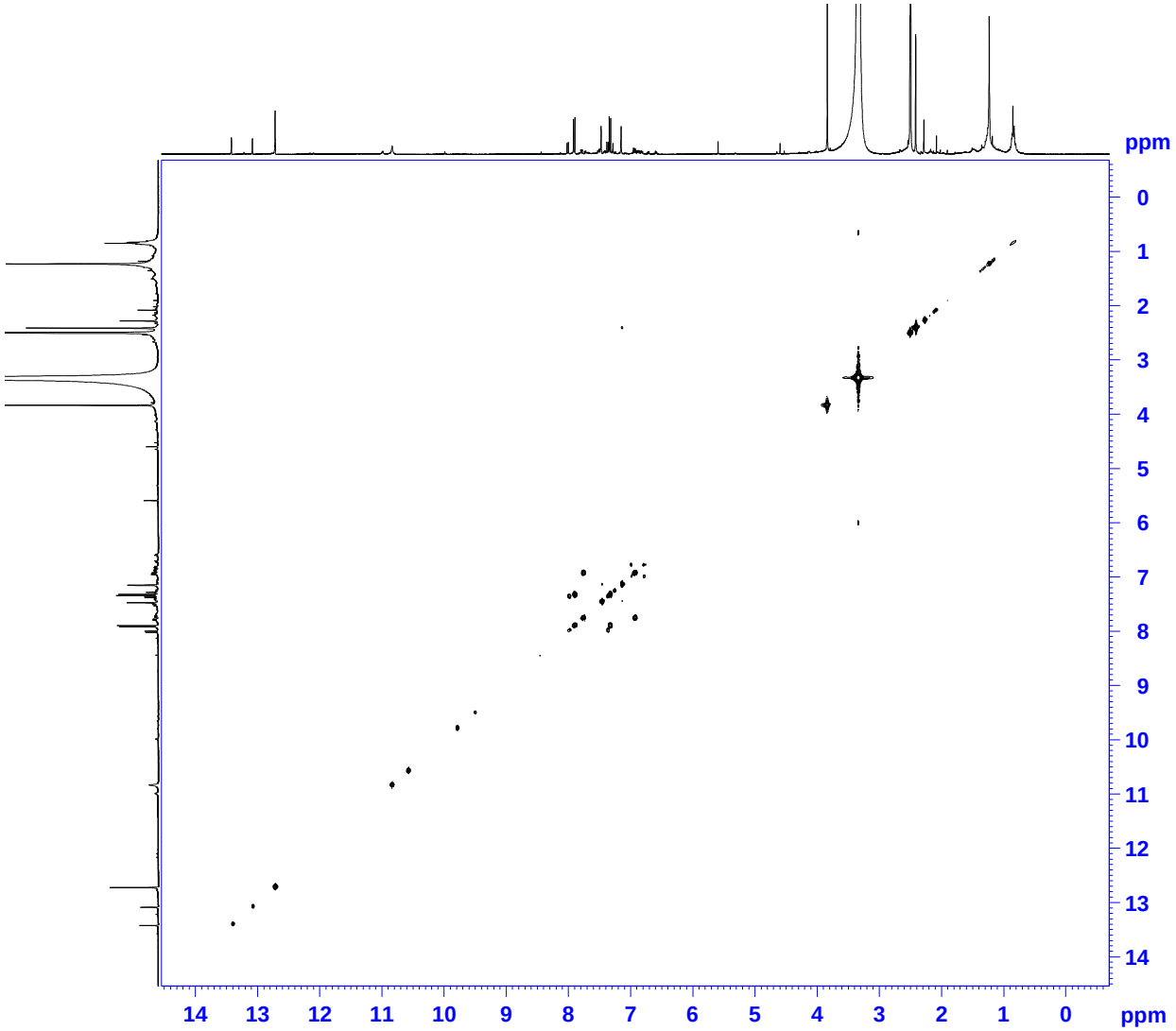

Plate 6e: HSQC NMR Spectrum of nataloe-emodin (2.28) in DMSO-d_6

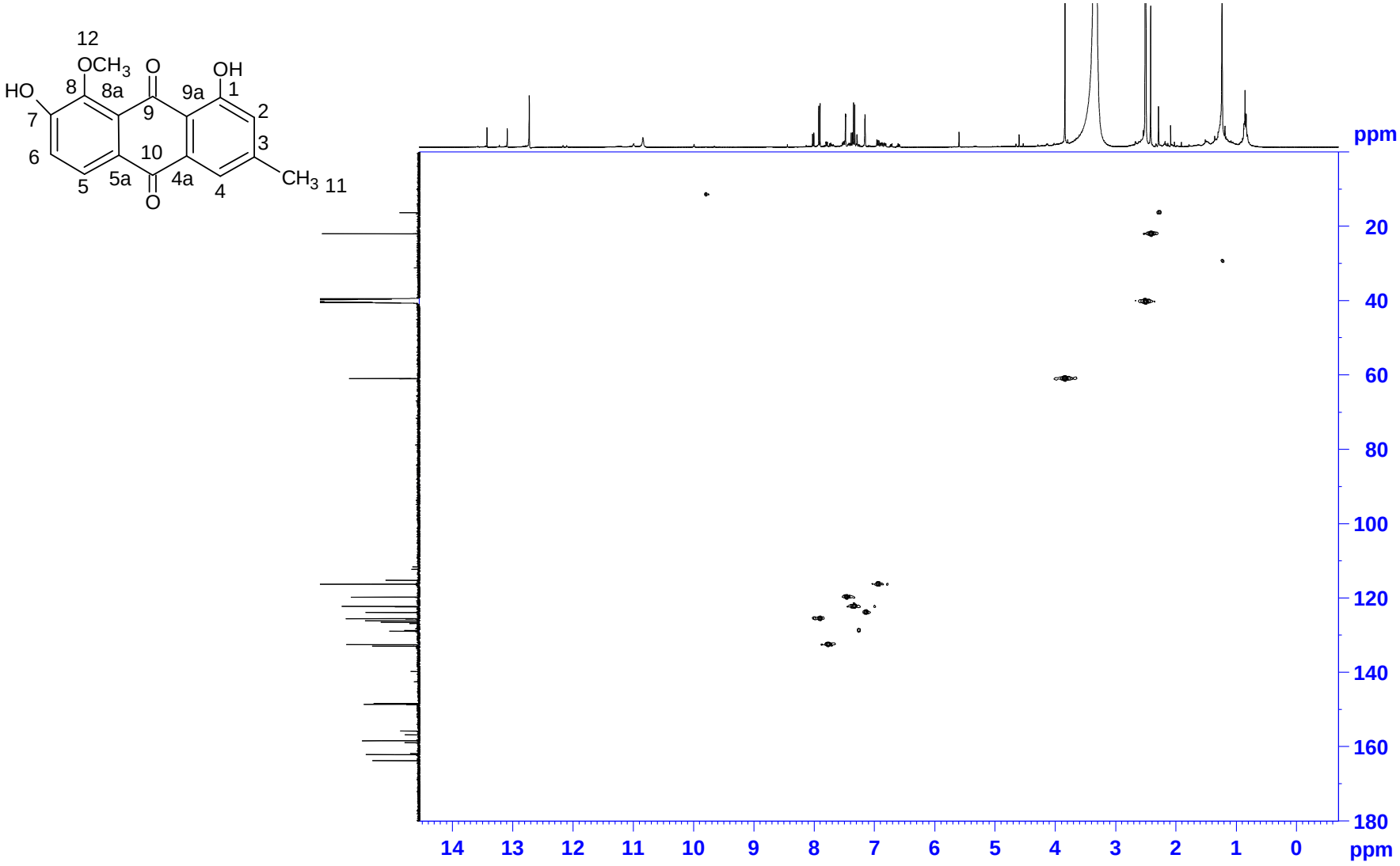

Plate 6f: HMBC NMR Spectrum of nataloe-emodin (2.28) in DMSO-d_6

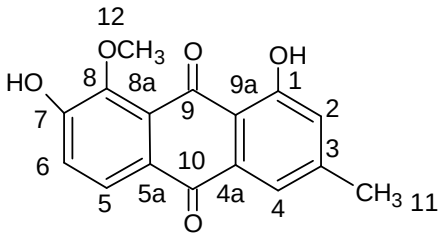

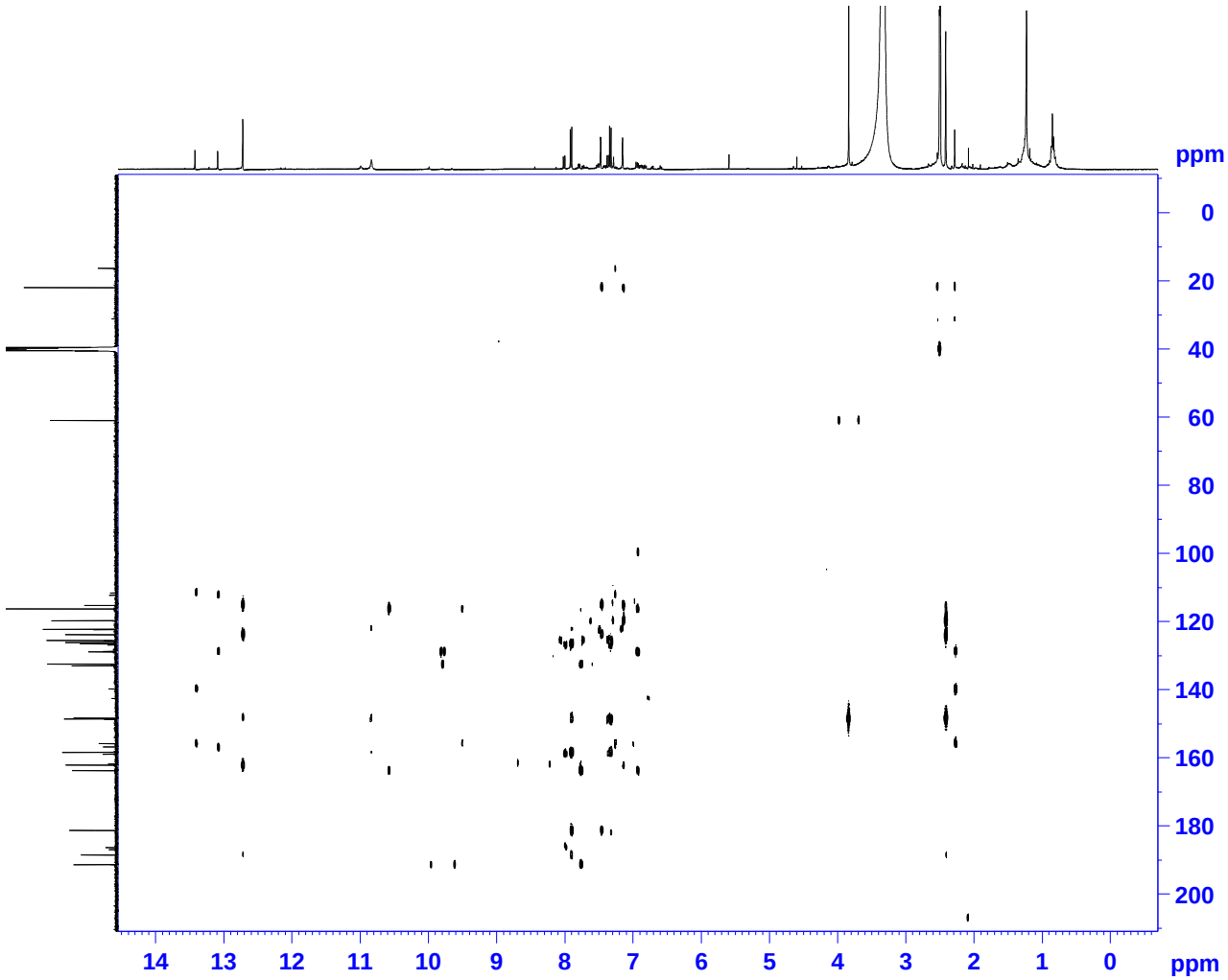

Plate 7a: ^{1}H NMR Spectrum of rheinal (2.29) in DMSO-d_6

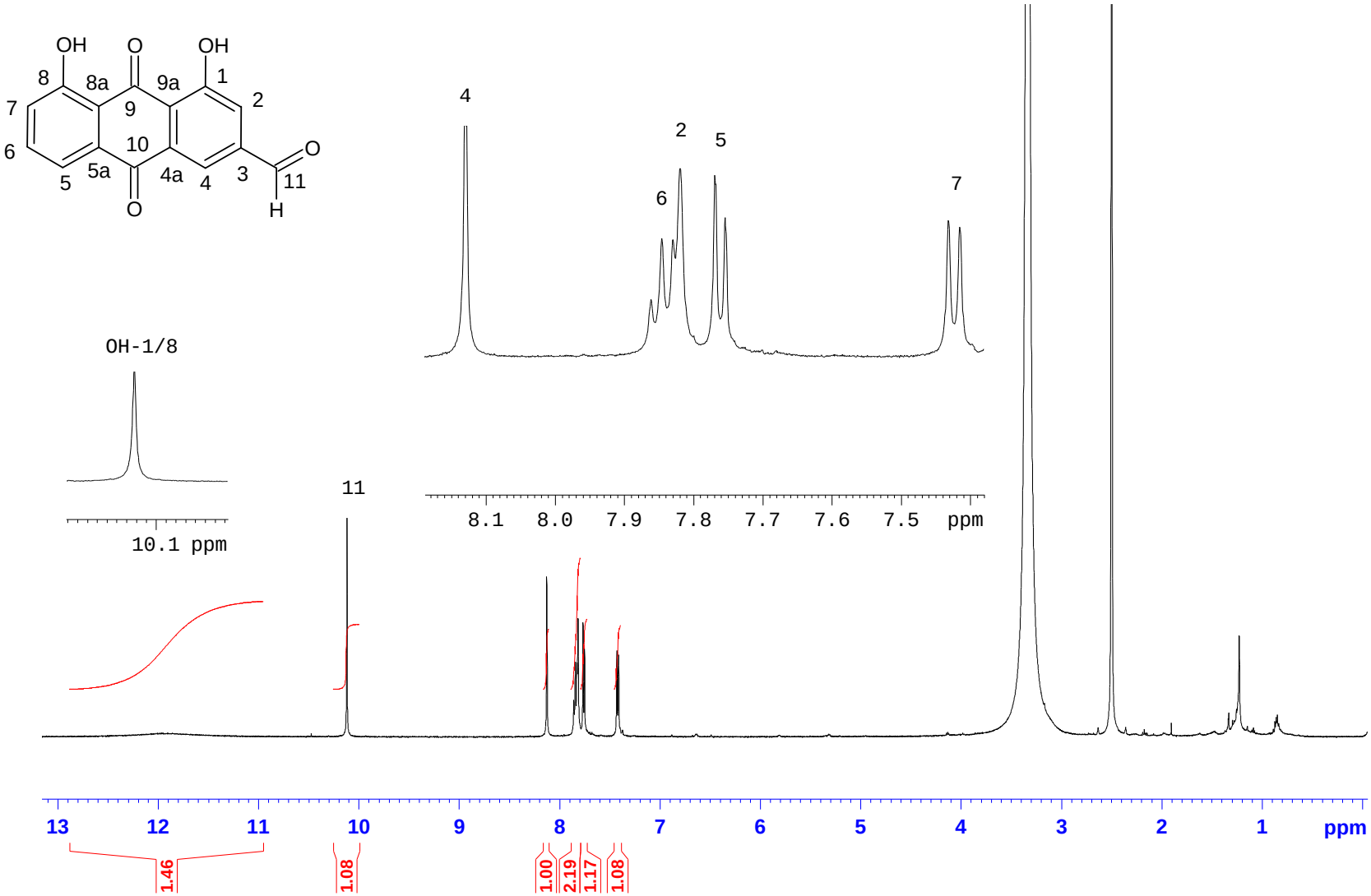

Plate 7b: ^{13}C NMR Spectrum of rheinal (2.29) in DMSO-d_6

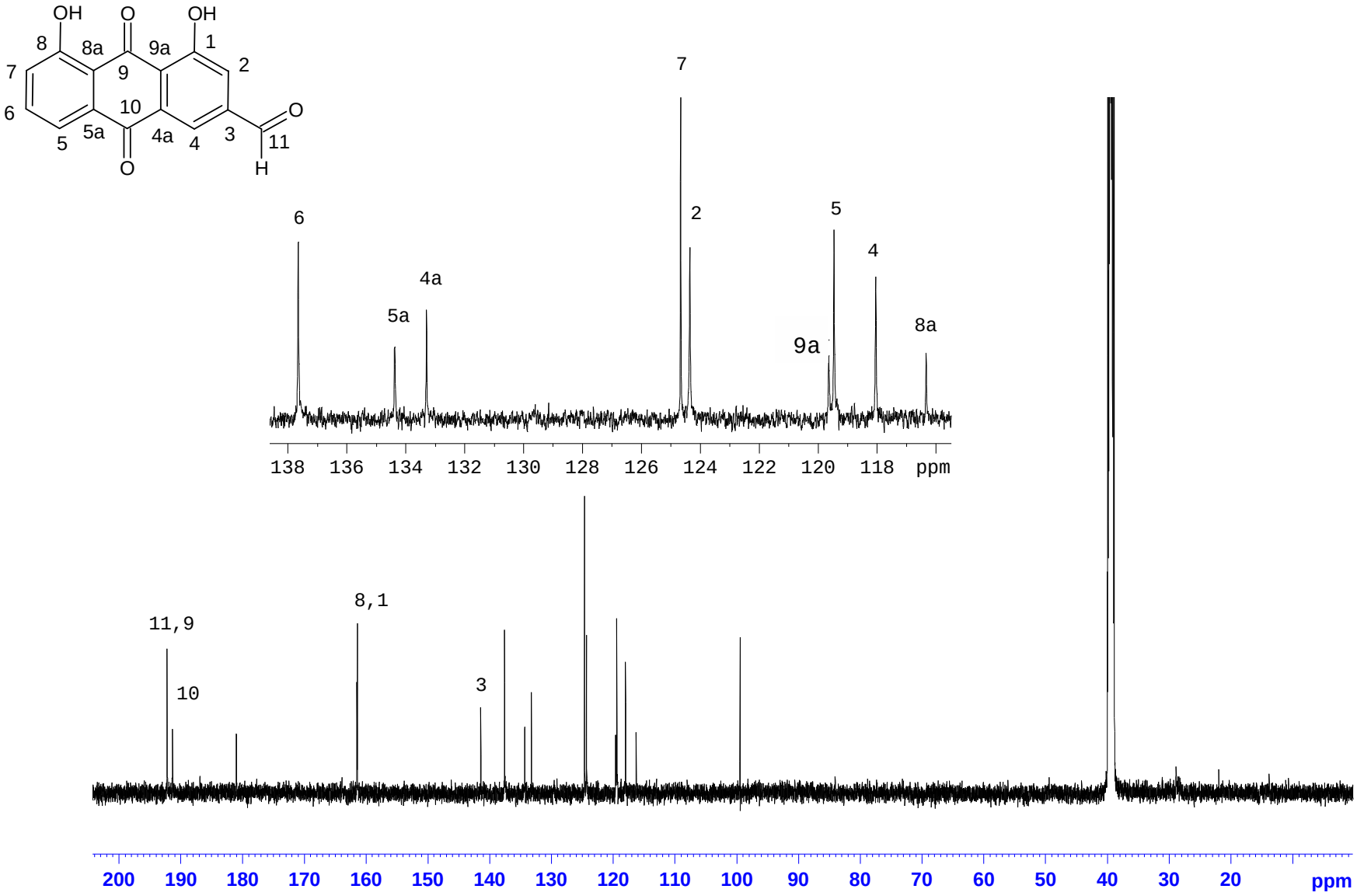

Plate 7c: COSY NMR Spectrum of rheinal (2.29) in DMSO-d_6

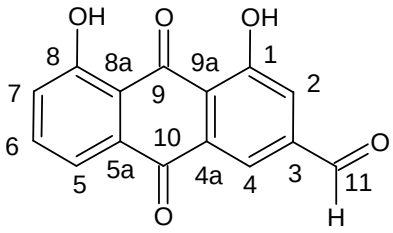

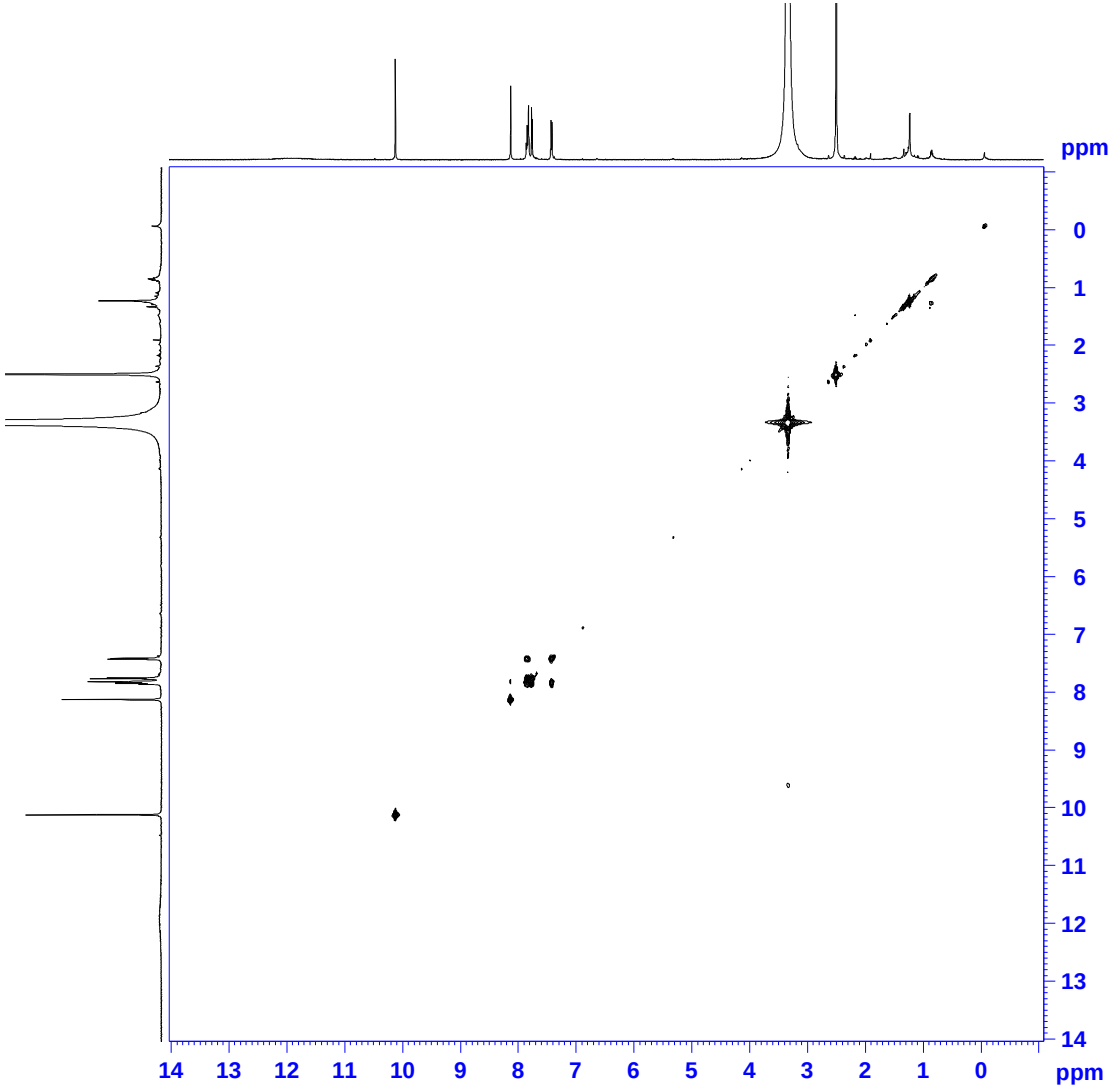

Plate 7d: HSQC NMR Spectrum of rheinal (2.29) in DMSO-d_6

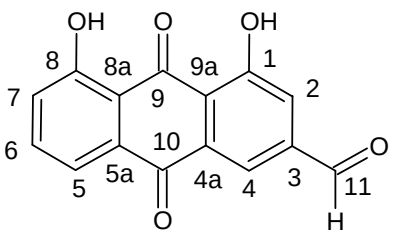

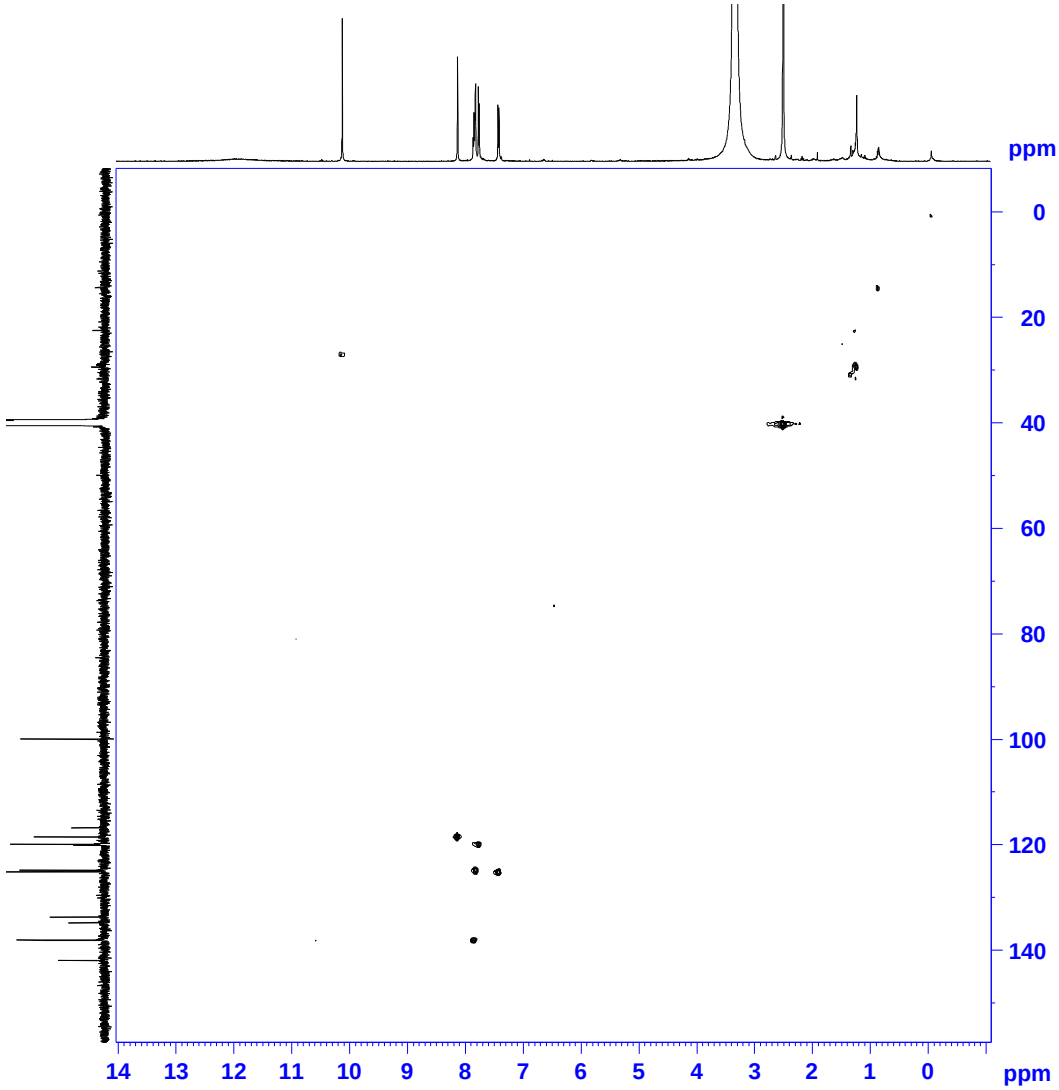

Plate 7e: HMBC NMR Spectrum of rheinal (2.29) in DMSO-d_6

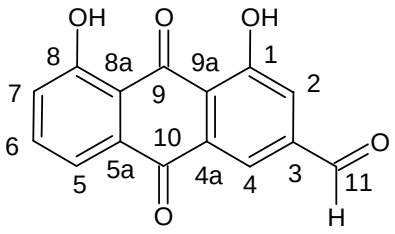

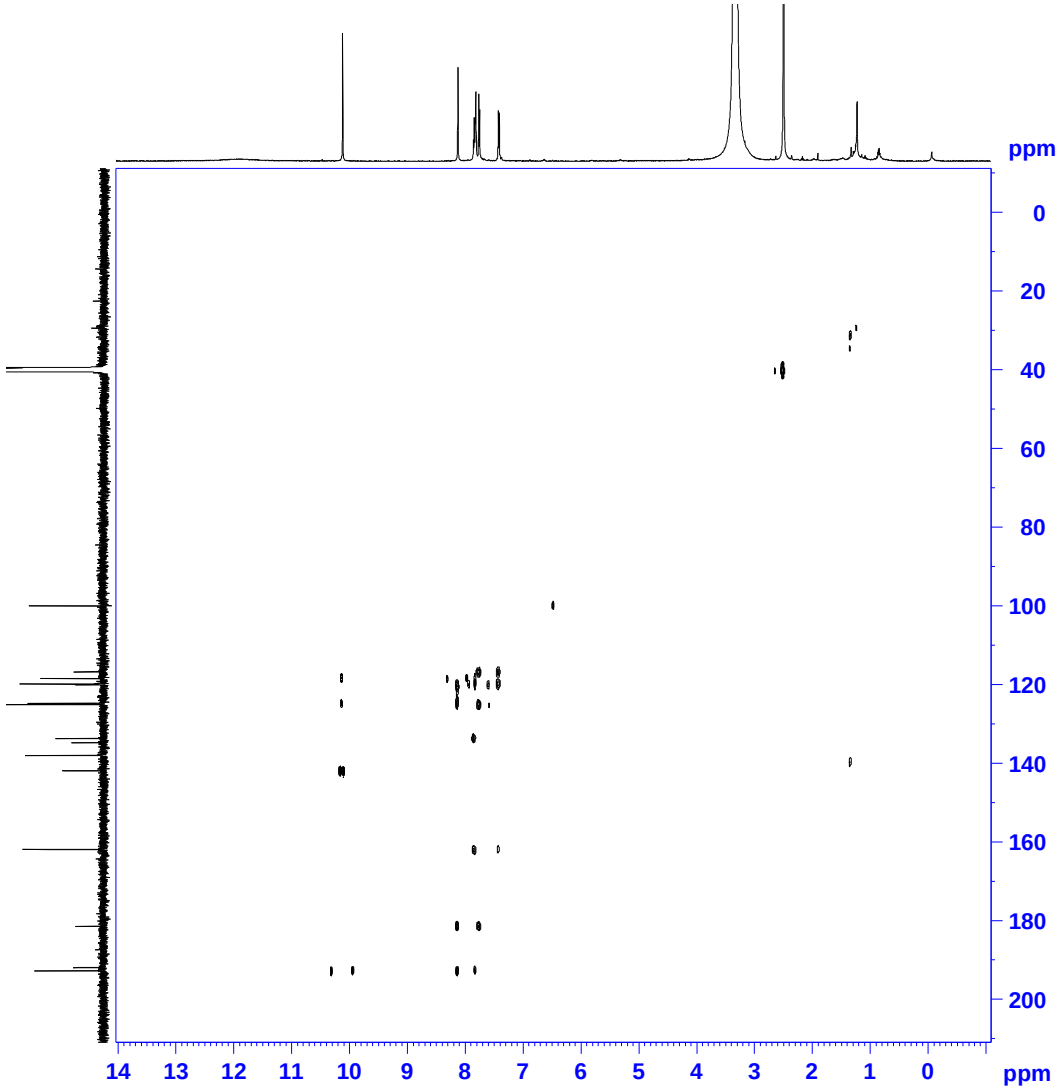

Plate 8a: ^{1}H NMR Spectrum of IBX (2.30) in DMSO-d_6

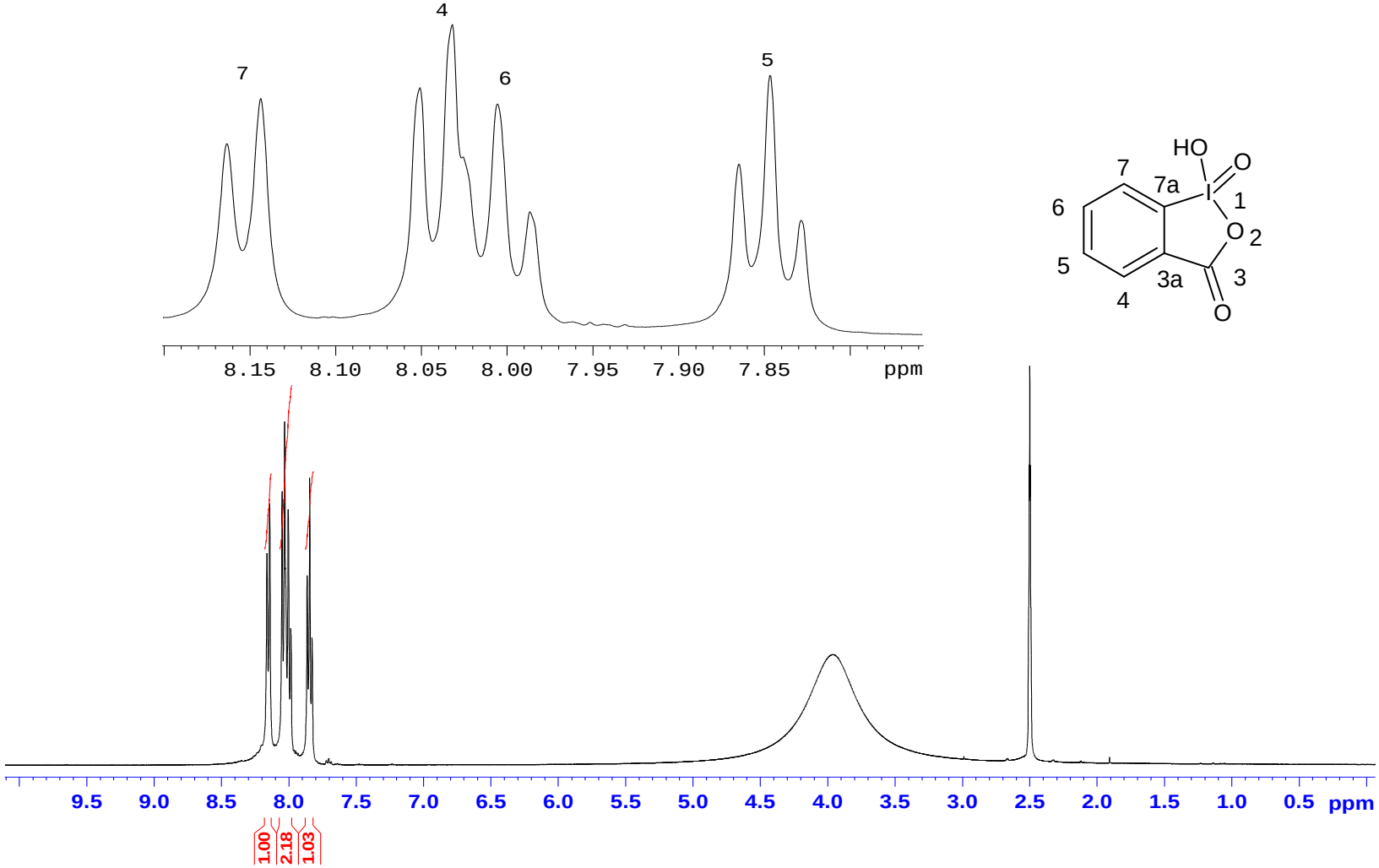

Plate 8b: ^{13}C NMR Spectrum of IBX (2.30) in DMSO-d_6

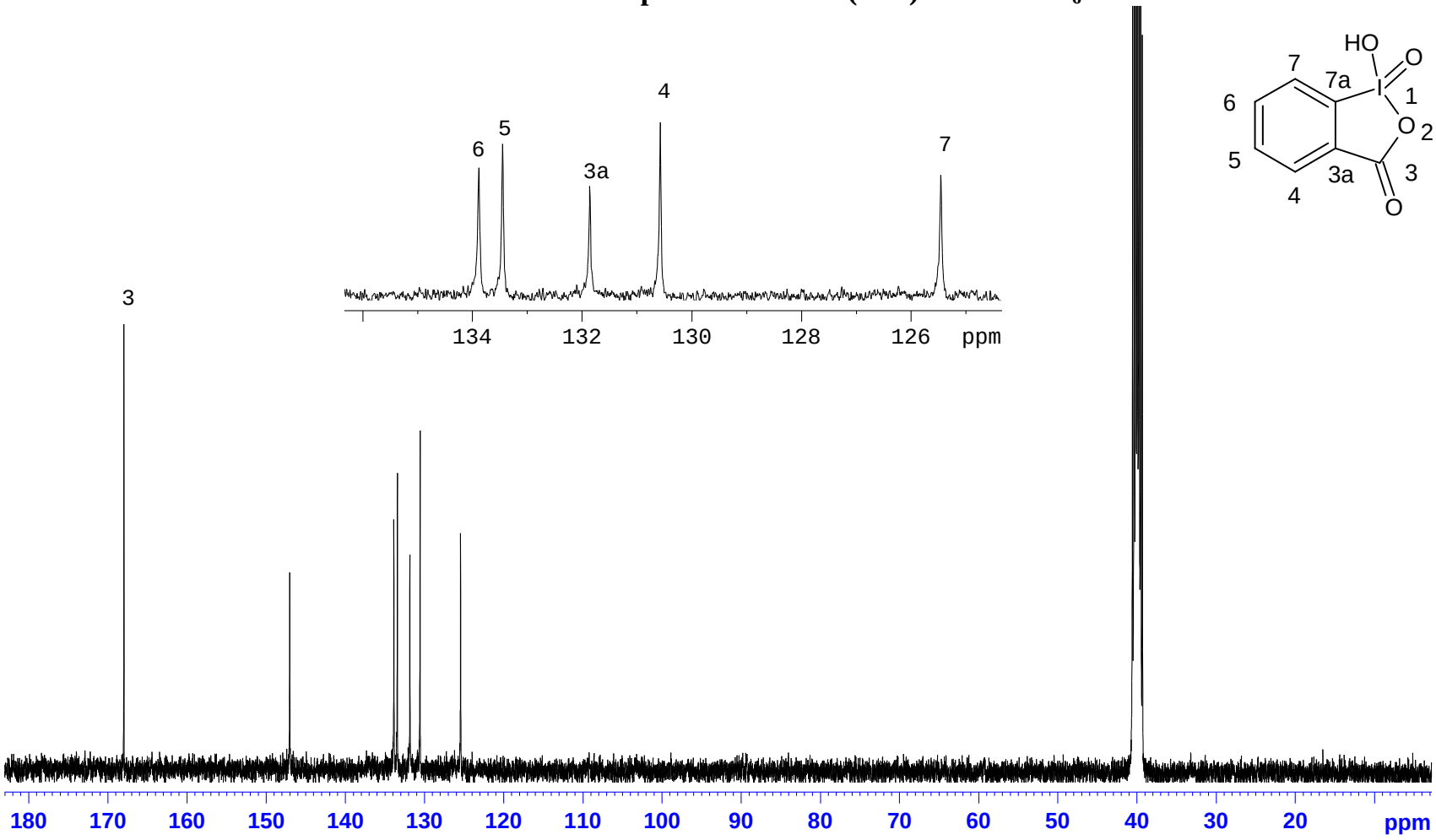

Plate 8c: COSY Spectrum of IBX (2.30) in DMSO-d_6

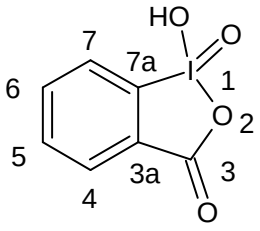

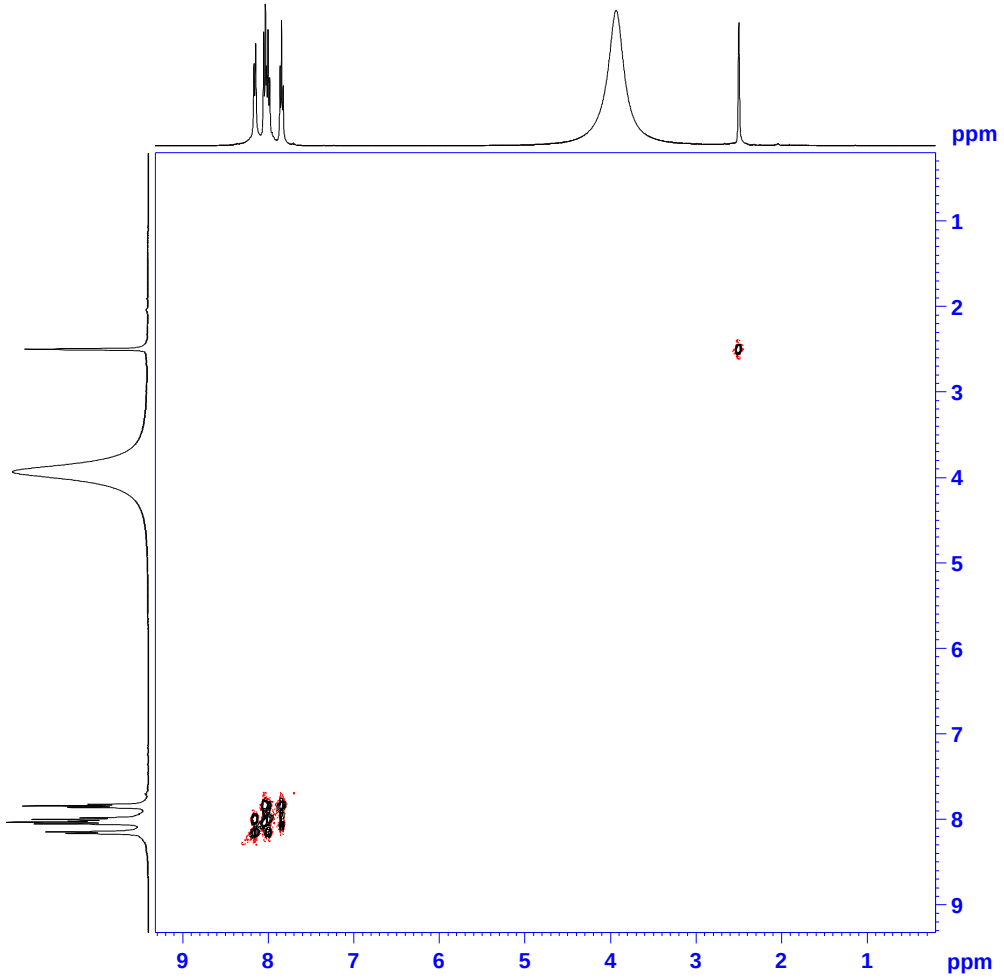

Plate 8d: HSQC Spectrum of IBX (2.30) in DMSO-d_6

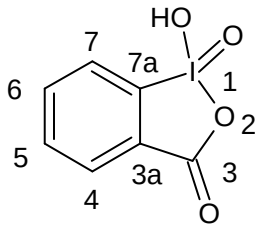

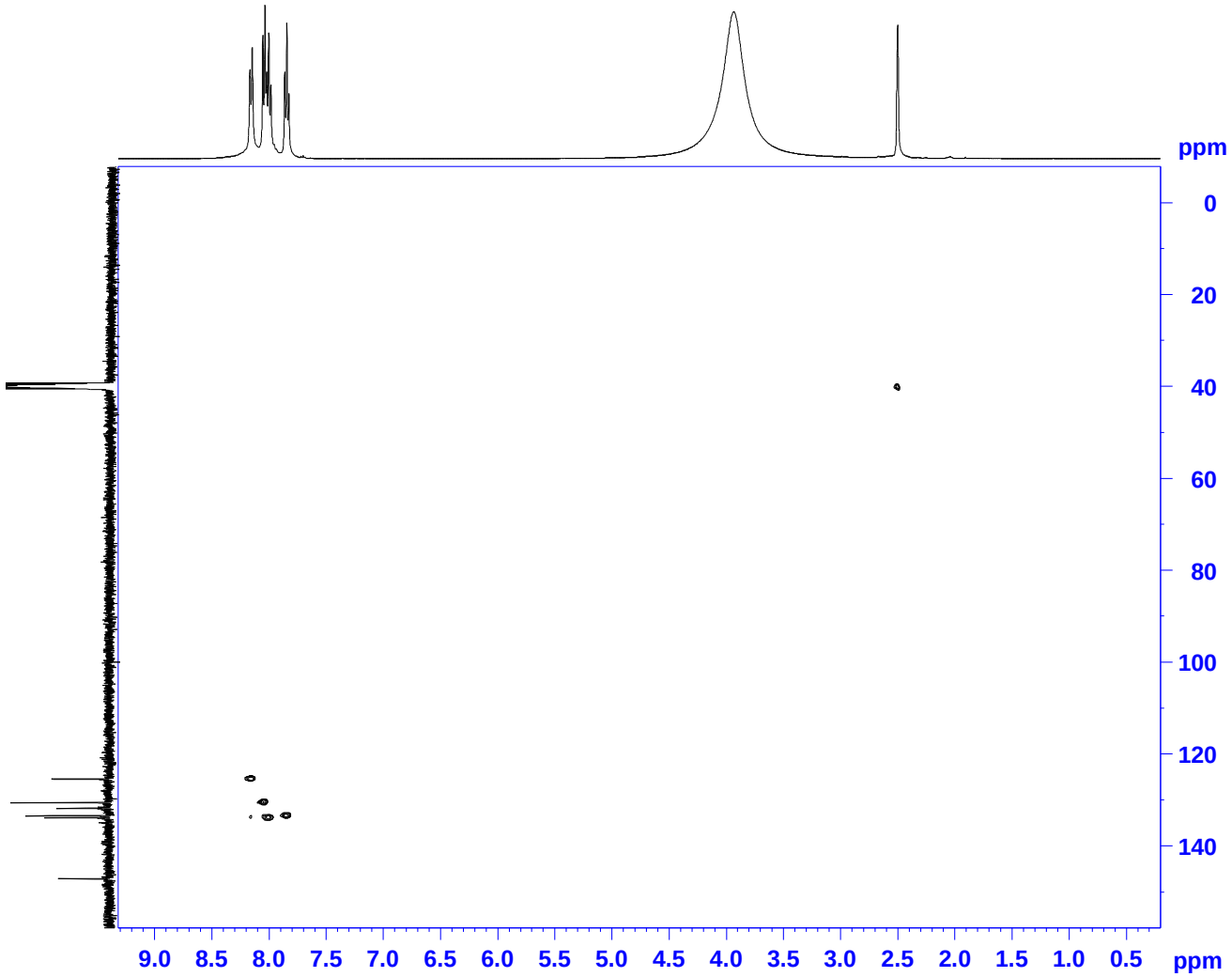

Plate 8e: HMBC Spectrum of IBX (2.30) in DMSO-d_6

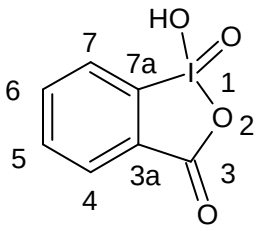

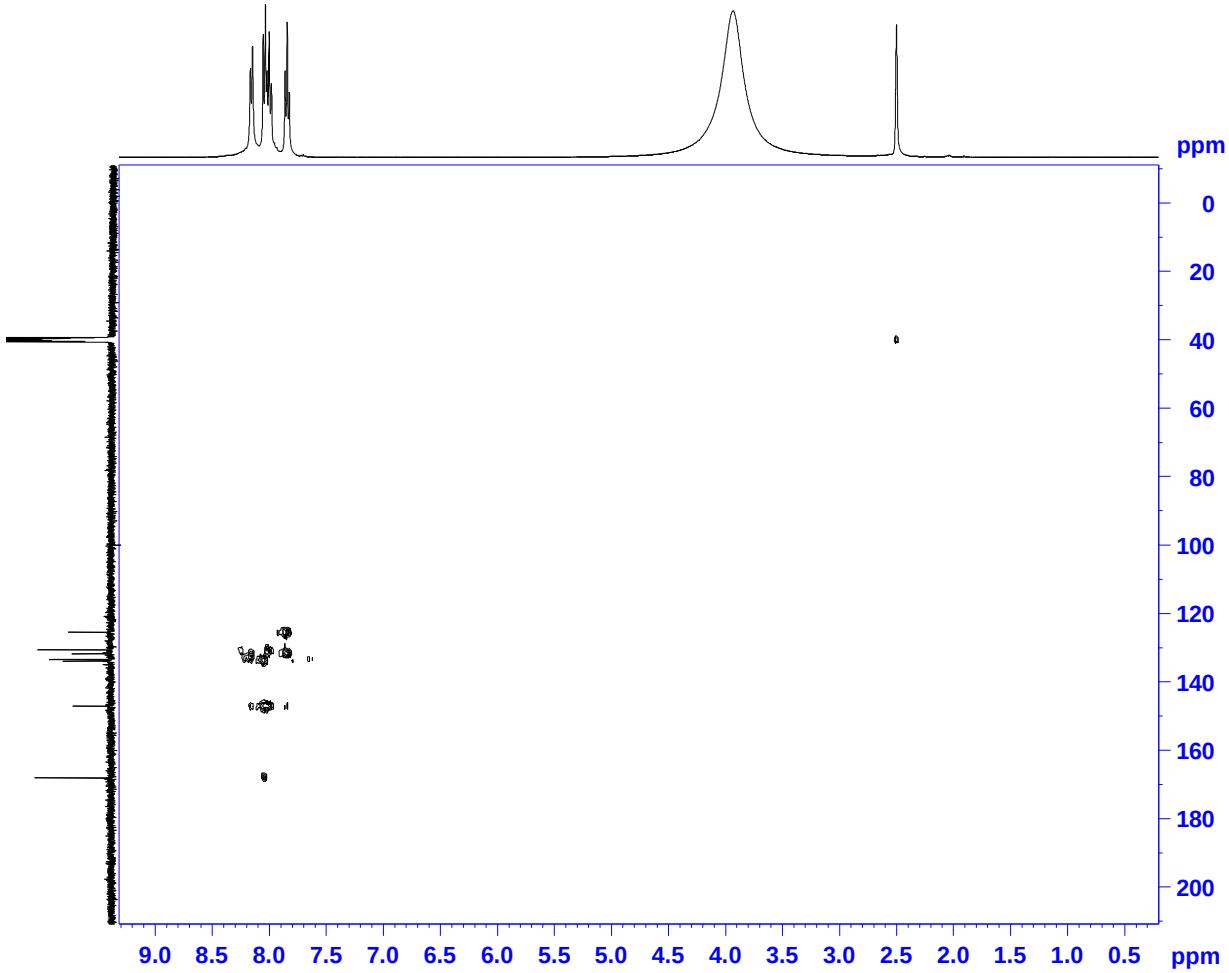

Plate 9a: ^{1}H NMR Spectrum of rhein (2.31) in DMSO-d_6

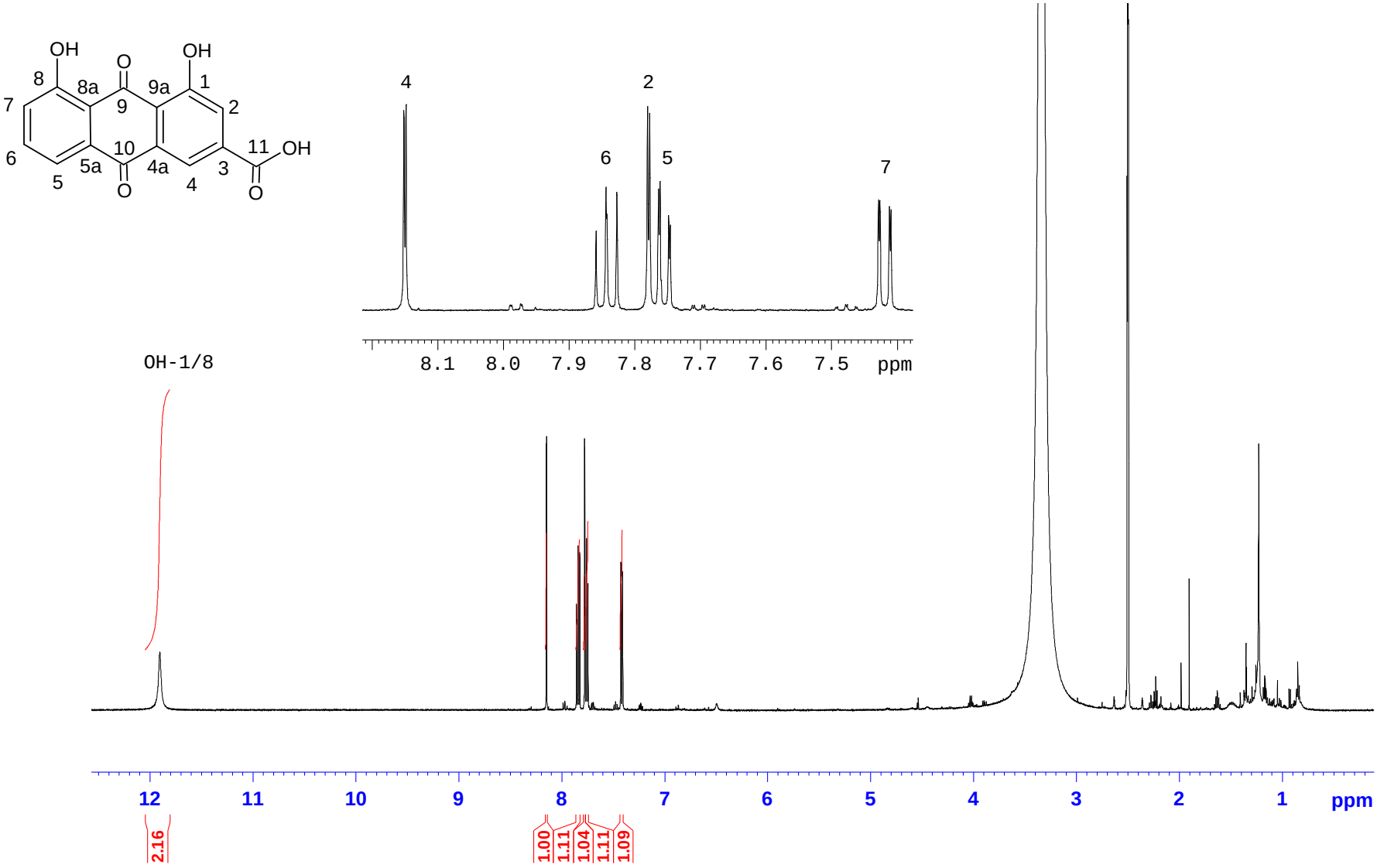

Plate 9b: ^{13}C NMR Spectrum of rhein (2.31) in DMSO-d_6

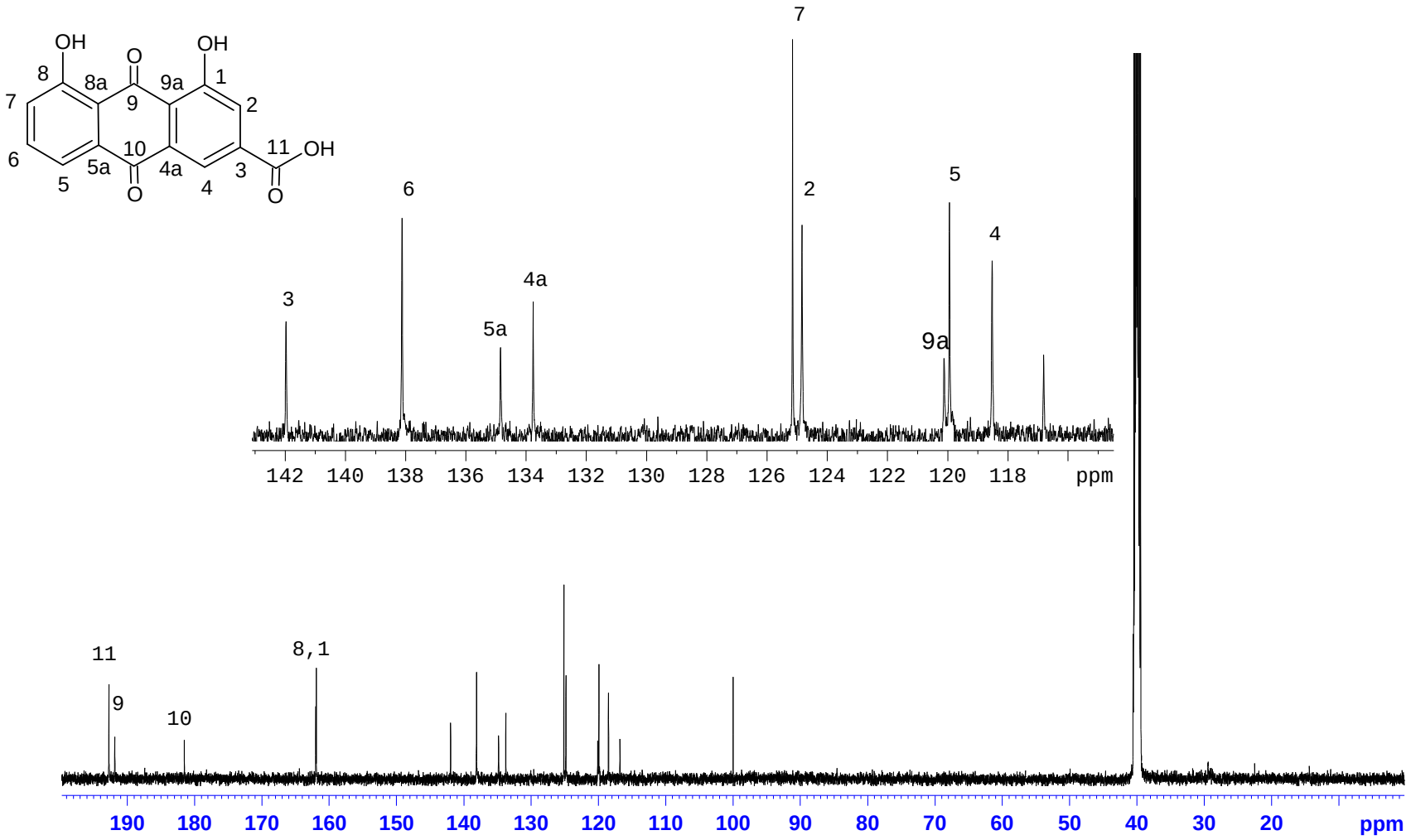

Plate 9c: COSY NMR Spectrum of rhein (2.31) in DMSO-d_6

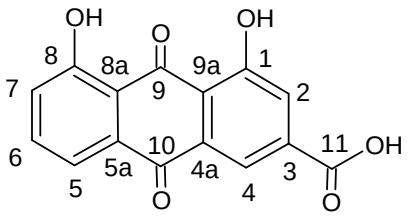

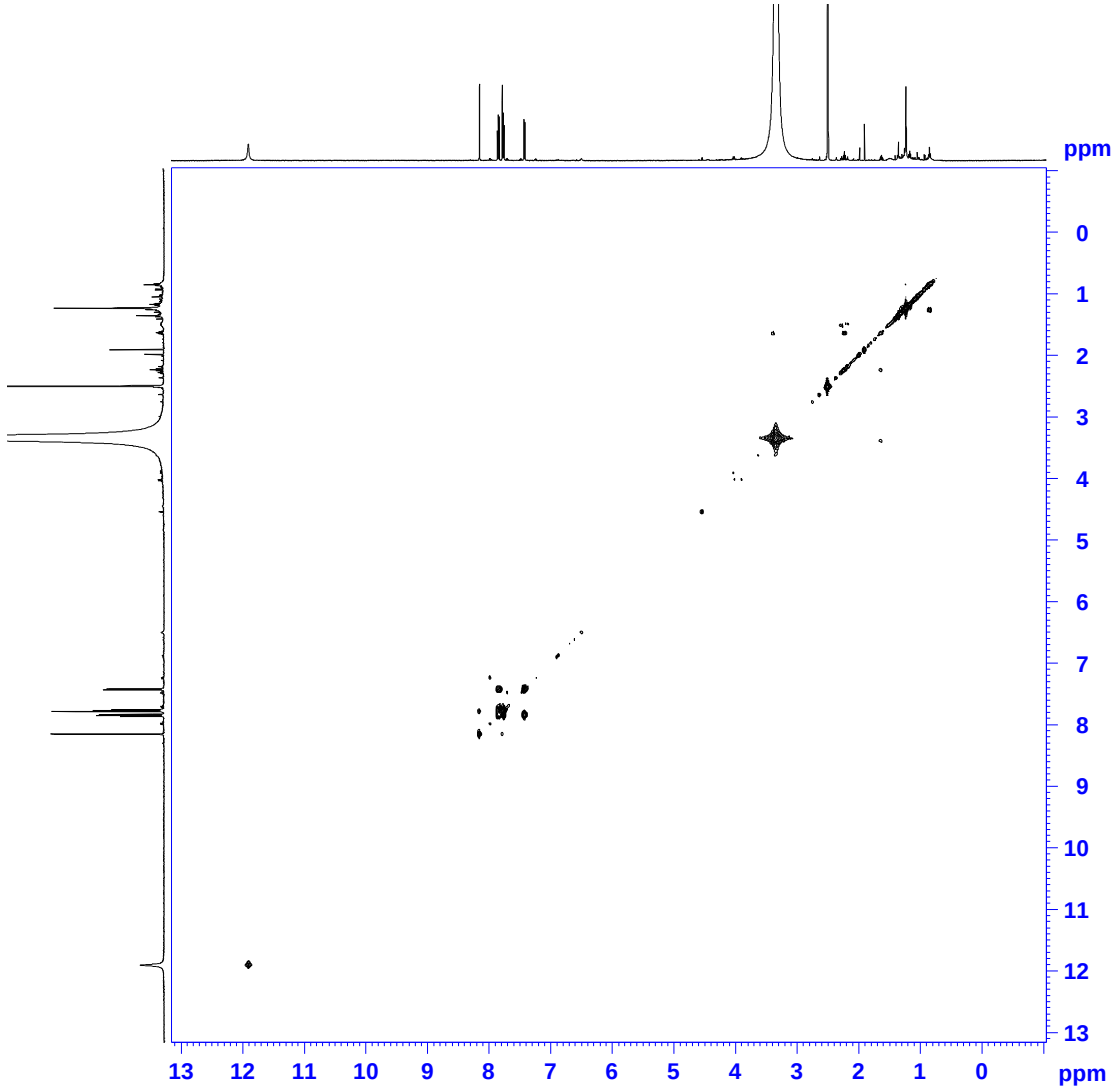

Plate 9d: HSQC NMR Spectrum of rhein (2.31) in DMSO-d_6

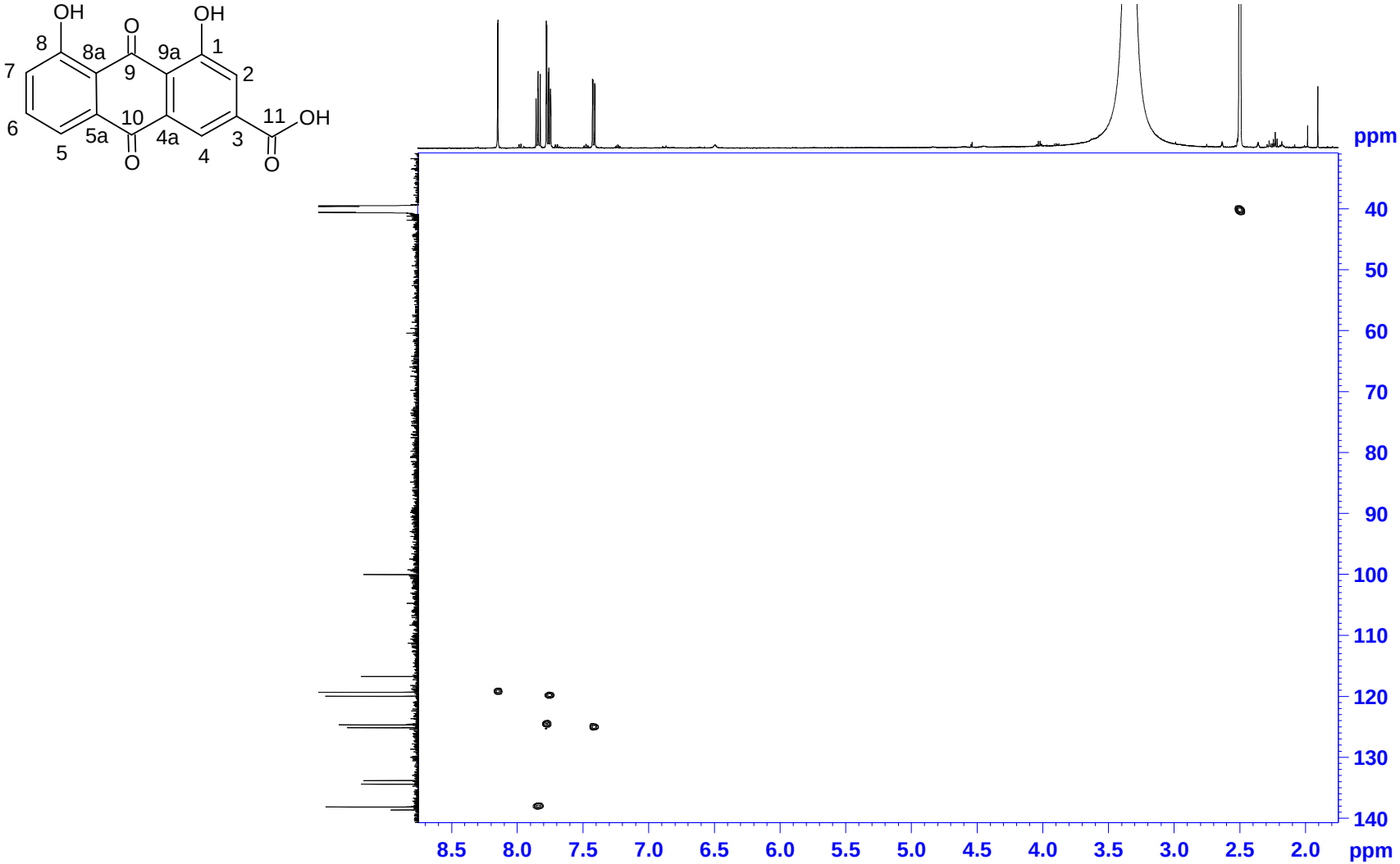

Plate 9e: HMBC NMR Spectrum of rhein (2.31) in DMSO-d_6

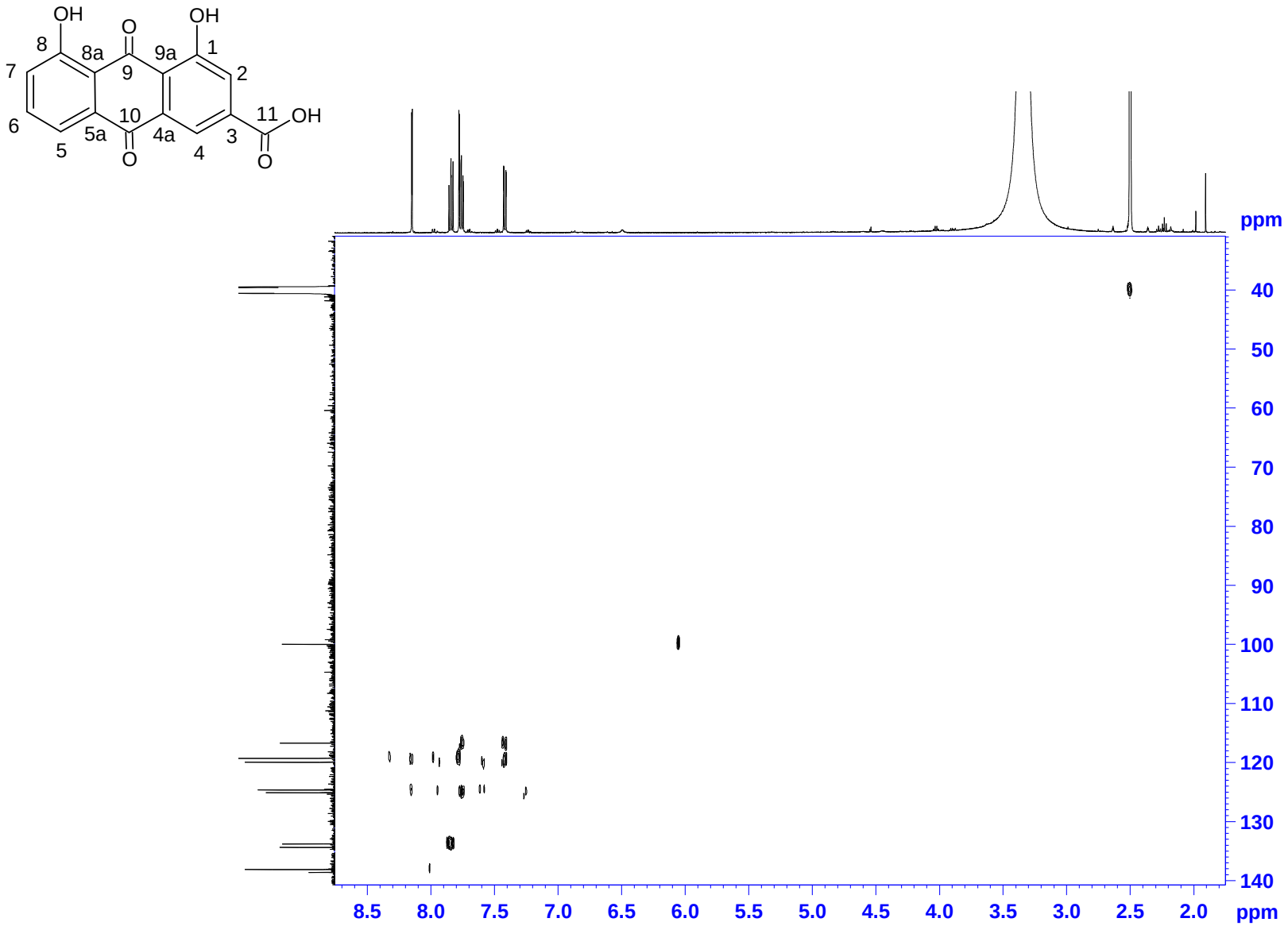

Plate 10a: ^{1}H NMR Spectrum of 11-bromo-chrysophanol (2.33) in DMSO-d_6

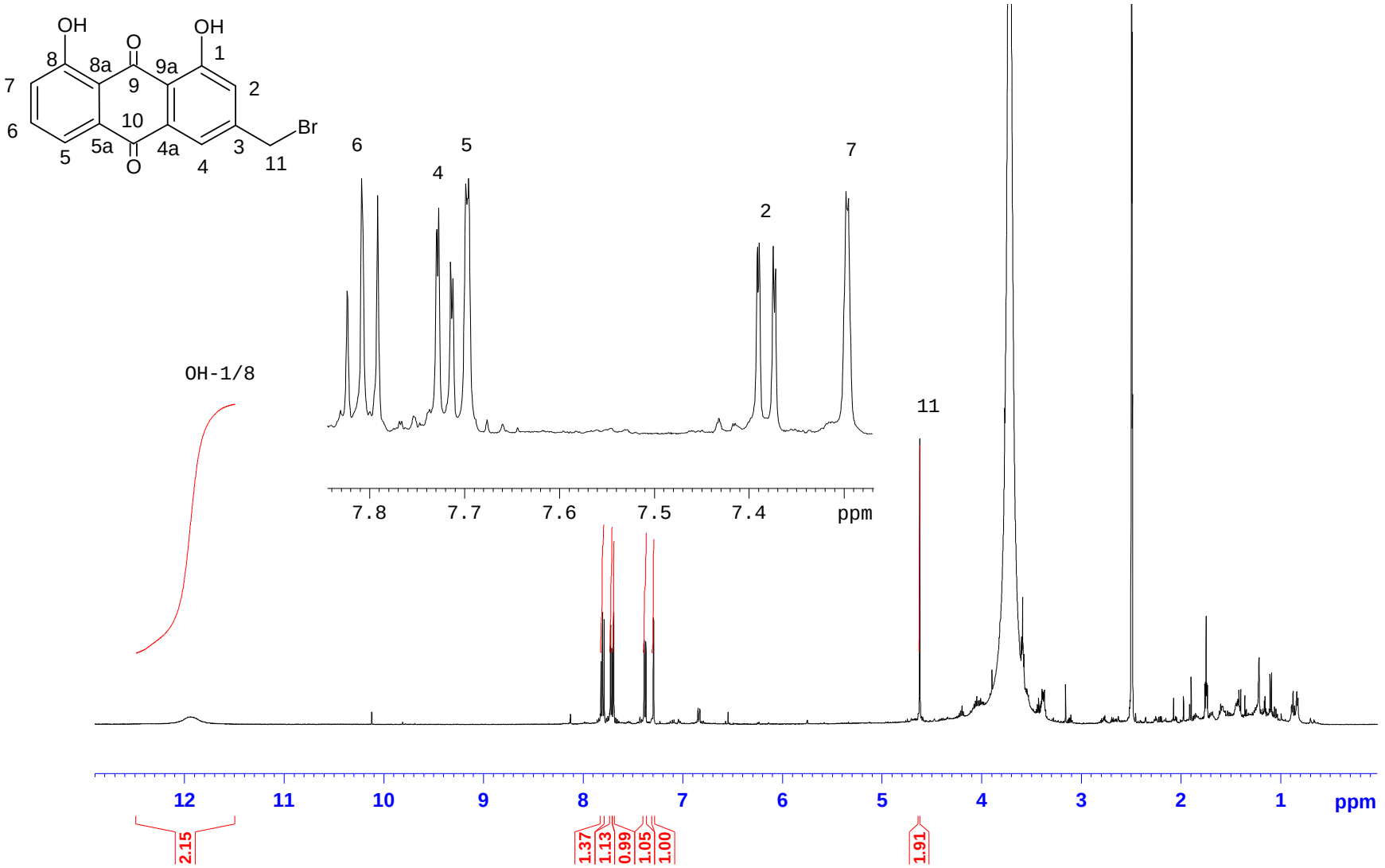

Plate 10b: ^{13}C NMR Spectrum of 11-bromo-chrysophanol (2.33) in DMSO-d_6

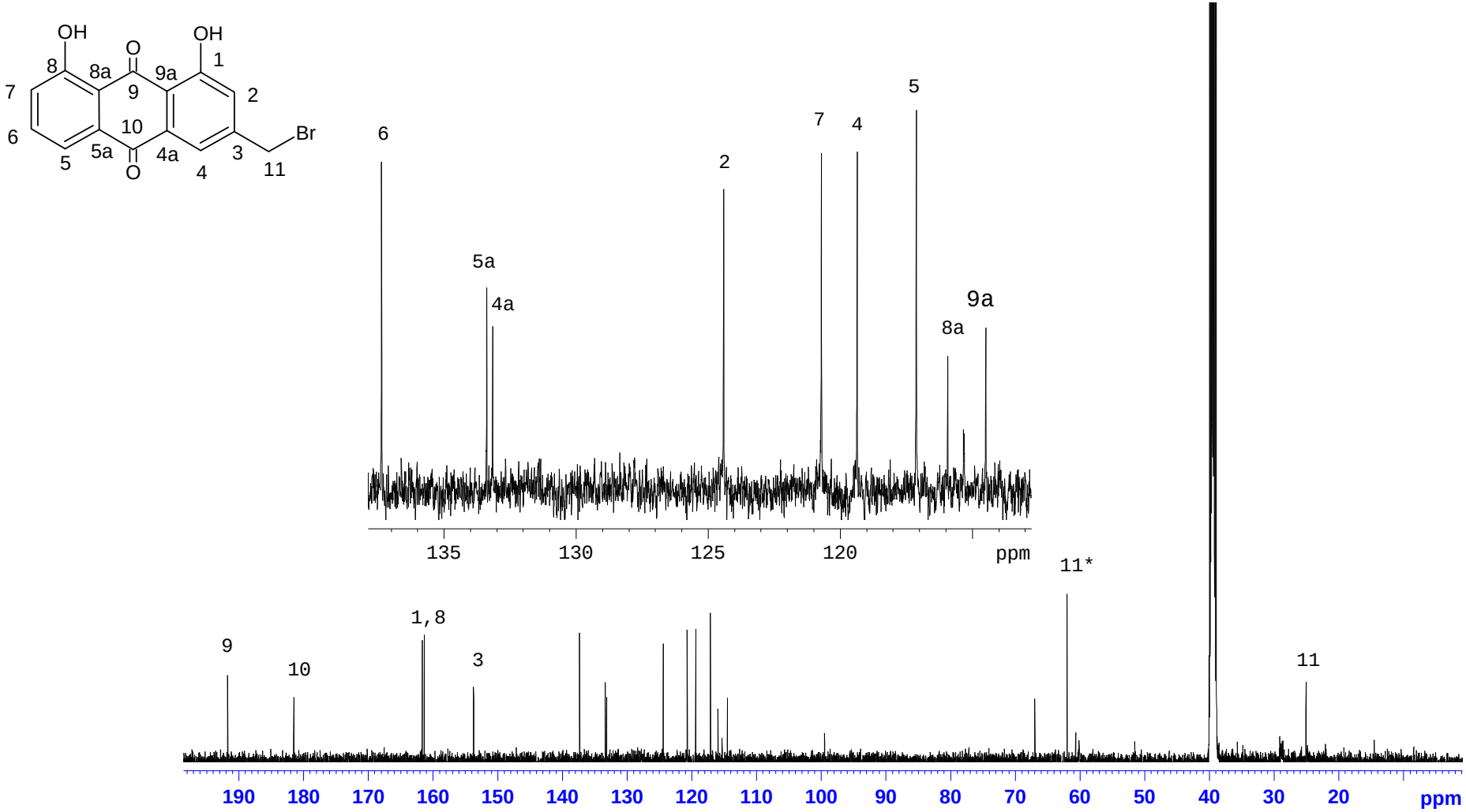

Plate 10c: COSY NMR Spectrum of 11-bromo-chrysophanol (2.33) in DMSO-d_6

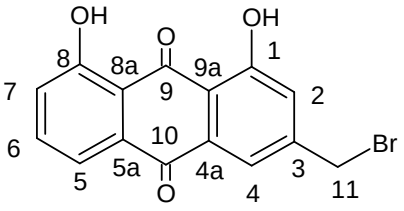

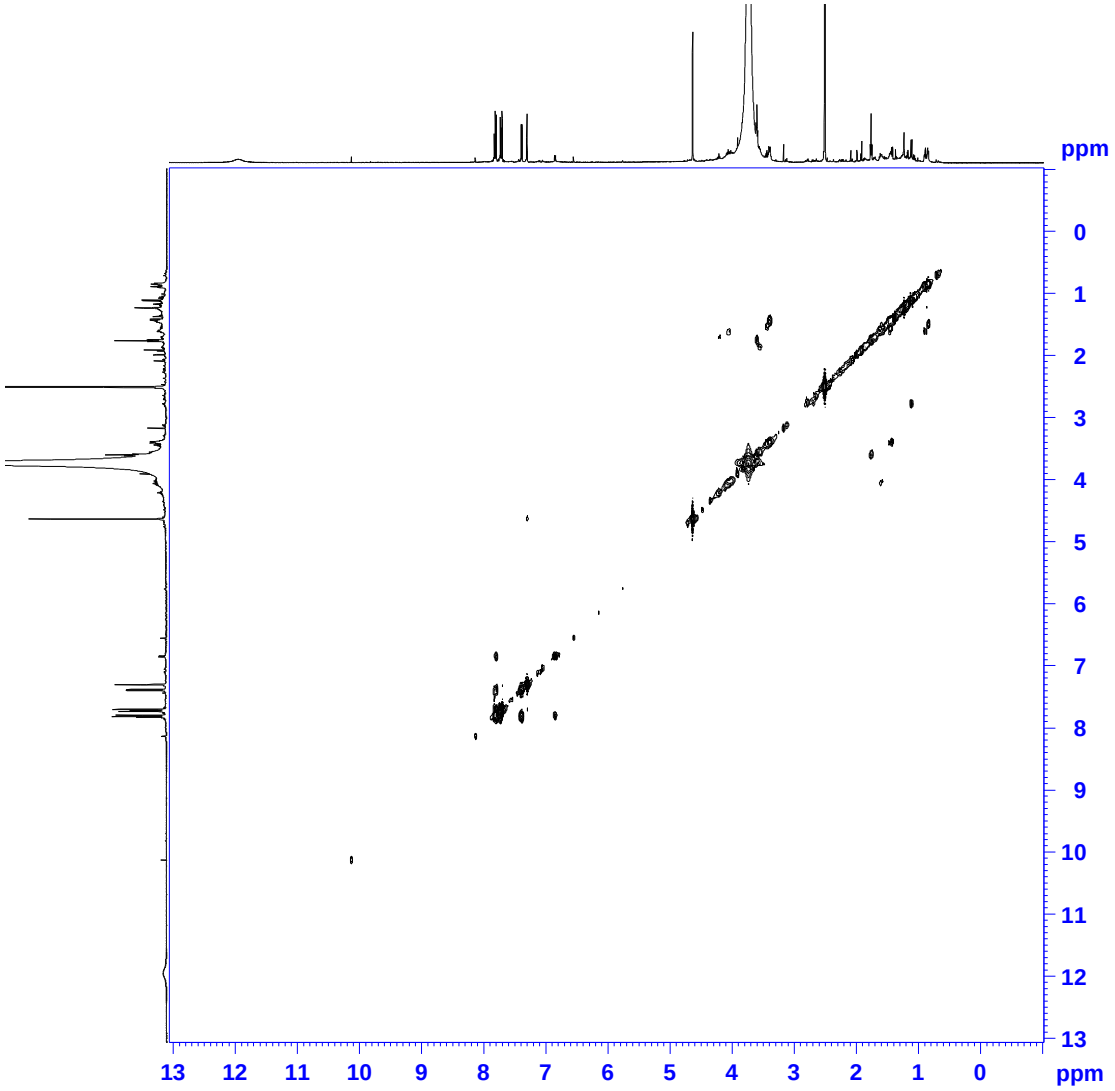

Plate 10d: HSQC NMR Spectrum of 11-bromo-chrysophanol (2.33) in DMSO-d_6

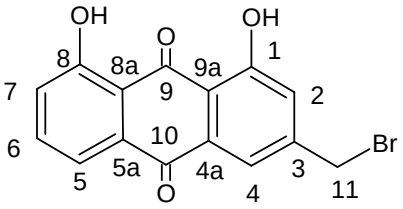

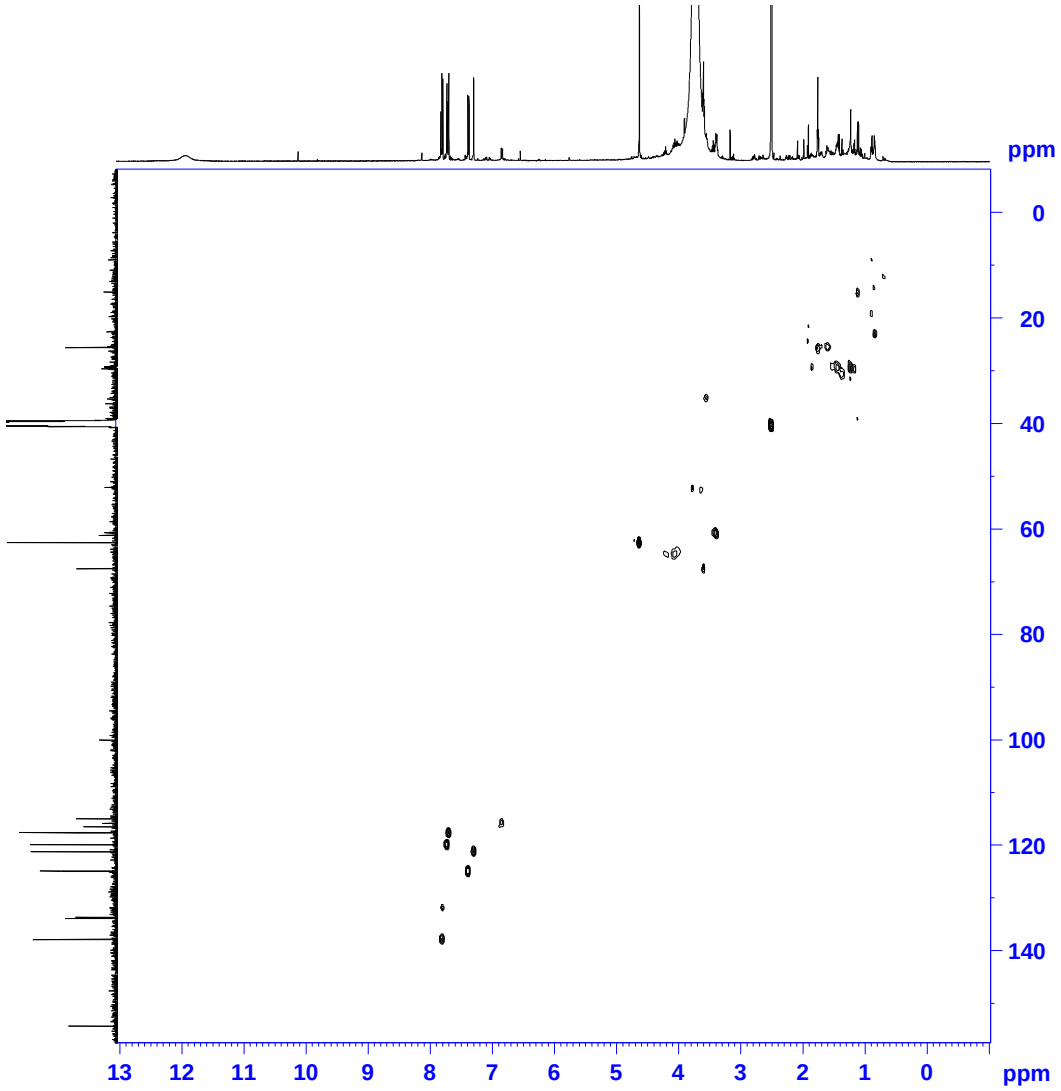

Plate 11a: ^{1}H NMR Spectrum of 11-(pyrrolidin-1-yl)chrysophanol (2.34) in DMSO-d_6

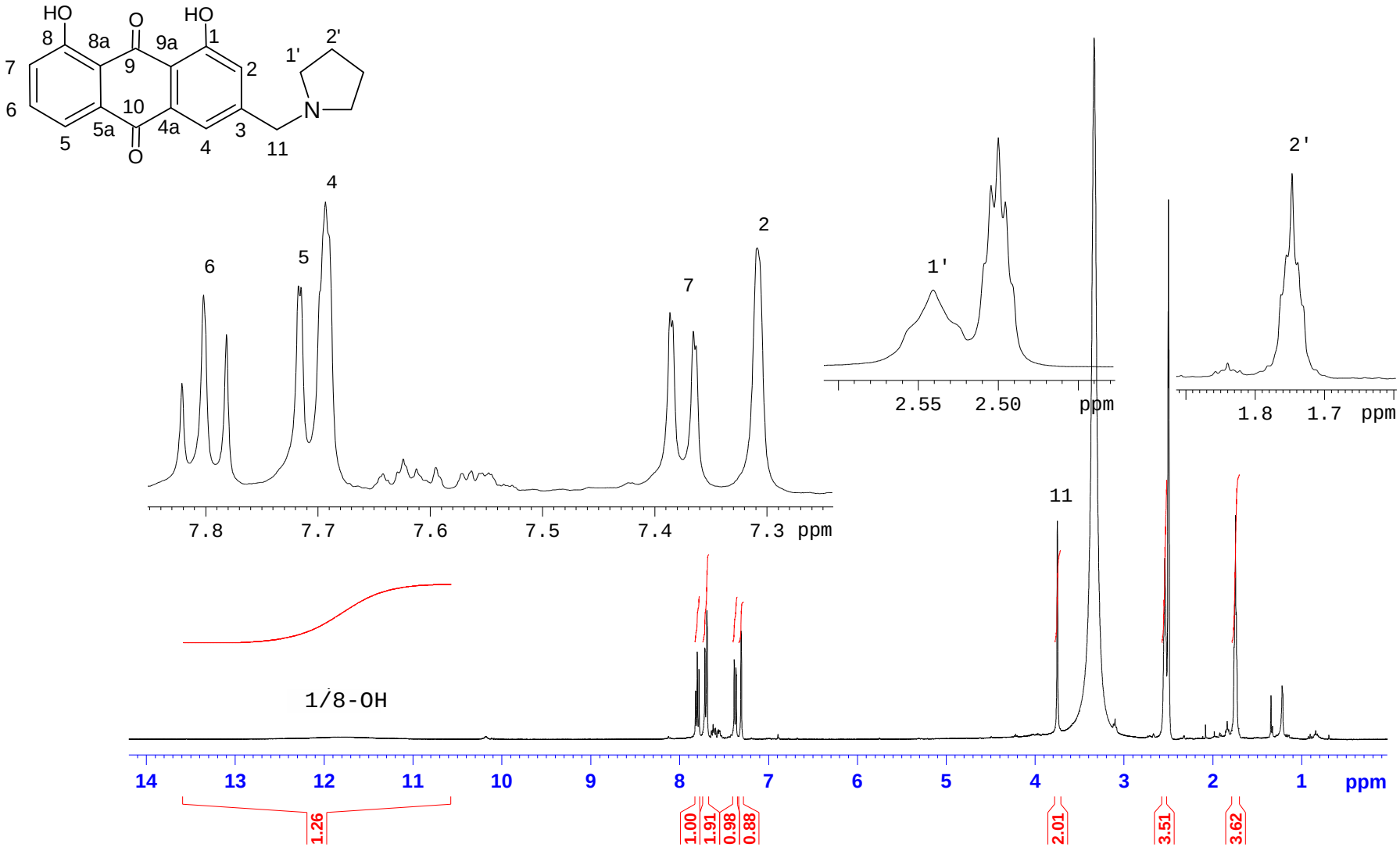

Plate 11b: ^{13}C NMR Spectrum of 11-(pyrrolidin-1-yl)chrysophanol (2.34) in DMSO-d_6

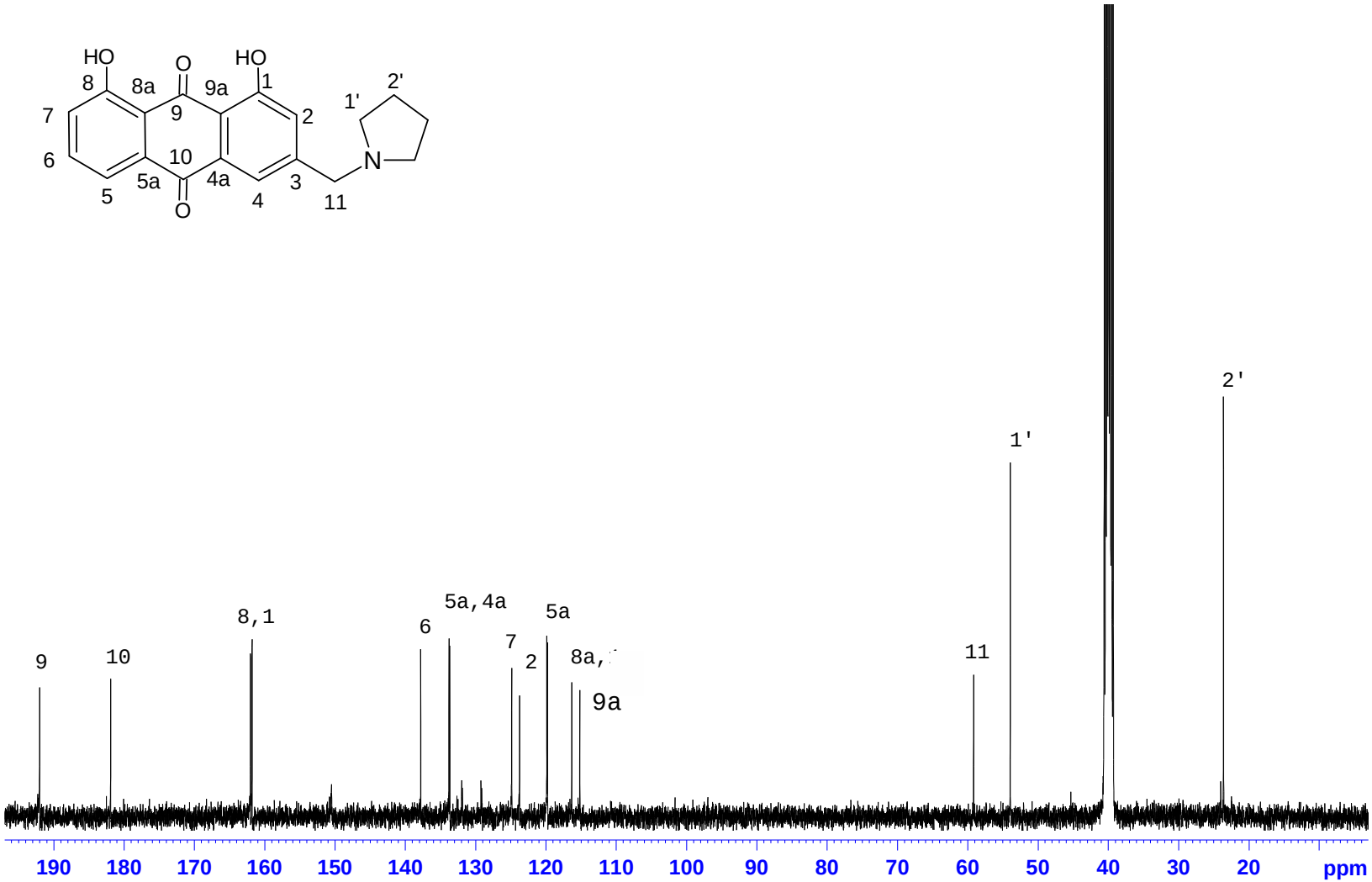

Plate 11c: DEPT 90 (i) and Dept 135 (ii) NMR Spectrum of 11-(pyrrolidin-1-yl)chrysophanol (2.34) in DMSO-d_6

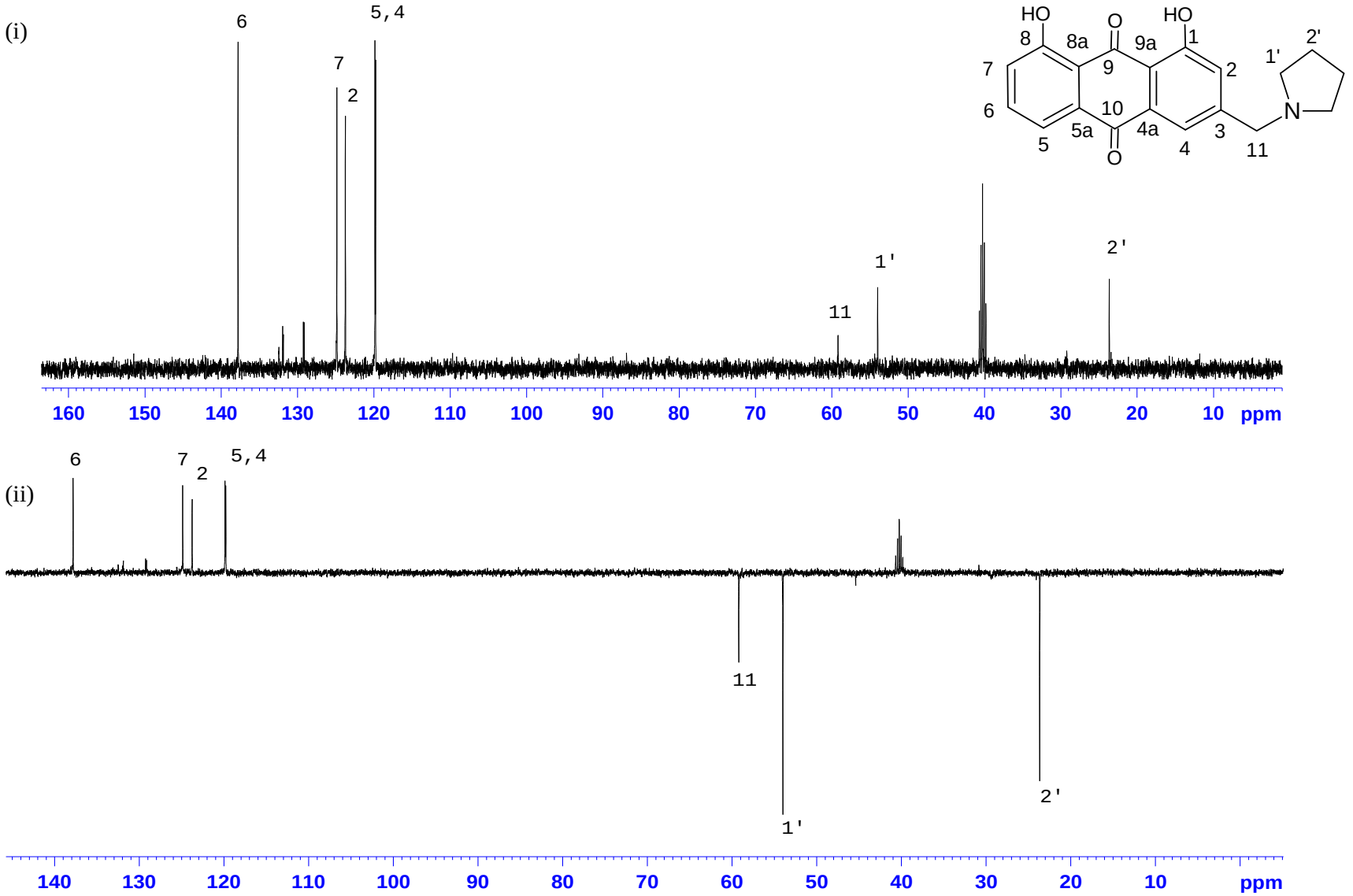

Plate 11d: COSY NMR Spectrum of 11-(pyrrolidin-1-yl)chrysophanol (2.34) in DMSO-d_6

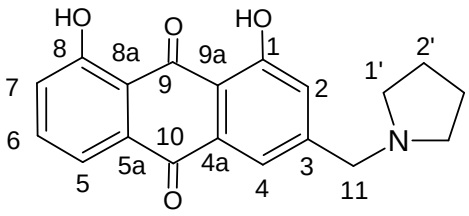

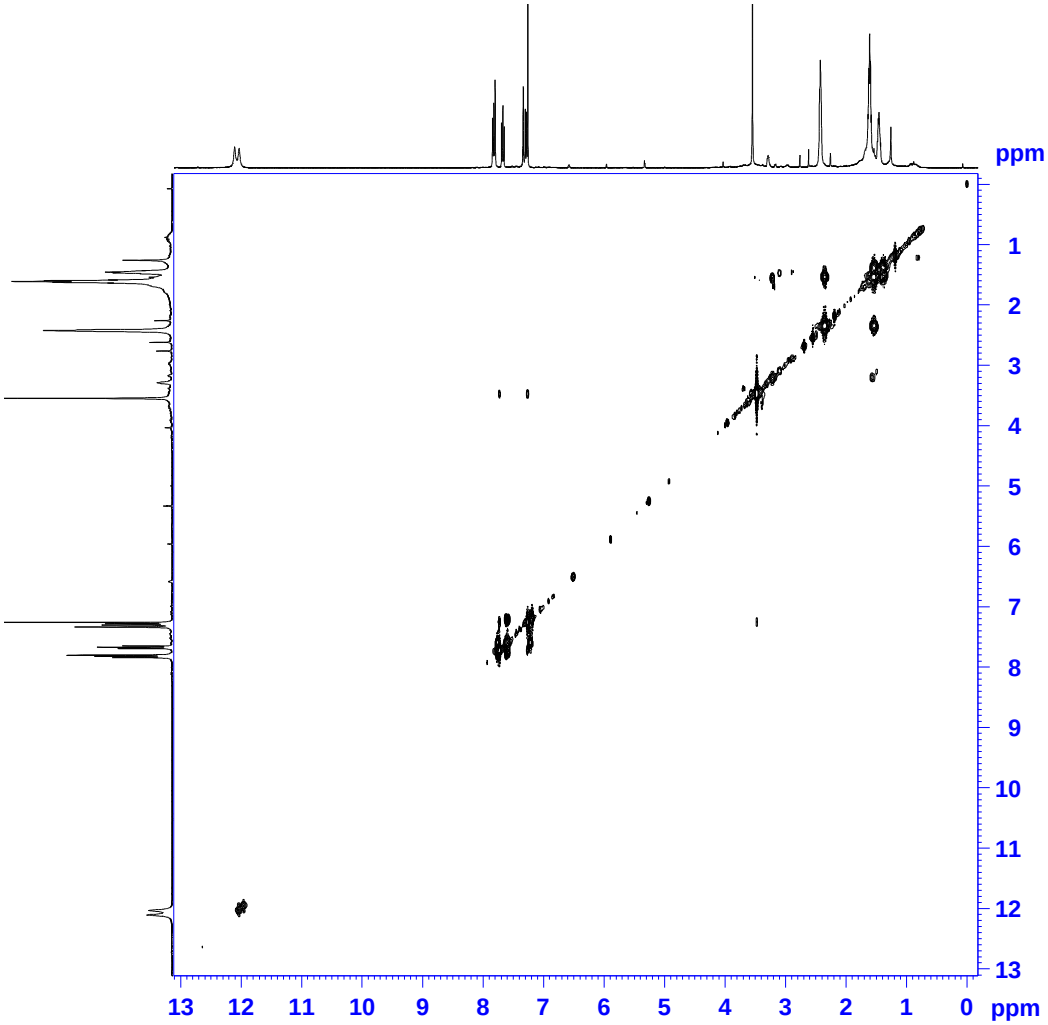

Plate 11e: HSQC NMR Spectrum of 11-(pyrrolidin-1-yl)chrysophanol (2.34) in DMSO-d_6

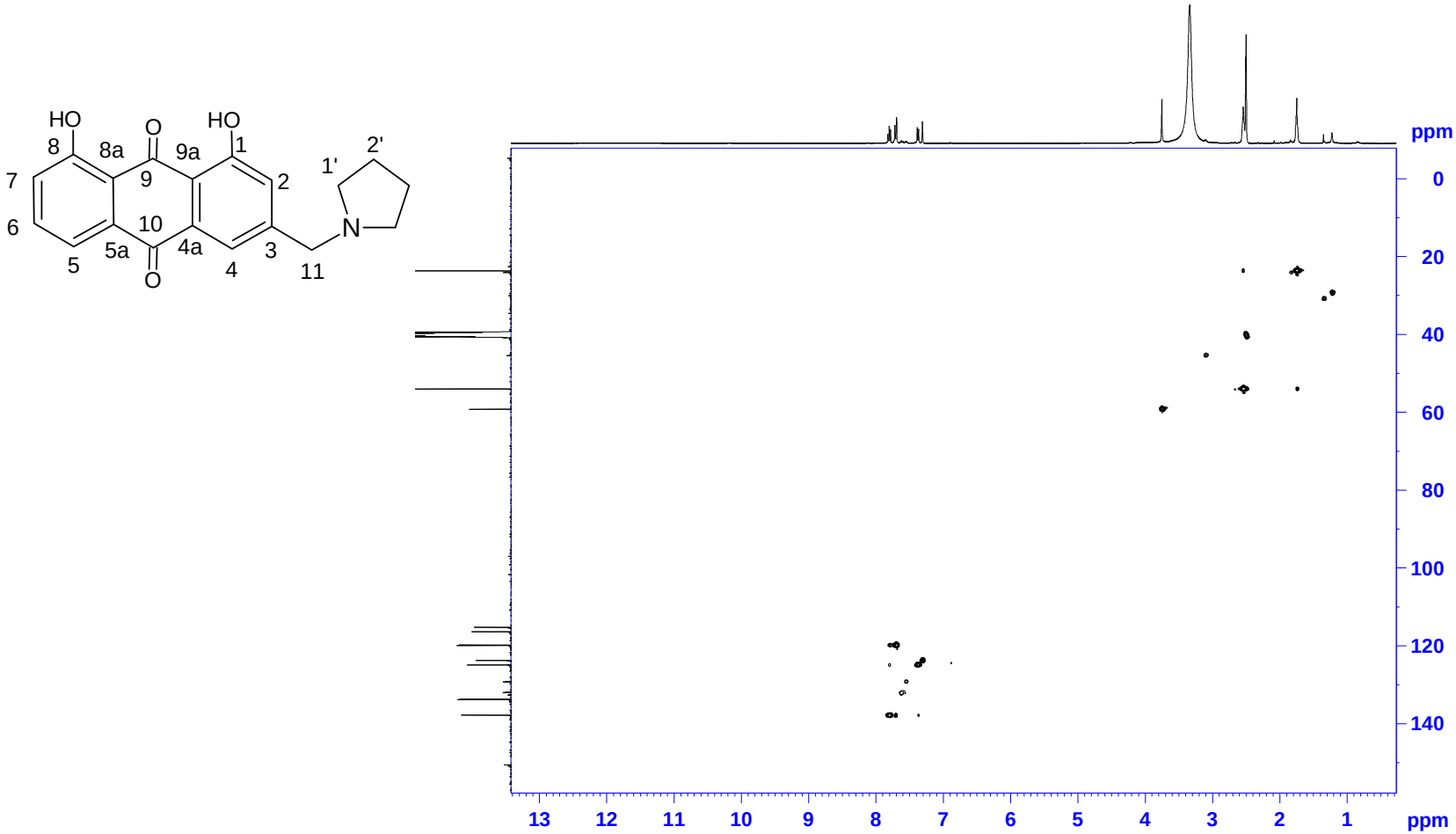

Plate 11f: HMBC NMR Spectrum of 11-(pyrrolidin-1-yl)chrysophanol (2.34) in DMSO-d_6

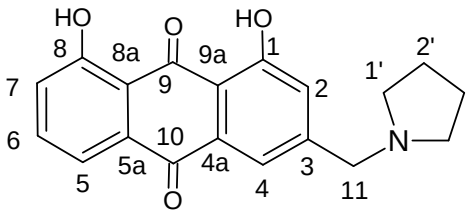

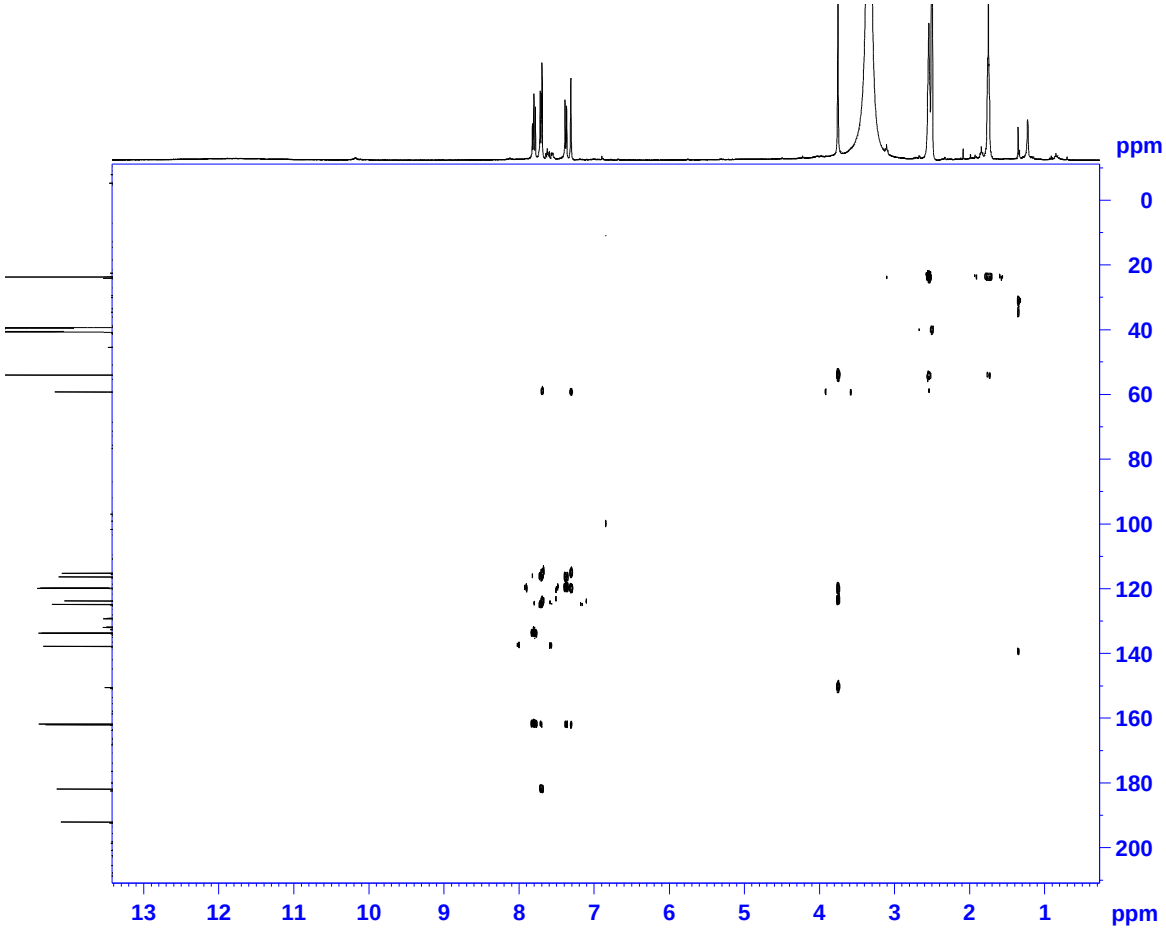

Plate 12a: ^{1}H NMR Spectrum of 11-(piperidin-1-yl)chrysophanol (2.35) in $CDCl_3$

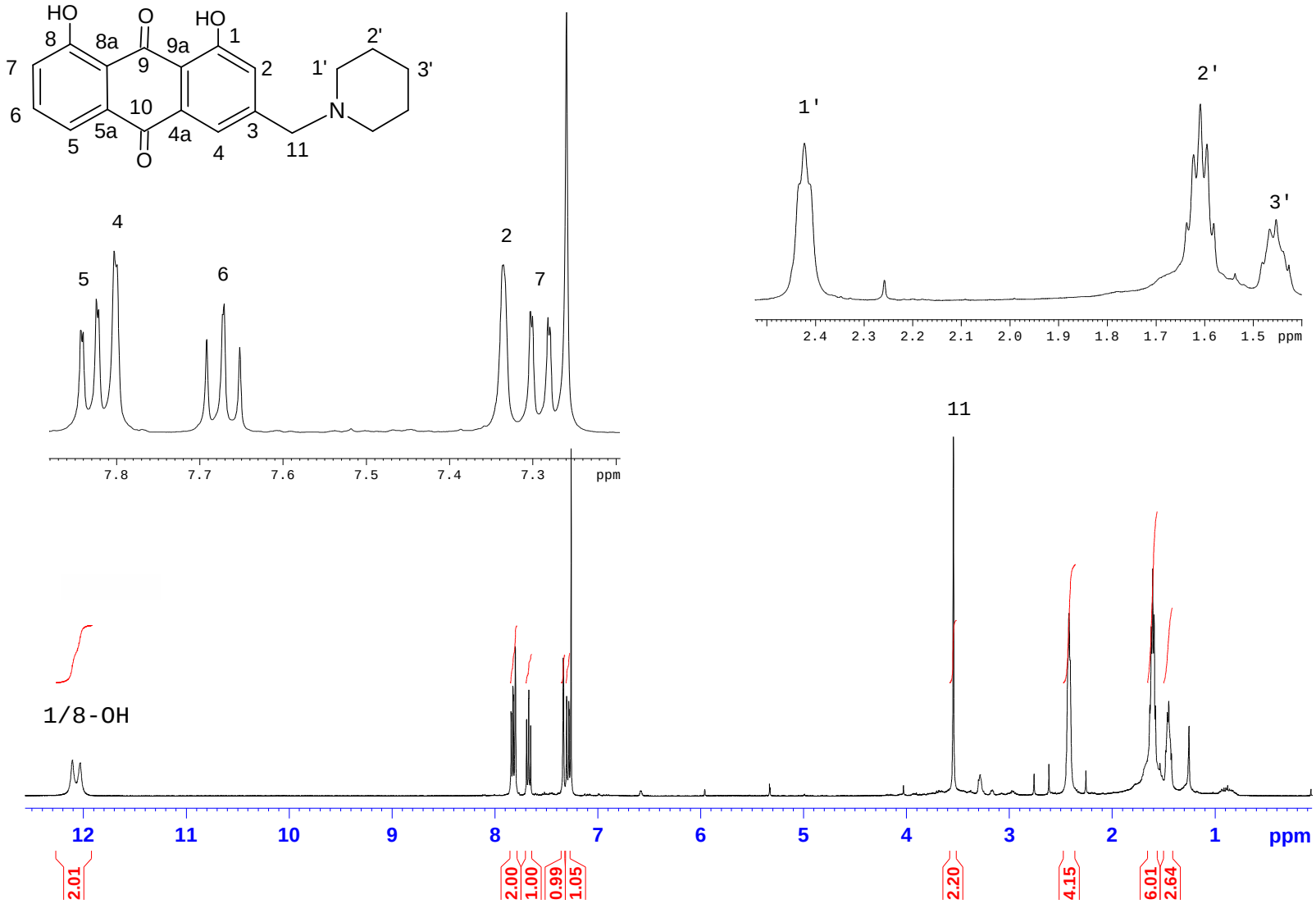

Plate 12b: ^{13}C NMR Spectrum of 11-(piperidin-1-yl)chrysophanol (2.35) in $CDCl_3$

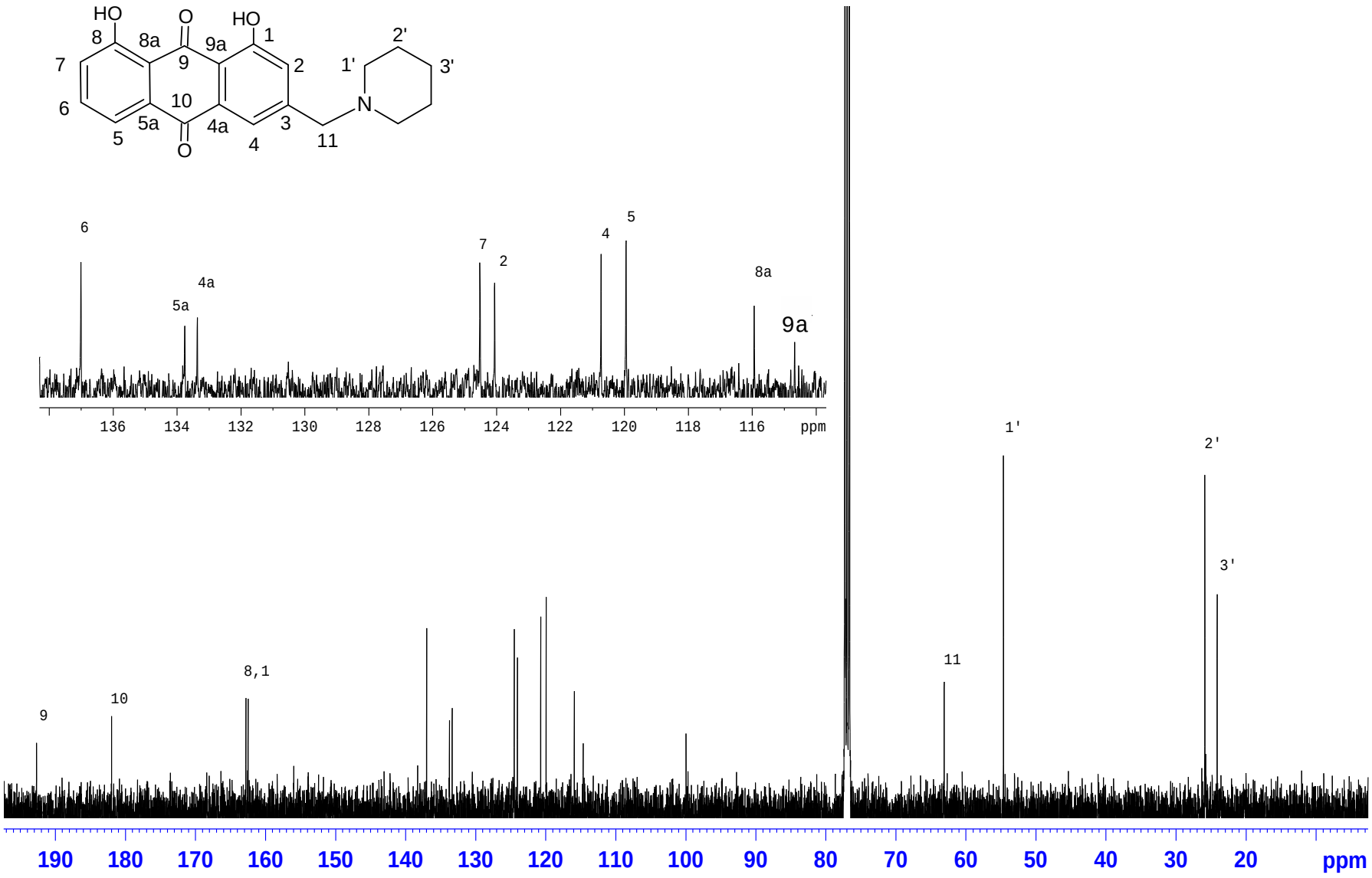

Plate 12c: DEPT 90 (i) and DEPT 135 (ii) NMR Spectrum of 11-(piperidin-1-yl)chrysophanol (2.35) in $CDCl_3$

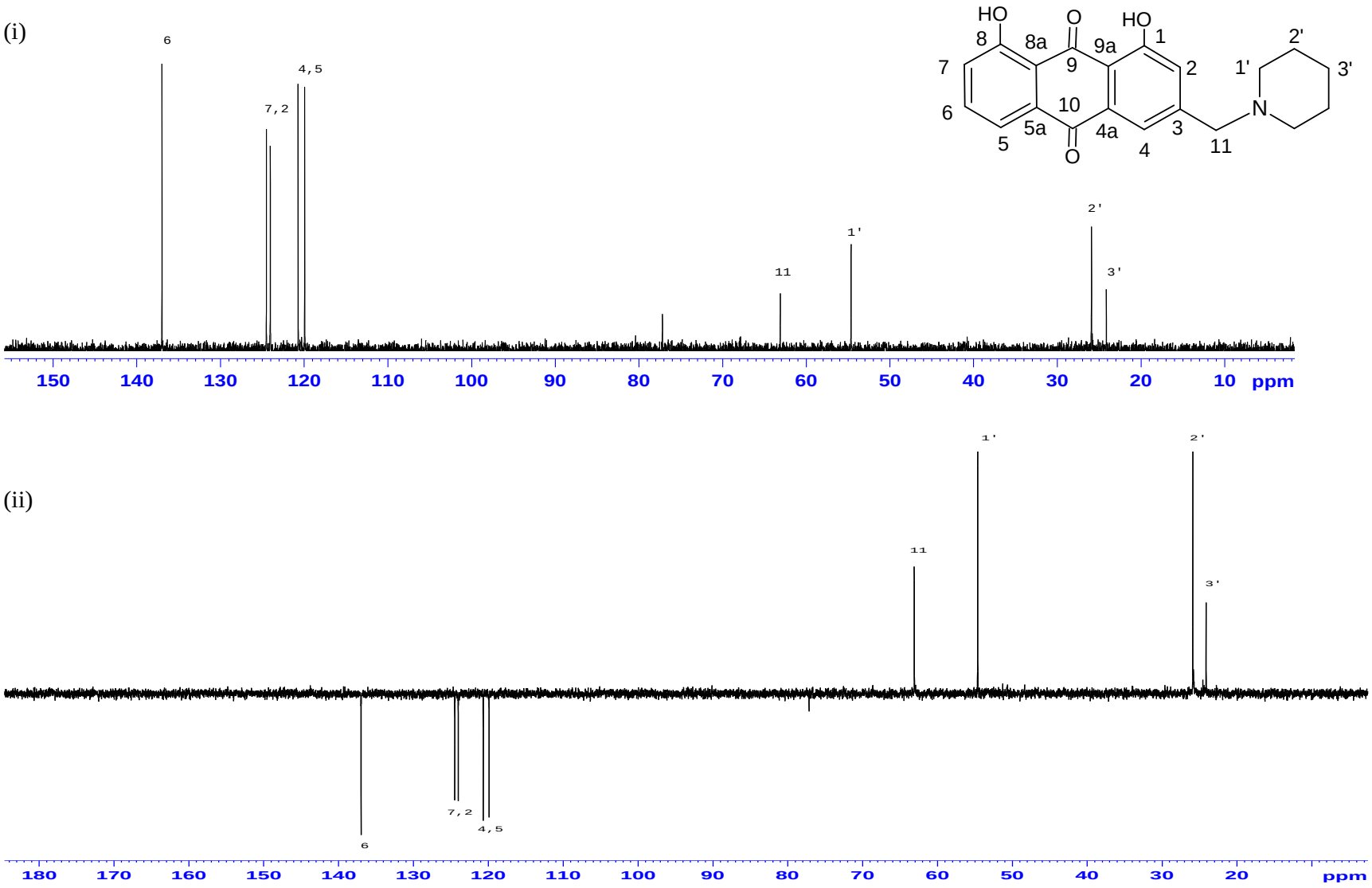

Plate 12d: COSY NMR Spectrum of 11-(piperidin-1-yl)chrysophanol (2.35) in $CDCl_3$

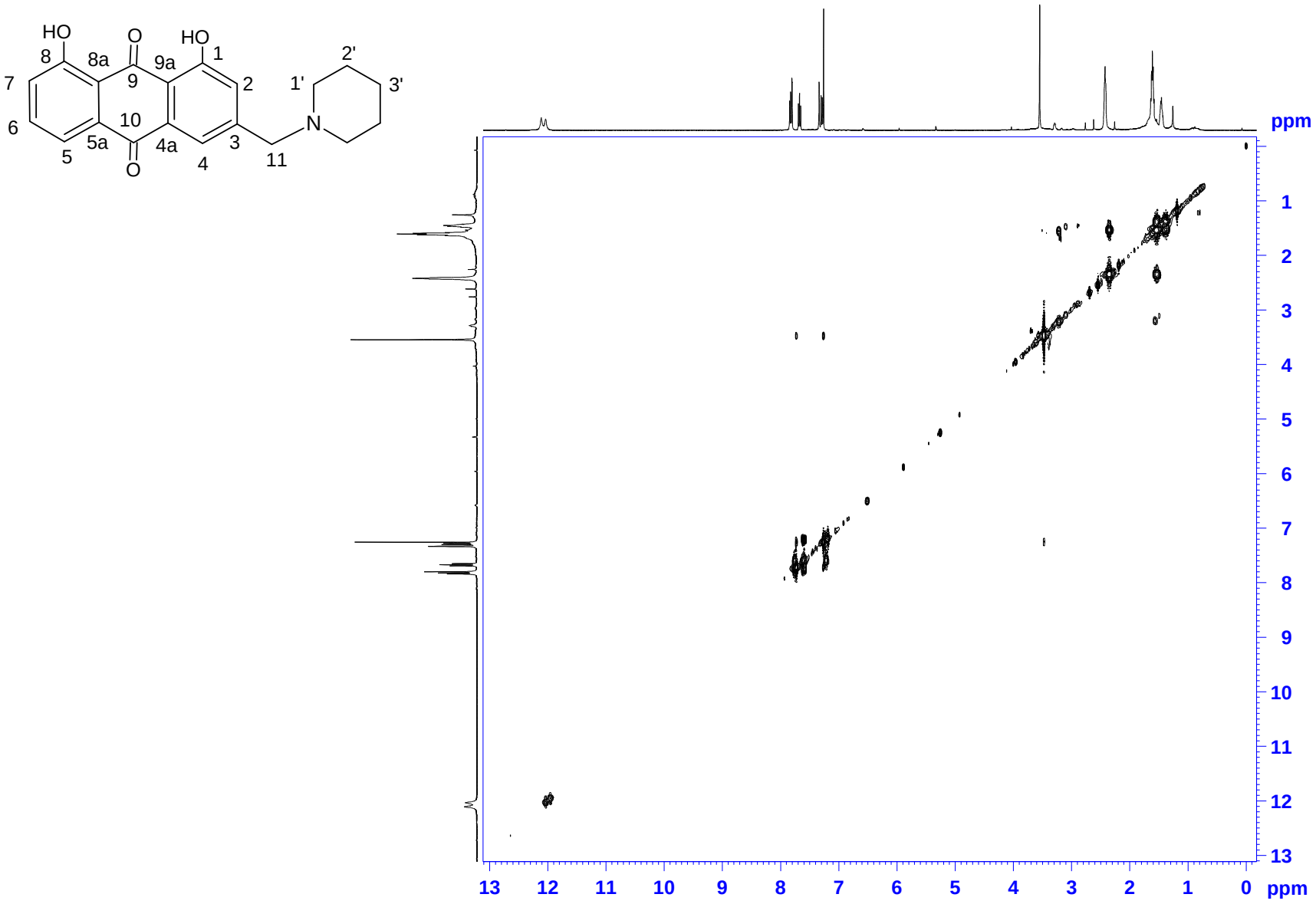

Plate 12e: HSQC NMR Spectrum of 11-(piperidin-1-yl)chrysophanol (2.35) in $CDCl_3$

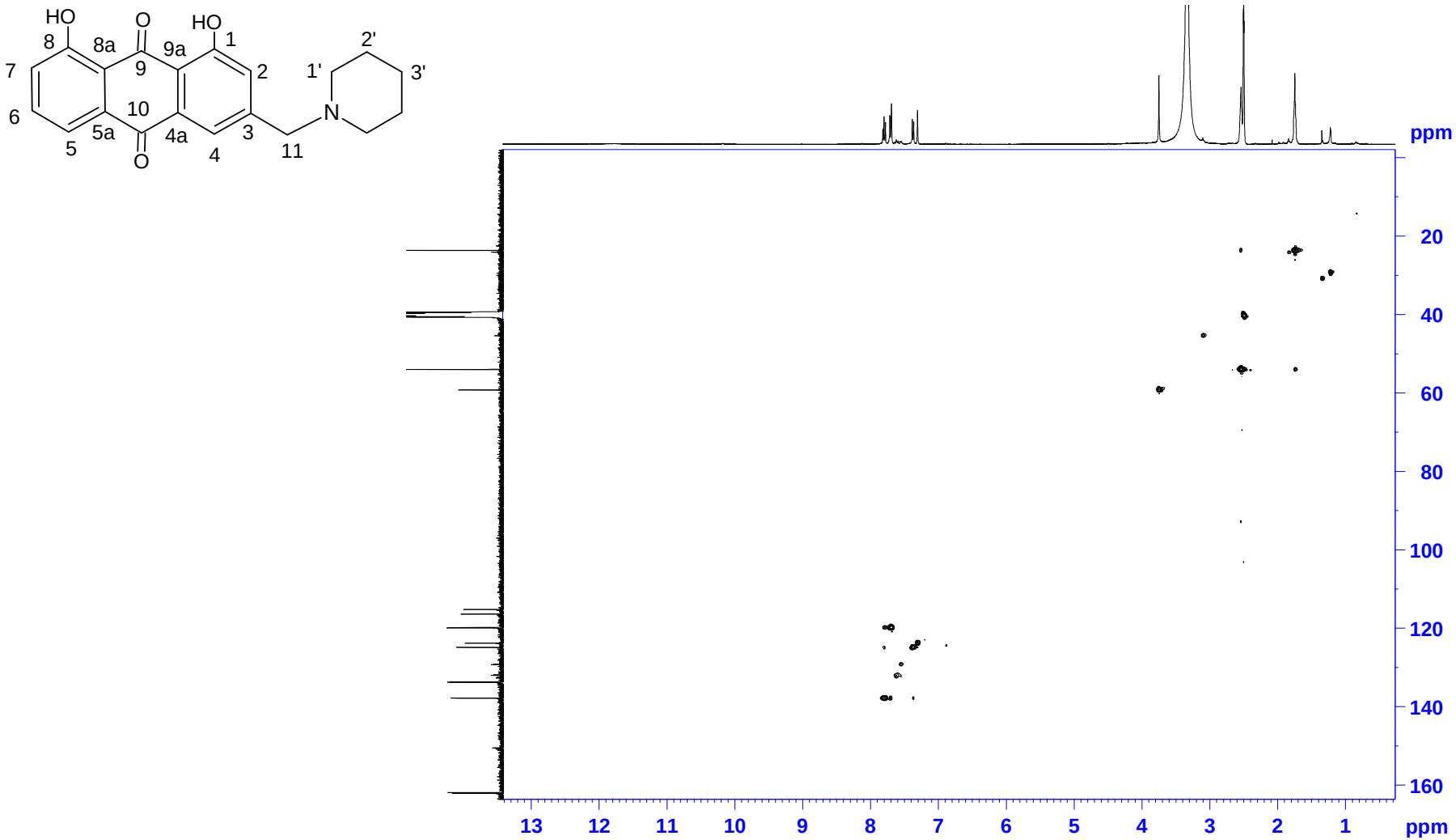

Plate 12f: HMBC NMR Spectrum of 11-(piperidin-1-yl)chrysophanol (2.35) in $CDCl_3$

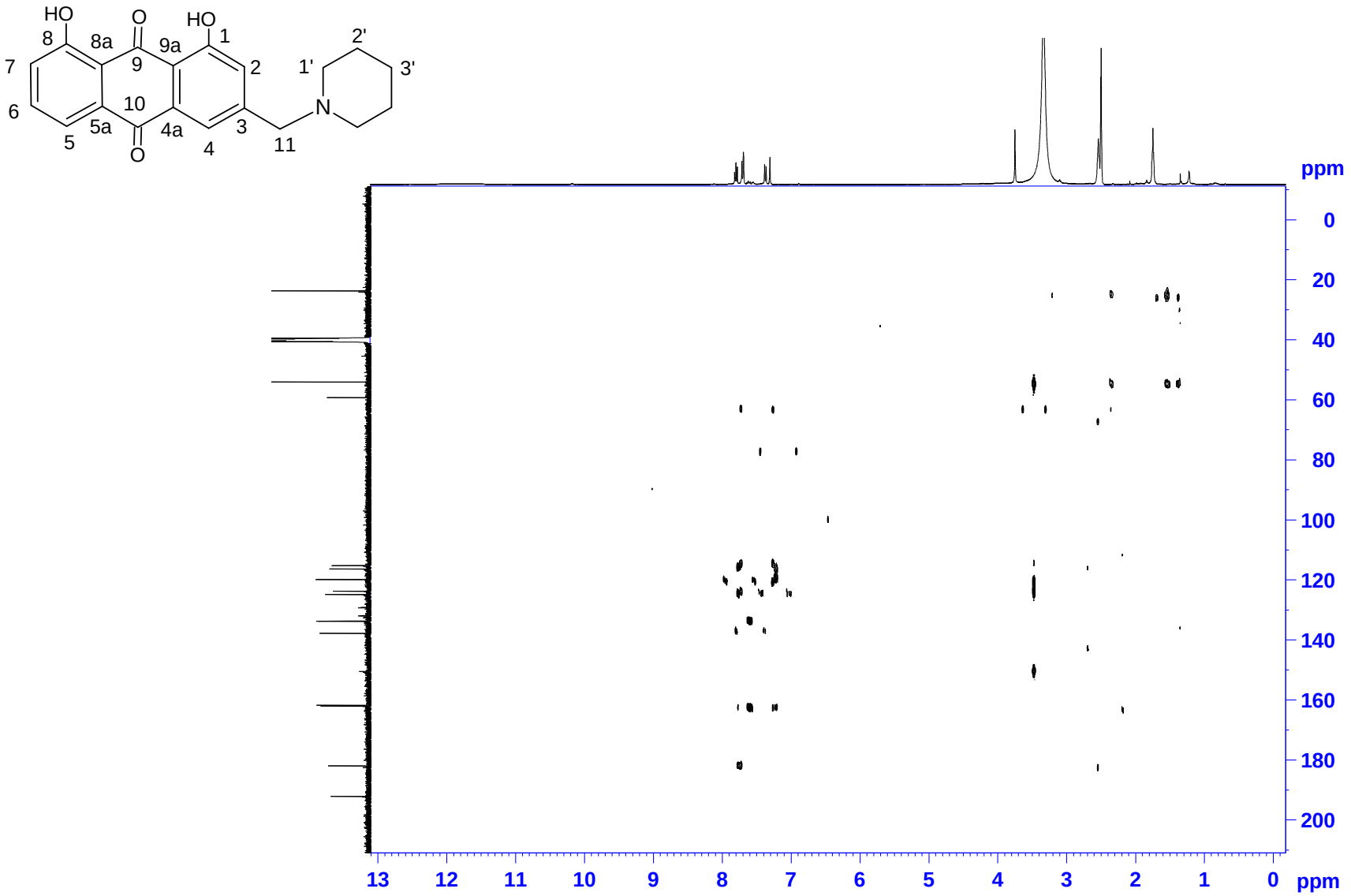

Plate 13a: ^{1}H NMR Spectrum of 11-(morpholin-1-yl)chrysophanol (2.36) in DMSO-d_6

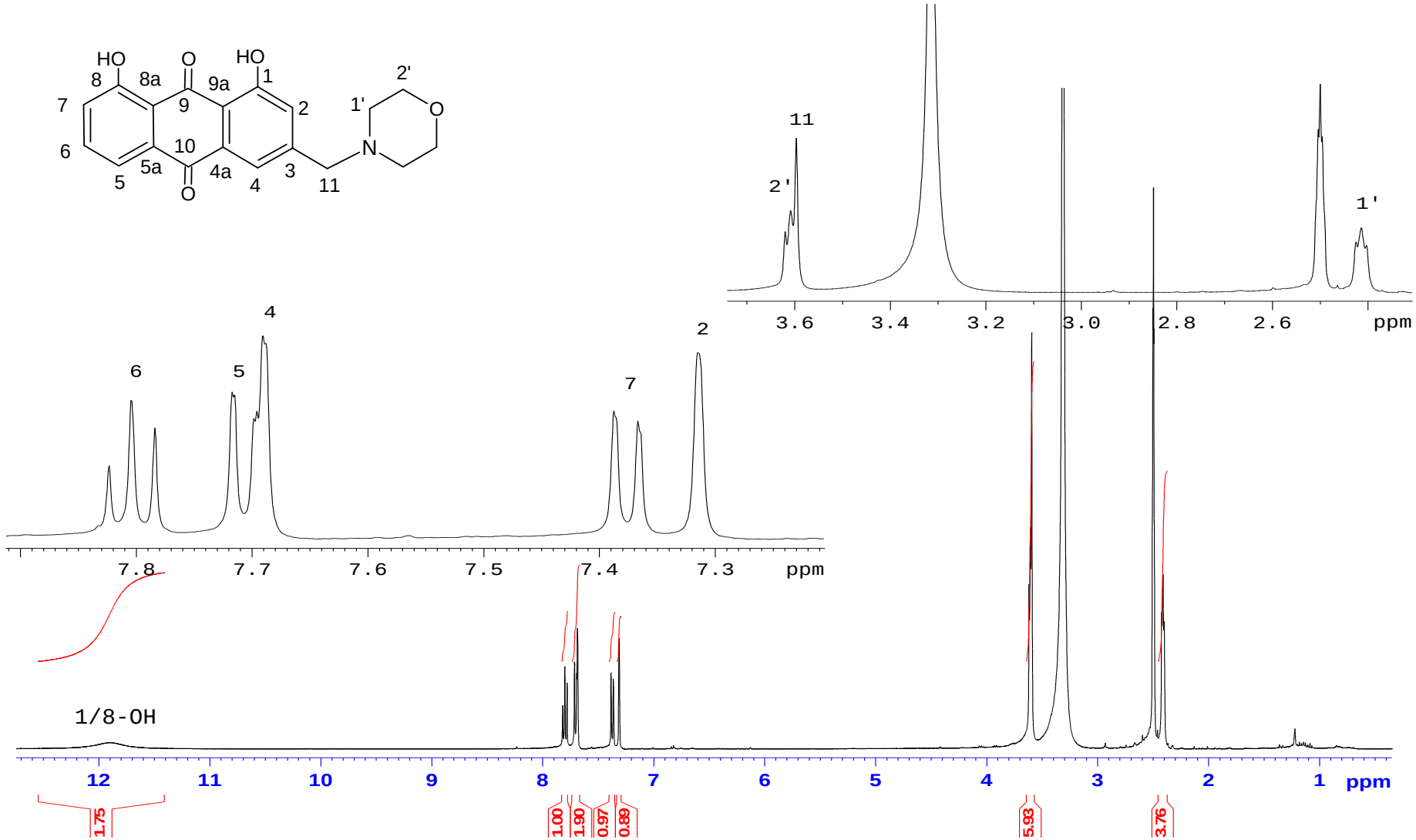

Plate 13b: ^{13}C NMR Spectrum of 11-(morpholin-1-yl)chrysophanol (2.36) in DMSO-d_6

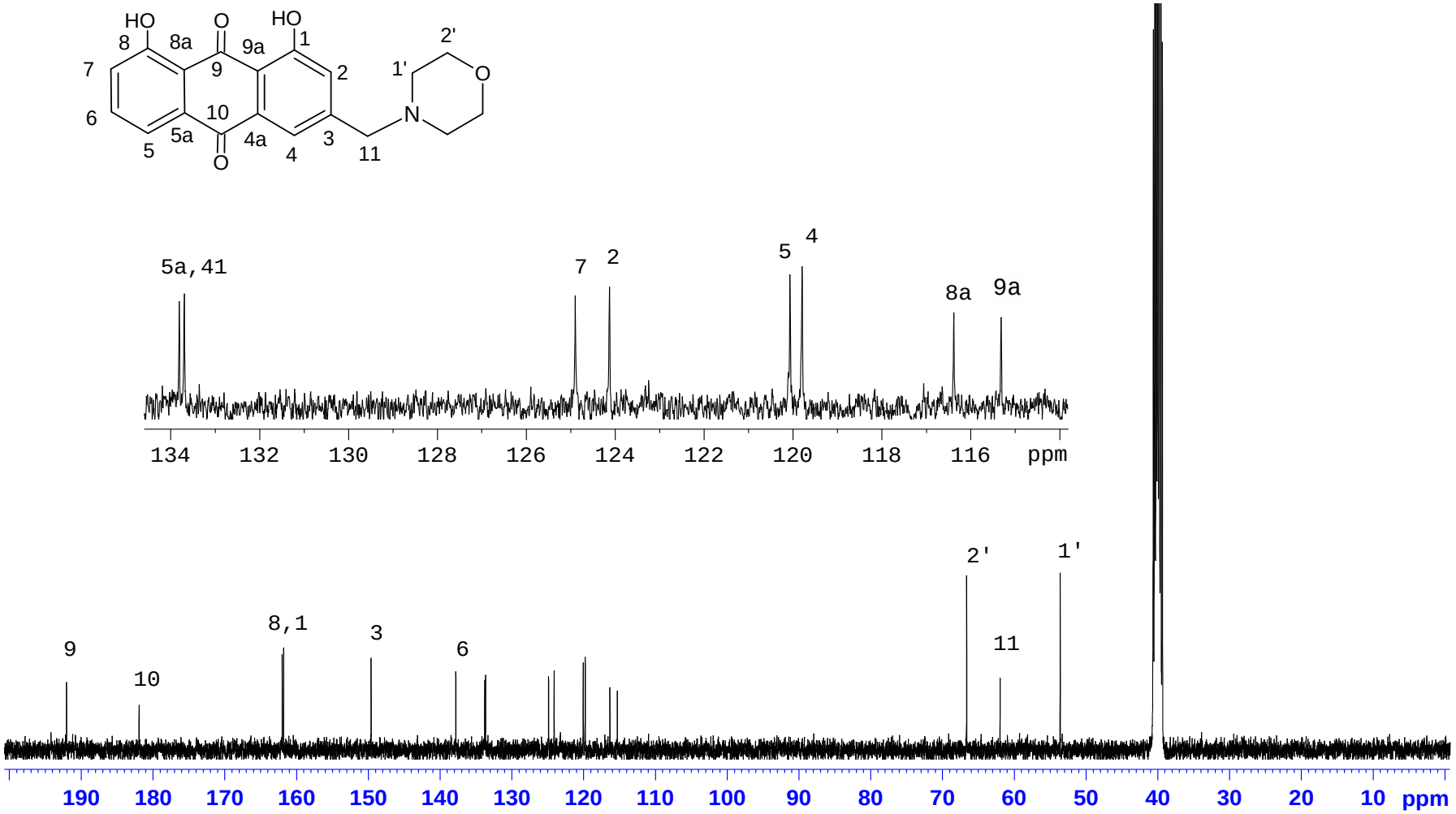

Plate 13c: DEPT 135 NMR Spectrum of 11-(morpholin-1-yl)chrysophanol (2.36) in DMSO-d_6

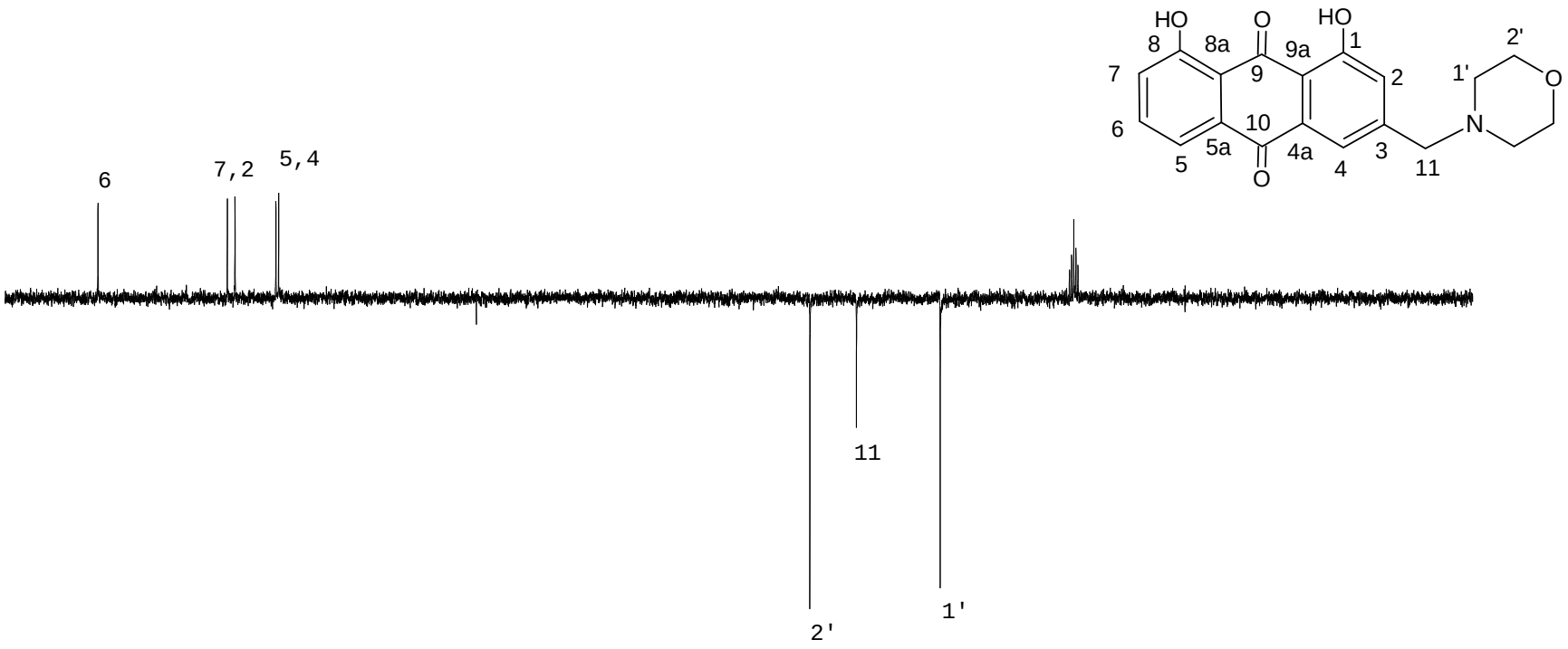

Plate 13d: COSY NMR Spectrum of 11-(morpholin-1-yl)chrysophanol (2.36) in DMSO-d_6

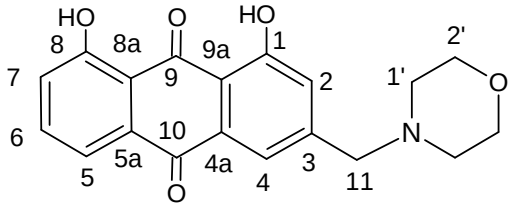

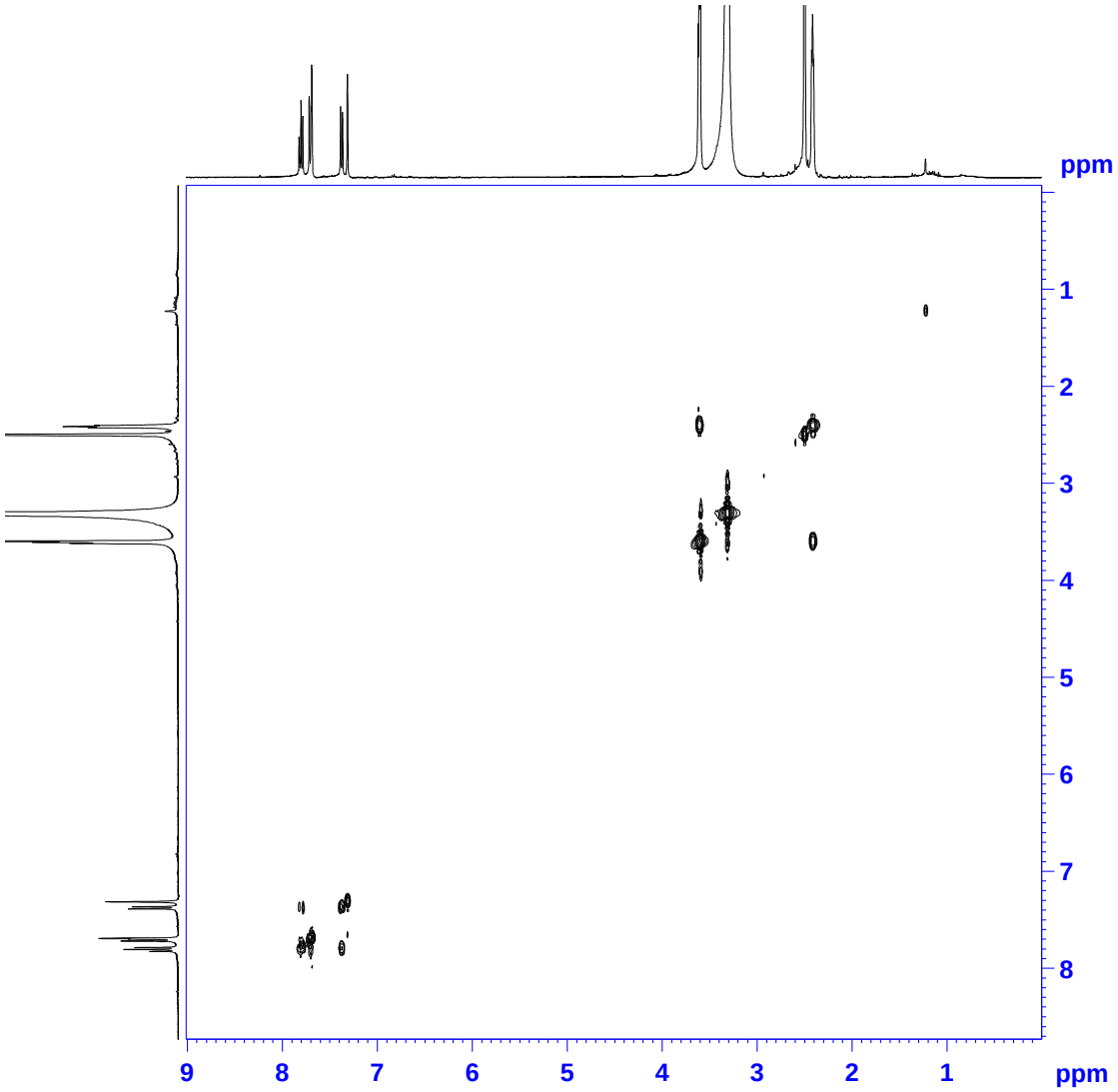

Plate 13e: HSQC NMR Spectrum of 11-(morpholin-1-yl)chrysophanol (2.36) in DMSO-d_6

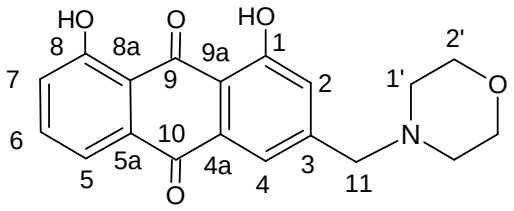

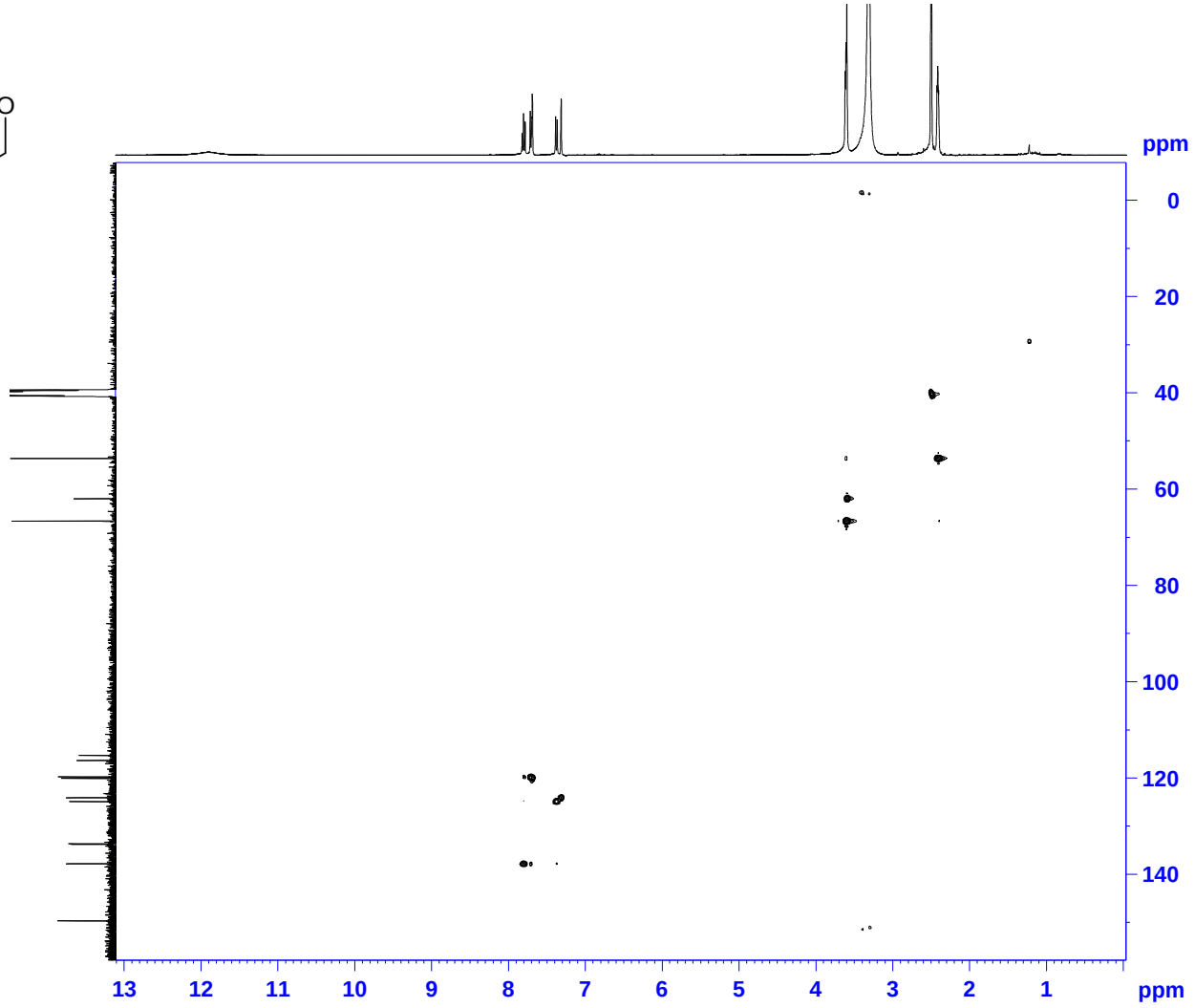

Plate 13f: HMBC NMR Spectrum of 11-(morpholin-1-yl)chrysophanol (2.36) in DMSO-d_6